In situ Dissection of the Virus-Cell and Cell-Cell Interplay in Granulomatous Lesions in Feline Infectious Peritonitis

Inaugural Thesis

to obtain the title of Doctor of Veterinary Medicine and Philosophy
(Dr. sc. med. vet.; corresponds to DVM, PhD)

from the Vetsuisse Faculty University of Zurich

submitted by

Alexandra Malbon

approved by

Prof. Dr. Anja Kipar (Supervisor)

Dr. Marina Meli (Co-advisor)

Prof. Dr. Volker Thiel (Mentor)

2019

Contents

Abstract

Feline infectious peritonitis (FIP) is an almost invariably fatal, feline coronavirus (FCoV)-induced disease of both small and large felids with a worldwide distribution. It arises from a combination of viral mutations of a ubiquitous enteric virus and an over-exuberant host immune response. The initial enteric infection often remains subclinical or causes a mild enteritis and may be associated with viraemia. A small minority of infected cats develops FIP, characterised by pyogranulomatous vasculitis, fibrino-suppurative serositis, and often protein-rich cavitary effusions. Neither the viral nor the host factors leading to this disease are completely understood, and it is almost unique in nature for its pathological presentation. Clinical and pathological features all point to excessive cytokine release, however the trigger and precise source(s) are unclear.

This present study focused on the host's local and systemic immune response to FCoV infection, with the mesenteric lymph nodes (MLN) the main organ of interest. The MLN is the likely first site of spread beyond the intestine and additionally has a crucial gatekeeper role against entry of enteric pathogens. A panel of relevant immune mediators was chosen, including the Toll-like receptors (TLRs) and STAT transcription factors; neither group was previously studied in FIP. Downstream mediators included type I and II interferons (IFN) and pro-inflammatory cytokines, colony stimulating factors and matrix remodelling enzymes. Using post mortem clinical cases, comparisons were made between cats with no detectable FCoV in the MLN, cats with FCoV in the MLN and no FIP, and infected cats with FIP. The second main focus was on the lesions themselves in order to evaluate the direct viral effect on mediator expression. Bone marrow and spleen were also studied to gain an appreciation of systemic immune mediator levels across groups.

The panel was evaluated across groups and organs, identifying TLR 2, 4, and 8 as the main TLRs upregulated in FIP (predicted to detect both viral proteins and genome). Correspondingly, the inflammatory cytokines IL-1β, IL-6, and TNF-α were also upregulated, as were the anti-viral IFN-α, -β, and -γ, the IFN despite the ineffectual defence response by the host. The greatest response was observed in the MLN, whilst cells within the lesions themselves upregulated many inflammatory cytokines still further, consistent with a direct viral trigger in addition to amplifying cascades. Transcriptional alterations in cases of FCoV infection without disease were rare. To examine both these and the effects of FIP itself in greater depth, MLN from the different groups were subjected to RNA-Seq by next generation sequencing (NGS). The greatest intergroup difference was still found between cats with FIP and controls, in which differentially expressed genes were linked to both pro-inflammatory and anti-viral aspects of the immune system, as well as cell cycle repression in FIP. However, between the two non FIP groups, cats with FCoV infection of the MLN exhibited lower mRNA expression of genes involved in immune responses known to be deleterious in FIP such as neutrophil chemotaxis and antibody production.

This reinforces the host dominance in disease development whilst opening up intriguing possibilities regarding host versus virus contribution to disease resistance.

A parallel aspect of the study assessed the virus, firstly for previously studied 'FIP specific' S gene mutations, confirming a link to systemic spread but not disease. Secondly the viral transcriptome via RNA-Seq. Initial results suggest there may be differential viral gene transcription occurring in FIP, affecting the viruses virion forming ability and thus hypothetically its pathogenic potential.

Introduction

History of the disease

Feline infectious peritonitis (FIP) is an almost universally fatal disease of felids with a worldwide distribution. It was first reported in 1963 although descriptions of a disease matching FIP can be found from Italy dating back earlier than this [1,2]. It was a further decade before a viral aetiology was shown, demonstrated to be a feline coronavirus (FCoV), which when causing the disease is a mutated form of a ubiquitous enteric coronavirus [3–5]. Both domestic and wild cats can be affected, with the disease being reported in big cats including mountain lions and cheetahs [6–9]. Cheetahs have been proposed to be particularly at risk because of their severely limited gene pool, meaning that 'susceptible' genes are likely to be carried by all [7]. Within domestic cats, pedigree animals and in particular certain pedigrees also show increased susceptibility, demonstrating that both viral and host factors contribute to disease [10,11].

Epidemiology

The epidemiology of the disease has many complexities and there remain many gaps in our understanding. Though the causative agent is a coronavirus, it is the cats' own immune system which inflicts the damage, combined with as yet only partially elucidated viral mutations.

The most common route of natural infection is faeco-oral, though experimentally virus has been administered intraperitoneally, intranasally, tracheally or orally with the rate of disease within cohorts related to the route of infection. This tends to be highest in peritoneal followed by tracheal then oral [12]. After experimental oral inoculation of the avirulent, enteric coronavirus (FECV), virus was found in the tonsils and small intestine within 24 hours and could be detected in the faeces by day two post infection [13]. Owing to faecal shedding, cats sharing litter trays or living in close proximity are at an increased risk of initial infection. Nevertheless it is only in very rare cases that FIP itself appears to be spread horizontally [14,15]. Despite this apparently low horizontal transmissibility of FIP, many cats with the disease also shed FCoV in their faeces [16]. Experimentally, some cats in fact stop shedding when they develop disease [17].

In experimental infection with the virulent form of the virus there are four possible outcomes: the cat resists disease, develops effusive disease, develops non-effusive disease, or develops enhanced disease [18]. The latter is usually seen in cats that were previously challenged e.g. with the avirulent form. This discrepancy between individual hosts shows clearly that the virus itself is not the deciding factor in terms of disease progression.

Antibodies against FCoV have been detected in up to 90% of cattery cats compared to 10-50% of animals in single cat households. In the former, seropositivity is thought to be maintained by reinfection [19–21]. Of these infected cats, longitudinal studies have shown that 5-10% in multi-cat households develop FIP [21]. Seropositivity itself is not an accurate predictor of the likelihood of developing FIP; cats may remain seropositive for years before disease develops, or may become spontaneously seronegative [20]. However, seronegative cats may also develop disease. Experimentally, kittens which seroconverted after infection with the virulent form (also referred to by some authors as FIP virus or FIPV) all developed disease and died within 6-10 days, whilst

half of the seronegative kittens did not develop FIP, and those that did developed the disease more slowly [22].

The role of antibody dependant enhancement (ADE) is controversial and it appears to be more common experimentally, where an enhanced form of disease exists in seropositive cats which are subsequently virus challenged (as mentioned above) [23,24]. This is defined by either a higher proportion developing disease, a shorter time course of disease, or an atypical gross picture [25]. ADE has proven particularly problematic in vaccine trials as prior exposure almost invariably worsened rather than prevented disease. No link between rising titre and development of FIP has been found [17]. On the other hand, maternally derived antibodies appear to be protective against FIP; these wane by 4-6 weeks when kittens become more susceptible [26].

Clinical findings

Coronaviruses in other species are frequently associated with enteric or respiratory disease. In farm animals, diarrhoea in neonates is especially common but some coronaviruses are not age specific (e.g. transmissible gastroenteritis virus [TGEV] of swine) [27]. Infection leads to exfoliation of viral infected villus tips leading to severe villus atrophy, blunting and fusion. The result is a malabsorptive diarrhoea with a minor secretory component [27]. In cats, infection with enteric coronavirus (FECV) is often subclinical but may lead to a transient enteritis. In rare cases, a severe fatal enteritis can develop [28]. In natural infection, therefore, most cases of FIP occur in animals with no recorded history of enteric disease.

FIP can present in many different guises, heavily influencing the ease of diagnosis. Classically FIP has been divided into wet and dry forms, with the wet form being that for which the disease was named. In reality these are a clinical distinction, representing the two ends of a spectrum of disease with the majority of cases being mixed forms. At pathological examination the overlap and continuum of lesion development becomes more evident [29].

Common clinical signs include a biphasic fever, lethargy, anaemia, anorexia, depression, and weight loss, though cats may have any combination or none of these. These are accompanied by signs relevant to the affected organs/body cavity e.g. abdominal distension in the case of ascites, dyspnoea and exercise intolerance in the case of pleural effusions, jaundice with extensive hepatic involvement, neurological signs, or renal failure [30]. The time scale can range from acute presentations to chronically progressing or waxing and waning disease [31,32]. Amongst the many differential diagnoses are neoplasia, congestive heart failure, toxoplasmosis and lymphocytic cholangitis [32].

Signalment can be helpful but is far from definite. Cats younger than two years and male are thought to be predisposed whilst neutered status is not a factor [31].

It is also not uncommon for animals to present with signs reflecting disease in a single organ system. This is especially well documented in the case of neurological FIP in which the brain may be the only affected organ and fits to the classic definition of ‘dry FIP’ [33].

The disease has also been reported presenting as orchitis [34], abdominal masses [35], ocular lesions [9,36] or cutaneous lesions [36–38].

Pathological findings

FIP is a disease of contradictions, one of these being that despite the myriad clinical presentations and many differentials diagnoses which can make intra-vital diagnosis highly problematic, it is an almost unique disease pathologically. To date, the only naturally occurring similar disease known is that in ferrets induced by ferret coronavirus [39]. Genetic engineering has created a similar disease in mice (discussed later).

In the initial enteric FCoV infection, histologically, the features are as seen with other coronaviruses, villus blunting and fusion, with epithelial necrosis, and FCoV antigen expression mainly in epithelial cells of the villous tips [13,28]. These are unlikely to be observed in natural infection as the usually mild disease rarely warrants investigation.

Early reported cases of FIP, or at least those which were recognised as such, mainly affected the peritoneum [1,2,40]; extra-serosal lesions were less common and first reported specifically in 1972 [41]. The authors found the kidneys, visceral lymph nodes (LN), lungs, liver, eyes, and leptomeninges to be the most commonly affected organs with disseminated granulomas and scant serosal lesions. The classical, almost pathognomonic, histological feature is a pyogranulomatous phlebitis, targeting particularly venules and small veins [42]. This was originally suggested to be immune-complex, i.e. type III hypersensitivity-mediated as C3, IgG and virus were seen together in vessel walls [22]. However, the distribution of and cellular composition within the vasculitis varies from immune mediated vasculitis of other species [42] and a type IV hypersensitivity reaction has also been suggested to cause the granulomas [23,43]. It is likely that a combination exists, reflecting the balance between humoral and cell-mediated responses in individual animals. FCoV is seemingly the only virus to induce immunological granulomas, though in contrast to these entities, granulomas in FIP lack multinucleate giant cells and epithelioid macrophages whilst having larger numbers of neutrophils. CD8+ cytotoxic T lymphocytes were found at the periphery of FIP granulomas and appeared to increase with the age of the lesions, whilst CD4+ helper T lymphocytes were more diffusely distributed [43]. There is also a progressive influx of B cells and plasma cells observed at the periphery of the lesions with time [44]. Despite common features, the distribution and precise type of lesions can vary between cats, and between organs within an individual [45]. Additional lesions include diffuse serosal inflammation, and lymphoplasmacytic infiltrates in more chronic cases [44]. The lymphocytic lesions are dominated by B cells and plasma cells and in some cases demarcate areas of inflammation from surrounding tissue [44]. Mesenteric lymph nodes without lesions have been variably found to show follicular hyperplasia with reduction in T cells, or moderate to severe depletion [44,46]. This may relate to viral presence [47]. An increase in the proportion of macrophages seems to be a more consistent feature, being observed in the splenic red pulp and lymph node sinuses in FIP cats [48]. Bone marrow is usually hyperplastic with a left shift and an increased proportion of cells of macrophage lineage in FIP [44,48].

Diagnosis

Intravital diagnosis is a particular challenge in FIP, especially in the dry form, and many methods are available (tending to indicate that no one method is ideal). The gold standard remains histological examination of lesions and immunohistology for FCoV antigen which requires an invasive procedure on frequently very sick cats.

The holy grail of FIP diagnosis is finding a test to reliably identify a pathogenic virus biotype alongside identifying host susceptibility. Antibody testing is rarely of benefit as the majority of cats have already been exposed. A negative correlation has in fact been found in cats with a higher virus load, implying immune exhaustion, and another study found that 10% of cats with FIP were antibody negative [49,50].

As well as developing an antibody response to FCoV, many healthy cats also become viraemic and may remain so for years, so that the presence of virus in the blood is not a feature defining the pathogenic biotype [51]. The same study also showed that remaining viraemic did not increase a cat's chances of developing FIP. As body cavity effusions result from an increased vascular permeability, it follows that a viraemic cat with e.g. ascites of cardiac origin may also have detectable virus in the fluid, as evidenced by specificities of immunostaining on effusions of around 70% [52,53]. The degree of viraemia is also not necessarily useful, as healthy FCoV infected cats may have high circulating levels [54]. Viral load in tissues tends to be higher in cats with FIP but this is currently more relevant to research than diagnosis as a precise cut off should first be established [55].

In FIP, as with other veterinary diseases with such a poor prognosis, the specificity of a test is arguably of more importance than the sensitivity, as a false positive result may lead to unnecessary euthanasia. A number of studies have compared the sensitivity and specificity of various *in vivo* tests for FIP. Quantitative RT-PCR (RT-qPCR) is nowadays one of the most common methods but there are still a multiplicity of samples to choose from as well as different laboratories with different protocols. Immunofluorescence and immunocytochemistry/ immunohistochemistry are the other main diagnostic modalities [32]. The Rivalta test is a simple method used to differentiate transudates and exudates and hence is a pointer towards the likelihood of FIP but not alone diagnostic [56].

If effusions or detectable masses are present then cytological examination is a non-invasive method which, whilst again not 100% diagnostic allows the likelihood of FIP to be determined [57].

Sensitivity, specificity, and positive and negative predictive value (PPV/NPV) are in all cases of course heavily influenced by the nature of the control group, and by the prevalence of FIP within the population [58].

As standard biopsy techniques are invasive, the utility of Trucut biopsies has also been evaluated on liver and kidney with the advantage of cost, safety, and surgical requirements but the expected disadvantage of a smaller sample requiring a degree of luck to target a diagnostic area [59].

Effusions have a higher diagnostic potential than blood, another factor complicating the diagnosis of cases without effusion. RT-qPCR on peripheral blood mononuclear cells (PBMCs), serum, and effusions found sensitivities of 28.6%, 15.4% and 88.9% respectively [60]. A positive immunocytology result on effusions was first thought to be 100% specific, a finding which was later questioned by the same group following further studies [50,52]. The nature of the effusion has a high positive predictive value (PPV), being yellow, gelatinous and transparent to cloudy with a high protein content and specific gravity [57]. The cell count can be variable but the population is composed of non-degenerate neutrophils, macrophages, and fewer lymphocytes [57].

Haematology and biochemistry reveal no pathognomonic changes and rely on increasing the suspicion of FIP when multiple suggestive results are obtained (leading to increased specificity but lower sensitivity). These include lymphopaenia, neutrophilia, anaemia, hyperproteinaemia, and

hypergammaglobulinaemia [61,62]. More selective analysis revealed that lymphopaenia tends to only affect acute cases and hyperproteinaemia subacute cases [45].

The hyperproteinaemia is due to an increased globulin fraction leading to an inverted albumin globulin ratio in many cases, which can also be used as a guide. The lymphopaenia is particularly due to decreased CD4+ T cell numbers (though CD8+, CD5+ and CD21+ cells were also found to be reduced); apoptosis was identified as the mechanism of reduction [63–65]. Lymphopenia is very non-specific when comparing cats with FIP to those with other diseases, so this feature is not a useful diagnostic tool but can help to rule out FIP as it has a high negative predictive value [65].

Host factors

In addition to searching for the key viral mutation, many studies have investigated which host genetics play a role in disease susceptibility.

As mentioned previously, breed susceptibilities have been identified, with those purebreds at an apparent higher risk of FIP including Abyssinians, Bengals, Holy Birmans, Himalayans, Ragdolls and Rexes [10,11].

The immune profile of Holy Birman cats has been further investigated to try to identify a reason for the breed's apparent predilection for FIP. Findings went against predictions of a skew towards humoral immunity (T helper (Th)2) and away from cell mediated immunity (Th1) as these cats instead had cytokine profiles favouring cell mediated immunity (CMI) [66].

Pathogenicity is affected by the viruses' ability to infect specific cell types but this also has a strong host aspect. From the side of the virus, peritoneal macrophages from SPF cats were shown to be susceptible to infection by both virulent and avirulent strains of FCoV, but the virulent strains infected a higher proportion of cells and were able to sustain replication [67]. This was despite comparable growth in CrFK cells. This study also observed that prior incubation with anti-FCoV antibodies led to enhanced uptake of virulent but not avirulent FCoV [67].

The host influence is shown in infection kinetic studies on PBMCs from healthy cats. Monocytes from just under half of cats are able to sustain viral replication of FIPV and not of FECV, a similar proportion can be infected but sustain neither, whilst just over 10% could not be infected at all at this time point [68]. PBMCs from a particular individual may also vary over time in their ability to sustain replication [69].

Many experimental studies have found that not all cats succumb to disease, as previously mentioned. A larger combined study looked into this further, confirming that some cats (approximately one third in this case) were resistant to FIPV challenge. However, a second challenge resulted in disease in some previously resistant animals. Prior exposure to avirulent FCoV did not increase the incidence but was sometimes associated with an earlier disease onset; resistance to FIP increased between six months and one year of age [70]. Counterintuitively, inbreeding of cats resistant to experimental FIP, with the aim of concentrating the gene pool and discovering which genes were relevant, produced cats more likely to succumb than the initial population [71].

Purebred cats have been shown to be predisposed. This is apparently a heritable trait, as the chances are much higher for a cat to develop FIP if an ancestor had FIP, and this seems to trace

back to common predisposed males. Persians and Birmans in particular show a heritability of at least 50% [72].

One study investigating the virus in an epidemic in Persian cats found that, regardless of viral factors, most affected kittens had a common sire and that by changing the sire the incidence dropped from 75% to 25% [73].

An analysis of Birman genetic susceptibility identified five possible candidate genes, ELMO1, TNFSF10, RRAGA, ERAP1 and ERAP2 [74]. Following on from this study, the aforementioned loci were compared in a genetically diverse population and not found to be significant. Instead, single nucleotide polymorphisms (SNPs) in TNF-α and DC-SIGN (CD209) were detected which appeared linked to susceptibility [75].

IFN-γ SNPs were separately identified in a targeted comparison of cats with and without FIP, suggesting the existence of polymorphisms linked to FIP resistance, as well as to circulating plasma levels of the protein [76].

Human leukocyte antigen (HLA) class II alleles correlate with e.g. viral load of HIV [77]. Feline LA class II polymorphisms were therefore studied, but no apparent link to susceptibility to FIP was found. However, this was a small study with many variables so may warrant further investigation [78].

Coronavirus biology and immune evasion strategies

Viral taxonomy

The causative agent of feline infectious peritonitis, feline coronavirus (FCoV), is a subspecies of coronavirus within the order Nidovirales.

Nidovirales is the order containing the largest known RNA genomes, which can exceed 30,000 bases [79]. All possess a single-stranded positive sense RNA genome which encodes their own replication machinery in addition to structural proteins, those involved in immune evasion, and proteins of as yet unknown function. Many features are shared by all nidoviruses. The current classification places FCoV as a subspecies within the species Alphacoronavirus 1, genus Alphacoronavirus, subfamily Coronavirinae and family Coronaviridae (Fig. 2.1) [80].

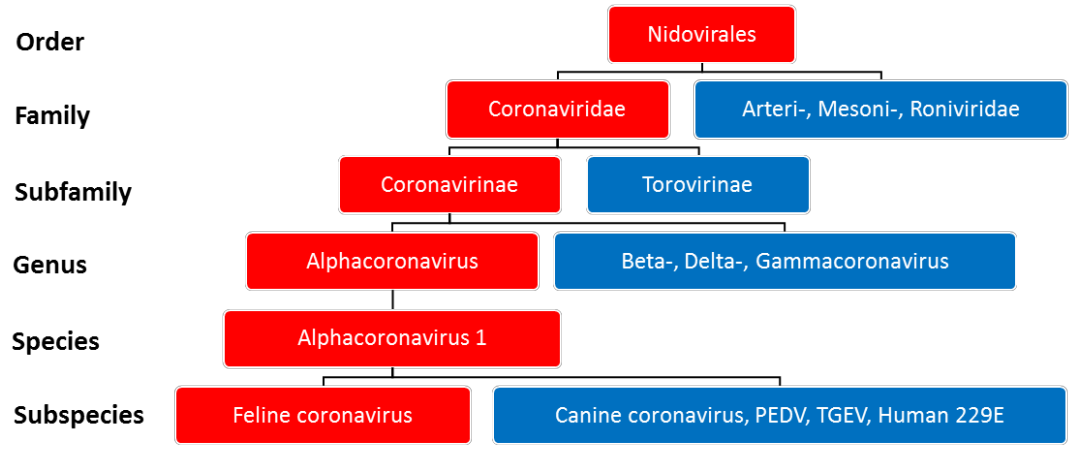

Figure 2.1: *Viral taxonomy adapted from the latest 2012 classification [80], which replaced the earlier classification of Coronavirus as a genus [81].*

The family Coronaviridae encompasses many viruses of human and veterinary significance. It includes the high profile severe acute respiratory distress syndrome (SARS) and Middle East respiratory syndrome (MERS) viruses, which led to a surge in interest in coronavirus research. MERS has a fatality rate of approximately one third of all diagnosed cases, eclipsing the importance of 229E, the common cold virus which is also an alphacoronavirus [82]. Alpha and betacoronaviruses infect mammals, gammacoronaviruses infect avians, whilst delta coronaviruses may infect both [82].

Unrelated to pathogenicity there are two serotypes of FCoV (I and II). The S proteins of serotype II FCoV were found to cluster with canine coronavirus (CCoV) and TGEV, whilst the M and N of both FCoVs clustered together away from the canine and porcine viruses [83]. Later, further work at the viral genome level showed that serotype II FCoV originates from more than one recombination event between FCoV serotype I and CCoV [84]. In addition to the S protein deriving largely from CCoV, 3c also differs between FCoV types, whereas 7b is the same, indicating it was not involved in the recombination [84]. It is known that CCoV can infect cats; CCoV exposure can cause ADE in FIP, and can also cause mild diarrhoea or even FIP itself [85].

In most parts of the world, FCoV type II is found in only a minority of FIP cases. Many studies have evaluated this, ranging from 2.5% in Malaysia to ~20% in Switzerland [86–91]. Owing to this relative rarity, and evaluation of viral sequences, it has been suggested that the recombination event in fact occurs within individuals rather than being a circulating form [92].

Coronavirus replication

Although this study focusses on the host response, the underlying viral mechanisms are of great importance in understanding which factors may affect this host response and which are potential targets in inhibiting viral replication or manipulating the immune response.

The large genome of the Coronavirinae comes with a unique replication strategy [93]. In common with other nidoviruses, they have a large replicase gene followed by structural and accessory genes; the replicase gene arrangement distinguishes the nidoviruses from other orders [79]. Nidoviruses, meaning ‘nest’ are named for their nested subgenomic mRNAs. Structural and accessory genes comprise only approximately one third of the genome, structural including S, E, M, and N (spike, envelope, membrane, and nucleocapsid respectively). The Coronavirinae are named for their distinctive club shaped spike proteins which project from the surface. The spherical virion is ~125 nm in diameter, with a helically symmetrical nucleocapsid (Fig. 2.2). This is uncommon amongst positive sense RNA viruses and instead is normally a feature of those which are negative stranded [93].

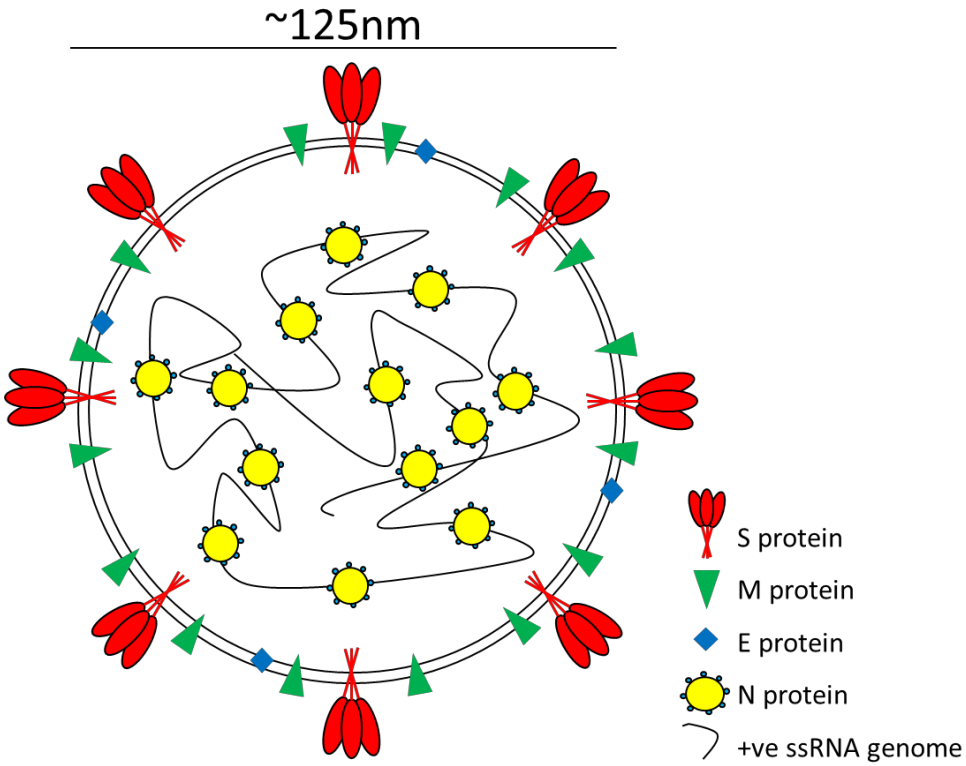

Figure 2.2: *Schematic image of coronavirus structure.*

The S protein is ~150 kDa and forms spikes made up of homotrimers [94,95]. M is the most abundant protein and may help with maintaining virus shape, whilst E is present at low levels and seems to enable assembly and release of the virus. N binds RNA and is heavily phosphorylated; this feature appears to lend the N protein a preference for binding viral over host RNA [96].

The coronavirus must first gain entry into the host cell and many utilise the aminopeptidase N protein (APN) of their respective host species as a receptor, including FCoV type II [93,97]. FCoV type I has been shown not to recognise this receptor but the search for its corresponding receptor is still ongoing [98,99]. Viruses are not always restricted to their host APN; the human HCoV-229E virus can additionally utilise the feline but not porcine APN [100] whilst the feline APN appears in general to be a receptor for multiple viruses within the same species as FCoV, with the potential to act as a mixing vessel as has occurred to form serotype II [97]. Many other receptors have also been identified as being used by other coronaviruses [82]. Despite the lack of a known primary receptor for FCoV type I, it has been shown that both type I and II use DC-SIGN as a co-receptor at least *in vitro* [101,102].

Apart from entering cells via the receptor, FCoV can enter via Fc receptor binding of the antibody against the FCoV S protein [103]. Further evidence of the crucial role of the S protein in this process is the ADE induced experimentally only by prior exposure to antibodies against the same serotype (i.e. the same S protein) [104].

The S protein is a class I fusion protein which mediates attachment to the host receptor [105]. It is then cleaved by a host cell furin-like protease to S1 (the receptor binding domain) and S2 (the stalk) [106]. It also has a transmembrane anchor and a short intracellular tail. The receptor binding

domain (RBD) of the S1 protein determines host specificity and tropism. Following binding, cleavage occurs at two sites in S2, the first cleavage separates the RBD and fusion domains, the second exposes the fusion peptide. The latter fuses the viral and host membranes and releases virus into the cell, this usually occurs in acidified endosomes but some may fuse at the plasma membrane [93].

Within coronavirus genera the S1 is very similar but may recognise different receptors. Between genera there is significant S1 variation yet it may still recognise the same receptor, a phenomenon still to be fully explored [82].

Having entered the host cell, the virus must now replicate. Replicase expression utilises frame shifting to make two alternate polyproteins, 1a and 1ab, although the precise ratio is unknown *in vivo*. These polyproteins then form the non-structural proteins (nsps) 1-16 [107]. The genome structure is portrayed schematically in Fig. 2.3. Coronaviruses encode their own proteases within these nsps, which then cleave the remainder. These include papain-like proteases (PLpro) from nsp3 and a main protease (Mpro) from nsp5. Many nsps form the replicase-transcriptase complex (RTC), responsible for transcription of sub-genomic RNAs. Nsp12 encodes the RNA-dependant RNA polymerase (RdRp) domain. The strand shifting ability of this RdRp helps explain the ability of the viruses to combine both homologously and non-homologously [93].

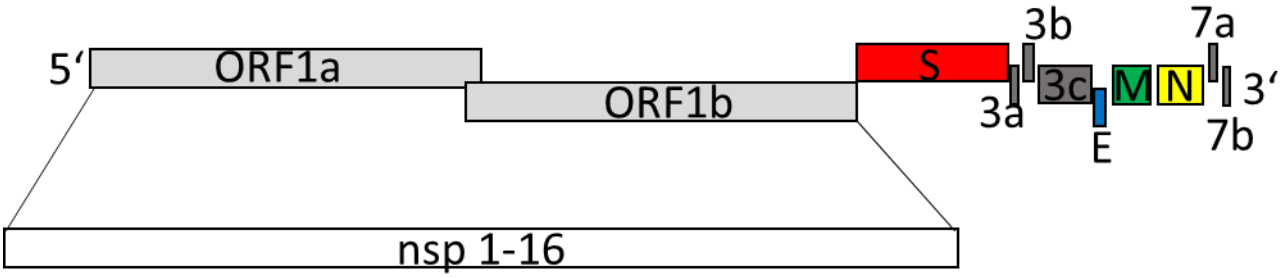

Figure 2.3: *Genomic organisation of FCoV. The light grey ORFs are encoded by the replicase gene, forming polyprotein 1ab which is cleaved to 16 nsps; structural proteins are coloured as in Fig. 2.2; accessory proteins dark grey.*

During replication, negative strand intermediates are formed which are ~1% as abundant as positive strand templates. Structural proteins S, E, and M are translated after replication and subgenomic RNA synthesis has been completed. These proteins insert into the ER, move to the ERGIC (endoplasmic reticulum-Golgi intermediate compartment), and viral genomes bud out to form mature virions [93]. Virus like particles can form with only E and M, but formation is enhanced by N [108]. S is not required at this stage. In some coronaviruses, S protein that is not packaged goes to the cell surface and mediates fusion between cells. This allows syncytia formation and mediates viral spread without the virus leaving cells, and hence aids evasion of the host immune response [93]. This phenomenon has not been observed in FCoV [93].

Coronaviruses also possess other and varied mechanisms of immune evasion. Host sensing of viral RNA relies largely on recognising viral features that are not found in host RNA. These features include 5' uncapped RNA and double stranded (ds)RNA [109]. Coronaviruses do however have a 5' cap, with capping enzymes encoded within the RTC [109,110]. They also encode an exoribonuclease to hydrolyse free RNA structures and remove them as targets for immune surveillance [111]. This enzyme additionally functions as a proofreading machine, endowing the virus with a very high

replication fidelity for an RNA virus [112]. A further viral evasion strategy is the apparent shielding of dsRNA within double membrane vesicles stolen from the host endoplasmic reticulum [109].

The above mechanisms are all designed to prevent host detection of viral presence. If these fail and receptors are activated, coronaviruses also possess other mechanisms to interfere with host signalling. The SARS PLpro enzyme for example inhibits TLR7 and TLR3 signalling via downstream pathway cleavage of Lys63-linked ubiquitin chains [113]. The same enzyme can also interact with the signalling complex formed by STING (stimulator of interferon genes) and others, preventing transcription of type I IFNs [114].

Viral factors

It was first suggested almost half a century ago that the causative agent of FIP, FIPV, is closely related to FECV, initially these were thought to be two separate viruses [26]. Despite host differences in susceptibility, experimental work clearly shows that pathogenic potential varies significantly between viruses. It was discovered in the 1980s that the two biotypes have different growth requirements in culture, with FECV replicating poorly in macrophages [18,67]. Dewerchin also found PBMCs were less supportive of FECV infection than of FIPV [68].

There has been some debate as to whether there are two circulating forms of the virus (the circulating virulent/avirulent strain hypothesis), or that mutations develop within individual animals, the so-called internal mutation (or *in vivo* mutation transition) theory [5]. The latter is now fairly widely accepted though disputed by some [115]. One of the main mysteries in the development of FIP is which mutations are relevant to viral pathogenicity. Many potential gene candidates have been explored, as discussed below, but as yet no single mutation/protein has been linked conclusively with disease. Identifying the viral changes of importance is a prerequisite for designing a distinguishing diagnostic test (setting host factors aside briefly) and trying to further understand the pathogenesis.

RNA viruses are inherently prone to mutations as they in general lack a proofreading mechanism. An average of 0.76 mutations/replication/μg of riboviral genome has been calculated and is fairly fixed per cycle, or ≈4 × 10^{-4} nucleotide substitutions/site/year [116,117]. Coronaviruses are an exception in possessing their own proofreading mechanisms and as such have lower mutation rates than most [112]. They nevertheless, like other RNA viruses, exist as quasispecies [112,118]. This is not due to selection pressure as viruses in cell culture exhibit the same quasispecies [119]. FCoV has a relatively low rate of mutation in cell culture, indicating relative stability [120].

Mathematically it can therefore be assumed that anything leading to an increased replication rate of the virus increases its chances of acquiring pathogenic mutations. Correspondingly, FCoV-infected cats with compromised immune systems e.g. those with FIV or FeLV infection have been shown to be at increased risk of developing FIP [12,86].

The increased replication is evidenced by a 10-100 fold higher FCoV titre in the faeces of experimentally infected FIV positive cats compared to FIV negative controls. These cats also shed for longer, and had lower antibody responses [121]. FECV infection led to FIP in 10% of FIV positive cats within 10 weeks, compared to none without [86,121]. This study also found evidence of independent (internal) mutations arising in cats infected with the same FECV to cause FIP.

This exemplifies one of the many contradictions of FIP, that despite being caused by an out of control immune response, cats with immunosuppression appear predisposed.

Beginning with the non-structural proteins, ORF1 proteins comprise the replicase machinery and have not thus far been implicated. ORF3abc appears to have been involved in a recombination with CCoV. Although it does not affect growth in CrFK or Fcwf-4 cells, its presence leads to a markedly lower replication in PBMCs [122]. FIPV isolated from an infected cat showed a truncated ORF3abc, with the theory that this truncation increases viral replication efficiency in and tropism for macrophages. This was narrowed down to being a 3c deletion/truncation. Addition of 3c in culture seemed to inhibit replication in Fcw-4 cells [123]. This theory was supported by *in vivo* studies, in which samples from faeces of healthy cats or organs/effusions of FIP cats showed that most healthy cats had an intact 3c whilst most FIP cats had a deletion or nonsense mutation [123,124]. It was subsequently found that cats with FIP may also have virus with intact 3c, so that this does not appear to be a determining factor in virulence [125]. Experimental work on this ORF, infecting cats either oro-nasally or intraperitoneally with FECVs (all having an intact 3c), or FIPVs (with and without intact 3c) found a close link between an intact 3c and the ability to replicate in the intestine, as well as showing again that FECVs had a lower ability to replicate systemically [126].

In vitro deletion of ORF3 or 7, or both, showed that ORF7 was required to maintain replication within PBMCs. The lack of only ORF3 still allowed sustained replication but at a much lower level compared to wildtype [127]. How closely this reflects the *in vivo* situation is unknown. *In vivo*, viruses with ORF7b deletions were found in both FIP effusions and faeces of healthy cats [128].

The viral 7a protein was shown *in vitro* (in Fcwf-4 cells) to help FIPV counteract IFN-α, as measured by the ability of the virus to replicate in the presence of the interferon, but that it also required ORF3 to achieve this [129].

The spike protein, with its importance in determining viral cell entry, is of particular interest. Its furin cleavage motif is conserved in FECV but was found to often be altered in FIPV [130]. This study compared cats before and after developing FIP, and cats in the same environment that did not get FIP. The same authors found that although all groups had mutations in S1/S2 they were often not in a functionally relevant site in cats that did not develop FIP [130].

Experimental recombinations between the type II cell culture adapted FECV (79-1683) and FIPV (79-1146) found that macrophage tropism is linked to the S protein, but that infectivity is not linked to receptor usage as both FIPV and FECV can be blocked by antibodies to the fAPN receptor. Tropism was found to be in the membrane proximal region of the ectodomain rather than the amino-terminal receptor-binding region itself [131]. Further S gene analysis compared FCoV sequenced from organs of cats with FIP with FCoV sequenced from the faeces of cats without FIP. Two mutations were found to identify over 95% of the cats with FIP, namely M1058L (the majority) and S1060A (another 4%, the first group still retained S at 1060) [132]. These mutations were then found in tissue samples of cats without FIP, though at a lower level, and the 'FIP mutation' found in virus within faeces [91,133]. This suggests that the mutations are indeed related to systemic spread but neither sufficient alone to cause FIP nor essential. Whether the difference then lies with the virus or with the host, and whether cats carrying mutated virus may later go on to develop FIP has not been determined.

Treatment and prevention

To date there is no successful treatment, although drug trials are ongoing. In order to succeed, any method relies on understanding the peculiarities of the virus. The following list of studies is not exhaustive as myriad compounds have been evaluated against FIP, but covers the range of tactics that researchers have adopted.

Vaccination has been attempted in multiple guises but as discussed briefly above with ADE, most attempts to immunise cats against subsequent challenge by FIPV have been unsuccessful, if not having the opposite effect of enhancing disease. Early efforts involved exposure to low levels of virus, to 'apathogenic' virus or to antisera from other animals. All led to increased susceptibility or to unpredictable responses which could not safely be applied clinically [22,23,134,135].

More recently, reverse genetics systems have been used to generate vaccines with varying success. One group found that viruses with deletions of either ORF3abc, ORF7ab, or both replicated well in cell culture (on Fcwf-4 cells), and caused no clinical signs in cats [136]. They then challenge tested these cats with virulent FCoV and found good protection (9/10 cats survived) when using the individual deletion viruses but the classic problem of enhanced disease using the double deletion virus [136]. A later study did not attempt vaccination but assessed these same deletion mutants in feline monocytes, finding impaired growth and/or infectivity in all [127]. The reasons for these differences must be host cell specific as both studies used the same viruses.

Another study found that a similar strategy of vaccinating with live ORF3abc attenuated vaccines protected SPF but not conventional cats. However as the conventional cats were British Short Hair purebreds and the SPF cats were domestic shorthairs, this extra variable of breed complicates interpretation of the relative effects of vaccination versus host genetics on outcome [137].

In the absence of a preventative vaccine, the search for a successful treatment becomes more critical and many antiviral therapies have been tried. Interferons, particularly the type Is, are a commonly used antiviral therapy in human medicine, later finding their way to veterinary medicine [138,139]. The first to be licensed for feline use was interferon omega, aimed particularly at retroviral infections [140]. The use of interferon omega in FIP has been reported as being of partial or no benefit [141,142]. The discrepancy may be in part due to the varying strictness of the diagnostic criteria of FIP used in the two trials. Less specific immune modulators include the immunosuppressive glucocorticoids, common in first opinion practice upon making a diagnosis of FIP but of no proven benefit [143]. Another immunosuppressant, cyclosporine, has had an *in vitro* effect on replication of a range of coronavirus species including FCoV [144,145].

Small interfering/silencing (si)RNAs can be designed to target specific regions of a viral genome to target the RNA for degradation and prevent its replication [146]. A side effect of the inherently high mutation rate of RNA viruses is the speed at which sequence alterations lead to therapy resistance [147]. Combination siRNA therapy targeting more than one region of the viral genome delayed the onset of viral resistance but has until now only been been tested *in vitro* [148].

In view of the fact that TNF-α is produced by virus infected macrophages and seen as a key mediator of the pathogenic effects of FIP, anti-TNF-α antibodies were clinically trialled. 1/3 compared to 3/3 untreated experimentally infected SPF cats developed FIP [149].

Another predicted inhibitor of inflammatory cytokines, propentofylline was clinically trialled and found to have no effect, the prediction having been that it would prevent the development of vasculitis and hence avoid the effects of the virus [150]. Other drugs trialled with varying success

include cholesterol inhibitors, platelet aggregation inhibitors, the antiviral ribavirin and the DNA alkylating melphalan [151–154].

Viral protease inhibitors are currently showing the most promise; different groups have reported the ability to reverse the clinical progression of FIP, though with more success in 'wet' cases [155–157]. By targeting this key viral enzyme the drugs interfere with viral replication and protein cleavage.

The host immune response

As described above, the host response is crucial to determining disease outcome. A range of immune mediators was chosen for the present study. These reflected those which were known, or thought likely, on the basis of previously published functions, to play a role in FIP pathogenesis; the aim was to evaluate disease associated quantitative changes. Their main functions, together with what is so far known for each as relates to FIP, are presented below. The specific members of each group involved in the study are given in brackets for each section.

Toll-like receptors (TLR) [TLR 1-9]

The immune system of mammals comprises two main branches. Whilst the innate immune response is found at a very early stage of evolution and allows for a rapid yet relatively unspecific response, the adaptive immune system is only possessed by higher vertebrates and leads to a more targeted response. There are various theories as to why the latter has evolved, with reduced energy expenditure by the host being one of these [158].

Four families of pathogen recognition receptors (PRRs) are currently known, TLRs, retinoic acid inducible gene I (RIG-I)-like receptors, nucleotide oligomerisation domain-like receptors, and HIN-200 family members [159,160].

TLRs are one of the most evolutionarily conserved defence mechanisms of the immune system, being found not only in humans and other mammals, but also in sponges, the phylogenetically oldest known extant metazoans [161]. Even the immune system of plants uses highly similar receptor proteins as the first line of defence, sharing leucine rich repeat (LRR) domains with the TLRs [162].

TLRs were the first PRRs to be discovered and as key components of the innate immune system are able to detect a wide range of pathogen associated molecular patterns (PAMPs) present on bacteria, viruses, fungi, parasites, and protozoa. PAMPs are those molecular signatures which are specific to pathogens and should not be present, or at least not exposed to the immune system, in the host. Most microbes are composed of multiple PAMPs, allowing simultaneous activation of multiple PRRs, which themselves exhibit receptor redundancy and crosstalk [163].

Another important function of TLRs is as inducers of dendritic cells which can then activate the second branch of the host immune response, adaptive immunity. TLRs are the bridge between innate and adaptive immunity which is crucial to co-ordinating an effective immune response and immune memory [164].

To date, 12 functional TLRs have been identified in mice, and ten in humans [163]. TLR 1-9 in the domestic cat have been sequenced and the lymphatic tissue TLR response to FIV assessed [165]. Their presence in feline pancreatic islet cells has also been assessed [166]. However, investigation into

their potential involvement in FIP has thus far only been undertaken for TLR9 and only *in vitro* [167]. Subsequently to completion of the experimental work in the current study, TLR4 was found incidentally by RNA-seq to be upregulated in peritoneal macrophages of cats with FIP [168]. Table 2.1 shows the reported ligands of TLR 1-9 and references studies of possible relevance to FIP.

Table 2.1: TLR 1-9 and their associated PAMPs, together with literature from other species which may be of relevance in FIP.

TLR	Main reported PAMPs[169–172]	Predicted relevance to FIP
1	Lipoproteins, LTA, PGN, lipoarabinomannan	- Possible role through TLR2 heterodimer formation [173]
2	Lipoproteins, LTA, PGN, lipoarabinomannan	- Possible S protein recognition [174]
3	dsRNA	- dsRNA is replicative intermediate of FCoV [93] - TLR3 has a protective role in MHV and SARS-CoV [175,176]
4	LPS	- Recognition of viral structural protein in other viral species [169,173]
5	Flagellin	- None known [173]
6	Lipoproteins, LTA, PGN, lipoarabinomannan	- Possible role through TLR2 heterodimer formation [173]
7	ssRNA	- Predicted FCoV genome recognition - Possible inhibition by viral PLpro [113]
8	ssRNA	- Predicted FCoV genome recognition
9	Unmethylated CpG motifs	- Possible inhibitory effect on viral replication [167]

LPS was the first identified TLR trigger, 20 years ago, with many more discovered since [177]. Despite crossover with other sensing systems and redundancy between TLRs, loss of one can markedly increase susceptibility to specific agents [178].

TLRs have three domains, an extracellular ligand binding domain specific to each, a transmembrane domain, and a cytosolic signalling domain, TIR, standing for Toll-interleukin 1 receptor homology domain [169]. They are grouped by family and by cellular localisation. Though mainly active in macrophages, dendritic cells, and B cells they can be expressed by many more cell types [178]. The TLR1 family includes TLR 1, 2, 6, and 10, and occurred by evolutionary duplication. These usually form heterodimers involving TLR2 upon ligand recognition and as such allow a greater diversity of detection and response [179]. The TLR1 family, plus TLR4 and 5 are found on the cell surface and, correspondingly, predominantly recognise membrane components. TLR 3, 7, 8, and 9 on the other hand are found within intracellular vesicles and recognise nucleic acid. The vesicle shields cellular nucleic acids from the TLRs to prevent auto-immune reactions, whereas extracellular free nucleic acids (e.g. following cell damage) are quickly degraded by nucleases. The intracellular TLRs require an acidic environment to function; drugs that prevent this from forming can also block TLR signalling [178].

Despite the degree of overlap, there is also huge scope to tailor a specific immune response by means of downstream signalling pathways. It remains in many cases to be elucidated exactly how a cell is able to correlate different ligands and responses. TLR signalling requires association of their TIR-domain with the TIR-domain of an adaptor protein, which occurs following ligand binding and induction of conformational changes [178]. All TLRs except TLR3 are able to signal through the

adaptor protein MyD88, with some being completely dependent on it [178]. This pathway usually leads to MAP kinase and NF-κB activation with induction of inflammatory cytokines [178]. These pathways are summarised in Fig. 2.4.

TLR3 and 4 use the alternative pathway activated by TRIF and culminating in interferon regulatory transcription factor (IRF)3 and NF-κB activation which induce type I interferons (IFN) as well as inflammatory cytokines [172].

The response to TLR4 activation is stage dependant, with early and late phase responses. It is able to activate two distinct signalling pathways, with an early phase MyD88 dependant pathway and a late phase TRIF-dependant [180]. Activation of only the TRIF-dependant pathway can induce type I IFN, whereas for inflammatory cytokine induction a more robust activation involving both pathways is required [180]. This implies a level of 'brake' on the immune system with a first defensive option which is less potentially aggressive to the host itself [180].

In comparison to bacteria, viruses lack common conserved features, therefore nucleic acid recognition is used. This is despite it being a slightly risky strategy on account of potential overlap with host nucleic acid [181]. Host RNA, if released from damaged cells, is usually broken down rapidly by extracellular RNAses [169]. In contrast, viral RNA is first contained within viral particles and then, upon uptake into phagosomes, released from the particle for detection by PRRs.

As shown in Table 2.1, many TLRs are known to have a role in viral sensing. TLR3 recognises dsRNA (with polyI:C the synthetic analogue) which comprises the nucleic acid of all Baltimore group III viruses e.g. the Reoviridae, or can be an intermediate replicative stage of ssRNA viruses, including the group IV (+)ssRNA Coronaviridae [93,182]; interestingly, negative stranded viruses do not produce detectable amounts of dsRNA during replication [182]. TLR 7 and 8 recognise ssRNA, whilst TLR9 is a DNA sensor but may also detect CpG motifs within RNA sequences [183]. Humans but not mice use TLR8 as a ssRNA sensor [184], the TLR8 has not been characterised in the cat. The precise motif for TLR 7 and 8 is as yet unknown [182].

In line with their role in viral defence, these intracellular TLRs (3, 7, 8, and 9) strongly upregulate type I IFN as well as inflammatory cytokines, the latter being the most common result of stimulation of other TLRs. There are two pathways; via signalling adapter TRIF to IRF3 phosphorylation to type I IFN transcription and translation, or via IRF7 transcription factor. The latter is downstream of TLR 7 and 9, primarily expressed in plasmacytoid dendritic cells and specialised to produce high levels of type I interferons [169,185]. It is thought that this is owing to these cells' high IRF7 levels, but delivery of TLR 7 and 9 to early endosomes in macrophages produces the same result [186]. Plasmacytoid dendritic cells (pDCs) are the main expressors of TLR 7 and 9 and are one of the two principal specialised subtypes of dendritic cells. They are characterised by distinct cell surface molecule expression in humans and mice, requiring further study in cats [185,187,188]. pDCs are specialised in sensing nucleic acids and are the primary type I interferon secreting cells of the immune system [188,189].

Viral proteins are also in some cases able to stimulate TLR pathways though this is relatively rare [169]. Viruses have an inherently high mutation rate, therefore they are often able to evade immune detection by alteration of their surface expressed proteins (particularly well-known in the case of influenza virus for example) [190,191]. As the TLRs are highly conserved, for a protein to be recognised it follows that the protein must be stable. This implies either that the conformation is required for viral function and hence the virus cannot mutate and remain competent, or that

receptor recognition is in fact of benefit to the virus. This has been shown in examples which induce a marked inflammatory response detrimental to the host [169].

In addition to these virus specific TLRs, other TLRs have been implicated in detecting viral proteins. TLR 2 and 4 in particular have been shown to have a role. TLR2 can recognise viral proteins including the SARS-CoV S protein, with a cell type-specific response [174,192]. In response to experimental vaccinia virus infection for example, macrophage expressed TLR2 led to downstream upregulation of inflammatory cytokines, whilst the same receptor expressed instead on monocytes led to type I IFN upregulation [192]. This is in contrast to the production of only inflammatory cytokines following bacterial ligand recognition [192]. As FCoV may infect both monocytes and macrophages, the same trigger may hypothetically induce both a pro-inflammatory cytokine and an interferon response via TLR2 signalling.

Unmethylated CpG motifs within bacteria were the first TLR9 ligands identified [193]. More accurately, these motifs were previously known to stimulate a marked, and often fatal, inflammatory response via an unidentified signalling pathway [194]. Having identified a new receptor which they named TLR9, Hemmi et al. tested the response of different knock out (KO) mice to CpG DNA challenge. TLR2 or 4-/- mice behaved as wildtypes, whilst $TLR9^{-/-}$ or $MyD88^{-/-}$ mice mounted no inflammatory response to challenge [193]. This demonstrated both the key role of TLR9 as well as the common signalling pathway with TLR2 and 4. In this study the spleen was the main source of TLR9 mRNA expression but other haematopoietic organs were not compared [193].

Since this discovery, many DNA viruses have also been found to activate TLR9, including herpes-, adeno-, and poxviruses [169]. RNA viruses are much rarer triggers of TLR9 but examples exist, including SARS-CoV and Dengue virus [195,196]. Whether this activation is direct or indirect is as yet unknown.

TLR9 is suggested to react to specific CpG motifs; the belief was that mammalian DNA, containing four times fewer CpG motifs than bacterial as well as being methylated, did not stimulate this receptor. In fact it has been shown that far more important than the sequence is the requirement for delivery to the endosomal compartment. This can be induced experimentally by transfection, where vertebrate DNA will then stimulate TLR9 [197]. Although synthetic CpG motifs are used experimentally and as adjuvants to stimulate TLR9, it has also been shown that the main role of these motifs is in increasing DNA uptake into endosomes and hence exposure to TLR9, rather than as a direct trigger [198].

Serum mitochondrial (mt)DNA, released from cells in trauma patients causes huge TLR9 elevations which then upregulate cytokines such as IL-6 triggering an inflammatory state [199].

Many factors can affect the downstream response to TLR9 binding e.g. early vs late endosomes, CpG features, and cell type. Different synthetic CpGs known as oligodeoxynucleotides (ODN) have been shown to stimulate different effects. Two classes with different molecular structures are defined based on their capacity to stimulate either DCs or B cells [181]. These comprise the preferentially DC acting type A (CpG-A ODN) and CpG-B ODN, type A remain in the early endosome longer, leading to stimulation of type I IFN whereas type B are quickly trafficked to endosomes and lysosomes and result in pro-inflammatory cytokine production [178]. pDCs are specialised to be preferentially driven to type I IFN, regardless of the stimulus [181].

DCs, regardless of subtype, are specialist antigen-presenting cells whose role it is to alert antigen specific cells of the adaptive immune system to the presence of said antigen [200,201]. They do this

by surface presentation of antigen by the MHCII molecule whilst simultaneously expressing co-stimulatory molecules such as CD80, CD86, and CD40. These co-stimulatory molecules, and MHCII, are upregulated following TLR ligand recognition allowing presentation of antigen to T cells; thus linking the adaptive and innate immune responses [164]. Furthermore, different DC subsets can react to triggering of the same TLR by the same ligand in different ways [164].

The role of TLRs in disease is complex; they have been variably implicated in both defence and induction of disease, and as such targeted therapeutics may aim to either stimulate or antagonise them [202].

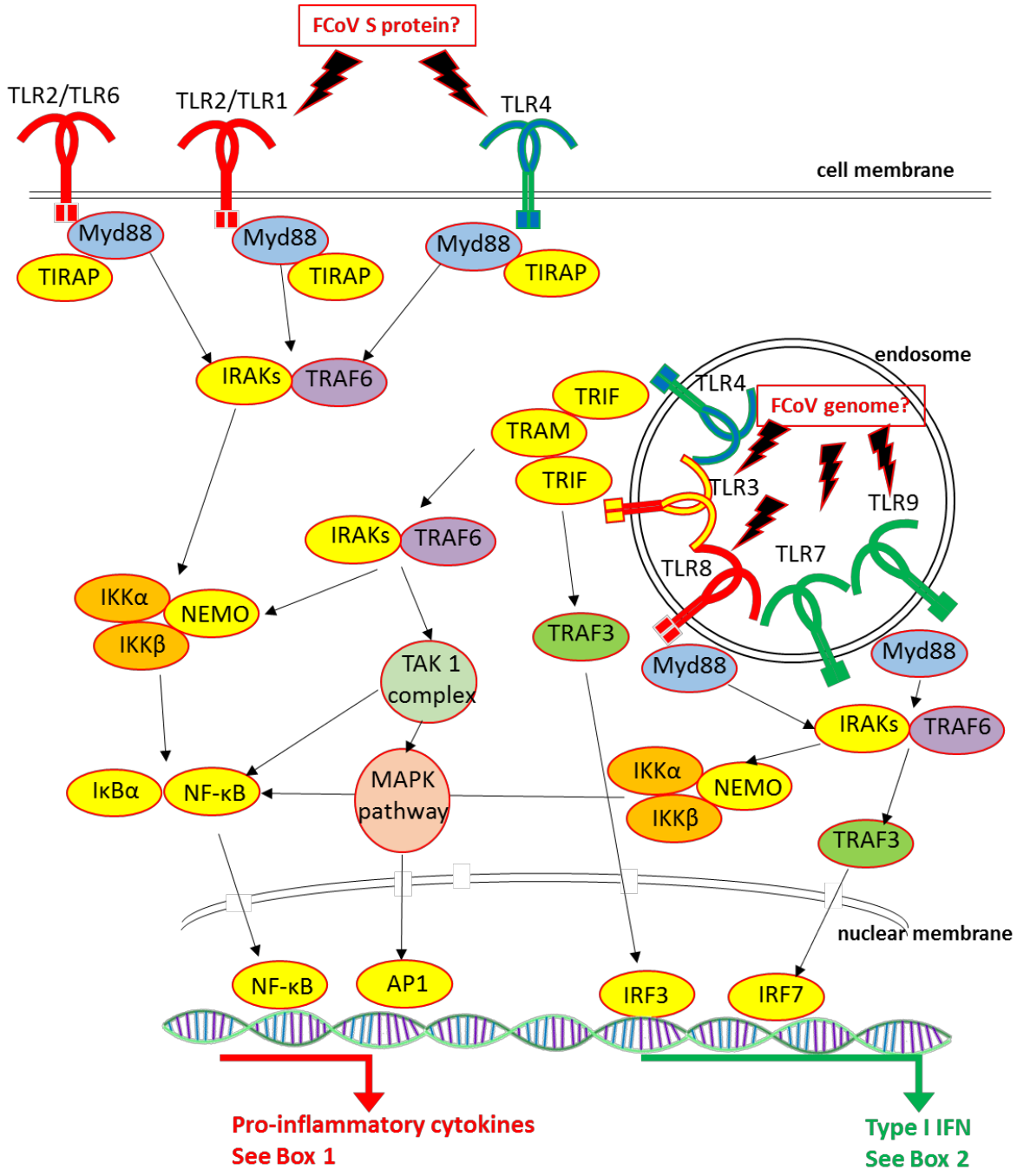

Figure 2.4: *Schematic summary of the main TLR signalling pathways, including receptor location, adaptor proteins utilised, and transcription factors induced. Compiled from* [172,178,179,203].

Cytokines [IL-1β, IL-6, IL-10, IL-15, IL-17, TNF-α, TGF-β]

Cytokines were first discovered in the 1970s and first named according to their producing cell e.g. lymphokine, but this soon proved impossible and the name cytokine took over [204]. With the exception of erythrocytes, all mammalian cells can produce and respond to cytokines though cells of the immune system are of course specialised in this role [204]. Evolutionarily they can be traced almost as far back as TLRs, with cytokine-like activity observed in *Drosophilia* [205]. Cytokines are divided by biological properties and family although huge overlap exists, indeed redundancy and pleiotropism are one of the defining features of these molecules. They are non-structural signalling proteins, usually signalling as soluble extracellular factors although some remain tethered to cell membranes [204]. It is difficult to classify cytokines into those with beneficial or detrimental effects, as even for a given disease their effects are often influenced by their concentration/dose and by the general cytokine milieu. In general they are highly potent, in comparison to e.g. hormones [204].

Cytokines are closely linked to TLRs not only via signalling pathways but also because their receptors share a conserved intracellular signalling domain, Toll-IL-1-Receptor (TIR; see above) [206]. Triggering of TLR pathways can induce a cytokine storm which should spontaneously subside when the infection is controlled and cytokine genes are again repressed by histone acetylation [204].

Amongst their myriad roles, cytokines are key determinants of lymphocyte differentiation, which itself is critical to host immune response and disease outcome [207].

From naïve precursor cells, T cells have many differentiation options open, determined by interactions with antigen-presenting cells, the cytokine milieu and multiple other variables. T helper cells are antigen specific effectors, which may be of different subsets depending on the direction of differentiation [208]. The naïve T helper cell is first activated by interaction of its TCR (T cell receptor) with antigen presented by an MHCII molecule. Subsequent division of this T cell leads to progeny all recognising the same antigen. All are CD4+ and may be of Th1, Th2 or Th17 phenotype [208]. Th1 cells are thought to be crucial to defence against FCoV as this is the subset specialising in defence against intracellular pathogens, and in particular viruses. Induced by IFN-γ and IL-12 they secrete mainly IFN-γ [209]. Th2 cells upregulate antibody secretion by production of cytokines including IL-10 [208]. The Th17 subset was discovered later, and secretes amongst other cytokines IL-6, IL-17 and TNF-α. Th17 cells have an important role in inflammation and neutrophil activation. Once T cells are driven in one direction, specific cytokine genes are activated. Genes of opposing subtypes are then suppressed, leading to stabilisation and potentiation of the phenotype [210]. The majority of TLR induced cytokines favour a Th1 phenotype [164].

Many studies on FIP have examined cytokines in various tissues and at various stages of disease in an attempt to establish a cytokine expression profile, yet results are inconsistent. Results of these studies are summarised below whilst cytokine effects in FIP which are predicted from the results of other studies are described with the individual mediators. Overproduction of pro-inflammatory cytokines in FIP is thought to be a key feature of disease progression but the precise source is unknown.

The Th1/Th2 balance is of frequent interest, testing the supposition that a Th2 biased antibody response is detrimental [22]. Following experimental infection of kittens with FIPV, an initial small increase in PBMC mRNA levels of IL-6 (a typical Th2 cytokine) and IFN-γ (a typical Th1 cytokine)

was observed following infection. As disease developed, IL-6 remained the same and IL-10 and IFN-γ became depressed [134], suggesting a lack of cell-mediated immunity.
Another study evaluated blood samples from immunised and challenge exposed cats, finding elevated TNF-α mRNA levels in all cats succumbing to disease together with unchanged or reduced IFN-γ. Only one of two surviving cats exhibited a strong IFN-γ elevation but neither upregulated TNF-α. IL-6 was unaltered, again suggesting a lack of cell-mediated immunity [24].
Dean et al. evaluated different lymphoid tissues following experimental infection for both cytokine mRNA expression and presence of FCoV as determined by PCR [47]. They found a majority of central lymphoid tissues (mediastinal and mesenteric lymph nodes, spleen) to be qPCR positive for FCoV, but only a minority of peripheral lymphoid tissues, such as popliteal lymph node. The latter were more likely to have lymphoid hyperplasia whilst lesions in central lymphoid tissues co-localised with virus, showing lymphoid depletion and pyogranulomatous inflammation. Correspondingly, leukopaenia was mainly represented by a decrease in lymphocytes. IL-10 was much higher in FCoV positive than negative central lymphoid tissue and an increased IL-10:IL-12 ratio suggested a Th2 bias. A later study on cytokine mRNA levels in haemolymphatic tissues compared bone marrow, spleen and mesenteric lymph nodes (MLN) of FCoV infected cats with and without FIP. The bone marrow showed no changes whilst IL-1β, IL-10 and TNF-α levels were higher in FCoV infected cats without FIP in the spleen. In the MLN, IL-1β and IL-6 were higher in FIP but TNF-α was lower [48].
Some of these effects are summarised in Fig. 2.5.

Interleukins [IL-1β, IL-6, IL-10, IL-15, IL-17]

Interleukins, as the name suggests, are a group of cytokines predominantly allowing communication between leukocytes including over 40 cytokines [207].
IL-1 was originally used to define a monocyte product and is now the name of a family, which includes IL-1α, IL-1β, and others. The IL-1 family, with currently 11 members, is the family most associated with innate immunity but also has a role in acquired immunity [206,211]. IL-1β is secreted as a precursor protein which must be cleaved by IL-1 converting enzyme (ICE, aka caspase-1), present within the inflammasome; an intracellular complex of molecules including NLRP3 (nucleotide-binding domain, leucine-rich-containing family, pyrin domain-containing-3) [206,212]. Caspase 1 inhibitors lead to accumulation of precursor protein which is not then cleaved to the secreted form. IL-1 may also be cleaved by other mechanisms, e.g. following the death of neutrophils in an area of inflammation, the released pro-IL-1 may be cleaved extracellularly by common neutrophil proteins such as proteinase-3. The IL-1 family also has inhibitory members including IL-1R2 and IL-1Ra. IL-1 signalling activates both MAPKs and NF-κB leading to further pro-inflammatory cytokine expression. Mice deficient in IL-1 exhibit no spontaneous disease but have abnormal reactions to inflammatory stimuli [206]. IL-1β is pyrogenic, induced through TLR signalling, and able to exert positive feedback on itself and remain high in the absence of microbial stimulants [206,213].
IL-6, now a prototypic member of its own family, was first discovered in 1973 as a soluble factor involved in antibody production [214]. It has had multiple previous names reflecting the functions that were attributed to it, including hepatocyte-stimulating factor and B cell differentiation factor, before it was discovered that all were one molecule. It is important in the maturation of B cells to

plasma cells, with plasma cells being a feature of chronic FIP lesions [44,215]. Antibody production is also stimulated; the observed hypergammaglobulinaemia and ADE in FIP [22,61,216] may therefore be connected. Chronic stimulation of plasma cells by IL-6 has been shown to lead to the production of auto-antibodies [216]. Synthesised early in infection, IL-6 induces acute phase protein production and reduces the production of albumin in the liver [217]; the latter may help contribute to the lowered A:G ratio in FIP. Following IL-6 receptor binding, JAK-STAT signalling is activated, leading to phosphorylation of STAT3. Soluble decoy receptors exist to counter its effect. In conjunction with TGF-β IL-6 pushes Th-17 differentiation in T cells [209]. It also helps with the link between innate and adaptive immunity and inhibits the TGF-β induced Treg differentiation. An upregulated Th17/Treg balance has been shown to contribute to chronic inflammation [216]. CD8+ differentiation to cytotoxic T cells, VEGF production, and vascular permeability are additionally stimulated [218,219]. Many cells produce IL-6, including leukocytes, endothelial cells, and mesenchymal cells [220]. Expression must be tightly regulated as IL-6 production warns the body of an emergency [216]. IL-6 mRNA expression and degradation are regulated both transcriptionally and post-transcriptionally so that levels of several proteins and microRNAs determine its fate. One of these methods is by microRNA inhibition of STAT3, the main IL-6 activated transcription factor [216]. IL-1β, TNF-α and TLR signalling can all upregulate IL-6 [216]. The products of some viruses, including HIV and hepatitis B virus, enhance the binding potential of transcription factors upstream of IL-6, including NF-κB and NF-IL-6 (nuclear factor IL-6 aka IRF1) [216]. Conversely, activation of the glucocorticoid receptor can repress transcription of IL-6, this is thought to be one of the anti-inflammatory mechanisms of glucocorticoid drugs; they are often used in FIP though with limited success [216,221]. IL-6 signals via a hexamer consisting of two of each molecule of IL-6, IL-6R and gp130; viral encoded IL-6 in KSHV infection can replicate native IL-6 and induce signalling [222]. Discovery of the molecular make up of IL-6 receptor helped solve the mystery of cytokine redundancy and pleiotropy [223]. gp130 is the signal transducing domain of the IL-6 receptor and has a broad range of expression [224]. The IL-6R may be membrane bound or soluble and when soluble it can then bind gp130 on any cell, known as trans-signalling. However, only select cell types express IL-6R meaning only these cells can respond directly [225]. Soluble gp130 also exists which can buffer IL-6 until its levels are overcome [226].

Following binding, IL-6 signals mainly via STAT3, but may also, less preferentially, use STAT1 and MAPK [216,226]. A negative feedback loop suppresses signalling and is designed to prevent an excessive inflammatory effect [227].

In the presence of IL-6, neutrophils are released more rapidly from the bone marrow, and exhibit enhanced chemotaxis in response to IL-8, but there is no apparent effect on survival [226]. This likely explains the early discovery that culture supernatant from cells within FIP ascites is chemotactic for neutrophils, as high IL-6 levels have been found in the ascites of cats with FIP, and cells within the abdominal exudate were shown capable of its production [228,229]. Serum levels of IL-6 in these cats did not differ greatly from the control cats, further supporting local production and effect [229].

IL-10 is also the head of a family of the same name, all typically anti-inflammatory. It was first named cytokine synthesis inhibitory factor before being designated a member of the interleukin family [230]. IL-10 inhibits production of IL-1β, IL-6, TNF-α, G-CSF and GM-CSF at the transcription level in stimulated human monocytes [230]. It also reduces MHCII expression from monocytes following LPS activation and is auto-regulatory [230]. IL-10 deficient mice develop spontaneous

inflammatory diseases which are often fatal [204]. Some viruses (including beta and gammaherpesviruses, though not coronaviruses) even encode their own IL-10 to act as an immunosuppressant including inhibiting IFN-γ [231].

IL-15 is a T cell regulator and is a part of the four alpha helix bundle cytokine family. It signals through a heterodimeric receptor combination [232]. Rarely for a cytokine its main method of signalling is through cell contact and it is produced by a wider cell range than most cytokines [233]. One of its main roles is in regulating cytotoxic lymphocyte function, giving it the potential either to help remove infected cells or to trigger widespread cell destruction if over or aberrantly produced [232]. This may be of relevance in the observed lymphocyte apoptosis in FIP [63].

The IL-17 family includes IL-17A (referred to simply as IL-17), and IL17B-F. Their major source is specialised T cells, the Th17 subset, active in innate immunity [234]. This subset has its own novel differentiation factors, including STAT3, which are distinct from Th1 and Th2 [235]. IL-17 is predominantly pro-inflammatory with downstream induction of other inflammatory cytokines [234]. It is often implicated in auto-immune disease or chronic inflammation, in particular as a triad with IL-6 and STAT3, two molecules with a main regulatory role in Th17 function, along with TGF-β [236,237]. Th17 differentiation requires cooperation between two cytokines (IL-6 and TGF-β) of opposing function [209]. IL-17 also has a defensive role, predominantly against bacteria at mucosal barriers; Th17 cells are able to mount a swift first line response to antigens by producing immunoregulatory mediators [234].

Tumour necrosis factor alpha (TNF-α)

The TNF superfamily consists of type II transmembrane proteins which are primarily produced by macrophages. They are secreted as transmembrane precursors of 26kDa which are cleaved to a 17kDa soluble form by TACE (TNF-α converting enzyme) before trimerising. The soluble form is the most potent. However the remaining membrane portion is further cleaved before translocating to the nucleus and itself inducing pro-inflammatory signalling [211]. TNF-α can signal through two receptors, sharing less than a third homology and with distinct biological effects. TNFR1 is the more important of the two receptors and has a death domain, allowing it to induce inflammation or apoptosis. Receptor binding is first possible at the cell membrane, forming complex I which leads to pro-inflammatory gene expression. If this fails, there is the opportunity for complex II to form intracellularly which instead has apoptosis as its downstream effect, i.e. defence as the first step followed by cell suicide should the defence fail [238].

TNF-α has myriad roles in inflammation, including triggering lipid mediator expression on vascular endothelium which promotes oedema, as well as adhesion molecule expression [211]. Adhesion molecules have been shown to be upregulated on peripheral leukocytes in FIP, as has CD18 on both intravascular monocytes and perivascular macrophages [42,239].

In vitro, TNF-α production by FIPV infected macrophages upregulates expression of the APN receptor, which is used by FCoV serotype II. Alveolar macrophages from cats with FIP have higher levels of both APN and TNF-α. Both virus titre and TNF-α are higher in macrophages cultured with virus and anti-S protein antibody than controls or those cultured with only one of these, demonstrating *in vitro* ADE. The supernatant of these dual cultured cells also induced higher levels of apoptosis in PBMCs [99,240].

It has been postulated that in FIP, TNF-α from lymphocytes induces apoptosis [47]. Ascitic fluid from cats with FIP had previously been shown to induce lymphocyte apoptosis *in vitro*, as had TNF-α [63].

Chemokines [CCL8 and CXCL10]

Both CCL8 and CXCL10 have been found to be upregulated *in vitro* in FIPV infection of CRFK cells [241,242].

The chemokines are divided into two main groups, the CC and CXC classes based on their structure [211]. Two further but less common subgroups exist, the C and the CXC3 subfamilies. All are small 8-12 kDa proteins which induce cell migration from the blood into target tissues [211]. They and their antagonists are seen as promising therapeutic options [243]. Initially, these molecules were classified as inflammatory or homeostatic, but several have since been shown to be dual function proteins [244].

Chemokines elicit their effect by binding seven-transmembrane G protein-coupled receptors, with uncoupled decoy receptors also existing which act as inhibitors and provide an extra layer of modulation potential [244].

As with the cytokines, there is extensive pleiotropy making extrapolation of individual functions difficult [243]. CCL8 (monocyte chemotactic protein (MCP)-2) is classified as an inflammatory cytokine involved in innate and adaptive immunity, able to bind CCR1, 2, 3, 5, and 11 [211,243,244]. CXCL10 (IFN-γ-inducible protein (IP)-10) on the other hand is a dual function chemokine involved in adaptive immunity which attracts CXCR3+ cells. These cells tend to be CD4+ T cells with subsequent Th1 differentiation and are a promising target for therapeutic intervention [211,244]. In addition to attracting CXCR3+ cells, CXCL10 blocks CCR3- cells (preferentially expressed by Th2), further contributing to a Th1 polarisation [244]. These effects should be beneficial in FIP.

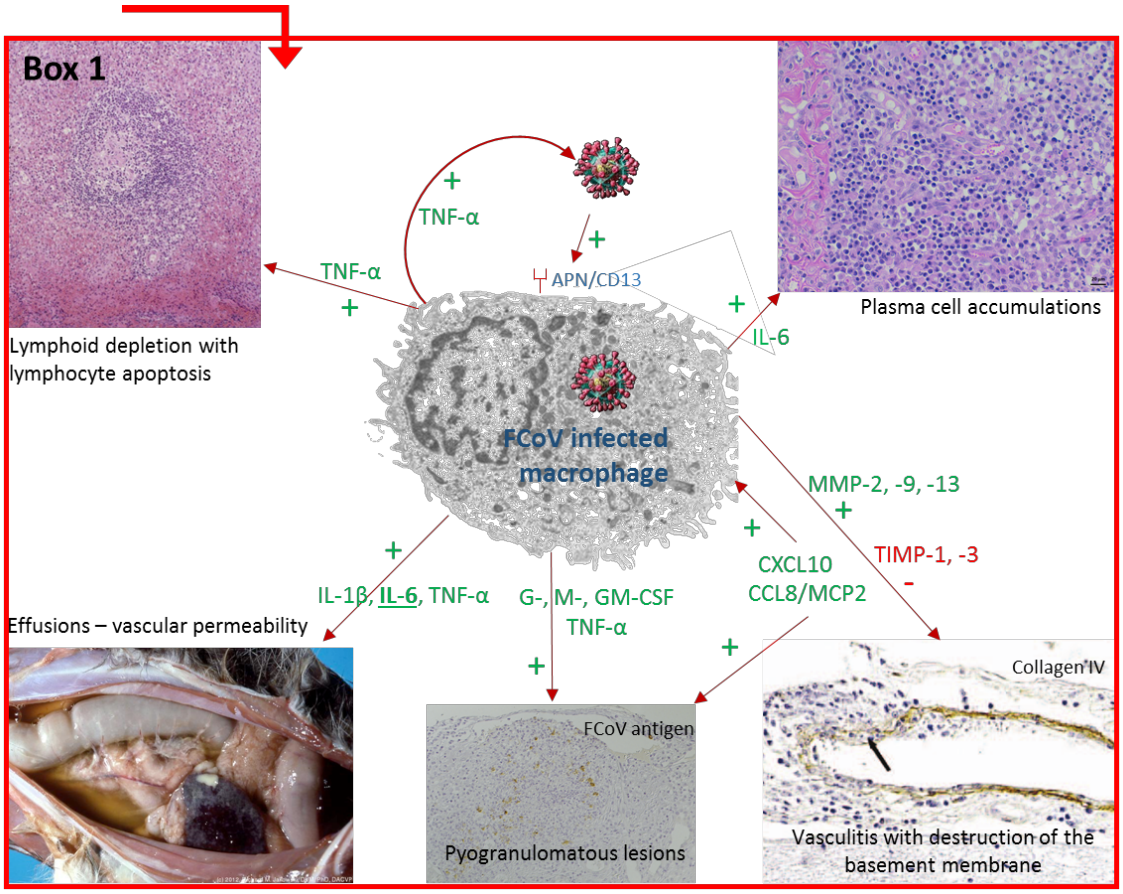

Figure 2.5: *Hypothesised contribution of inflammatory mediators to the pathogenesis of FIP, following on from Fig. 2.4.*

Transforming growth factor (TGF)-β

TGF-β was found in one study to be present at very low levels in the ascites of cats with FIP [63], but appears otherwise to not have been of much interest in FIP studies.

TGF-β is produced as an inactive compound requiring activation; this step is an important layer of regulation [245]. It classically signals via Smad pathways but may also use MAPK, PI3K and others [246]. Simultaneously it stimulates self-regulatory pathways [245]. TGF-β plays a crucial role in regulating T cell activation; TGF-$\beta^{-/-}$ mice die early from multi-organ inflammatory disease with widespread T cell activation and wasting [247].

TGF-β has context dependant effects on T cells [245]. It promotes apoptosis of CD8+ T cells to limit clonal expansion after activation by reducing anti-apoptotic Bcl2 and upregulating pro-apoptotic Bim [248,249]. However, it may also promote survival by blocking FasL-mediated apoptosis [250]. Lymphocyte apoptosis, particularly of T cells, is a recognised feature of FIP [44,63,251]. Overall TGF-β has mainly anti-inflammatory functions, enhancing Treg differentiation together with IL-2, and blocking both Th1 and Th2. Together with IL-1β and IL-6 it is able to stimulate Th17, it is rare that Th17 cells can develop in the absence of TGF-β [245]. The concentration of TGF- β may determine whether a T cell becomes an induced Treg or a Th17 cell. Another indirect mechanism of Th1 inhibition is by inhibition of IFN-γ production; interfering with the positive feedback loop between IFN-γ and Th1 [245]. Though Th1 responses appear to be the initial targets, Th2 responses can also

be potently downregulated by TGF-β [249]. Induced overexpression of TGF-β in mice can protect them from the effects of allergic airway disease [252].

Type I interferons [IFN-α and IFN-β]

The type I interferons (IFN) include IFN-α and IFN-β, cytokines specialised in anti-viral defence [253,254]. These cytokines are intricately linked to the adaptive immune system; phylogenetic studies indicate that interferons developed in jawed vertebrates in parallel with it. The adaptive immune system, in contrast to the innate, requires B and T cells; no species has been found which has these cells without having IFN-α and -β and vice versa [254].

Two pathways can induce type I IFN; one pathway includes ubiquitous cytosolic receptors for PAMPs such as RIG-1 and MDA5, requiring the cell to be infected (cell-intrinsic). The second pathway involves the TLRs and can be used by uninfected cells (cell-extrinsic innate immune recognition) [170]. This is possible as antigen can be presented either at the cell membrane or in endosomes following processing. Those TLRs which induce type I IFN tend to be those which detect nucleic acids, with the exception being TLR4 which detects LPS but can lead to IFN production. TLR 7 and 9 are especially responsible for the high type I IFN levels observed in many experimental viral infections, they are (seemingly uniquely amongst the TLRs) expressed by both conventional and plasmacytoid dendritic cells rather than just conventional dendritic cells. The intracellular TLR 3, 7 and 9 require an acidified endosomal compartment; if TLR9 is relocated to the cell membrane it can no longer recognise its ligand [255].

Almost all cells can produce type I IFNs and one of the main roles of these proteins is to restrict viral replication. Downstream effects are focussed on inducing an antiviral state, with the aim being to make the cell an inhospitable host for the virus, these effects include induction of apoptosis and the shutting down of protein translation. Signalling through STAT1 and STAT2 represents the canonical pathway of type I IFNs. Type I IFN signalling also leads to differentiation and activation of natural killer (NK) cells, which are able to kill virally infected cells using MHC downregulation in an attempt to evade the immune system [254]. The IFN-stimulated gene factor 3 (ISGF3) complex is formed by interferon regulatory factor (IRF)9 and phosphorylated STAT1 and 2 coming together following type I IFN binding of its receptor [256]. This complex then binds IFN stimulated response elements (ISRE) in gene promoters, leading to hundreds of IFN-stimulated genes (ISGs) being transcribed [256]. This is summarised in Fig. 2.6. These genes function to control viral infection but also infection by other pathogens. To enhance the anti-viral response they include the PRRs, STAT1 and 2, and IRFs, providing a positive feedback mechanism [256]. Induced proteins have a more direct antiviral effect, e.g. viperin, which is upregulated in FCoV infected CRFK cells *in vitro,* and serves to inhibit viral egress [241,256].

Type II interferons [IFN-γ]

IFN-γ mRNA levels within lesions of FIP have been examined previously by RT-PCR and found to be increased [257]. This was supported by the finding of higher IFN-γ protein levels in effusions than serum of cats with FIP [258]. The same study found that serum levels of IFN-γ were higher in healthy FIP in-contact cats than either unexposed or FIP cats, suggesting a protective effect. A separate

study found that mRNA levels of IL-1β and IFN-γ both peaked in the whole blood of healthy cats following exposure to another cat with FIP, with the same implication [259].

IFN-γ is the only type II IFN. It has no structural homology with type I IFNs but was originally classified together with these owing to their ability to 'interfere' in viral replication, there is significant overlap between the downstream effectors of type I and II IFN [260]. IFN-γ is predominantly produced by T cells and NK cells [261]. Although IFN-γ production is restricted to certain cell types, almost all cells express the receptor and are hence able to respond [262]. Canonical signalling involves IFN-γ dimerisation and subsequent binding to the IFNGR. Receptor chains bind JAK 1 and 2 which in turn phosphorylate STAT1, which translocates to the nucleus and binds gamma interferon activation site elements (GAS) [263]. In the absence of STAT1, STAT3 may be activated, along with other non-canonical pathways which involve various responses to IFN-γ [263]. IFN-γ does not induce the ISGF3 complex as type I IFN do, so it cannot induce genes with only an ISRE and not a GAS in their promoters [260].

Chronic exposure to a low level of IFN-γ can prime cells and lead to overreaction to stimuli, the type I and II IFNs become able to utilise each others signalling pathways and hence amplify their effects [263].

Mouse hepatitis virus (MHV) is another CoV existing as two biotypes; enterotropic and polytropic [264]. IFN-$\gamma^{-/-}$ mice also develop FIP like lesions in response to the enterotropic form which exogenous IFN-γ can partially dampen [265,266]. Interestingly, even in the highly controllable environment of experimental mice, with controlled genotype and virus dose, the disease was not reliably reproducible [266]. IFN-$\gamma^{-/-}$ mice are also able to sustain the replication of MHV, unlike wildtype mice [267].

Colony stimulating factors [G-, M-, GM-CSF]

The colony stimulating factors (CSFs) are members of the cytokine superfamily, first named CSF-1, -2, -3 for their ability to act as growth factors for haematopoietic cells *in vitro*. They have since been renamed monocyte (M)-CSF, granulocyte monocyte (GM)-CSF and G-CSF respectively. The CSFs have overlapping but non-redundant roles. M-CSF is important in homeostasis, being detectable in plasma and constitutively expressed by many cell types including macrophages, endothelial cells, and fibroblasts [268]. GM-CSF is more involved in inflammation and as such is mainly produced by activated leukocytes [269]. A slightly oversimplified version of their effect on mature cells is that they induce an anti- vs pro-inflammatory state (M vs GM-CSF) in macrophages. Both M- and GM-CSF, derived from a fibroblast lineage, are commonly used to direct bone marrow derived cell differentiation in culture [270,271].

Matrix metalloproteinases (MMPs) and tissue inhibitors of matrix metalloproteinases (TIMPs) [MMP-2, -9, -13, TIMP-1, -3]

MMP9 was found in intravascular monocytes and occasional perivascular infiltrating macrophages of FIP lesions and is believed to contribute to basement membrane destruction as a byproduct of monocyte emigration [42].

MMPs are a family of zinc dependant endoproteinases which function in tissue remodelling as well as processes such as cell proliferation and migration, through their ability to degrade extracellular matrix components [272]. Over 25 MMPs have so far been characterised in vertebrates [273]. These are grouped and subgrouped. There are four groups, including archetypal MMPs and gelatinases. Within the archetypal enzymes are the collagenases, and the stromelysins. The former comprise three MMPs including collagenase-3 or MMP-13 which was chosen for the present study. In addition to collagen, these enzymes are able to process a number of molecules to their active form, including TNF-α [274]. The gelatinases are MMP-2 and MMP-9, otherwise known as gelatinase-A and -B. They have a broad spectrum of substrates, overlapping with the collagenases, which includes components of the basal membrane, collagen IV and laminin [275]. MMP-2 and -9 can also cleave cytokines including TNF-α, TGF-β and IL-1β, and monocyte chemoattractant protein (MCP)-3 to their active forms [274,276]. Gene expression is regulated primarily, though not exclusively, at the transcriptional level, making RT-PCR a meaningful method of measurement [277]. Physiological transcription is usually at a low level and there is often co-expression in response to stimuli as a result of shared promoter elements [278]. Some MMP genes e.g. *MMP-2* have reduced regulatory elements in their proximal promoters and are therefore less responsive to stimuli and more important constitutively [279]. In inflammation, cytokines such as IL-1β and TNF-α activate signalling pathways with intermediates including NF-κB, MAPK, and STATs which can induce MMP transcription [280]. STATs may also inhibit transcription by sequestering required proteins (e.g. c-jun) as may occur with MMP-9 and MMP-13. MMP-13 may be induced by TGF-β via Smad proteins and MAPK pathways [281,282]. In addition to regulation at the transcriptional level, and by various post-transcriptional methods, levels are also controlled by endogenous inhibitors [273,283]. The major inhibitor types are α_2-macroglobulin and TIMPs; the former are acute phase proteins but do not have a major role in cats [284]. Three TIMPs are described, of which TIMP-3 appears to be the least redundant *in vivo*. In addition to targeting MMPs, they may also inactivate other enzymes. One of these is thought to be ADAM17 (TACE), as TIMP-3$^{-/-}$ mice exhibit inflammatory changes owing to elevated TNF-α levels [283].

Signal transducers and activators of transcription (STATs)

The JAK-STAT signalling pathways are an essential, extensively studied, and highly conserved, aspect of cytokine receptor signalling [285]. These have not yet been studied in FIP. JAK-STAT pathways are responsible for controlling gene expression downstream of cytokine receptor binding, and as in most signalling systems there are elements of both redundancy and pleiotropy [286]. The JAK family has four, and the STAT family seven members which may combine to induce different downstream effects. However, the same combinations can also induce different effects. As such, a response may be cell specific or molecule specific. IL-6 for example classically signals via STAT3, as does IL-10, though the two induce conflicting downstream transcription [287]. IL-10 may also use STAT1 [288].

Knock out mice for each STAT have been studied, with some (e.g. *Stat3*$^{-/-}$), being embryonically lethal [287]. The simplified version of the pathway is that the binding of a cytokine to its receptor causes association with JAK, phosphorylation of the receptor, and STAT recruitment. The recruited STAT is in turn phosphorylated causing it to dimerise and translocate to the nucleus to function as

a transcription factor [287]. The MAP kinase pathways are the other main pathways involved in cytokine signalling.

The pathogenesis of SARS-CoV has been linked to STAT1, STAT1 being of more importance than either type I, II, or III IFNs in determining disease outcome. Experimentally infected *STAT1*$^{-/-}$ mice developed severe disease in contrast to a wild type phenotype exhibited by any of the interferon knock out mice [289].

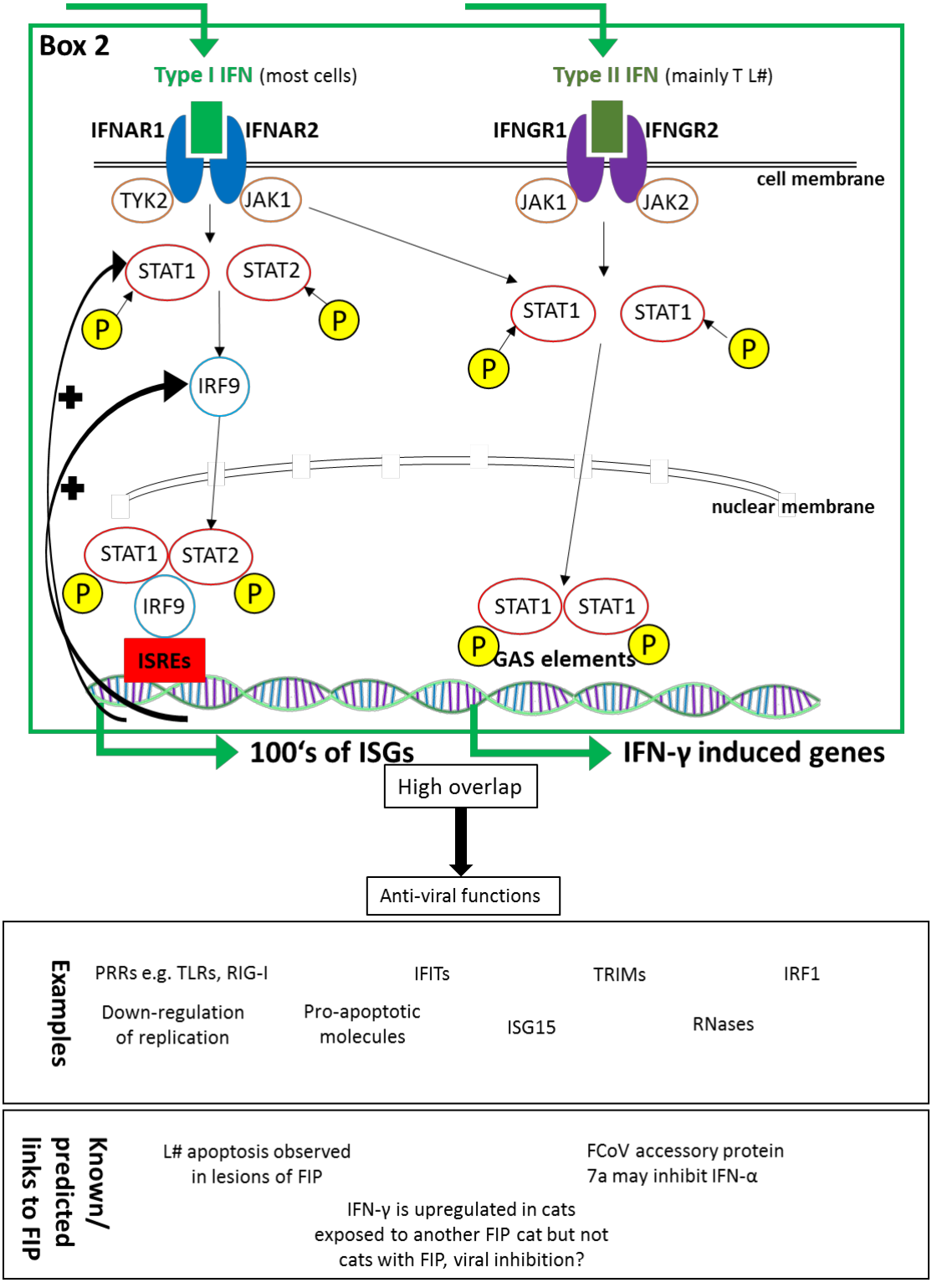

Figure 2.6: *IFN signalling through JAK-STAT pathways and its downstream effects. Compiled from* [63,129,256,259,260,290].

The molecules discussed here comprise only a fraction of those involved in regulating the immune response to viral infection, but have been chosen to represent different levels of signalling pathways from receptors to responders. The ability to respond to stimuli is not restricted to leukocytes but these cells are of course those tasked with the greatest responsibility in regulating immunity. As such, haemolymphatic tissues with their role in producing and moulding leukocytes are among the first tissues of interest in studying FIP.

The MLN are at the gateway between the intestine, with its direct exposure to the outside world, and the rest of the body. In terms of exposure to orally derived bacteria they act as a firewall and are of great importance in inducing immune tolerance [291]. The MLN are known as the site of 'first pass' as antigens or pathogens entering the intestinal lymphatics are first directed here, where the MLN 'decides' whether to pass on the possible threat to the systemic immune system [292]. In FCoV infection, induction of tolerance to the virus could be seen as a highly beneficial process. Cats may be long term or transient systemic carriers without disease and in these carriers, beyond the colon the MLN are one of the most frequently virus positive tissues [293]. For this reason, the immune status of this organ and its potential positive or negative effects warrants more in depth study.

Aims and Hypotheses

Aims

- Design and or optimise a panel of primer and probe sets for assessing inflammatory mediator levels in the cat
- Assess the role of the mesenteric lymph node in the development of FIP
- Determine which TLR's are likely to be involved in the pathogenesis of FIP
- Screen samples for the presence of coronavirus and viral S gene mutations and assess relationship between viral load, disease state, S gene mutations and the inflammatory response
- Determine which cell pathways are upregulated in FIP and whether this is more specific to the presence of disease or virus
- Determine cell type expression of significant TLRs and assess co-localisation to FCoV-infected cells

Hypotheses

- FCoV infection without disease induces a specific immune mediator expression profile, distinct from that in uninfected cats or those with FIP
- There is a skew towards a pro-inflammatory rather than an interferon dominated response in cats with FIP
- The anti-viral, RNA detecting TLRs 3, 7, 8, and 9 are failing to adequately respond to infection whilst the more pro-inflammatory TLR2 and 4 are upregulated in FIP
- The mediator response is enhanced within the lesions themselves
- The response to virus is more pronounced locally than systemically

Materials and Methods

Case Material

A number of different approaches were taken to address the aims of the project, as shown in Table 4.0.1. Cases were prospectively obtained in collaboration with the University of Zurich Small Animal Clinic and local veterinary practices. Retrospective cases were available from the University of Bristol's existing biobank of cases which had been seen in the university clinic and surrounding practices (Table 4.0.1). All animals were client owned cats euthanased on purely clinical grounds. Cats were those with a clinical suspicion of FIP, or with unrelated diseases (used as control animals). All cats underwent routine diagnostic necropsies with the owners' full permission, with additional histological and immunohistological examination to confirm FIP or an alternative diagnosis. Case numbers with corresponding sample numbers and pathological findings are found in each chapter where relevant, the signalment of all cases is provided in Tables 4.0.2-4.0.4.

Sampling

Necropsies were performed within 1 h of death with routine sampling of a standard organ set (brain, heart, lungs, liver, stomach, duodenum, pancreas, jejunum, ileum, caecum, colon, mesenteric lymph node, spleen, bone marrow, kidney, bladder, [reproductive organs], thyroid gland, adrenal gland, pituitary gland; where permitted by the owner), as well as macroscopical lesions, into 10% neutral buffered formalin. Additionally, cubes of tissue up to 5 mm in diameter were taken at the time of necropsy into RNAlater (Qiagen, Hombrechtikon, Switzerland) for subsequent RNA extraction and downstream analysis. These were from bone marrow (BM), spleen, mesenteric lymph nodes (MLN), and additional organs e.g. liver, omentum, and kidney as part of the biobank development. In some cases, on owners' request, only selected organs were available to sample. After 24-48 h at 4°C in order to allow permeation of the tissues, samples in RNAlater were transferred to -80°C for longer term storage. Bristol samples had had the RNAlater removed before storage. Within the Zurich cohort, when classical serosal, or pyogranulomatous parenchymatous lesions were grossly visible, these were sampled and cryoblocks prepared (see chapter 4).

After at least 24 h and a maximum of 72 h in formalin tissues were trimmed and routinely paraffin wax embedded. Sections (3-5 µm) were prepared and stained with haematoxylin and eosin (HE). In addition to the histological examination, lesions from FIP cases underwent immunohistology to demonstrate FCoV antigen within infected monocytes and macrophages. This was carried out by the Institute of Veterinary Pathology Zurich (IVPZ) histology laboratory as previously described [44], using a mouse monoclonal primary antibody (clone FIPV3-70 SC 65653, Santa Cruz, Heidelberg, Germany). It is a routine accredited diagnostic method (ISO/IEC 17025), further details are given in Chapter 4.

For the purpose of this study, in addition to a routine diagnostic number for each case, a number per sample (i.e. organ or selected region) for RT-qPCR was also allocated. Control cats were allocated Group 1, and cats with FIP Group 2.

Table 4.0.1: Cases used for each section of the study, with origin, original case number and group.

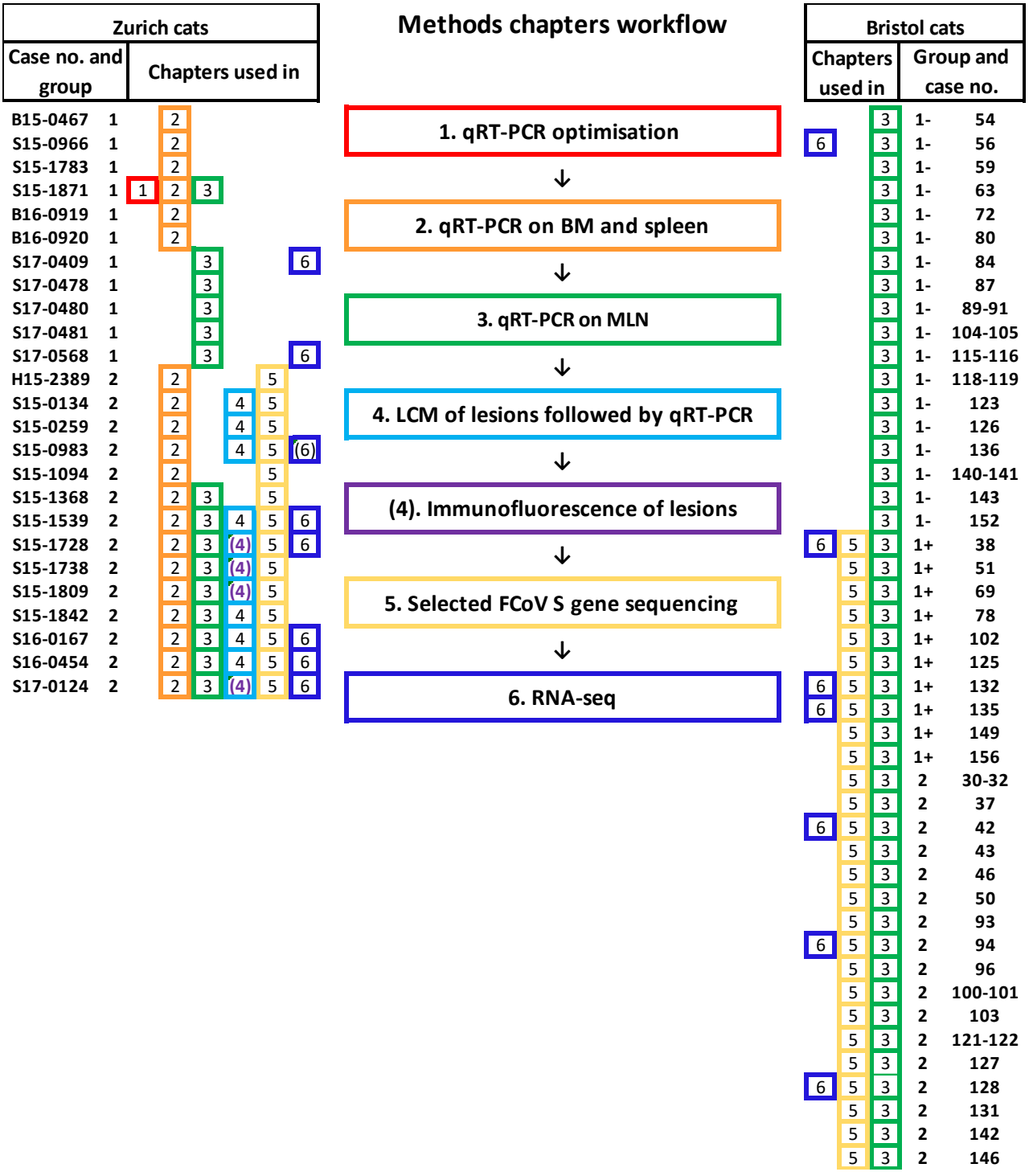

Table 4.0.2: Signalment of Zurich cases and sample numbers corresponding to organ and chapter. BM: bone marrow; MLN: mesenteric lymph node; LCM: laser capture microdissection; NGS: Next Generation Sequencing (RNA-Seq); DSH: domestic short hair; BSH: British short hair; y: years; m: months; M(N): male (neutered); F(N): female neutered; CRD: chronic renal disease; CHF: congestive heart failure; DCM: dilated cardiomyopathy.

Case no.	Sample numbers				Group	Breed	Age	Sex	Diagnosis in control cases
	BM	spleen	MLN	LCM/NGS					
B15-0467	1	2			1	DSH	Adult	MN	Intestinal lymphoma
S15-0966	3	4			1		Adult	MN	CRD and hyperthyroidism
S15-1783	5	6			1	DSH	9 y	FN	Pulmonary thromboembolism
S15-1871	7	8	50		1	Ragdoll	4.5 y	MN	CHF and CRD
B16-0919	9	10			1	DSH	Juvenile		Behavioural
B16-0920	11	12			1	DSH	Juvenile		Behavioural
S17-0409			51		1	Bengal	11 y	MN	Colonic adenocarcinoma
S17-0478			52		1		Adult	FN	DCM, CRD
S17-0480			53		1	DSH	Adult	MN	Acute myeloid leukaemia
S17-0481			54		1	Birma	1 y	F	Hippocampal necrosis
S17-0568			55		1	House cat	14 y	MN	Haemorrhage in brain
H15-2389		13			2	DSH	9 y	M	
S15-0134	37	36		122	2	Birma	4 y	FN	
S15-0259	35	34		123-125	2	House cat	4 y	F	
S15-0983	33	32		116	2	DSH	1 y	FN	
S15-1094	31	30			2	DSH	Juvenile	ME	
S15-1368		16	17		2	Norwegian Forest	8 m	MN	
S15-1539	26	25	24	117	2	Maine Coon	1 y	MN	
S15-1728	29	28	27	115, 118, 126	2	DSH	6 m	MN	
S15-1738	20	19	18	109-114, 127, 128	2		4 m	M	
S15-1809	23	22	21	106-108, 129, 130	2		1.5 y	MN	
S15-1842	41	42	43	102-105, 137	2	DSH	4 m	F	
S16-0167		14	15	119, 131, 132	2	DSH	10 y	FN	
S16-0454	44	45	46	120, 133	2	BSH	6 y	MN	
S17-0124	47	48	49	121, 132-136	2	Persian	5 m	F	

Table 4.0.3: Signalment and sample numbers of Bristol control cat cases. DSH: domestic short hair; DLH: domestic long hair; y: years; m: months; M(N): male (neutered;) F(N): female (neutered); HCM: hypertrophic cardiomyopathy; IBD: inflammatory bowel disease; FATE: feline aortic thromboembolism; CRD: chronic renal disease.

Case no.	Sample no.	Group	Breed	Age	Sex	Diagnosis
54	63	1-	DSH	8 y	MN	Chemodectoma
56	64	1-	Birman	13 y		Pyothorax and pneumonia
63	65	1-	DSH	6 y	MN	Astrocytoma
80	66	1-		10 y	MN	Diabetes mellitus
84	67	1-	DSH	12 y		Aplastic anaemia
87	68	1-	DSH	6 y		Diarrhoea, suspected torovirus
89	69	1-	DLH	8 y		Gastric lymphoma
90	70	1-	DSH	5 y	MN	Suppurative meningitis
91	71	1-	DSH	3 y	MN	Lymphocytic cholangiohepatitis
115	79	1-	DSH	2 y	MN	Hepatitis and pyelonephritis
116	80	1-	DSH	4 y	FN	Granulomatous rhinitis & encephalitis
118	81	1-	DSH	8 y	FN	Chronic enteropathy
119	82	1-	DSH	1 y	FN	Poxviral pneumonia
123	85	1-	DSH	4 y	FN	Hepatic encephalopathy
126	87	1-	Ragdoll	3 y	MN	HCM
136	93	1-	DSH	13 y	FN	Focal intestinal necrosis
140	94	1-	DSH		F	Behavioural
141	95	1-	DSH	3 y	FN	Invasive meningioma
143	97	1-	Maine Coon	9 y		Meningioencephalitis
152	100	1-	DSH	5 y	FN	Pulmonary adenocarcinoma
59	154	1-	Devon Rex	8 y		IBD
72	156	1-	DSH	9 y	MN	Multicentric lymphoma
104	160	1-	DSH	10 m	MN	HCM and FATE
105	161	1-	Bengal	7 y	FN	Small intestinal neoplasia
38	60	1+	Maine Coon	1 y		Connective tissue abnormality
51	62	1+	DSH	3y	MN	Lethargy, weight loss, anaemia
102	77	1+	DSH	10 y	MN	Diabetes mellitus
125	86	1+	Ragdoll	4 m	M	Severe interstitial pneumonia
132	91	1+	Havana	4 y	FN	Nasal lymphoma
135	92	1+	DSH	10 y	FN	Round cell neoplasia
149	99	1+	DSH	8 y	MN	Pleural effusion (PCR neg)
156	101	1+	DSH	18 y	FN	CRD
69	155	1+	DSH	10 y	MN	Lymphoma
78	158	1+	DSH		F	Anaesthetic death

Table 4.0.4: Signalment and sample numbers of Bristol FIP cat cases. DSH: domestic short hair; BSH: British short hair; y: years; m: months; M(N): male (neutered); F(N): female (neutered).

Case no.	Sample no.	Group	Breed	Age	Sex
30	56	2		3 y	
31	57	2	Burmese	3 m	M
32	58	2	Abyssinian	4 m	F
37	59	2	DSH		
42	61	2	DSH	5 m	
93	72	2	Siamese	1 y	
94	73	2	BSH	10 m	MN
96	74	2	DSH	2 y	MN
100	75	2	Siamese	3 y	MN
101	76	2	Birman	12 y	MN
103	78	2	BSH	1 y	FN
121	83	2	DSH	2 y	MN
122	84	2	Oriental	3 y	M
127	88	2	Birman	8 m	M
128	89	2	Ragdoll	10 m	FN
131	90	2	BSH	2 y	MN
142	96	2	DSH	6 m	F
146	98	2	DSH	1 y	
43	150	2	DSH	4 m	
46	151	2	DSH	7 m	
50	152	2	DSH		M

1. Establishment of quantitative reverse transcriptase polymerase chain reaction (RT-qPCR) protocols

The first stage of the study was to design, where required, or optimise, two step RT-qPCR protocols to study mRNA expression levels of a panel of immune mediators. This panel (Table 4.1.1) was chosen as described in the introduction.

Table 4.1.1. Summary of target molecules investigated by RT-qPCR.

Target group	Targets
Pathogen recognition receptors	TLR1-9
Cytokines and chemokines	IL-1β, -6, -10, -15, -17, TNF-α, TGFβ, CXCL10, CCL8
Interferons	IFN-α, -β, -γ
Transcription factors	STAT1-3
Matrix remodelling enzymes	MMP2, 9, 13, TIMP1, 3
Colony stimulating factors	G-CSF, M-CSF, GM-CSF

RNA extraction and cDNA synthesis

A test sample (spleen cDNA from cat S15-1871) was used for all trials. The RNeasy Plus Mini Kit (Qiagen) was used following the manufacturer's instructions. The kit includes an on column gDNA removal step. Briefly, the sample was removed from -80°C and thawed on ice. Approximately 30 mg of tissue was placed into RNA extraction buffer with added β-mercaptoethanol (Sigma-Aldrich, St Gallen, Switzerland) in a 2 ml round bottomed Eppendorf tube. A 5 mm steel bead (Retsch, Haan, Germany) was added to each tube and tissues were disrupted using a tissue homogeniser (Mixer-Mill 300, Retsch) set to 30 Hz for 40 s before on-column extraction and elution of RNA. Two elutes were performed per sample, giving a final elute volume of 80 µl. Multiple extractions were performed from the test spleen to obtain sufficient RNA for all trials.

The High-Capacity cDNA Reverse Transcription Kit (Thermo Fisher Scientific; Waltham, MA, USA) was then used according to the manufacturer's protocol; this results in 20 µl cDNA per 10 µl of input RNA. Eight reactions were performed per sample (totalling 160 µl) and the cDNA pooled, to which 160 µl RNase free water was added.

Primer Design

TaqMan qPCR requires specifically designed primer probe combinations; published protocols utilising a different method e.g. SYBR Green could therefore not be used. For the planned panel of markers, a number of suitable protocols were however already published (Table 4.1.2).

Table 4.1.2: Primer and probe sequences used for RT-qPCRs and conventional RT-PCRs.

Gene	Reference/Acc. no.	Primer and probe sequences (5'-3') where not previously published		PCR product length (bp)
GAPDH, IL-10	Leutenegger et al. 1999[294]			
FCoV (RT-qPCR)	Gut et al. 1999[295]			
FCoV (conventional)	Porter et al. 2014[133]			
TLR1, 2, 4, 5 ,6, 7, 9	Ignacio et al. 2005[165]			
TLR3, 8, IL-15, IFNα, -β	Robert-Tissot et al. 2011[296]			
IL-1β, IL-6, TNF-α	Kipar et al. 2001[297]			
TGF-β	Taglinger et al. 2008[298]			
G-CSF, M-CSF, GM-CSF	Kipar et al. 2006[48]			
IL-17	XM_006931816.1	F-16	ACTTCATCCATGTTCCCATCACT	126
		R-141	CACATGCTGAGGAAAATTCTTGTC	
		P-83	CATTCCCACAAAATCCAGGATGCCC	
STAT-1	XM_006935443	F-1649	TTGACCTCGAGACGACCTCTCT	135
		R-1783	GCGGGTTCAGGAAGAAGGA	
		P-1686	CTCCAATGTCAGCCAGCTCCCGAGT	
STAT-2	XM_003988893	F-1182	GCCCAGGTCACGGAGTTG	122
		R-1303	ACAGTGAACTTGCTCCCTGTCTT	
		P-1212	CTGCACAGAGCCTTTGTGGTAGAAACCC	
STAT-3	XM_006940361.2	F-1626	GCCAGTTGTGGTGATCTCCAA	133
		R-1758	TTGATCCCAGGTTCCAATCG	
		P-1696	CTGACCAACAACCCCAAGAACGTGAACTTT	
CCL8	XM_003996558	F-95	GGCCACCTTCAGCATCCA	82
		R-176	CCCTTTGACCACACTGAAGCA	
		P-121	CTCAGCCAGGTTCAGTTTCCATCCCA	
CXCL10	XM_003985274.3	F-386	TGCCATCATTTCCCTACATTCTT	78
		R-463	CAGTGGTTGGTCACCTTTTAGGA	
		P-411	CAAGCCCTAATTGTCCCTGGATTGCAG	
IFNγ	NM_001009873.1	F-214	TGGAAAGAGGAGAGTGATAAAACAA	122
		R-335	TCCTTGATGGTGTCCATGCT	
		P-284	ACCTGAAAGATGATGACCAGCGCATTCAA	
MMP2	XM_003998042.3	F-1633	CAAGTTCTGGAGGTACAATGAAGTAAAG	102
		R-1734	ACGGCGTCCAGGTTATCG	
		P-1681	CCCCAAGCTCATCGCGGATGC	
MMP9	XM_003983412.5	F-917	CCCAACCCGAGCTGACTCT	104
		R-1020	CCCTGGTGCATGTTGAGTACTC	
		P-964	AGCTGTGTGTCTTTCCCTTCATCTTCCTGG	
MMP13	XM_003992308.2	F-297	TGTGGGCGAGTACAACGTTTT	72
		R-368	TTCACAATCCTGTAGGTTAAGTTCGT	
		P-319	CCCCGAACGCTCAAGTGGTCCA	
TIMP1	XM_011291721.1	F-319	GCTGCTGGCTGCGAAGA	72
		R-390	GTGAGTGTCATTCTGCAGTTTGC	
		P-337	TGCACCGTATTTTCCTGTTCATCCATCC	
TIMP3	XM_003989216.5	F-41	GATGGTAAGATGTACACAGGACTATGC	127
		R-167	AGTAGCAGGATTTGATCTTGCAGTT	
		P-89	CAGCTCACCCTCTCCCAGCGCA	

Acc. no.: NCBI accession number; F: forward primer and start site; R: reverse primer and start site; P: probe and start site; bp: base pairs. All final reactions contained equivalent F and R concentrations of 900 nM, and P concentration of 250 nM, with the exception of FCoV RT-qPCR: 300 and 250 nM; FCoV conventional: 500nM; TGF-β: 200 and 50 nM; STAT3: 600 and 250 nM respectively.

Those newly developed were designed using Primer Express software (v3.0.1, Thermo Fisher Scientific) to span an exon-exon junction in order to prevent accidental detection of any genomic DNA, with the exception of possible pseudogenes. Where possible the junction was covered by a probe so that the full gene could not be detected by RT-qPCR (amplification would still be possible). Conventional PCR would be capable of amplification and thus detection on a gel (see Fig. 4.1.1). Where a suitable primer probe set could not be found meeting these criteria, one of the primers was instead placed over the junction. The aim was for these control measures against gDNA detection to be rendered superfluous by successful gDNA removal. All primers were checked in NCBI BLAST for specificity.

All primers and probes were manufactured by Microsynth (Balgach, Switzerland). The hydrolysis probes were labelled with a 5' reporter dye FAM (6-carboxyfluorescein), and a 3' quencher TAMRA (6-carboxytetramethylrhodamine).

Each new primer set was tested for specificity by conventional PCR. Conditions were as for RT-qPCR below except with omission of the probe. Primer concentrations for this step were 900 nM. The PCR product was subjected to gel electrophoresis and the resulting band(s) purified using a MinElute Gel Extraction Kit (Qiagen) according to the manufacturer's instructions. The resulting DNA solution was submitted to Microsynth for sequencing following dilution as per Microsynth's submission protocol. NCBI BLAST was used to evaluate the sequence obtained.

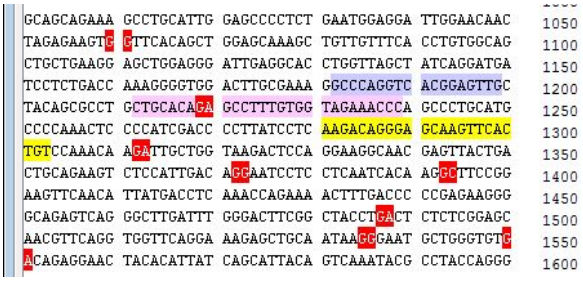

Figure 4.1.1: *Example primer probe design for STAT2. Exon-exon junctions, marked in red, were manually inputted into the Primer Express Software using gene annotation data from the NCBI database.*

Primer probe concentration optimisation

For all newly designed primer probe sets, varying concentrations were tested to determine the optimum (giving the best amplification efficiency). First, a single sample dilution, run in duplicate, was used to compare 300 nM, 600 nM, and 900 nM of primer, together with 150 nM vs 250 nM probe. Taqman RT-qPCR was performed on an Applied Biosystems 7500 Fast PCR System (Thermo Fisher Scientific). The master mix comprised 12.5 µl of Taqman Fast Universal Master Mix (2x) (Thermo Fisher Scientific), primer and probes diluted to 10 µl in RNase free water to give the desired concentration for a 25 µl final volume, and 2.5 µl sample cDNA. The thermal profile for all RT-qPCR was as follows: 50°C for 2 min, 95°C for 10 min, and 45 cycles of 95°C for 10s, and 60°C for 1 min. Data collection occurred during the extension phase (60°C).

The Applied Biosystems 7500 Software v2.0.6 was used to visualise results and calculate a threshold cycle (C_T) for each sample within the exponential phase of the amplification curve as per

the manufacturer's guidelines. The threshold was equilibrated between runs for each different target.

The primer probe concentration combinations giving the earliest and strongest signal (i.e. highest fluorescence) were then evaluated in a sample dilution series for efficiency and replicability. Where possible this consisted of seven 1:5 dilutions (i.e ~5 logs); depending on the starting C_T the dilution curve was adapted accordingly.

All final protocols (see Table 4.1.2) had an efficiency >95% (see Fig. 4.1.3 for example) and R^2 value >0.95 (though the majority were >0.99).

The first primer probe set for IFN-γ did not give reproducible results in a dilution curve (Fig. 4.1.2) so a new set was designed and tested as above, yielding appropriate results (Fig. 4.1.3).

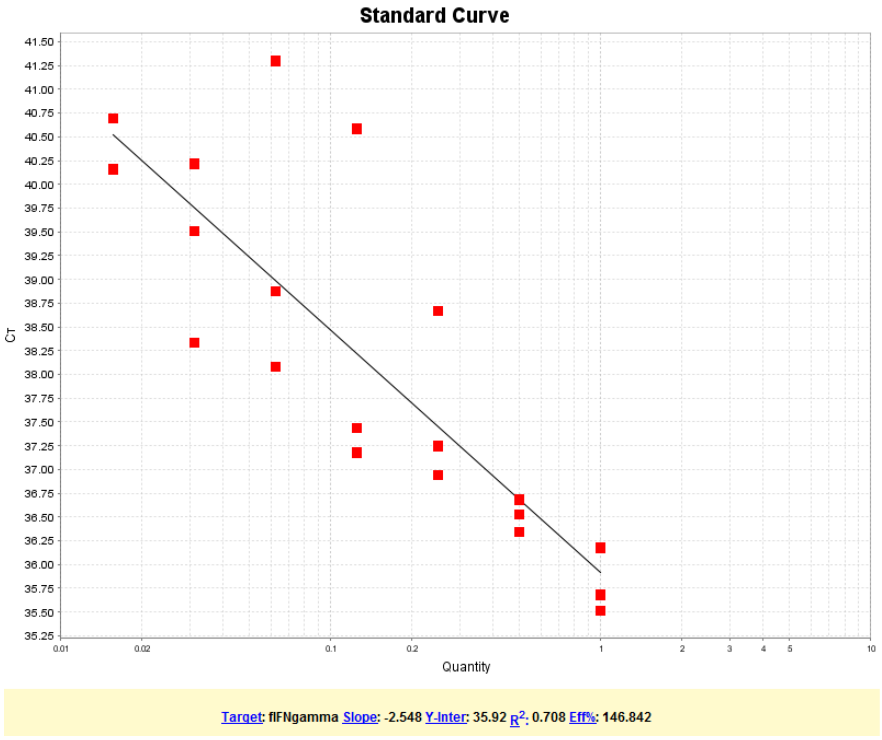

Figure 4.1.2: *Standard curve for dilution series in triplicate for the first IFN-γ primers and probe.*

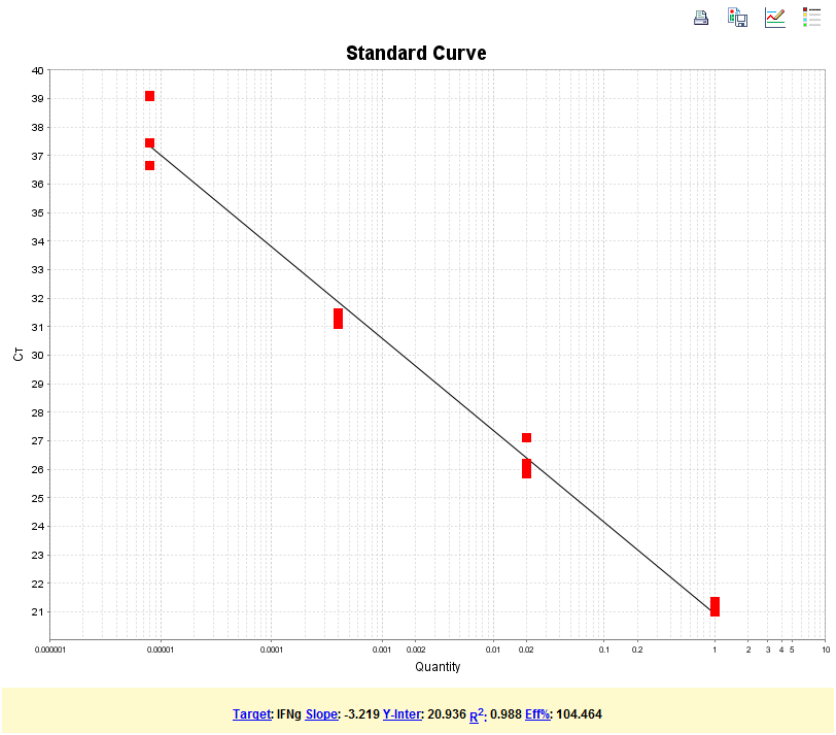

Figure 4.1.3: *Standard curve for dilution series in triplicate for the second IFN-γ primers and probe.*

Testing for gDNA contamination

The RNA purification protocol is designed to enzymatically remove gDNA, however during conventional PCR to test the newly designed STAT2 primers, two bands were obtained. In this case the probe spans an exon-exon junction but neither primer does, meaning that by RT-qPCR the gene would not be detected as it would not bind the probe, but it could still be amplified and its presence interfere with the assay, by competing for primers. Gel electrophoresis revealed a band at the predicted PCR product weight of ~120 (122bp) and a heavier band at ~230bp. Sanger sequencing revealed the heavy band to derive from the full gene (Fig. 4.1.4) rather than the mRNA product. The lighter band was as predicted (Fig. 4.1.5).

Figure 4.1.4: *Alignment of forward and reverse primer sequencing products of the heavy weight band with the STAT2 gene, showing the sequence spans an intron.*

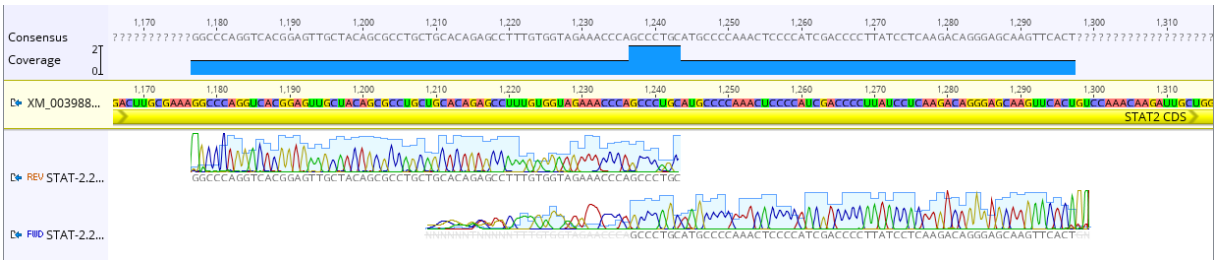

Figure 4.1.5: *Alignment of forward and reverse primer sequencing results from the lighter band shows these correspond to the STAT2 mRNA sequence.*

To test for gDNA contamination by assessing possible pseudogene presence, all PCR protocols were run in parallel on two sets of samples. cDNA was resynthesized in two reactions on a test sample, with the reverse transcriptase excluded from one reaction, i.e. the only available DNA will be genomic DNA extracted with the RNA (the Qiagen website states that Taq DNA Polymerase cannot amplify RNA under PCR reaction conditions; https://www.qiagen.com/ch/resources/faq?id=65b9b97f-1961-492f-8510-2de502a15159&lang=en).

qPCR reactions were then run in duplicate for each target gene and each reaction condition (i.e. four reactions per target).

Table 4.1.3 shows the cycle difference between runs with and without reverse transcriptase (RT). The positive results in the absence of RT enzyme indicate the presence of genomic DNA (in this case the contribution is given by the pseudogenes) within the sample despite the supposed gDNA removal step. The high variation in results depends on the abundance of pseudogenes present. When primers/probe designed over an intron-exon junction still give positive results, this indicates the presence of processed pseudogenes. In the absence of pseudogenes, gDNA would not be detectable but may still interfere with the efficiency of the PCR reaction [299].

Table 4.1.3: Test for gDNA contamination, cDNA synthesis reaction performed with and without the inclusion of reverse transcriptase (RT).

Target	+RT	-RT	C_T difference
GAPDH	19.55	32.00	12.4
TLR1	24.34	30.50	6.2
TLR2	24.33	31.02	6.7
TLR3	25.36	31.32	6.0
TLR4	22.86	30.80	7.9
TLR5	27.49	30.00	2.5
TLR6	27.16	32.75	5.6
TLR7	26.25	32.24	6.0
TLR8	23.79	33.40	9.6
TLR9	27.70	31.21	3.5
IL-1β	28.37	-	-
IL-6	30.88	-	-
IL-10	27.63	38.12	10.5
IL-15	30.82	-	-
IL-17	34.01	35.23	1.2
TNF-α	27.09	-	-
TGF	23.73	-	-
IFN-α	27.68	28.50	0.8
IFN-β	28.93	30.18	1.3
STAT1	21.72	34.74	13.0
STAT2	24.66	32.52	7.9
STAT3	23.77	-	-
CCL8	30.00	-	-
MMP2	26.25	36.65	10.4
MMP9	22.66	37.02	14.4
G-CSF	31.11	-	-
M-CSF	23.87	-	-

Genomic DNA removal

As a result of the contamination testing, an extra step was added to further remove gDNA. The DNA-*free*™ DNA Removal Kit (Thermo Fisher Scientific) was tested following the manufacturer's instructions to determine whether DNA removal had been successful, and whether there was a negative impact on RNA levels. The precise level of contaminating gDNA was unknown as samples were measured on a Nanodrop (although the 260/280 absorbance ratio will give an indicator of RNA purity, the concentration of RNA and DNA are combined as these cannot be distinguished). It can, however, be assumed to be heavy; some targets such as the interferons resulted in a C_T without reverse transcriptase almost equivalent to that with. The DNA removal kit (utilising DNase) is limited in the amount it is able to remove to 50 μg DNA/ml RNA, therefore it was predicted that the samples would need to be further diluted in order to allow effective enzyme activity. A second option was an extension of the clean-up step of the process, these were trialled as below.

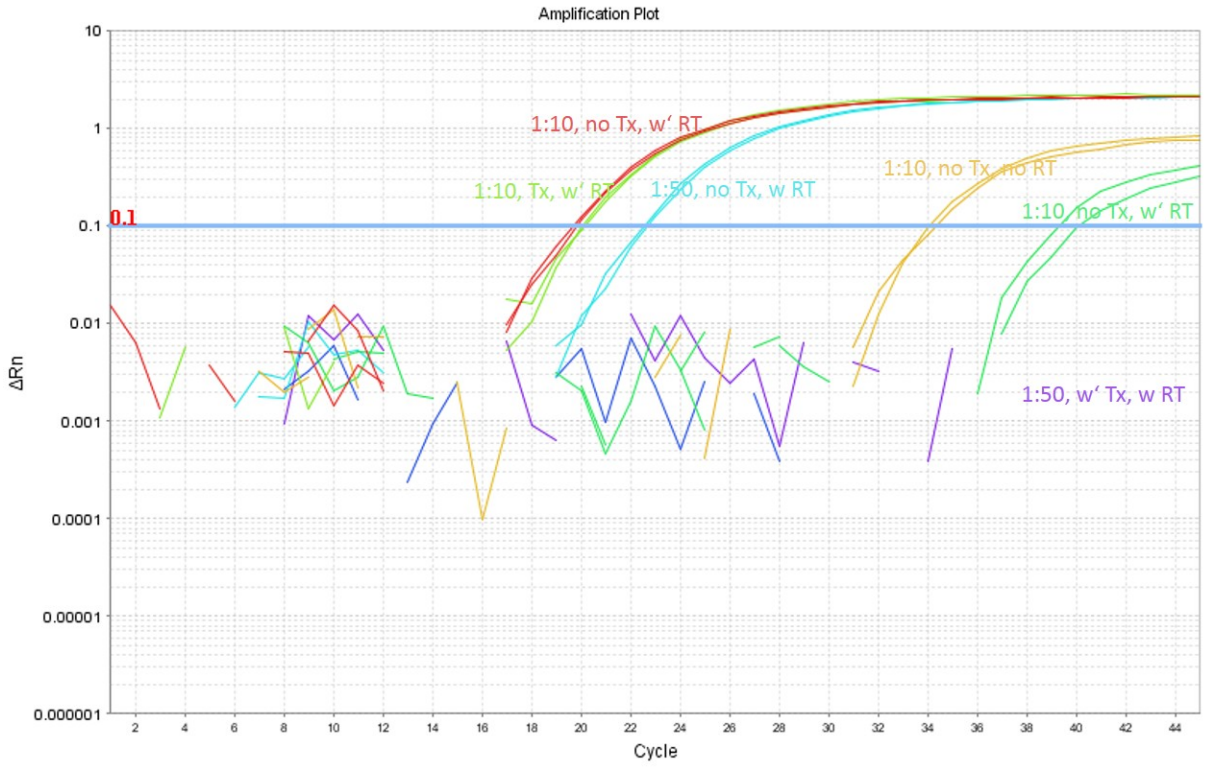

Figure 4.1.6: *qPCR amplification plot for GAPDH comparing DNase treatment (Tx) at different dilutions, with and without reverse transcriptase (RT).*

Table 4.1.4: Tabulated version of Fig. 4.1.7, comparing GAPDH C_T levels under different treatment conditions.

Dilution/condition	**+RT**	**-RT**	**C_T difference**
1:10 / untreated	19.73	34.14	14.41
1:10 / DNase treated	20.07	39.64	19.57
1:50 / DNase treated	22.59	-	>22.41

These results show that at a 1:10 dilution the DNase treatment reduced gDNA contamination by 5 C_Ts, or ~32 times (Fig. 4.1.6, Table 4.1.4). It also shows a small but fairly negligible effect on RNA levels, which were slightly reduced by the treatment (<0.4 of a cycle). At 1:50 the DNase treatment was more effective but with a corresponding reduction in starting level this is risky for low expressed genes. A further trial was carried out using IFN-α and an extended treatment step. IFN-α had originally shown less than a cycle difference between ±RT reactions, however as a low expressed gene it was not used for the first trials as the high starting C_T level reduces the possible comparisons available. At 1:10 and 1:20 dilutions with an extended DNase treatment (as per manufacturer's protocol trouble shooting options) 'with RT' C_T values of 32.9 and 33.6 respectively were detected. 'Minus RT' reactions were negative indicating that this protocol achieves an improvement exceeding the 5 cycles reduction with the standard protocol.

RNA extraction and cDNA synthesis were therefore repeated as described above with exclusion of on-column DNA removal and addition of an intervening DNase treatment. Concentrations were normalised to ~50ng/µl following Nanodrop 2000 (Thermo Fisher Scientific) measurement.

Alternative internal reference gene trials

GAPDH is commonly used and has been published as a reliable reference (housekeeping) gene for amplification control in felines [294,298,300,301], however under inflammatory conditions it may sometimes be altered [302]. RPS7 and GUSB were trialled as alternatives by comparing a subset of group 1 and 2 cats. Levels of both reflected GAPDH levels fairly closely so no change to the protocol was made [303].

GAPDH duplex trial

Owing to the number of targets and samples, it would of course not be possible to run all required reactions on one plate. Therefore as an extra internal control, and to reduce the total reaction number, a duplex GAPDH which could be run with each sample and target was tested. The second GAPDH probe was labelled with 5' VIC and 3' BHQ (black hole quencher), also supplied by Microsynth. The probe concentration was tested at 50, 150 and 250 nM, being optimal at 250 nM where C_T levels were however still ~1 cycle lower than with the FAM-TAMRA probe.
The duplex was then trialled on three targets, known to have a range of expression levels, each run alone and in combination with GAPDH, shown in Table 4.1.5.

Table 4.1.5: GAPDH duplex trial on selected targets.

Target	C_T alone	C_T with GAPDH	C_T 'loss'
GAPDH	22.2792	-	
STAT3	24.877449	24.4080505	-0.5
IL-6	32.0183182	33.8927383	1.9
TLR1	29.0191936	32.0472107	3.0

These results showed that for highly expressed genes, expressed at a similar level to GAPDH, there was no loss of signal. However, those expressed at far lower relative levels were outcompeted and detection efficiency was significantly lower. Interestingly, and counter-intuitively, detected levels of GAPDH itself were also reduced when combined with lower expressed targets.
As the results showed that this method could therefore not be applied to all targets without extensive individual optimisations it was decided from a cost benefit viewpoint not to pursue this further.
Table 4.1.2 above shows the final primer and probe concentrations used.

2. Determination of FCoV and mediator transcription levels in bone marrow and spleen using RT-qPCR

The protocols were first applied to BM and spleen (tissues with a known involvement in FIP [46]) from the first 20 cats within the Zurich cohort in order to provide early results on the likely relevance of the previously untested mediators, particularly the TLRs.

Group 1 contained six control cats and Group 2 14 cats with FIP. From these cases, all had spleen available whilst BM was available from 11 of the 14 G2 cats. Pathological findings are shown in Table 4.2.1.

Statistical analysis

All samples were run in duplicate and any samples with discordant results repeated. After confirmation of the automatic threshold for each run, or input of a manual threshold, results were exported to Windows Excel. This step ensured that samples from different runs had the same threshold for each target. Relative mRNA transcription levels were calculated using the comparative C_T method [304]. The C_T of each sample was first normalised to GAPDH as the endogenous reference (ΔC_T) and then, for each target, expressed relative to the G1 ΔC_T bone marrow mean for that target as the calibrator ($2^{-\Delta\Delta CT}$). The exception was FCoV, for which $2^{-\Delta CT}$ was used.

The statistical programme SPSS v.25 (IBM Statistics) was used for all analyses and graphical data presentation. Data were first assessed for normality using a Shapiro-Wilk test. As almost all data failed the test, non-parametric measures were applied. A two-tailed Mann-Whitney test with a significance level of $p \leq 0.05$ was used to compare results between groups for each target molecule, with the null hypothesis that there is no difference between groups.

Table 4.2.1: Histological and immunohistological (IH) findings in association with case numbers used for the BM and spleen studies. NS: not sampled; NAD: no abnormality was detected; mϕ: macrophages; MF: multifocal; +ve: positive; -ve: negative.

Case no.	BM			spleen		
	Sample no.	Histological findings	IH	Sample no.	Histological findings	IH
H15-2389		NS		13	Multiple small pyogranulomas	+ve
S15-0134	36	NAD	-ve	36	Serositis	+ve
S15-0259	35	NS		34	Mild multifocal serositis, neutrophilic splenitis	rare +ve
S15-0983	33	High cellularity	-ve	32	Serositis and histiocytosis	+ve serosa
S15-1094	31	NS		30	MF follicular necrosis and granulomas, scant serositis.	+ve serosa and follicles
S15-1368				16	Mild follicular hyperplasia	-ve
S15-1539	26	Moderate cellularity, NAD	-ve	25	Serositis and subserosal splenitis, histiocytosis	+ve, predominantly serosa
S15-1728	29	High cellularity	-ve	28	Moderate serositis	+ve
S15-1738	20	High cellularity, increased mϕ	-ve	19	Cell poor serositis	+ve
S15-1809	23	High cellularity	-ve	22	Serositis, follicular hyperplasia	+ve, predominantly serosa
S15-1842	41	High cellularity, increased m0	-ve	42	Mild serositis	rare +ve
S16-0167		NS		14	Serositis and histiocytosis	+ve
S16-0454	44	Moderate cellularity, NAD	-ve	45	Very mild serositis	rare +ve, mainly in follicles
S17-0124	47	NS		48	Serositis and subserosal splenitis	+ve

3. Determination of FCoV and mediator transcription levels in the mesenteric lymph nodes (MLN) using RT-qPCR

Following promising results from BM and spleen, the study was extended to evaluate MLN from a greater number of animals. At this stage Bristol biobank cases were used. Macroscopical findings, histological, and immunohistological results from the MLN were available from almost all cases, giving information such as whether effusions were present and whether or not the MLN itself had histologically evident FIP lesions. These details were used to create and compare subgroups.

From the Bristol database, many tissue samples had already been tested for FCoV and undergone pyrosequencing for previous publications [91,133] but the available cDNA stock had been largely exhausted necessitating shipping of tissue samples on dry ice to Zurich. A customs delay unfortunately resulted in partial thawing of the samples which may have impacted on the RNA quality as discussed below.

Cases used together with histological findings in the MLN are shown in Tables 4.3.2-3.

RNA extraction

RNA extraction was performed as above on 50 Bristol MLN samples. These were eluted twice into a total volume of ~50 µl (accounting for loss to the spin column filter).

RNA levels were measured using a Nanodrop 2000 (ThermoFisher Scientific) and four samples with a concentration of <30 ng/µl were excluded. Those remaining had measured levels ranging from 34.5 ng/µl to 1994.1 ng/µl; the occasional low levels likely to be related to the thawing in transit.

Prior to cDNA synthesis, the RNA concentrations were equilibrated to ~400ng/µl with RNase free water. Where the starting concentration was lower than this, multiple synthesis reactions were carried out and the resulting cDNA pooled with a correspondingly lower volume of water added to achieve the same end concentration (e.g. if the starting concentration equilibrated to 200ng/µl then two synthesis reactions instead of one contributed to the final cDNA sample).

cDNA synthesis

As starting material was limited, and following the experience of the previous stage which required up to eight cDNA synthesis reactions per sample to provide sufficient starting material, an alternative cDNA synthesis protocol was trialled.

The SuperScript IV VILO kit with ezDNase (Thermo Fisher Scientific) includes a gDNA removal step so was tested in comparison to the previous method on a single sample (84) for TLR6.

Table 4.3.1: Comparison between the original HC-cDNA synthesis protocol (method 1) and the SuperScript IV VILO protocol (method 2), with and without reverse transcriptase (RT).

Method	C_T +RT	C_T -RT
1	25.09	28.67
2	22.13	-
C_T ***difference:***	2.96	

These results showed that there was an almost three cycle difference (8 x concentration) between the methods, therefore only one reaction per sample was carried out. It also shows that the ezDNase step was effective at removing contaminating gDNA so this simpler method was used in place of the RNA clean up step previously described.
cDNA synthesis was carried out according to the manufacturer's protocol, resulting in 20 µl from 8 µl of starting RNA per sample. All samples were then made up to 250 µl with molecular grade water.

RT-qPCR

This was carried out as described. In total, there were 40 cats in Group 1 (G1), including six cats from Zurich, and 30 cats in G2, including 9 cats from Zurich. FCoV results led to subgrouping of G1 to G1+ and G1-, with 10 and 30 cats positive and negative for FCoV respectively.

Statistical analysis

Data were processed as in section 2, an exception being that for FCoV RT-qPCR results, the mean of G1+ was instead used as the calibrator (to allow for better visualisation graphically).
In the accepted manuscript, the MLN results were presented as stand-alone results and therefore the MLN G1 mean was used. The change to the BM mean does not affect statistical comparisons within the MLN group, as the same function was applied to all, but meant that relative values were comparable between organs (though not between targets).
As there were now three groups of cats, first cats with and without FIP (G1 vs G2) were compared. This was followed by comparisons between G1- and G1+, and between G1+ and G2. Within G2, comparisons were made between cats with and without cavitary effusions and with and without histologically observed FIP lesions in the MLN. Correlation between relative FCoV levels and inflammatory mediator levels, and also between individual inflammatory mediators, was analysed within G2 using a one-tailed Spearman's rank test. Here a cut off of $p \leq 0.01$ was used, with $p \leq 0.05$ indicating weak correlation.

Table 4.3.2: Group 1, histological and immunohistological (IH) findings; ND: not done. -ve indicates negative immunohistological result.

Case no.	Sample no.	Group	MLN histology and immunohistology
S15-1871	50	1-	Normal, IH -ve
S17-0409	51	1-	Normal, IH ND
S17-0478	52	1-	Follicular hyalinosis, IH -ve
S17-0480	53	1-	Leukaemia, IH -ve
S17-0481	54	1-	Normal, IH -ve
S17-0568	55	1-	Follicular hyalinosis, IH ND
54	63	1-	Normal, IH -ve
56	64	1-	Pyogranulomatous inflammation, IH -ve
63	65	1-	Normal to reactive, IH -ve
80	66	1-	Reactive hyperplasia & amyloidosis, IH -ve
84	67	1-	Neutrophilic inflammation, IH -ve
87	68	1-	ND
89	69	1-	Normal, IH -ve
90	70	1-	Mild depletion, IH -ve
91	71	1-	Normal to reactive, IH ND
115	79	1-	Reactive hyperplasia & sinus histiocytosis, IH -ve
116	80	1-	ND
118	81	1-	ND
119	82	1-	Multifocal pyogranulomas, IH -ve
123	85	1-	ND
126	87	1-	ND
136	93	1-	Normal, IH ND
140	94	1-	Normal to reactive, IH -ve
141	95	1-	Normal to reactive, IH -ve
143	97	1-	Normal, IH -ve
152	100	1-	Tumour emboli, IH ND
59	154	1-	Normal, IH -ve
72	156	1-	Reactive hyperplasia, IH -ve
104	160	1-	Reactive hyperplasia & sinus histiocytosis, IH -ve
105	161	1-	Follicular depletion, IH -ve
38	60	1+	ND
51	62	1+	ND
102	77	1+	Reactive hyperplasia with collagen scars, IH -ve
125	86	1+	Normal to hyperplastic, IH -ve
132	91	1+	ND
135	92	1+	Sinus histiocytosis, IH -ve
149	99	1+	Normal, IH -ve
156	101	1+	Sinus histiocytosis, IH ND
69	155	1+	Focal cortical inflammation, IH -ve
78	158	1+	Normal to reactive, IH -ve

Table 4.3.3: Group 2, pathological, histological and immunohistological (IH) findings; Y: yes; N: no; A: ascites; P: pericardial effusion; T: thoracic effusion; M: multicavitary effusion; ND: not done; LPC: lymphoplasmacytic.

Case no.	Sample no.	Group	Effusions present?	LN lesions	MLN histology and immunohistology
S16-0167	15	2	Y - A	Y	Necrotising & pyogranulomatous, IH +ve
S15-1368	17	2	N	Y	Necrotising, pyogranulomatous, LPC, IH +ve
S15-1738	18	2	Y - A	Y	Granulomatous, IH +ve
S15-1809	21	2	Y - A	Y	Pyogranulomatous, IH +ve
S15-1539	24	2	Y - A	Y	Pyogranulomatous & LPC, IH +ve
S15-1728	27	2	Y - A&P	Y	Granulomatous, IH +ve
S15-1842	43	2	Y - M	Y	Granulomatous, IH +ve
S16-0454	46	2	Y -A	Y	Pyogranulomatous, IH +ve
S17-0124	49	2	Y -A	Y	Pyogranulomatous, IH +ve
30	56	2	Y -A	Y	Granulomatous, IH +ve
31	57	2	Y - T	Y	Necrotising and granulomatous, IH +ve
32	58	2	Y - A	Y	Pyogranulomatous, IH +ve
37	59	2	Y - T	-	ND
42	61	2	Y - A&T	Y	Necrotising & pyogranulomatous, IH +ve
93	72	2	Y	Y	Pyogranulomatous, IH +ve
94	73	2	Y	N	Sinus histiocytosis, IH -ve
96	74	2	Y	N	Reactive hyperplasia, IH -ve
100	75	2	Y - A&T	N	Normal, IH -ve
101	76	2	Y - M	N	Reactive hyperplasia, IH +ve
103	78	2	Y - A&T	Y	Pyogranulomatous, IH +ve
121	83	2	N	Y	Granulomatous, IH +ve
122	84	2	N	Y	Granulomatous, IH +ve
127	88	2	N	-	ND
128	89	2	-	Y	Necrotising & granulomatous, IH +ve
131	90	2	Y - A	Y	Necrotising & pyogranulomatous, IH +ve
142	96	2	N	N	Normal, IH -ve
146	98	2	Y - A	N	Reactive hyperplasia, IH -ve
43	150	2	-	N	Reactive hyperplasia, IH -ve
46	151	2	N	Y	Pyogranulomatous, IH +ve
50	152	2	Y - A	Y	Pyogranulomatous, IH +ve

4. Laser Capture Microdissection (LCM) and RT-qPCR

The Zurich case cryoblocks from organs/tissues with FIP lesions in Group 2 cats were prepared as follows: Firstly, an appropriately sized tissue sample (rough dimensions 1 x 1 cm and not exceeding 5 mm in depth) was removed from the organ using a scalpel. The side of interest was placed face down in a mould onto a drop of Cellpath OCT embedding matrix (Thermo Fisher Scientific) before placing the block into isopentane cooled by liquid nitrogen. The block was removed from the isopentane when a 1 mm bubble of liquid OCT remained centrally at the surface, separated from the surrounding mould and placed into a micro-Petridish for storage at -80°C.
In total, 23 cryoblocks were obtained from 11 cats as in some cases, small lesions were lost following block trimming.

Sample optimisation

To reduce the time pressure on the LCM stage, and to obtain the maximum possible RNA quality, an extra step of first placing the tissue sample in RNAlater prior to OCT was tested. As OCT is not designed to preserve protein structure, the morphology was unfortunately too compromised so this method was not taken further.
Cryosections of a single sample were tested by scrape test (removal of the whole section from a slide using a scalpel) for approximate RNA levels by RNA extraction and RT-qPCR for GAPDH. This was for practical reasons in order to optimise the laboratory workflow and determine which steps are under time pressure. Six sections were cut as shown in Table 4.4.1. During the LCM procedure itself slides are at room temperature and humidity, with the required time span difficult to accurately predict in advance. RNA was extracted using a Qiagen RNeasy Microkit according to the manufacturer's protocol. The RT-qPCR reaction was run as a one step reaction with the following reagents per sample: 12.5 µl One step RT-qPCR MasterMix (Eurogenteq, Seraing, Belgium); 0.5 µl each of 20 µM forward and reverse primer (see chapter 1), 0.75 µl of 10 µM probe, 0.125 µl of Moloney Murine leukemia virus reverse transcriptase and RNase Inhibitor (EuroScript RT 0.25 U/ml and RNase Inhibitor 0.1 U/ml, Eurogentec). The one step method was used to exclude other variables e.g. in the cDNA transcription stage and as there was no requirement to store the samples for future testing.

Table 4.4.1: Comparison of C_T levels obtained from sections under different conditions.

Condition	**GAPDH** C_T
Direct scrape	26.77
HE stain then direct scrape	19.91
1h RT	17.72
1h on ice	18.06
2h RT	18.05
2h on ice	22.67
Positive control	15.74

This small test only included one sample per condition and as such it would be speculative to draw too precise conclusions. The result of the direct scrape is not easily explained as, in the absence of

any potentially RNA damaging treatments, this would be expected to give the lowest C_T (suggesting an error at some stage). However, the results otherwise suggest that working with the slides at room temperature for a few hours is unlikely to have any significant detrimental effect. The use of RT-qPCR is however much more lenient in terms of sample quality than e.g. next generation sequencing. Room temperature actually appeared preferable to ice, though the difference was negligible. As dehydration is the most important factor for preventing RNase activity, it is possible that the more humid atmosphere under ice conditions played a role.
Samples were also compared when the work flow was completed the same day as sectioning, or sections being left for two days at -20°C (to allow for weekend work on slides prepared during normal laboratory working hours). There was again no observable difference.

Cryosectioning

Sections were cut to 10 µm thickness and mounted onto PEN Membrane Glass slides (Thermo Fisher Scientific) using sterile and RNase free technique on a CryoStar NX50 Cryostat (Thermo Fisher Scientific) with the temperature set according to the tissue (e.g. mesentery ~-35°C, spleen ~-10°C). Tests carried out for a parallel project showed that from 20 to 10 µm there was no significant loss of yield but there was a significant loss of morphological details from 10 to 20 µm. Two consecutive sections of 6 µm were mounted onto positively charged glass slides and routinely stained with HE or immunohistologically stained for FCoV antigen (see Chapter 1), to confirm the presence of virus within selected lesions.

Staining procedure

The staining protocol for LCM requires a compromise between the optimal morphology (usually provided by HE staining), and the optimal RNA quality (no staining procedure). A number of staining procedures were tested for their practicality and effectiveness. These included:

- with and without acetone fixation
- with and without a final xylene step
- basic dehydration with no staining
- Ambion staining protocol (increased ethanol gradient steps, xylene steps at end [305]).
- haematoxylin staining with ammonium hydroxide as blueing agent (replacing tap water)

The final staining protocol was based on a previously published protocol as follows [306]:

Table 4.4.2: Staining protocol for cryosections prior to LCM.

Solution	Incubation time
95% ethanol	30 s
75% ethanol	30 s
1% wt/vol cresyl violet in pH 8.0 75% ethanol	40 s
75% ethanol	30 s
95% ethanol	30 s
100% ethanol	30 s
100% ethanol	30 s
100% ethanol	5 min

All reagents were diluted to the required concentration using diethyl pyrocarbonate (DEPC) treated-water (to inactivate any RNase contaminants which autoclaving alone may not remove). DEPC treated water was prepared using concentrated DEPC (Sigma Aldrich) added to ultrapure Milli-Q water (Merck, Lucerne, Switzerland) at a concentration of 0.1%, mixed on a magnetic stirrer overnight and autoclaved to inactivate the toxin. Each staining solution was prepared fresh each time in a 50 ml Falcon tube filled to 35 ml. Following the last ethanol step, slides were air dried on the bench for at least 10 min before proceeding to LCM.

Laser capture microdissection of samples

An automated Arcturus XT Laser Microdissection Instrument based on a Nikon Eclipse Ti-E motorized Microscope was used. The system consists of an inverted microscope equipped with an UV-cutting laser and an infrared laser for capturing dissected material. The main aim was to select areas highly enriched for FCoV-infected macrophages and to try to compare between serosal inflammation and granulomas. Additional samples of interest were taken from some blocks (e.g. follicles in the MLN to gain a brief overview of lymphocyte contribution). Consecutive sections of the frozen blocks were stained with HE, and by immunohistology for FCoV antigen. This gave additional confirmation that the correct regions of interest had been selected.

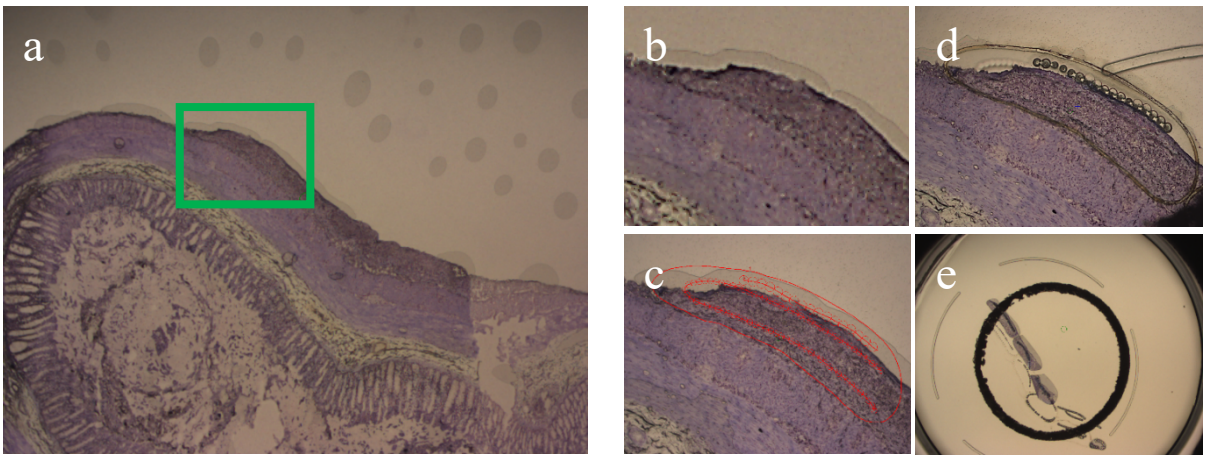

Figure 4.4.1: *Intestine (S15-0134) a) Overview; b) close up of selected area showing serositis; c) selection of desired area; d) tissue following UV cut and IR capture; e) cap with this region and adjacent areas.*

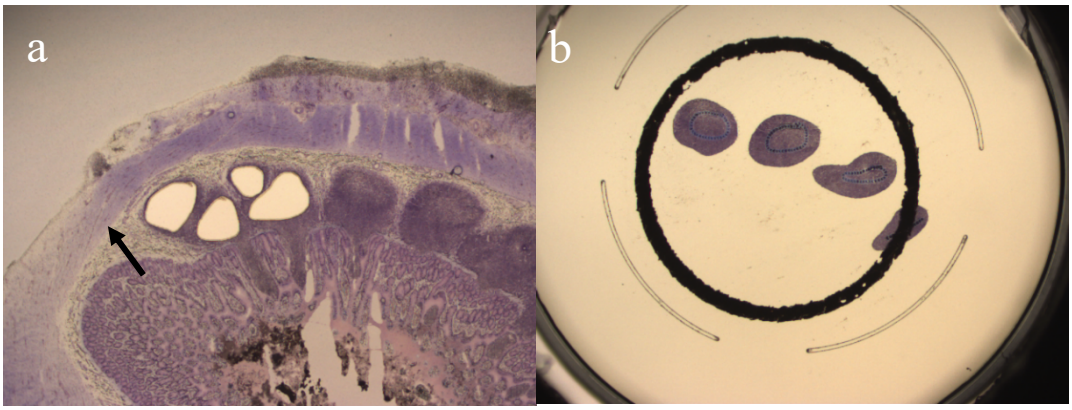

Figure 4.4.2: *Intestine (S15-1842) a) After LCM of Peyers patches (e.g. arrow); b) cap with captured tissue*

Table 4.4.3: Cases used for LCM and final sample numbers allocated for RT-qPCR studies.

Case no.	Sample no.	Organ	Region sampled by LCM
S15-1842	102	Small intestine	Serosal inflammation
S15-1842	103	Small intestine	Peyer's patches (no lesion)
S15-1842	105	Liver	Serositis
S15-1809	106	Spleen	Serositis
S15-1809	107	Spleen	Follicles (no lesion)
S15-1738	109	Spleen	Follicles (no lesion)
S15-1738	110	Spleen	Serositis
S15-1738	112	Mesentery	Pyogranulomatous vasculitis
S15-1738	113	MLN	Serositis
S15-1738	114	MLN	Follicles (no lesion)
S15-1728	115	Liver	Serositis
S15-0983	116	MLN	Serositis (small granulomas)
S15-1539	117	MLN	Granulomas
S15-1728	118	MLN	Granulomas and vasculitis
S16-0167	119	MLN	Granulomas
S16-0454	120	MLN	Granulomas
S17-0124	121	MLN	Pyogranulomatous inflammation
S15-0134	122	Large intestine	Serositis
S15-0259	123	MLN	Granulomas
S15-0259	124	Spleen	Serositis
S15-0259	125	Liver	Serositis
S15-1738	128	Liver	Macrophages in serositis
S15-1809	129	Kidney	Serositis
S15-1809	130	Omentum	Granulomas
S16-0167	131	Spleen	Serositis
S16-0167	132	Omentum	Granulomatous inflammation
S16-0454	133	Liver	Serositis
S17-0124	134	Liver	Serositis (with small subcapsular granulomas)
S17-0124	135	Spleen	Serositis
S17-0124	136	Small intestine	Pyogranulomatous vasculitis in muscularis
S15-1842	137	Small intestine	Serositis

RNA extraction

For the final lesion samples, this step was performed using the RNAqueous Micro Total RNA Isolation Kit (ThermoFisher Scientific AM1931) kit according to the manufacturer's protocol [307]. The change from the previously used Qiagen extraction kit was based on other users' experience. Briefly, the LCM membrane was removed from the cap with a sterile scalpel blade and transferred to a 500 µl Eppendorf tube containing 100 µl of Lysis buffer. This was placed in an incubator set to 42°C for 30 min before progression to on-column RNA elution. At the final elution step, two elutions were performed with a volume varying from 10-14 µl per elution depending on the amount of starting material.

cDNA synthesis

The initial optimisation for LCM was carried out in parallel with optimisation of the PCR protocols (Chapter 1). As such, the High Capacity cDNA synthesis kit (Thermofisher) was first tested. From a 10 µl RNA input, 25 µl cDNA are obtained. A test sample of control kidney was first trialled, from which microscopic regions were sampled, to mimic small lesional areas. Following RNA extraction and cDNA synthesis the samples were subjected to qPCR for GAPDH using undiluted, 1:4, 1:8 and 1:16 dilutions to evaluate the suitability for large numbers of PCR runs. The undiluted sample had a C_T of 30.1, increasing to 32.0, 34.0 and 34.5 respectively. This indicated that the protocol was not feasible for small samples either in terms of increasing the number of PCR runs possible, or in detecting targets with low expression.

Instead, the SuperScript IV VILO Master Mix with ezDNase (Thermo Fisher Scientific) was used (as per Chapter 3).

A single qPCR for GAPDH was carried out on all samples prior to pre-amplification, using 1 µl of undiluted sample, to ensure successful RNA extraction and cDNA synthesis.

Pre-amplification of cDNA

Owing to earlier tests showing that the cDNA yield would be insufficient for large numbers of PCR reactions, the sample first underwent pre-amplification. The TaqMan PreAmp Master Mix Kit (Thermo Fisher Scientific) was used according to the manufacturer's protocol with some adaptations. The kit is predominantly designed for use with TaqMan's own primer and probe sets which are supplied as one assay mix at 20x for which the concentrations of individual reagents are not provided. A maximum of 100 assays may be pooled. As the precise calculations could therefore not be replicated, the concentrations were calculated approximately relative to the most common qPCR concentration of 900nM primer (used for reactions without pre-amplification). Allowing for a maximum of 50 reactions, 1 µl of each 20 µM primer was added per 100 µl pooled assay mix for reactions usually requiring 900nM, adjusted accordingly for those at lower concentrations.

One trial run was carried out on a single test sample of myocardium from another study (not an FIP sample) to ensure that all targets were amplified following the pre-amplification. This was successful. Only GAPDH was run on a non pre-amplified sample (1 µl), to ensure there was starting material for the pre-amplification.

Each pre-amplification reaction consisted of 25 µl of TaqMan PreAmp Master Mix (2x), 12.5 µl of pooled assay mix, 7.5 µl of nuclease free water and 5 µl of sample cDNA. All except the cDNA were prepared as a single master mix, from which 45 µl per well was pipetted. The reaction thermal profile was as shown in Table 4.4.4.

Table 4.4.4: Reaction conditions for pre-amplification RT-PCR

Stage	**Temperature**	**Time**	
Hold	95°C	10 min	
Denaturation	95°C	15 s	14 cycles
Annealing/extension	60°C	4 min	
Hold	4°C	∞	

The PCR product was then diluted 1:20, giving a total of 1ml per sample.

RT-qPCR

This was performed as described above (see Chapter 1), though using 5µl of pre-amplified sample cDNA per reaction. A CAS-1200 pipetting robot (Corbett Robotics Pty. Ltd., Queensland, Australia) was used to pipette the samples into each reaction.

Pre-amplification correction calculations

Initial comparisons of results showed many targets to be expressed at a lower level than expected, including FCoV which should have been higher than in non laser microdissected samples as areas high in infected macrophages were specifically chosen. This led to the suspicion that the pre-amplification step was not amplifying all targets equally.

There was of course insufficient sample to carry out all PCR reactions on non-pre-amplified cDNA therefore it was decided to assess and hopefully correct the error mathematically.

As all samples already had a GAPDH result, the level of cDNA in each was already known approximately (ie. low, medium, high). Groups of samples were then made, each containing 6 samples over a range of cDNA content. The targets were randomly assigned a group, and the PCR repeated with 1 µl of cDNA reactions. For each target, the before and after pre-amplification C_T values were plotted against each other. When this resulted in a straight-line graph (correlation graph), the equation of this line was used to calculate an artificial 'before pre-amplification' C_T for all samples (Fig. 4.4.3 and Table 4.4.5). Targets without a close line of best fit were not used for statistical comparisons as it was assumed that the pre-amplification stage was introducing an unpredictable rather than a predictable error. This however tended to only apply to targets already expressed at low levels such that the direct sample C_T was towards the detection limit, e.g. Fig 3.2.

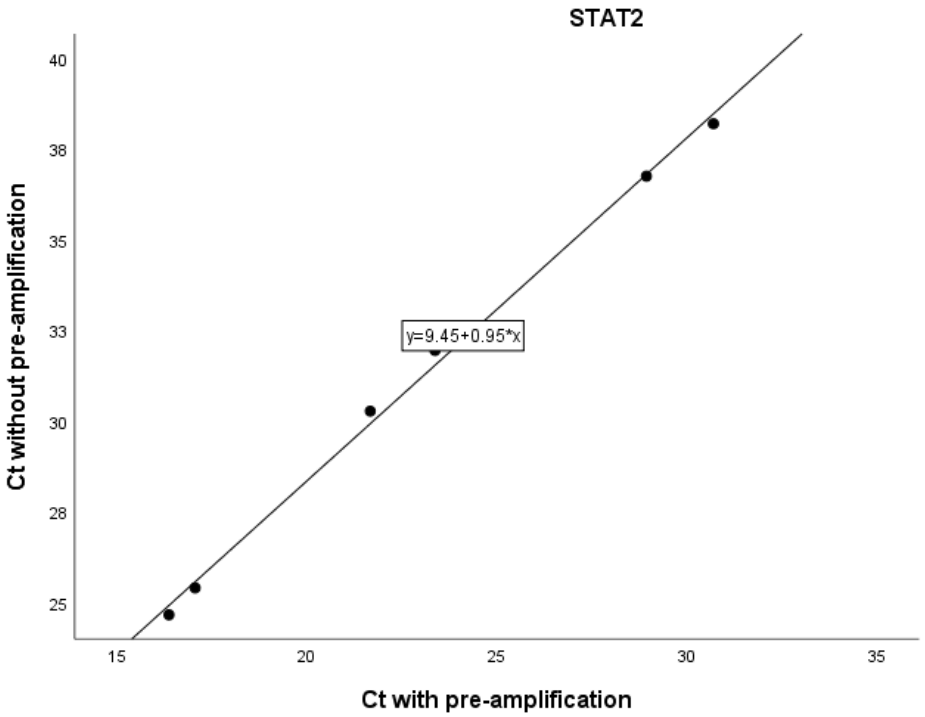

Figure 4.4.3: *Example of method used to predict the pre-amplification C_T values of all samples; STAT2 showing all points are in agreement with the line of best fit.*

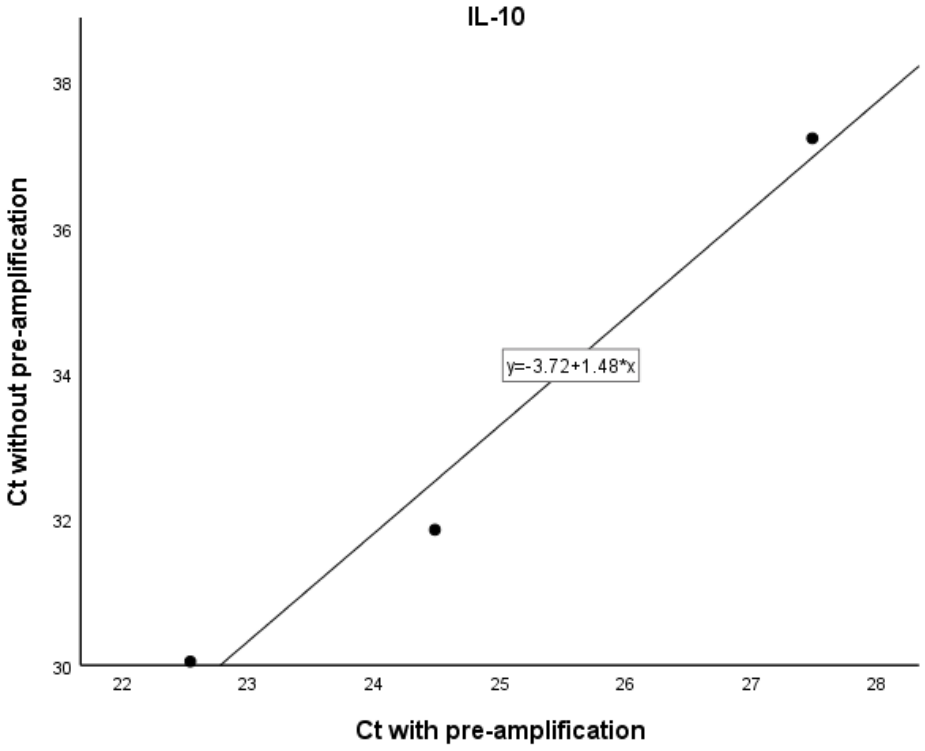

Figure 4.4.4: *Example of line of best fit deemed insufficiently accurate, target removed from final calculations.*

Table 4.4.5: Equations used to calculate a 'before pre-amplification' C_T value, derived from graphs exemplified above in Fig. 4.4.3.

Mediator	Equation
GAPDH	y= 8.8+0.99x
FCoV	y=5.06+1.09x
TLR1	y=7.37+1.05x
TLR2	Y=7.12+0.98x
TLR3	y=5.98+1.06x
TLR4	y=8.75+0.89x
TLR5	y=8.47+0.97x
TLR6	-
TLR7	y=6.67+1.05x
TLR8	y=8.57+0.90x
TLR9	y=6.41+1.07x
IFN-α	y=6.71+0.96x
IFN-β	y=3.54+1.21x
IFN-γ	y=5.17+1.07x
STAT1	y=8.25+0.93x
STAT2	y=9.45+0.95x
STAT3	y=9.85+0.90x

Mediator	Equation
IL-1β	y=7.86+1.00x
IL-6	y=10.4+0.93x
IL-10	-
IL-15	-
IL-17	-
TNF-α	y=8.51+1.00x
TGFβ	y=7.42+1.13x
CCL8	y=10.73+0.87x
CXCL10	y=5.97+1.10x
MMP2	y=4.74+1.04x
MMP9	-
MMP13	-
TIMP1	y=8.67+0.99x
TIMP3	y=7.67+1.05x
G-CSF	-
M-CSF	y=12.48+0.79x
GM-CSF	-

Statistical analysis

The calculated 'without pre-amplification' values were used for all statistical analyses, meaning that not all targets could be evaluated. Results were otherwise evaluated as before. Samples from lesions were compared as a whole with results from the group 2 MLN, (non-lesional sites were excluded from this analysis). Comparisons were then also made between granulomatous and serosal lesions.

(4). Immunohistology (IH) and Immunofluorescence (IF)

Following RT-qPCR, the genes of most interest for further investigation were chosen as being TLR 2, 4, and 8, upregulated in FIP, and STAT2 which showed an intermediate expression in the FCoV infected control cats. None of these genes had been previously evaluated in FIP and it was hoped to first confirm protein expression by immunohistology and then to correlate this with cell type, cellular location, and co-expression of FCoV. Immunohistology allows better visualisation of cell morphology, whilst for assessing co-expression, immunofluorescence was planned to allow for double labelling. Antibodies directed against FCoV and Iba-1 (a macrophage marker) were already in routine and accredited diagnostic use in the Histology Laboratory at the Institute of Veterinary Pathology and required optimising only for immunofluorescence.
Trialled and final protocols for all antibodies are presented in Tables 4.4.6-8.

Antibody trials

Antibodies were obtained from various sources as shown in Table 4.4.6-8x, based on manufacturers' recommendations regarding their sequence homology and likely cross reactivity. To our and the manufacturers' knowledge, none had been previously tested on feline tissue. An archived diagnostic biopsy of a reactive feline lymph node was used as control tissue. As no published data on expression in feline haemolymphatic tissues was found, whenever possible 'The Human Protein Atlas' (https://www.proteinatlas.org/) was used as an approximate predictor of the staining pattern to be expected.

TLR8

The expectation from function and 'The Human Protein Atlas' was of a low level of macrophage staining. This antibody showed selective cell staining (see Tables 4.4.6 and 4.4.7 for conditions) which could be replicated in IH, IF, and IF double-staining with FCoV.
TLR8 and the routinely used Iba-1 antibody share a common secondary antibody, so could not be used for double labelling. Instead, an alternative Iba-1 was trialled (see Table 4.4.8). This had been used successfully in other species but did not appear to cross-react with feline antigen so that this particular double staining approach could not be further optimised.

TLR2, TLR4, STAT2

'The Human Protein Atlas' only had information available for TLR4, for which moderate staining of cells in the lymph node with a macrophage morphology was expected (no image annotation is provided). None of the trialled reaction conditions (Table 4.4.8) yielded reliable results for any of these antibodies with sections either negative or heavily background stained; these antibodies were not applied to case material.
All IH reactions were visualised by 3,3'-Diaminobenzidine (DAB) chromagen (Dako, Waldbronn, Germany; 1 drop of DAB+ chromagen in 1ml of DAB+ substrate buffer) for 10 min followed by 2 s counterstaining in haematoxylin (Gill no. 1, 20%, Merck).
All IF sections were counterstained with 0.1µg/ml DAPI (Thermo Fisher Scientific) at room temperature for 15 min to visualise nuclei.

Table 4.4.6: Final conditions of antibodies used for immunohistology. aa: amino acid; M: mouse; R: rabbit; M: monoclonal; P: polyclonal; NA: not applicable; basic/acidic antigen retrieval indicate 20 min incubation in pH 9.0 EDTA buffer/pH 6.0 citrate buffer in a pressure cooker set to 98°. HRP: horseradish peroxidase.

Primary antibody							Secondary antibody/detection system and conditions
Directed against	**Immunogen**	**Type**	**Homology with feline**	**Source**	**Antigen retrieval**	**Dilution and incubation**	
FCoV	clone FIPV3-70	MM	NA	Santa Cruz (SC 65653)	Basic	1:200, RT, 1h	Mouse EnVision+ System HRP labelled polymer (Dako)
Iba-1 (anti-human/ rat/mouse)	Synthetic peptide corresponding to C terminus region	RP	unknown	Wako (WDE 1198)	Acidic	1:750, RT, 1h	Rabbit EnVision+ System HRP labelled polymer (Dako)
TLR8 (anti-human)	Recombinant fragment corresponding to aa 849-1041	RP	93%	Abcam (ab180610)	None	1:50, RT, 2h	Rabbit EnVision+ System HRP labelled polymer (Dako)
Iba-1 (anti-human/ rat/mouse)	Synthetic peptide corresponding to C terminus region	RP	unknown	Wako (WDE 1198)	Acidic	1:750, RT, 1h	Rabbit EnVision+ System HRP labelled polymer (Dako)

Table 4.4.7: Final conditions of antibodies used for immunofluorescence. aa: amino acid; M: mouse; R: rabbit; M: monoclonal; P: polyclonal; NA: not applicable; basic/acidic antigen retrieval indicate 20 min incubation in pH 9.0 EDTA buffer/pH 6.0 citrate buffer in a pressure cooker set to 98°.

Primary antibody							Secondary antibody conditions
Directed against	**Immunogen**	**Type**	**Homology with feline**	**Source**	**Antigen retrieval**	**Dilution and incubation**	
FCoV	clone FIPV3-70	MM	NA	Santa Cruz (SC 65653)	Basic	1:50, RT, 1h	Goat anti-mouse 488 (Invitrogen A11001), 1:400, RT, 1h
TLR8 (anti-human)	Recombinant fragment corresponding to aa 849-1041	RP	93%	Abcam (ab180610)	None	1:50, RT, 2h	Goat anti-rabbit 594 (Invitrogen A11012), 1:400, RT, 1h
Iba-1 (anti-human/ rat/mouse)	Synthetic peptide corresponding to C terminus region	RP	unknown	Wako (WDE 1198)	Acidic	1:300, RT, 1h	Goat anti-rabbit 546 (Invitrogen A11010), 1:400, 1h

Table 4.4.8: Details and trialled conditions of unsuccessful antibodies. KLH: Keyhole Limpet Haemocyanin; aa: amino acid; M: mouse; R: rabbit; M: monoclonal; P: polyclonal; RT: room temperature; prot K: proteinase K (Dako, 25 min RT in a 1x solution).

Primary antibody							Secondary antibody/detection system and conditions
Antibody	**Immunogen**	**Type**	**Homology with feline**	**Source**	**Antigen retrieval**	**Dilution and incubation**	
TLR2 (anti-human)	KLH conjugated synthetic peptide corresponding to aa 711-774	RP	95%	Bioorbyt (orb11487)	Basic/acidic	1:50/100; 1h/overnight; RT/4°C	Rabbit EnVision+ System HRP labelled polymer (Dako)
TLR2 (anti-human)	Synthetic peptide corresponding to aa 364-379	RP	88%	Abcam (ab191458)	Basic/acidic /prot K	1:100/300; 1h/overnight; RT/4°C	Rabbit EnVision+ System HRP labelled polymer (Dako)
TLR4 (anti-rat)	KLH-conjugated synthetic peptide encompassing a sequence within the C-term region	RP	unknown	Abbiotec (251111)	Basic/acidic	1:50/100; 1h/overnight; RT/4°C	Rabbit EnVision+ System HRP labelled polymer (Dako)
TLR4 (anti-human)	KLH-conjugated synthetic peptide corresponding to aa 100-200	MM	88%	Abcam (ab22048)	Basic/acidic	1:100/300; 1h/overnight; RT/4°C	Mouse EnVision+ System HRP labelled polymer (Dako)
Iba-1 (anti-human)	Synthetic peptide corresponding to aa 135-147	GP	85%	Abcam (ab5076)	Acidic	1:100; overnight; RT	Donkey anti-goat (Invitrogen A11055), 1:500, 30 min
STAT2 (anti-human)	Recombinant fragment (His-T7-tag) corresponding to aa 616-849	RP	81%	Abcam (ab233177)	Basic/acidic	1:100/200/400/ 500/1000; 1h/overnight; RT/4°C	Rabbit EnVision+ System HRP labelled polymer (Dako)

Immunohistology on case material

All cases had routinely undergone FCoV IH staining (see Chapters 2 and 3) to confirm the absence of lesions in group 1 and the presence of lesions in Group 2. A subset of Group 1 and Group 2 cases were stained for TLR8 and Iba-1 to attempt localisation of TLR8 staining.

Immunofluorescence on case material

Cases and organs selected for IF were those from which cryoblocks and hence LCM sections had also been taken. These were double-stained for TLR8 and FCoV. The aims were to correlate protein expression levels with the RT-qPCR results and to assess the frequency of double-staining.

Staining documentation

All IH and IF slides were first evaluated by AM. Selected cases were scanned to provide appropriate files for digital image analysis. This was performed using a NanoZoomer 2.0HT Hamamatsu slide scanner.

A Nikon Eclipse Ni photomicroscope was used for higher quality photodocumentation of specific regions. Filters applied to the IF images were DAPI (AHF, Tübingen, Germany; F36-500), TRITC (AHF; F36-503), FITC (AHF; F36-501), and TxRed (AHF; F36-504).

Image analysis

The image analysis software Visiopharm was used to classify the images and allow digital quantification. An application protocol package (APP) was created to evaluate the TLR8-FCoV double-IF-stained slides including searching for co-expression. This APP first used thresholding to detect intensity in the DAPI, FITC and TRITC channels (set at 50, 50, and 30 respectively) in order to classify the staining. The following post-processing corrections were then applied:

Classifying nuclei:

- An inversion was applied to the DAPI stain to attempt improved nuclear segregation as many nuclei overlapped in tissues such as the mesenteric lymph node. 255 was then added to the pixels to return a positive value.
- Stained areas smaller than 5 μm^2 were excluded.
- 'Separate by size' at a 4 μm limit was applied, in conjunction with the blob feature to better define nuclei.

Classifying FCoV antigen- and TLR8-positive cells:

- Following thresholding for staining, designed to exclude auto-fluorescent staining of erythrocytes, 'change surrounded' was applied, at a coverage of 0.01.

Classifying overlapping staining:

- As FCoV staining was labelled prior to TLR8 staining, and both are cytoplasmic, overlap would still be labelled for the first marker. Therefore an intensity correction was used to look for staining in the TRITC channel beneath the FITC channel.

The outputs were defined as:

- the count of DAPI stained nuclei in the region of interest (ROI),
- the count of nuclei touching FITC/FCoV staining,
- the count of nuclei touching TRITC/TLR8 staining,
- the count of overlapping cells.

In total, nine regions of interest were selected from the scanned slides. These corresponded to regions taken by LCM from the cryoblocks of the same animal and organ.

5. Selected S gene Sanger sequencing

All samples that had positive FCoV RT-qPCR results and were not already sequenced (i.e. all Zurich samples including LCM samples and a proportion of the Bristol samples) were subjected to conventional PCR and subsequent Sanger sequencing using published primer sequences [133]. Faeces were not subjected to PCR from Zurich cases but Bristol faecal results were evaluated where available from previous sequencing.

The PCR protocol involved 12.5 µl 2x GoTaq master mix, 0.5 µl of 10 µM forward and reverse primer (final concentration 0.25 µM), 9.5 µl molecular grade water, and 2 µl of sample cDNA per reaction, to a total of 25 µl. Primers used were degenerate and had been designed using multiple known FCoV Type I sequences to maximise the binding potential. The primer positions below are given relative to the published genome of FCoV strain C1Je, accession number DQ848678.

Forward: 5'-GCHCARTATTAYAATGGCATAATGG-3'; 23436-23460

Reverse: 5'-AAGYCTRGCYTGYACTTGCAT-3'; 23588-23568

Reaction conditions were as follows; 95°C for 2 min, 40 cycles of 95°C for 15 s, 52°C for 20 s and 72°C for 20 s, before being held at 4°C.

The resulting product was run on a standard 2 % agarose gel for 40 min at 100 V with 5 µl of 6x DNA gel loading dye (Thermo Fisher Scientific) per well, before visualisation using a Benchtop UV Transilluminator (Analytik Jena Ag, Jena, Germany). 5 µl GeneRuler (Thermo Fisher Scientific) was run to either side of the gel. Visible bands were excised using sterile single use scalpel blades and the DNA purified using the MinElute Gel Extraction Kit (Qiagen) according to the manufacturer's instructions. A Nanodrop 2000 (Thermo Fisher Scientific) was then used to determine the correct concentration to be submitted to the commercial laboratory Microsynth for sequencing.

This protocol was tested on a previously sequenced and published sample (no. 58) in addition to two untested samples and was at first trial successful. Using samples with higher FCoV RT-qPCR C_T values however, many PCR products could not be sequenced and a low level of repeatability was noted between runs using positive controls, including one run of all negative results. To troubleshoot this problem, a test sample was run again with the qRT-qPCR protocol for GAPDH and the C_T compared, in case of sample degradation. As the RT-qPCR sequences are slightly shorter and may thus be detected in more degraded samples than longer sequences (though the difference in this case is negligible), RNA was freshly extracted and cDNA newly synthesised. Results were still unreliable therefore a new protocol was developed.

The master mix was changed to Phusion Flash High-Fidelity PCR Master Mix (Thermo Fisher Scientific), containing Phusion Flash II DNA Polymerase which is designed to offer a higher degree of replication fidelity https://www.thermofisher.com/order/catalog/product/F548S. The datasheet states an improvement of 25x in comparison to Taq polymerase, providing a higher chance of sequence amenable DNA from low input samples.

The reaction components (Table 4.5.1) and protocol (Table 4.5.2) were calculated according to the manufacturer's recommendations, though with an increased cycle number based on previous experience with these samples. A 3-step protocol rather than a 2-step protocol was used as Tm

values were lower than recommended for a 2-step one (at least 69°C for primers >20 nucleotides). The manufacturer provides an online calculator (www.thermofisher.com/tmcalculator) as the enzyme has different annealing rules than the Taq polymerase. This does not include degenerate bases in the calculation. Suggested temperatures were: forward primer 62°C, reverse primer 57.6°C. A gradient PCR was then run on a known positive sample (no. 14) ranging from 52 – 65°C over 12 lanes (Table 4.5.3).

Table 4.5.1: Components per reaction for S gene conventional PCR.

Component	**20 µl reaction (µl)**	**Final concentration**
2 x Phusion Flash PCR Master Mix	10	1x
H_2O	6	
Forward primer (10µM)	1	0.5 µM
Reverse primer (10µM)	1	0.5 µM
Template DNA	2	

Table 4.5.2: Reaction conditions for S gene conventional PCR.

Cycle step	**3-step protocol**		**Cycles**
	Temp (°C)	**Time**	
Initial denaturation	98	10 s	1
Denaturation	98	1 s	40
Annealing	See gradient	5 s	
Extension	72	15s/1 kb = 3s	
Final extension	72	1 min	1

Table 4.5.3: Gradient PCR settings and results.

Lane	1	2	3	4	5	6	7	8	9	10	11	12
T °C	52				56.2							65
Result	+	+	+	+	+	+	(+)	-	-	-	-	-

Lanes 1 and 5 were selected as the optimal two lanes, see Fig. 4.5.1 below, producing the brightest and most condensed bands respectively.

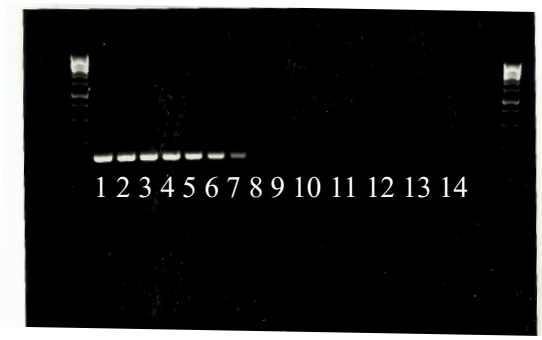

Figure 4.5.1: *Gradient PCR of sample 14 with positive results in lanes 2-8.*

The majority of cases were then sequenced without further problems. Those with a low viral genome level required 50 cycles or in some cases PCR of the purified region of an expected band

(Fig. 4.5.2). First, simple repeat PCR of the product was attempted and compared to PCR of purified product; the former was unsuccessful. For all G1+ cases, in which C_Ts were generally over 35, cDNA was newly synthesised from previously extracted RNA using the SuperScript IV VILO kit (see above, Chapter 3). The product was not diluted as it had previously been for qPCR in order to increase the starting copy number. All of these high C_T cases required double PCR; positive samples were run in alternate lanes to target the regions to be incised.

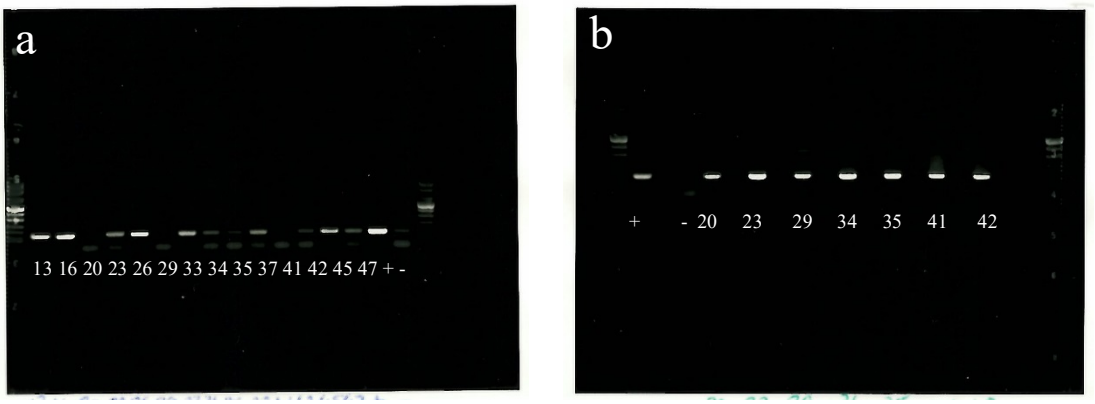

Figure 4.5.2: *a) initial PCR run with no or negligible bands visible for many samples, b) results of second PCR on purified product of initial run.*

6. RNA-Seq by Next Generation Sequencing (NGS)

Samples were chosen for RNA-Seq on the basis of RT-qPCR results. Mesenteric lymph node samples from each of Groups 1-, 1+ and 2 were submitted for initial quality testing. This was performed on a Bioanalyzer 2100 (Agilent, Waldbronn, Germany) based in the Functional Genomics Centre Zurich (FGCZ) a Core Facility of the University of Zurich, to obtain a RIN (RNA integrity number). Among the Bristol samples were occasional samples of very low quality, despite performing satisfactorily with RT-qPCR. This may be related to the thawing in transport, meaning not all samples were available to select from.

To utilise a complete run (recommended by the FGCZ for this protocol as 15 samples), three bulk MLN samples from each group were selected, in addition to six MLN LCM samples. Three is the mathematical minimum number of biological replicates required in order to reliably group results and be able to spot outliers (if two samples give different results the difference could be real or due to error in one, but which one could not be determined; as for PCR replicates).

All samples were DNase treated with the Superscript IV VILO ezDNase step as described above (Chapter 3). Before application of this method to all samples, sample quality with and without this treatment was compared with no deleterious effect on concentration detected.

Steps subsequent to RNA extraction and cleaning were carried out by the FGCZ.

The final submitted cases were as in Table 4.6.1 below.

Table 4.6.1: Cases used for RNA-Seq NGS. The starred sample failed the pre-sequencing quality checks so is not included in the results section. Superscript E indicates effusions, and L lesions. All LCM samples were granulomatous.

		Group and sample number			
NGS sample number	**Case number**	**G1- (G1)**	**G2**	**G1+ (G3)**	**LCM**
p2762_4449/1	56	64			
p2762_4449/2	S17-0409	51			
p2762_4449/3	S17-0568	55			
p2762_4449/4	42		$61^{E,L}$		
p2762_4449/5	128		89^{L}		
p2762_4449/6	94		73^{E}		
p2762_4449/7	38			60	
p2762_4449/8	132			91	
p2762_4449/9	135			92	
p2762_4449/10	S15-0983				116*
p2762_4449/11	S15-1539				117
p2762_4449/12	S15-1728				118
p2762_4449/13	S16-0167				119
p2762_4449/14	S16-0454				120
p2762_4449/15	S17-0124				121

Two methods were applied, one to the standard MLN samples, and one to the LCM samples, owing to the huge differences in starting concentrations.

Library preparation for samples p2762_4449/1-9 (bulk MLN)

The quality of the isolated RNA was determined with a Qubit® (1.0) Fluorometer (Life Technologies, California, USA) and a Bioanalyzer 2100. Only those samples with a 260 nm/280 nm ratio between 1.8–2.1 and a 28S/18S ratio within 1.5–2 were further processed. The TruSeq RNA Sample Prep Kit v2 (Illumina, Inc, California, USA) was used, following the manufacturer's protocol. Briefly, total RNA samples (100-1000 ng) were poly A enriched and then reverse-transcribed into double-stranded cDNA. The cDNA samples were fragmented, end-repaired and polyadenylated before ligation of TruSeq adapters to each end. These contain the index for multiplexing fragments and were selectively enriched by PCR. The quality and quantity of the enriched libraries were validated using Qubit® (1.0) Fluorometer and the Caliper GX LabChip® GX (Caliper Life Sciences, Inc., USA). The product is a smear with an average fragment size of approximately 260 bp. The libraries were normalized to 10nM in Tris-Cl 10 mM, pH8.5 with 0.1% Tween 20.

Oligonucleotide adapter sequences for TruSeq™ RNA and DNA Sample Prep Kits were as follows, in order from sample 1-9:

TruSeq Universal Adapter

5' AATGATACGGCGACCACCGAGATCTACACTCTTTCCCTACACGACGCTCTTCCGATCT

TruSeq™ Adapters

TruSeq Adapter, Index 1

5’ GATCGGAAGAGCACACGTCTGAACTCCAGTCAC**ATCACG**ATCTCGTATGCCGTCTTCTGCTTG

TruSeq Adapter, Index 2

5’ GATCGGAAGAGCACACGTCTGAACTCCAGTCAC**CGATGT**ATCTCGTATGCCGTCTTCTGCTTG

TruSeq Adapter, Index 3

5’ GATCGGAAGAGCACACGTCTGAACTCCAGTCAC**TTAGGC**ATCTCGTATGCCGTCTTCTGCTTG

TruSeq Adapter, Index 4

5’ GATCGGAAGAGCACACGTCTGAACTCCAGTCAC**TGACCA**ATCTCGTATGCCGTCTTCTGCTTG

TruSeq Adapter, Index 5

5’ GATCGGAAGAGCACACGTCTGAACTCCAGTCAC**ACAGTG**ATCTCGTATGCCGTCTTCTGCTTG

TruSeq Adapter, Index 6

5’ GATCGGAAGAGCACACGTCTGAACTCCAGTCAC**GCCAAT**ATCTCGTATGCCGTCTTCTGCTTG

TruSeq Adapter, Index 7

5’ GATCGGAAGAGCACACGTCTGAACTCCAGTCAC**CAGATC**ATCTCGTATGCCGTCTTCTGCTTG

TruSeq Adapter, Index 8

5’ GATCGGAAGAGCACACGTCTGAACTCCAGTCAC**ACTTGA**ATCTCGTATGCCGTCTTCTGCTTG

TruSeq Adapter, Index 9

5’ GATCGGAAGAGCACACGTCTGAACTCCAGTCAC**GATCAG**ATCTCGTATGCCGTCTTCTGCTTG

Cluster generation and sequencing

The TruSeq SR Cluster Kit HS4000 (Illumina) was used for cluster generation using 10 pM of pooled normalised libraries on the cBOT. Sequencing was performed on the Illumina HiSeq 4000 single end 100 bp using the TruSeq SBS Kit HS4000.

Library preparation for samples p2762_4449/10-15 (LCM)

The quantity and quality of the isolated RNA was determined with a Qubit® (1.0) Fluorometer (Life Technologies) and a Tapestation (Agilent). The SMARTer Stranded Total RNA-Seq Kit - Pico Input Mammalian (Clontech Laboratories, California, USA) was then used, following the manufacturer’s protocol. Briefly, total RNA samples (0.25–10 ng) were reverse-transcribed using random priming into double-stranded cDNA in the presence of a template switch oligo (TSO). When the reverse transcriptase reaches the 5’ end of the RNA fragment, the enzyme’s terminal transferase activity adds non-templated nucleotides to the 3’ end of the cDNA. The TSO pairs with the added non-templated nucleotide, enabling the reverse transcriptase to continue replicating to the end of the oligonucleotide. This results in a cDNA fragment that contains sequences derived from the random priming oligo and the TSO. PCR amplification using primers binding to these sequences can now be performed. The PCR adds full-length Illumina adapters, including the index for multiplexing. Ribosomal cDNA is cleaved by ZapR in the presence of the mammalian-specific R-Probes. The remaining fragments are enriched by a second round of PCR amplification using primers designed to match Illumina adapters.

The quality and quantity of the enriched libraries were validated using Qubit® (1.0) Fluorometer and the Tapestation (Agilent)**.** The product is a smear with an average fragment size of

approximately 360 bp. The libraries were normalized to 10nM in Tris-Cl 10 mM, pH8.5 with 0.1% Tween 20.

All samples used the i7 Index R3 adapter sequence CGCTCATT, together with i5 index adapter sequences as follows:

sample 10	F1	TATAGCCT
sample 11	F2	ATAGAGGC
sample 12	F3	CCTATCCT
sample 13	F4	GGCTCTGA
sample 14	F5	AGGCGAAG
sample 15	F6	TAATCTTA

Cluster generation and sequencing was performed as for samples 1-9.

Data Analysis

In the main analysis comparing the G- and LCM groups, reads were quality-checked with FastQC. Sequencing adapters were removed with Trimmomatic [308] and reads were hard-trimming by 5 bases at the 3' end. Successively, reads at least 20 bases long, and with an overall average phred quality score greater than 10 were aligned to the reference genome and transcriptome of *Felis Catus* (FASTA and GTF files, respectively, downloaded from Ensembl, build 6.2) with STAR v2.5.1 [309] with default settings for single end reads. In this Ensembl build, genes TLR7 and TLR9 are not annotated, therefore the UCSC build *felCat5* was used instead to estimate the expression of those two genes.
Distribution of the reads across genomic isoform expression was quantified using the R package GenomicRanges [310] from Bioconductor Version 3.0. Differentially expressed genes (DE) were identified using the R package edgeR [311] from Bioconductor Version 3.0.
A gene is marked as DE if it possesses the following characteristics:

- at least 10 counts in at least half of the samples in one group;
- $p \leq 0.01$
- fold change ≥ 2

The Gene Ontology (GO) gene set analysis was performed via a contingency table-based Fisher's exact test.
Additionally, a quantification of the viral transcriptome in the different samples was attempted. The reference Feline Coronavirus (Accession DQ848678) was obtained from uniprot and RSEM v1.2.31 [312] was used to directly estimate the expression of the viral segments.

Results

1. RT-qPCR on bone marrow and spleen

The entire panel of immune mediators were expressed constitutively by both organs with only rare negative results. The latter were most frequent for IL-17 which was always recorded at a high C_T, indicating the levels were close to the detection limit and hence not always measurable in this system. In the control group, for all targets except MMP9 and MMP13 mRNA levels were higher in the spleen than in the bone marrow (BM), frequently without overlap between groups. Results are summarised in Figs. 5.1.1-7 and Table 5.1.1.

FCoV

Nine of the eleven cats with FIP (G2) for which the BM was available for testing had detectable FCoV in the BM. This was despite negative FCoV IH from all cases. The samples for routine embedding were of course not the same samples as those used for PCR, but this finding is consistent with previous findings in the BM [48]. All fourteen cats with FIP had detectable FCoV in the spleen and at a higher level than in the BM with no overlap of the interquartile ranges between organs. This corresponds to the observed histological lesions present in most, and the FCoV positivity observed in all. There was no FCoV detectable in either organ of cats without FIP (G1; n=6). See Fig. 5.1.1.

Toll-like receptors

TLR9 mRNA levels were significantly higher in G2 for both organs whilst TLR1 and 6 were significantly lower in the BM and TLR3 and 6 significantly lower in the spleen. TLR2, 5, and 7 showed a trend to be increased in the BM with the opposite shown by TLR3. In the spleen, the same tendencies were observed, however, here the increase in TLR2 and decrease in TLR3 reached significance. See Fig. 5.1.2.

Cytokines and chemokines

Of the pyrogenic triad of IL-1β, IL-6 and TNF-α, only IL-1β was significantly increase in G2, and only in the BM. However, all three showed a slight trend to increase in the spleen whereas only IL-6 levels showed no tendency in the BM. IL-15 and IL-17 were both negligibly altered. The chemokines CCL8 and CXCL10 were both significantly increased in G2 in the spleen, whilst in the BM both were increased but only CXCL10 significantly so. Of the predominantly anti-inflammatory cytokines IL-10 and TGF-β, the latter was significantly reduced in G2 for both organs with no change in IL-10. See Fig. 5.1.3.

Interferons

A significant increase in IFN-β was observed in both organs in G2. For IFN-γ a significant increase was observed in the spleen only, with little change in the BM, whilst for IFN-α both organs showed a non-significant slight increase. See Fig. 5.1.4

STATs

Both organs showed significantly increased STAT1 and 2 mRNA levels in G2, with no change in STAT3. See Fig. 5.1. 5

Matrix remodelling enzymes

In the BM, MMP2 and MMP9 were significantly lower in G2, whereas in the spleen, MMP2 and MMP13 were significantly lower. TIMP1 and 3 were significantly lower in G2 for both organs. See Fig. 5.1.6

Colony stimulating factors

Within the BM, both G- and M-CSF were significantly lower in G2, and the latter was also significantly lower in the spleen. See Fig. 5.1.7.

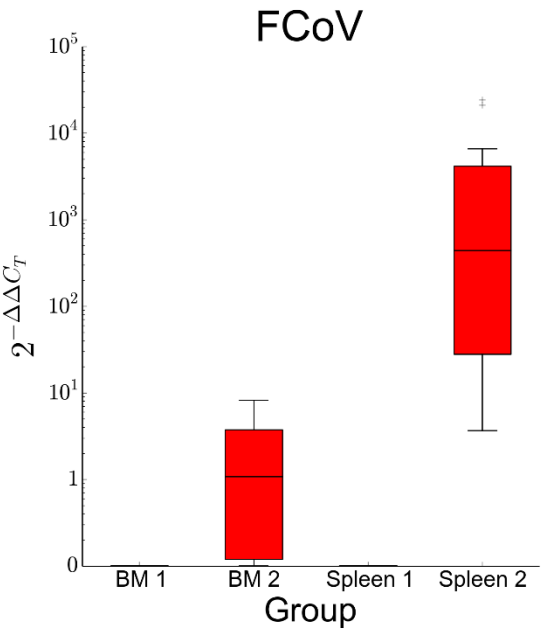

Figures 5.1.1: *Boxplots of relative levels of FCoV in each group.*

Groups 1 and 2 refer to the control cases and FIP cases respectively. The amount of target was calculated by $2^{-\Delta\Delta CT}$, using fGAPDH as the internal reference gene for normalisation and expressed as an n-fold difference relative to the G1 mean of the BM samples as a calibrator. The boxes depict the median and interquartile (IQ) range with whiskers extending to the highest and lowest values which are within 1.5 x the IQ range. Outliers beyond this are individually marked.

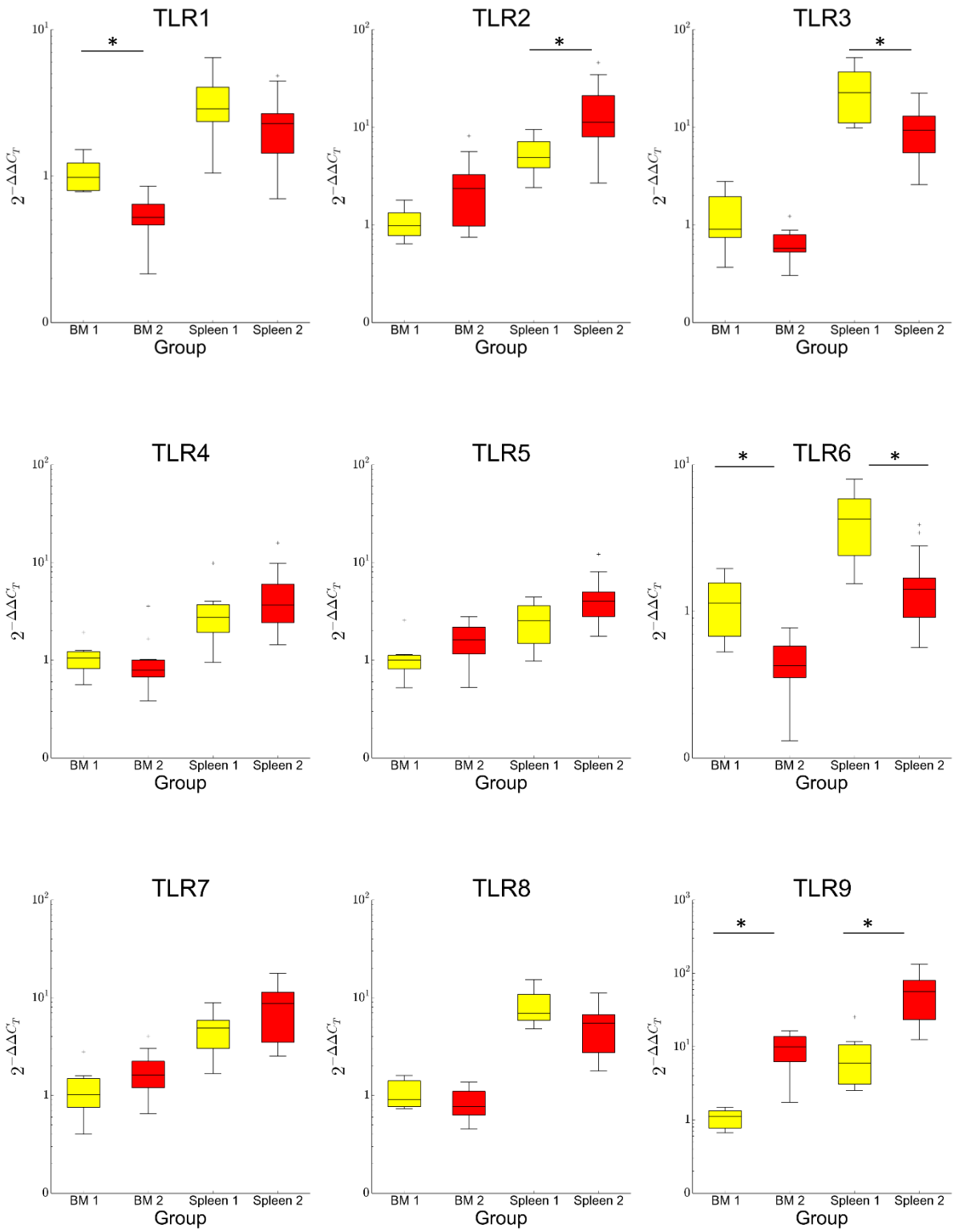

Figures 5.1.2: *Boxplots of relative mRNA levels of Toll-like receptors in each group.*

*Groups 1 and 2 refer to the control cases and FIP cases respectively. The amount of target was calculated by $2^{-\Delta\Delta CT}$, using fGAPDH as the internal reference gene for normalisation and expressed as an n-fold difference relative to the G1 mean of the BM samples as a calibrator. The boxes depict the median and interquartile (IQ) range with whiskers extending to the highest and lowest values which are within 1.5 x the IQ range. Outliers beyond this are individually marked. * marks significant differences between groups (p≤0.05).*

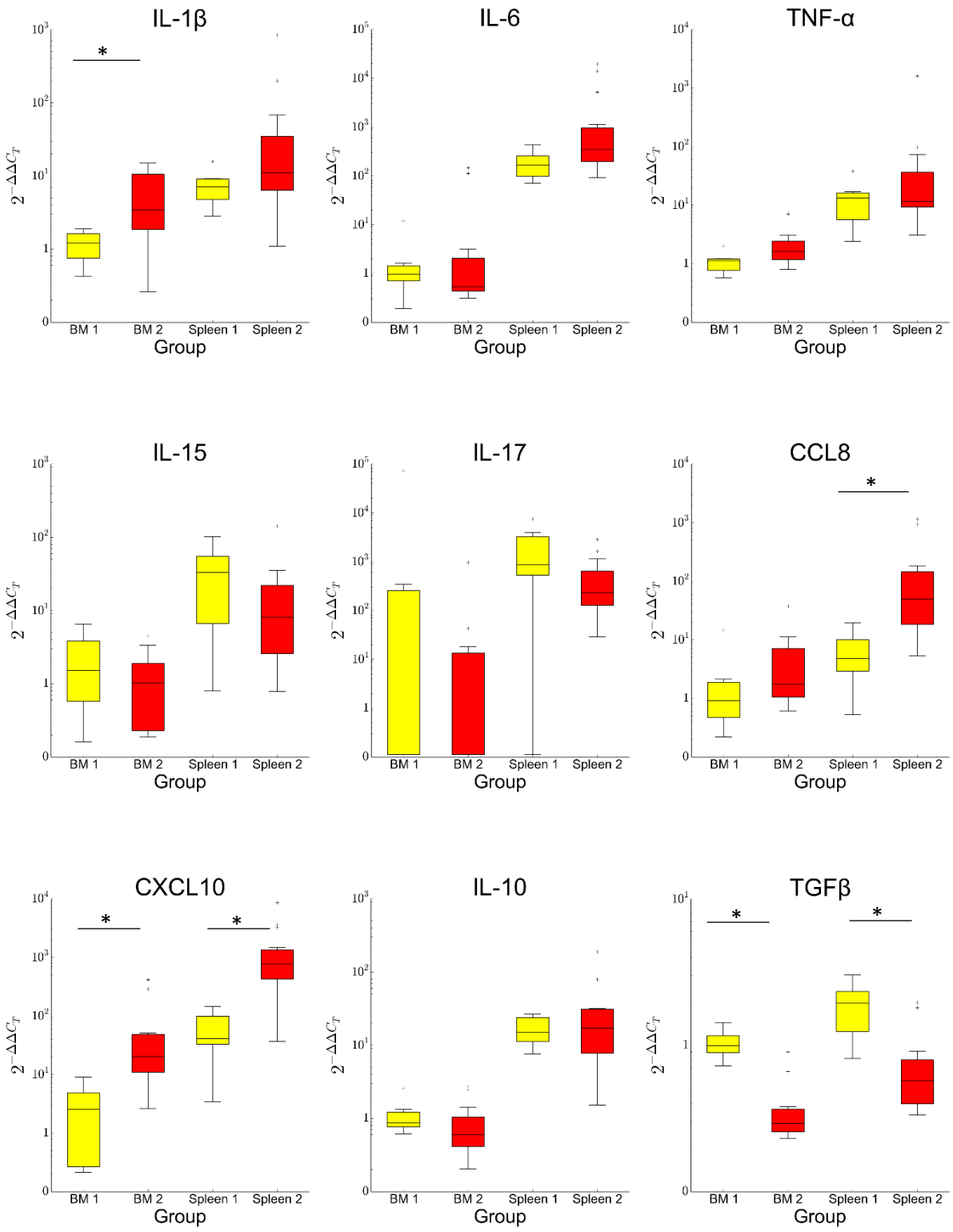

Figures 5.1.3: *Boxplots of relative mRNA levels of cytokines and chemokines in each group.*

*Groups 1 and 2 refer to the control cases and FIP cases respectively. The amount of target was calculated by $2^{-\Delta\Delta CT}$, using fGAPDH as the internal reference gene for normalisation and expressed as an n-fold difference relative to the G1 mean of the BM samples as a calibrator. The boxes depict the median and interquartile (IQ) range with whiskers extending to the highest and lowest values which are within 1.5 x the IQ range. Outliers beyond this are individually marked. * marks significant differences between groups (p≤0.05).*

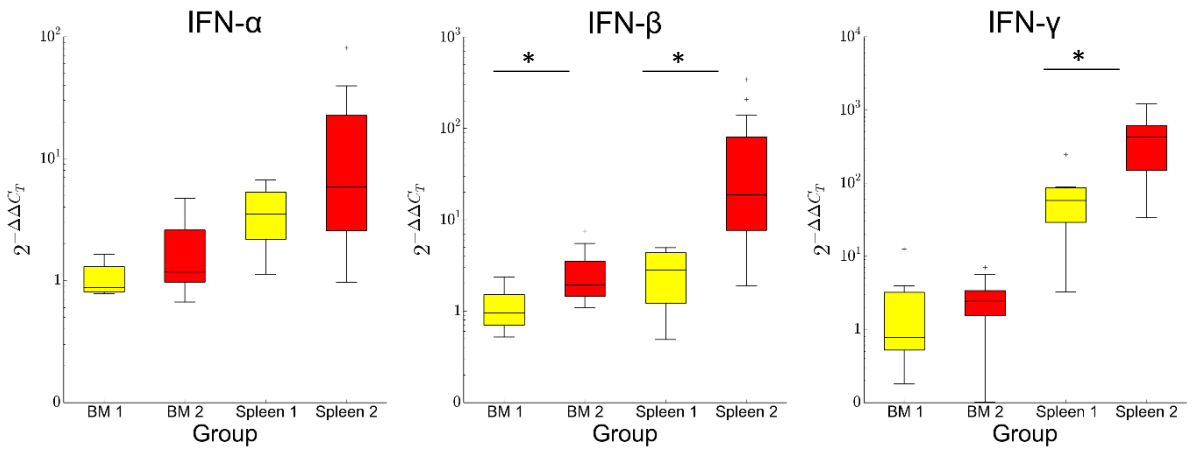

Figures 5.1.4: *Boxplots of relative mRNA levels of interferons in each group.*

*Groups 1 and 2 refer to the control cases and FIP cases respectively. The amount of target was calculated by $2^{-\Delta\Delta CT}$, using fGAPDH as the internal reference gene for normalisation and expressed as an n-fold difference relative to the G1 mean of the BM samples as a calibrator. The boxes depict the median and interquartile (IQ) range with whiskers extending to the highest and lowest values which are within 1.5 x the IQ range. Outliers beyond this are individually marked. * marks significant differences between groups (p≤0.05).*

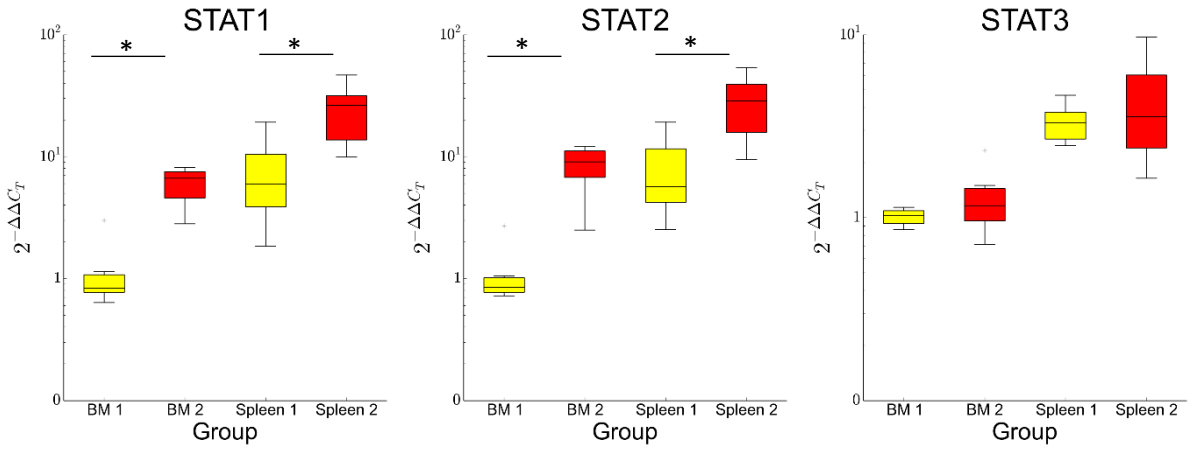

Figures 5.1.5: *Boxplots of relative mRNA levels of STATs in each group.*

Groups 1 and 2 refer to the control cases and FIP cases respectively. The amount of target was calculated by $2^{-\Delta\Delta CT}$, using fGAPDH as the internal reference gene for normalisation and expressed as an n-fold difference relative to the G1 mean of the BM samples as a calibrator. The boxes depict the median and interquartile (IQ) range with whiskers extending to the highest and lowest values which are within 1.5 x the IQ range. Outliers beyond this are individually marked. * marks significant differences between groups (p≤0.05).

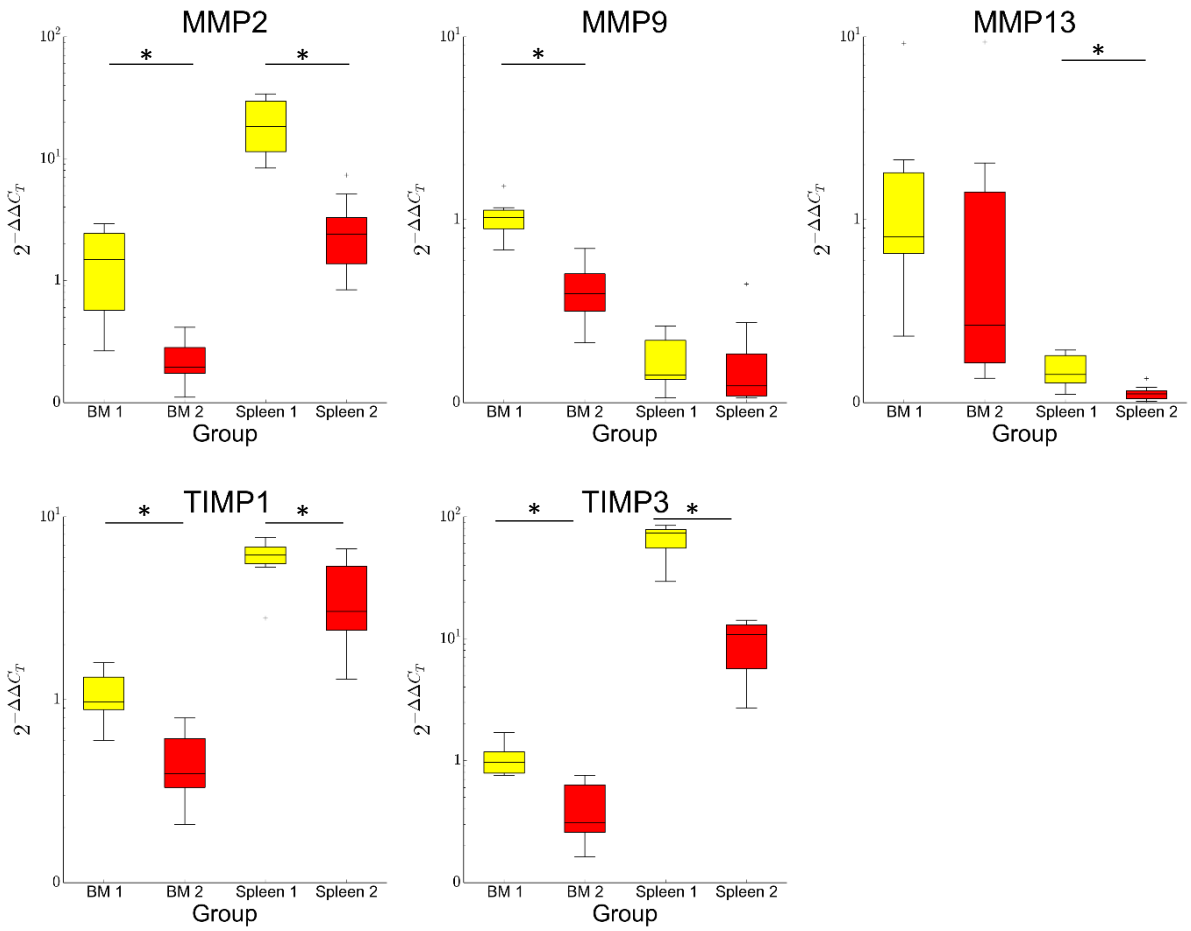

Figures 5.1.6: *Boxplots of relative mRNA levels of matrix remodelling enzymes in each group.*

Groups 1 and 2 refer to the control cases and FIP cases respectively. The amount of target was calculated by $2^{-\Delta\Delta CT}$, using fGAPDH as the internal reference gene for normalisation and expressed as an n-fold difference relative to the G1 mean of the BM samples as a calibrator. The boxes depict the median and interquartile (IQ) range with whiskers extending to the highest and lowest values which are within 1.5 x the IQ range. Outliers beyond this are individually marked. * marks significant differences between groups (p≤0.05).

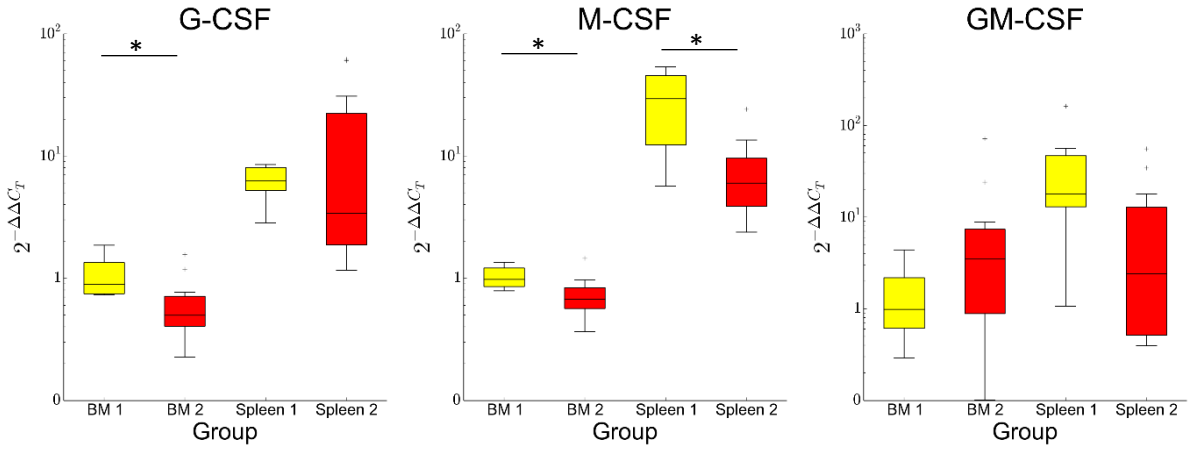

Figures 5.1.7: *Boxplots of relative mRNA levels of colony stimulating factors in each group.*

Groups 1 and 2 refer to the control cases and FIP cases respectively. The amount of target was calculated by $2^{-\Delta\Delta CT}$, using fGAPDH as the internal reference gene for normalisation and expressed as an n-fold difference relative to the G1 mean of the BM samples as a calibrator. The boxes depict the median and interquartile (IQ) range with whiskers extending to the highest and lowest values which are within 1.5 x the IQ range. Outliers beyond this are individually marked. * marks significant differences between groups (p≤0.05).

Table 5.1.1: Statistical results of Mann-Whitney test, comparing G1 vs G2 for bone marrow and spleen. Highlighted results indicate p≤0.05 and arrows indicate whether G2 was higher or lower.

	BM		**spleen**	
Target	**G1 vs G2**		**G1 vs G2**	
TLR1	0.001	↓	0.274	
TLR2	0.062		0.015	↑
TLR3	0.216		0.033	↓
TLR4	0.404		0.444	
TLR5	0.149		0.130	
TLR6	0.005	↓	0.009	↓
TLR7	0.216		0.179	
TLR8	0.350		0.130	
TLR9	0.000	↑	0.001	↑
STAT1	0.000	↑	0.002	↑
STAT2	0.000	↑	0.003	↑
STAT3	0.301		1.000	
IFN-α	0.149		0.239	
IFN-β	0.020	↑	0.001	↑
IFN-γ	0.404		0.003	↑
IL-1β	0.048	↑	0.153	
IL-6	0.591		0.051	
IL-10	0.149		0.779	
IL-15	0.404		0.397	
IL-17	0.884		0.207	
TNF-α	0.098		0.659	
TGF-β	0.001	↓	0.002	↓
CCL8	0.216		0.003	↑
CXCL10	0.007	↑	0.000	↑
MMP2	0.003	↓	0.000	↓
MMP9	0.000	↓	0.494	
MMP13	0.216		0.003	↓
TIMP1	0.001	↓	0.041	↓
TIMP3	0.000	↓	0.000	↓
G-CSF	0.027	↓	0.602	
M-CSF	0.037	↓	0.015	↓
GM-CSF	0.216		0.051	

2. Accepted manuscript

The following accepted manuscript includes results from the MLN RT-qPCR experiments and part of the Sanger sequencing work, such that there is some overlap between chapters. Related and further results which were not included in the manuscript are presented subsequently. Alternative graphs are also displayed for this chapter, as the manuscript focussed on the MLN only. RT-qPCR results were calculated by the $\Delta\Delta C_T$ method, relative to levels of the reference gene GAPDH and calibrated to the mean of the control group ΔC_T levels for each target. This calibrator was the MLN control group for the publication in order for the results to be stand-alone. However, the BM control group was used for these additional graphs, as in the previous chapter, for comparability between organs (this affects the y axis of the graphs but has no effect on the statistics as the same function is applied to all results for a given target).

Manuscript title: "**Inflammatory mediators in the mesenteric lymph nodes, site of a possible intermediate phase in the immune response to feline coronavirus and the pathogenesis of feline infectious peritonitis?"**

Author's contribution:

AM was responsible for case collection and the pathological investigations undertaken on the Zurich cases. AM carried out all laboratory work (with the exception of certain Bristol sequencing results as stated in the manuscript), data evaluation, figure production, and writing, with input and advice from all co-authors, but in particular AK and MM.

J. Comp. Path. 2019, Vol. 166, 69–86

Available online at www.sciencedirect.com

ScienceDirect

ELSEVIER

www.elsevier.com/locate/jcpa

INFECTIOUS DISEASE

Inflammatory Mediators in the Mesenteric Lymph Nodes, Site of a Possible Intermediate Phase in the Immune Response to Feline Coronavirus and the Pathogenesis of Feline Infectious Peritonitis?

A. J. Malbon[*,†,‡], M. L. Meli[‡,§], E. N. Barker[¶], A. D. Davidson[#], S. Tasker[‖] and A. Kipar[*,††]

[*] Institute of Veterinary Pathology, Vetsuisse Faculty, University of Zurich, [†] Graduate School for Cellular and Biomedical Sciences, Bern, [‡] Center for Clinical Studies, [§] Clinical Laboratory, Vetsuisse Faculty, University of Zurich, Switzerland, [¶] Langford Vets, Langford House, [‖] Bristol Veterinary School, [#] School of Cellular and Molecular Medicine, Faculty of Life Sciences, University of Bristol and [††] Institute of Global Health, Faculty of Health and Life Sciences, University of Liverpool, UK

Summary

Feline infectious peritonitis (FIP) is an almost invariably fatal feline coronavirus (FCoV)-induced disease thought to arise from a combination of viral mutations and an overexuberant immune response. Natural initial enteric FCoV infection may remain subclinical, or result in mild enteric signs or the development of FIP; cats may also carry the virus systemically with no adverse effect. This study screened mesenteric lymph nodes (MLNs), the presumed first site of FCoV spread from the intestine regardless of viraemia, for changes in the transcription of a panel of innate immune response mediators in response to systemic FCoV infection and with FIP, aiming to identify key pathways triggered by FCoV. Cats with and without FIP, the latter with and without FCoV infection in the MLN, were compared. Higher expression levels in FIP were found for toll-like receptors (TLRs) 2, 4 and 8. These are part of the first line of defence and suggest a response to both viral structural proteins and viral nucleic acid. Expression of genes encoding inflammatory cytokines and chemokines, including interleukin (IL)-1β, IL-6, IL-15, tumour necrosis factor (TNF)-α, CXCL10, CCL8, interferon (IFN)-α, IFN-β and IFN-γ, was higher in cats with FIP, consistent with inflammatory pathway activation. Expression of genes encoding transcription factors STAT1 and 2, regulating signalling pathways, particularly of the interferons, was also higher. Among cats without FIP, there were few differences between virus-positive and virus-negative MLNs; however, TLR9 and STAT2 expression were higher with infection, suggesting a direct viral effect. The study provides evidence for TLR involvement in the response to FCoV. This could open up new avenues for therapeutic approaches.

Keywords: cytokines; feline coronavirus; mesenteric lymph nodes; toll-like receptors

Introduction

Feline infectious peritonitis (FIP) is a well-known and widely distributed coronavirus-induced disease of felids. With as yet no effective vaccine or viable treatment options, FIP is almost invariably fatal, and understanding the pathogenetic and immunological mechanisms involved in disease development is crucial to aiding chances of combating FIP and identifying novel avenues for possible treatment.

After initial enteric infection, feline coronavirus (FCoV) may spread beyond the intestine, resulting

Correspondence to: A. Kipar (e-mail: anja.kipar@uzh.ch).

0021-9975/$ - see front matter
https://doi.org/10.1016/j.jcpa.2018.11.001

in a monocyte-associated viraemia, with or without the development of FIP. In cases progressing to FIP, which may have a time lag of weeks to years, viral and host factors combine to turn an initial, usually subclinical, enteritis into an overt immune-mediated disease (Pedersen *et al.*, 1981; Kipar and Meli, 2014). Much research has focussed on viral mutations and has partially elucidated the function of various viral proteins in the pathogenesis of FIP. The viral spike (S) protein gene has been of particular interest, and a switch from methionine (M) to leucine (L) at amino acid residue 1,058 (M1058L) has been strongly associated with a gain of virulence (Chang *et al.*, 2012). A second switch from serine (S) to alanine (A) at amino acid residue 1,060 (S1060A) distinguished tissue-associated FCoV in a further small subset of FIP cases from FCoV shed with the faeces by healthy cats (Chang *et al.*, 2012). These mutations have since been associated with systemic spread of FCoV, rather than providing proof of virulence (Porter *et al.*, 2014; Barker *et al.*, 2017; Felten *et al.*, 2017a), so the two forms are subsequently referred to here as 'systemic' and 'enteric' FCoV.

Early experiments demonstrated that not all cats are susceptible to FCoV infection, even with known pathogenic strains (Pedersen and Boyle, 1980), indicating the importance of host genetic factors/immune mechanisms in disease development. More recently it was shown that cultured monocytes from different cats vary in their ability to sustain viral replication, again suggesting that there is a subset of animals who can resist disease (Dewerchin *et al.*, 2005; Tekes *et al.*, 2010). Monocytes/macrophages are not the only cell type beyond enterocytes that may be infected by FCoV, but they are also key cells in the innate immune defence system. They are able to detect pathogen-associated molecular patterns (PAMPs), triggering a number of intracellular signalling pathways leading to activation of an antiviral state in the host (Abbas *et al.*, 2017). Chief amongst these pathways are those triggered by engagement of toll-like receptors (TLRs); highly evolutionarily conserved, membrane-bound pathogen recognition receptors (PRRs) (Lester and Li, 2014). Their presence on both the cell surface membrane and internal membrane-bound vesicles allows detection of external and internal PAMPs; their ligands include those associated with viruses, bacteria and fungi (Arpaia and Barton, 2011). Downstream mediators include inflammatory cytokines and interferons that have been assessed in cats with FIP, with sometimes conflicting results (Dean *et al.*, 2003; Kipar *et al.*, 2006b). Interferons and the inflammatory cytokine interleukin (IL)-6 can activate members of the signal transducer and regulator of transcription (STAT) family with downstream effects on replication, differentiation or inflammatory potential (Aaronson and Horvath, 2002). Cats with a compromised immune system appear to be more susceptible to FIP, while, paradoxically, the lesions are caused by an excessive immune response (Pedersen, 1987, 2014; Kipar and Meli, 2014). This has been attributed, at least in part, to increased viral replication in immunosuppressed animals and, therefore, an increased likelihood of viral mutations occurring and accumulating (Poland *et al.*, 1996).

TLRs have been associated with susceptibility to many diseases, including chronic inflammatory, viral and more specifically coronaviral diseases (e.g. severe acute respiratory syndrome, SARS) (Dosch *et al.*, 2009). Intriguingly though, both TLR stimulation and antagonism/knock-outs have contributed to exacerbation of disease in different contexts and there exists considerable crossover between receptors and their potential ligands (Arpaia and Barton, 2011).

When FCoV is able to leave the intestine, the mesenteric lymph nodes (MLNs) are the presumed first site of viral spread, potentially representing the interface between local and systemic immune response; support for this assumption are FIP cases that present only with MLN lesions (Kipar *et al.*, 1999). We therefore chose the MLN as our organ of interest, with the aim of comparing key mediators of the innate immune system between uninfected cats and FCoV-infected cats with and without FIP. We hypothesized that in addition to an excessive pro-inflammatory cytokine response, there would be a deficient interferon response, and aimed to gain an insight into which TLR pathways are involved in triggering this response. We also wished to further evaluate the presence and significance of previously published viral S gene variations and determine whether a connection with the host immune response could be detected.

Materials and Methods

Case Selection

The study was undertaken on cats that had all been seen initially as patients at the university small animal clinics and local veterinary practices of Bristol, UK, or Zurich, Switzerland, and humanely destroyed with or without FIP for clinical reasons unrelated to this study (Table 1). A post-mortem examination was performed on each cat with owner consent and samples of MLN were collected into RNAlater® (Qiagen, Hombrechtikon, Switzerland) within 2 h of

Table 1A
Signalment, histological and immunohistochemical findings and Sanger sequencing results of all cases. Group 1−: cats without FIP and without evidence of systemic FCoV infection

	Breed	*Age*	*Sex*	*Diagnosis*	*Mesenteric lymph node*	
					Histology	*IHC (FCoV Ag)*
1	Ragdoll	4 y	MN	Congestive heart failure	Normal	–
2	Bengal	11 y	MN	Colonic adenocarcinoma	Normal	ND
3	DSH	Adult	FN	DCM, chronic kidney disease	Follicular hyalinosis	–
4	DSH	Adult	MN	Acute myeloid leukaemia	Leukaemia	–
5	Birma	1 y	MN	Hippocampal necrosis	Normal	–
6	House cat	14 y	MN	Haemorrhage in brain	Follicular hyalinosis	ND
7	DSH	8 y	MN	Chemodectoma	Normal	–
8	Birman	13 y		Pyothorax and pneumonia	Neutrophilic and histiocytic inflammation	–
9	DSH	6 y	MN	Astrocytoma	Normal to reactive hyperplasia	–
10		10 y	MN	Diabetes mellitus	Reactive hyperplasia and amyloidosis	–
11	DSH	12 y		Aplastic anaemia	Neutrophilic inflammation	–
12	DSH	6 y		Diarrhoea, suspected torovirus	ND	ND
13	DLH	8 y		Gastric lymphoma	Normal	–
14	DSH	5 y	MN	Suppurative meningitis	Mild depletion	–
15	DSH	3 y	MN	Lymphocytic cholangiohepatitis	Normal to reactive hyperplasia	ND
16	DSH	2 y	MN	Hepatitis and pyelonephritis	Reactive hyperplasia and sinus histiocytosis	–
17	DSH	4 y	FN	Granulomatous rhinitis and encephalitis	ND	ND
18	DSH	8 y	FN	Chronic enteropathy	ND	ND
19	DSH	1 y	FN	Poxviral pneumonia	ND	ND
20	DSH	4 y	FN	Hepatic encephalopathy	ND	ND
21	Ragdoll	3 y	MN	Hypertrophic cardiomyopathy	ND	ND
22	DSH	13 y	FN	Focal intestinal necrosis	Normal	ND
23	DSH		F	Behavioural	Normal to reactive hyperplasia	–
24	DSH	3 y	FN	Invasive meningioma	Normal to reactive hyperplasia	–
25	Maine Coon	9 y		Meningoencephalitis	Normal	–
26	DSH	5 y	FN	Pulmonary adenocarcinoma	Tumour emboli	ND
27	Devon Rex	8 y		Inflammatory bowel disease	Normal	–
28	DSH	9 y	MN	Multicentric lymphoma	Reactive hyperplasia	–
29	DSH	10 m	MN	Hypertrophic cardiomyopathy	Reactive hyperplasia and sinus histiocytosis	–
30	Bengal	7 y	FN	Jejunal constriction	Follicular depletion	–

FIP, feline infectious peritonitis; FCoV, feline coronavirus; MLN, mesenteric lymph node; IHC, immunohistochemistry; Ag, antigen; DSH, domestic shorthair; DLH, domestic longhair; blank, data not available; F, female; M, male; FN, female neutered; MN, male neutered; DCM, dilated cardiomyopathy; ND, not done; –, negative.

euthanasia and stored at −80°C until use. The Bristol cases form part of the University of Bristol FIP Biobank built up as a resource for multiple studies; many of these cases were utilized previously (Porter *et al.*, 2014; Barker *et al.*, 2017).

Group 1 (G1) comprised of 40 control cats confirmed to not have FIP and with an alternate confirmed diagnosis (Tables 1A and 1B), and group 2 (G2) consisted of 30 cats confirmed to have FIP (Table 1C). A diagnosis of FIP was based on relevant clinical findings and compatible gross and/or histological lesions together with immunohistological demonstration of FCoV antigen-positive macrophages within typical lesions (Kipar *et al.*, 1998). The immunohistochemistry was carried out as previously described (Kipar *et al.*, 1998), using a mouse monoclonal primary antibody (clone FIPV3-70 SC 65653, Santa Cruz, Heidelberg, Germany). Based on the results of the reverse transcriptase quantitative polymerase chain reaction (RT-qPCR) for FCoV undertaken on the MLNs, group G1 was then subdivided into G1+ (FCoV positive) and G1− (FCoV negative).

RNA Extraction and cDNA Synthesis

RNA extraction was carried out using the RNeasy Plus Minikit® (Qiagen) according to the manufacturer's protocol. Briefly, 30 mg of MLN tissue were disrupted in extraction buffer using a tissue homogenizer (Mixer-Mill 300, Retsch, Haan, Germany) for 40 sec at 30 Hz before on-column extraction and elution of RNA. As pilot tests revealed that significant genomic DNA contamination remained, an optional DNase step was included prior to use of the Superscript IV VILO® kit (ThermoFisher Scientific, Waltham, Massachusetts, USA) for cDNA synthesis, following the manufacturer's instructions, in order

Table 1B
Group 1+: cats without FIP, but with evidence of systemic FCoV infection

	Breed	*Age*	*Sex*	*Diagnosis*	*Mesenteric lymph node*					
					Histology	*IHC (FCoV Ag)*	*Sequencing*			
							Codon 1,048		*Codon 1,050*	
1	Maine Coon	1 y		Pleural effusion (FCoV RT-qPCR negative)	ND	ND	Not possible			
2	DSH	3 y	MN	Lethargy, weight loss, anaemia	ND	ND	TTG	Leu	ND	
3	DSH	10 y	MN	Diabetes mellitus	Reactive hyperplasia with collagen scars	–	CTG	Leu	ND	
4	Ragdoll	4 m	M	Severe interstitial pneumonia	Normal to reactive hyperplasia	–	CTG	Leu	TCC	Ser
5	Havana	4 y	FN	Nasal lymphoma	ND	ND	TTG	Leu	TCT	Ser
6	DSH	10 y	FN	Round cell neoplasia	Sinus histiocytosis	–	Not possible			
7	DSH	8 y	MN	Pleural effusion (FCoV RT-qPCR negative)	Normal	–	TTG	Leu	ND	
8	DSH	18 y	FN	Chronic kidney disease	Sinus histiocytosis	ND	TTG	Leu	TCT	Ser
9	DSH	10 y	MN	Lymphoma	Normal	–	CTG	Leu	ND	
10	DSH	–	F	Anaesthetic death	Normal to reactive hyperplasia	–	CTG	Leu	ND	

FIP, feline infectious peritonitis; FCoV, feline coronovirus; IHC, immunohistochemistry; Ag, antigen; DSH, domestic shorthair; MN, male neutered; FN female neutered; ND, not done; Leu, leucine; Ser, serine.

to avoid possible interference with the RT-qPCR results. Starting RNA levels were equilibrated between samples to 400 ng/μl, using a NanoDrop 2000® (ThermoFisher Scientific). Samples were further diluted 1 in 20 prior to RT-qPCR.

Reverse Transcriptase Quantitative Polymerase Chain Reaction

TaqMan RT-qPCR was performed on an Applied Biosystems 7500 Fast PCR System® (ThermoFisher Scientific) using newly developed, or previously published, primer and probe protocols for: FCoV; feline TLR 1 to 9; STAT 1 to 3; interferon (IFN)-α, -β and -γ; IL-1β, -6, -10, -15, and -17; tumour necrosis factor (TNF)-α; CXC motif chemokine 10 (CXCL10); CC motif chemokine ligand 8 (CCL8); transforming growth factor (TGF)-β1; and glyceraldehyde 3-phosphate dehydrogenase (GAPDH), as the reference gene (Table 2) (Leutenegger *et al.*, 1999). This gene was chosen based on previous experience in our laboratory and following reference gene comparisons during optimization. All primers and probes were manufactured by Microsynth (Balgach, Switzerland). The hydrolysis probes were labelled with a 5′ reporter dye FAM (6-carboxyfluorescein) and a 3′ quencher TAMRA (6-carboxy-tetramethylrhodamine).

Those primers and probes that were newly developed were designed using Primer Express® software (v3.0.1, Thermo Fisher Scientific) to span an exon–exon junction. These were tested for specificity by conventional PCR of a test sample, gel electrophoresis, sequencing of the resulting extracted band (Microsynth) and evaluation using NCBI BLAST. Conditions were as for RT-qPCR except for omission of the probe. Primer concentrations for this step were 900 nM. Varying primer/probe concentrations were then tested to determine the optimal efficiency and dynamic range as well as replicability using a sample dilution series. All final protocols (Table 2) had an efficiency >95%. Those previously published were tested again in our system, omitting the conventional RT-PCR step. Each reaction comprised 12.5 μl TaqMan Fast Universal Master Mix® (ThermoFisher Scientific), with 2.5 μl cDNA, primer and probe volumes as per Table 2, made up to 25 μl with RNase-free water. The thermal profile for all RT-qPCRs was: 50°C for 2 min, 95°C for 10 min, and 45 cycles of 95°C for 10 sec and 60°C for 1 min. All samples were run in duplicate and any samples with discordant results were repeated. Data collection occurred during the extension phase at 60°C. Appropriate controls were included in each run.

The Applied Biosystems 7500 Software® v2.0.6 was used to visualize results and allocate a quantification cycle (C_q) to each sample, and the threshold was equilibrated between runs for each target.

Viral Sequencing

The particular codons of interest within the FCoV S gene were 1,058 and 1,060 (Chang *et al.*, 2012). With reference to the sequence used in the original paper, the mutations in question appear to be at positions 1,048 and 1,050 rather than 1,058 and 1,060

Table 1C
Group 2: cats with FIP

	Breed	*Age*	*Sex*	*Effusion*	*Mesenteric lymph node*					
					FIP lesions	*IHC (FCoV Ag)*	*Sequencing*			
							Codon 1,048		*Codon 1,050*	
1	DSH	10 y	FN	+ (A)	Necrotizing and pyogranulomatous	+	TTG	Leu	TCT	Ser
2	Norwegian Forest	8 m	MN	–	Necrotizing and pyogranulomatous and lymphoplasmacytic	+	CTG	Leu	TCT	Ser
3		4 m	M	+ (A)	Granulomatous	+	ATG	Met	GCT	Ala
4		1.5 y	MN	+ (A)	Pyogranulomatous	+	TTG	Leu	TCA	Ser
5	Maine Coon	1 y	MN	+ (A)	Pyogranulomatous and lymphoplasmacytic	+	TTG	Leu	TCC	Ser
6	DSH	6 m	MN	+ (A, P)	Granulomatous	+	TTG	Leu	TCT	Ser
7	DSH	4 m	F	+ (M)	Granulomatous	+	TTG	Leu	TCT	Ser
8	BSH	6 y	MN	+ (A)	Pyogranulomatous	+	TTG	Leu	TCC	Ser
9	Persian	5 m	F	+ (A)	Pyogranulomatous	+	TTG	Leu	TCT	Ser
10		3 y		+ (A)	Granulomatous	+	TTG	Leu	ND	
11	Burmese	3 m	M	+ (T)	Necrotizing and granulomatous	+	TTG	Leu	ND	
12	Abyssinian	4 m	F	+ (A)	Pyogranulomatous	+	TTG	Leu	ND	
13	DSH	–		+ (T)	ND	ND	TTG	Leu	ND	
14	DSH	5 m		+ (A, T)	Necrotizing and pyogranulomatous	+	TTG	Leu	ND	
15	Siamese	1 y		+	Pyogranulomatous	+	CTG	Leu	TCC	Ser
16	BSH	10 m	MN	+	Sinus histiocytosis	–	TTG	Leu	TCC	Ser
17	DSH	2 y	MN	+	Reactive hyperplasia	–	TTG	Leu	TCT	Ser
18	Siamese	3 y	MN	+ (A, T)	Normal	–	c/tTG	Leu	TCT	Ser
19	Birman	12 y	MN	+ (M)	Reactive hyperplasia	+	TTG	Leu	TCC	Ser
20	BSH	1 y	FN	+ (A, T)	Pyogranulomatous	+	ATG	Met	TCC	Ser
21	DSH	2 y	MN	–	Granulomatous	+	ATG	Met	GCC	Ala
22	Oriental	3 y	M	–	Granulomatous	+	TTG	Leu	TCC	Ser
23	Birman	8 m	M	–	ND	ND	TTA	Leu	TCA	Ser
24	Ragdoll	10 m	FN		Necrotizing and granulomatous	+	TTG	Leu	TCC	Ser
25	BSH	2 y	MN	+ (A)	Necrotizing and pyogranulomatous	+	TTG	Leu	TCC	Ser
26	DSH	6 m	F	–	Normal	–	CTG	Leu	TCT	Ser
27	DSH	1 y		+ (A)	Reactive hyperplasia	–	FCoV Type II			
28	DSH	4 m			Reactive hyperplasia	–	TTG	Leu	TCC	Ser
29	DSH	7 m		–	Pyogranulomatous	+	TTG	Leu	ND	
30	DSH		M	+ (A)	Pyogranulomatous	+	TTG	leu	ND	

FIP, feline infectious peritonitis; FCoV, feline coronavirus; MLN, mesenteric lymph nodes; IHC, immunohistochemistry; Ag, antigen; DSH, domestic shorthair; blank, data not available; BSH, British longhair; F, female; M, male; FN, female neutered; MN, male neutered; +, positive/present; –, negative/absent; A, abdominal; P, pericardial; M, multicavitary; T, thoracic; ND, not done; Leu, leucine; Ala, alanine; Met, methionine; Ser, serine. Nucleotide bases in lower case indicate a mixed infection.

as previously described, and will be referred to subsequently by the former numbers.

Following initial FCoV RT-qPCR, all positive samples not analysed for previous studies by Porter *et al.* (2014) or Barker *et al.* (2017) underwent additional conventional RT-PCR and Sanger sequencing targeting the S gene region of interest. PCR was performed using the previously published degenerate primers (Porter *et al.*, 2014). Each reaction comprised 10 µl Phusion Flash Master Mix® (ThermoFisher Scientific), with 2 µl cDNA, 0.5 µM each of forward and reverse primers, made up to 20 µl with RNase-free water. Reactions were run on a T Professional® thermocycler (Biometra GmbH, Göttingen, Germany) with the following thermal profile: 98°C for 10 sec, 40 cycles of 98°C for 1 sec, 52°C for 5 sec, 72°C for 3 sec, followed by 72°C for 1 min. Appropriate controls were included in each run.

The reaction product then underwent gel electrophoresis. Bands of appropriate size were extracted using the GeneJET Gel Extraction Kit® (ThermoFisher Scientific) and submitted for Sanger sequencing at a commercial laboratory (Microsynth). When no band was visible, the reaction was repeated using 50 cycles and the product was subjected to gel electrophoresis. Samples still appearing negative were cut out in the region of the expected band, purified and re-subjected to PCR. The bioinformatics software Geneious 9.1.7®, (Biomatters Limited, Silkeborg, Denmark) was used to map the resulting sequences to the reference gene FCoV C1Je (Accession number DQ848678) (Chang *et al.*, 2012).

Table 2
Primer and probe sequences used for RT-qPCR and conventional RT-PCR

Gene	*Reference or accession number*		*Primer and probe sequences (5′-3′) where not previously published*	*PCR product length (base pairs)*
GAPDH, IL-10	Leutenegger *et al.* (1999)			
FCoV (RT-qPCR)	Gut *et al.* (1999)			
FCoV (conventional)	Porter *et al.* (2014)			
TLR1, 2, 4, 5, 6, 7, 9	Ignacio *et al.* (2005)			
TLR3, 8, IL-15, IFN-α, -β	Robert-Tissot *et al.*, 2011			
IL-1β, IL-6, TNF-α	Kipar *et al.* (2001)			
TGF-β	Taglinger *et al.* (2008)			
IL-17	XM_006931816.1	F-16	ACTTCATCCATGTTCCCATCACT	126
		R-141	CACATGCTGAGGAAAATTCTTGTC	
		P-83	CATTCCCACAAAATCCAGGATGCCC	
STAT1	XM_006935443	F-1649	TTGACCTCGAGACGACCTCTCT	135
		R-1783	GCGGGTTCAGGAAGAAGGA	
		P-1686	CTCCAATGTCAGCCAGCTCCCGAGT	
STAT2	XM_003988893	F-1182	GCCCAGGTCACGGAGTTG	122
		R-1303	ACAGTGAACTTGCTCCCTGTCTT	
		P-1212	CTGCACAGAGCCTTTGTGGTAGAAACCC	
STAT3	XM_006940361.2	F-1626	GCCAGTTGTGGTGATCTCCAA	133
		R-1758	TTGATCCCAGGTTCCAATCG	
		P-1696	CTGACCAACAACCCCAAGAACGTGAACTTT	
CCL8	XM_003996558	F-95	GGCCACCTTCAGCATCCA	82
		R-176	CCCTTTGACCACACTGAAGCA	
		P-121	CTCAGCCAGGTTCAGTTTCCATCCCA	
CXCL10	XM_003985274.3	F-386	TGCCATCATTTCCCTACATTCTT	78
		R-463	CAGTGGTTGGTCACCTTTTAGGA	
		P-411	CAAGCCCTAATTGTCCCTGGATTGCAG	
IFN-γ	NM_001009873.1	F-214	TGGAAAGAGGAGAGTGATAAAACAA	122
		R-335	TCCTTGATGGTGTCCATGCT	
		P-284	ACCTGAAAGATGATGACCAGCGCATTCAA	

Accession number, NCBI accession number; F, forward primer and start site; R, reverse primer and start site; P, probe and start site. All final reactions contained equivalent F and R concentrations of 900 nM and 250 nM for P, with the exception of FCoV RT-qPCR, 300 and 250 nM; FCoV conventional, 500 nM; TGF-β, 200 and 50 nM; STAT3, 600 and 250 nM, respectively.

Statistical Analysis

Relative mRNA transcription levels were calculated using the comparative C_q method (Pfaffl, 2001). The C_q of each target was first normalized to GAPDH as the endogenous reference (ΔC_q) and then expressed relative to the G1 ΔC_q mean as the calibrator ($2^{-\Delta\Delta Cq}$). For FCoV RT-qPCR results, the mean of G1+ was instead used as the calibrator (to allow for visualization graphically).

The statistical programme SPSS Statistics v.25® (IBM, Armonk, New York, USA) was used for all analyses and graphical data presentation. Data were first assessed for normality using a Shapiro–Wilk test. As almost all data failed the test, non-parametric measures were applied. A two-tailed Mann–Whitney test with a significance level of $P \leq 0.05$ was used to compare results between groups for each target molecule. Firstly, cats with and without FIP (G1 versus G2) were compared, followed by comparisons between each of the three groups (G1−, G1+ and G2) in turn. Within G2, comparisons were made between cats with and without cavitary effusions and with and without histologically observed FIP lesions in the MLNs. Correlation between relative FCoV levels and inflammatory mediator gene expression levels, and also between individual inflammatory mediator gene expression levels, was analysed within G2 using a one-tailed Spearman's rank test. Here a cut off of $P \leq 0.01$ was used, with $P \leq 0.05$ indicating weak correlation.

Results

Feline Coronavirus Status within the Study Population

Signalments of the cats are shown in Tables 1A–C. All MLN samples from cats with FIP (G2) were positive for FCoV ($n = 30$). Of the 40 cats without FIP (G1), 10 (25%) also had a positive FCoV RT-qPCR result; these were assigned to a new sub-group (G1+). However, the relative FCoV load was clearly, and significantly, lower in G1+ than in G2 (Fig. 1).

None of the G1 cats exhibited histological changes suggestive of FIP in any tissue examined, including the MLNs when available for histology (25 of 30 from G1− and seven of 10 from G1+). Inflammation

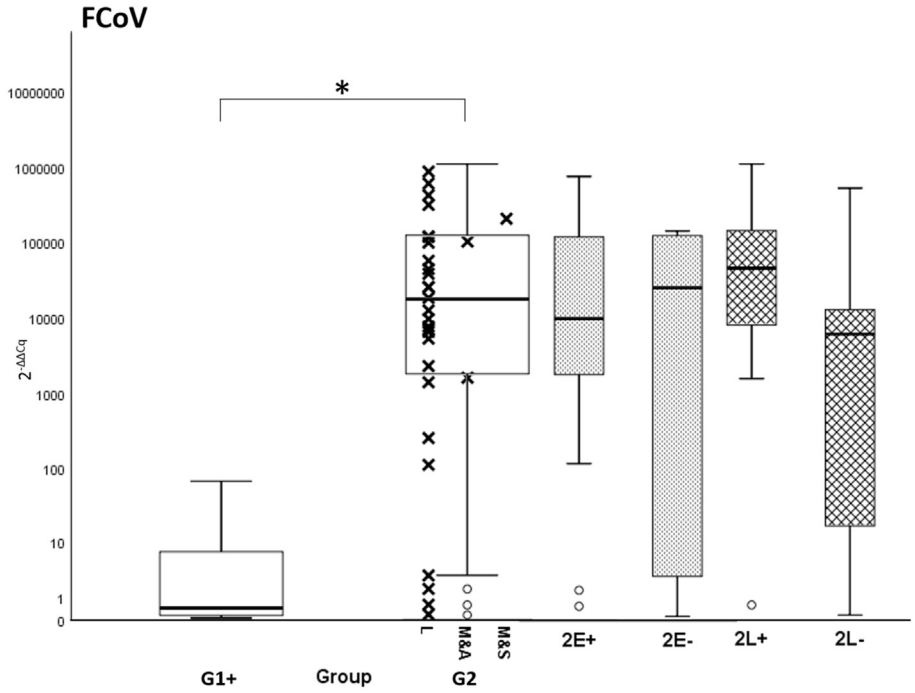

Fig. 1. Boxplots demonstrating relative levels of FCoV transcription in G1+ and G2. The amount of FCoV was calculated by $2^{-\Delta\Delta Cq}$, using fGAPDH as the internal reference gene and expressed as an n fold difference relative to the G1+ mean as a calibrator. The boxes depict the median and interquartile (IQ) range with whiskers extending to the highest and lowest values, which are within 1.5× the IQ range. Outliers beyond this are individually marked. The three columns of individual crosses within G2 depict the three variations in the viral S protein at codons 1,048 and 1,050, respectively. From left to right: L, leucine at 1,048 ('systemic' virus); M&A, methionine and alanine ('systemic' virus); M&S, methionine and serine ('enteric' virus). 2E+, 2E−, 2L+ and 2L− represent relative FCoV levels among MLN of cats with and without effusions/lesions.

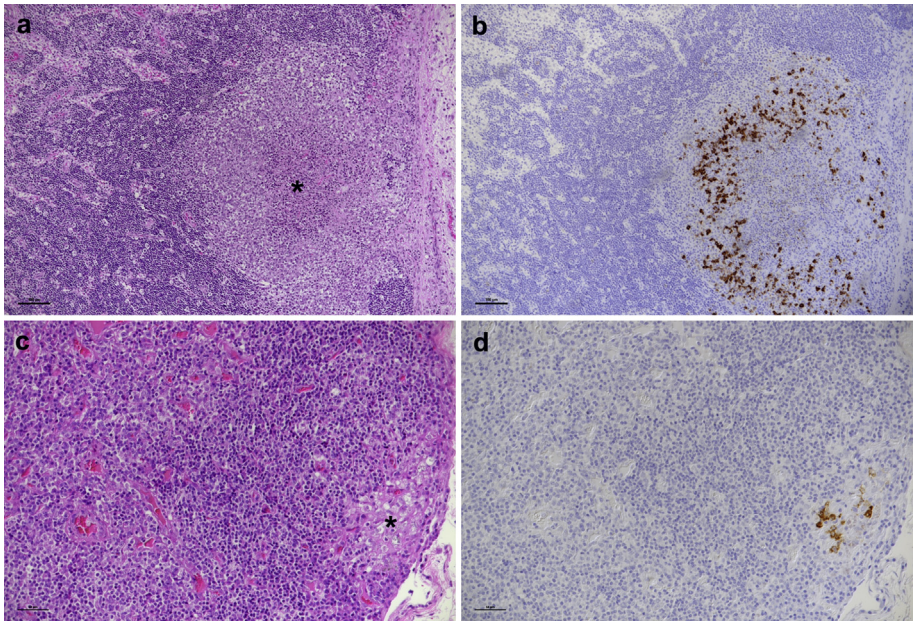

Fig. 2. Examples of MLNs with and without lesions from cats with FIP. (a, b) Case G2.5. (a) Focal pyogranulomatous inflammation with central necrosis (*). HE. (b) Viral antigen expression is seen in abundant intact lesional macrophages. IHC. (c, d) Case G2.19. (c) Reactive hyperplasia with expansion of the marginal sinus by macrophages (*). HE. (d) Some of the latter are FCoV antigen positive. IHC.

Table 3
Results of statistical comparisons between groups of cats, using a two-tailed Mann–Whitney test

	Statistical comparison between			*FIP group*	
	G1 versus G2	*G1− versus G1+*	*G1+ versus G2*	*Effusions present versus absent*	*MLN lesions present versus absent*
FCoV	0.000[a]	0.000[a]	0.000[a]	0.764	0.071
TLR1	0.610	0.914	0.794	0.643	0.533
TLR2	0.000[a]	0.724	0.002[a]	0.259	0.048[a]
TLR3	0.569	0.724	0.656	0.682	0.189
TLR4	0.019[a]	0.794	0.022[a]	1.000	0.208
TLR5	0.053	0.508	0.396	0.806	0.756
TLR6	0.859	0.286	0.469	0.764	0.228
TLR7	0.059	0.770	0.272	0.427	0.568
TLR8	0.012[a]	0.246	0.015[a]	0.566	0.435
TLR9	0.991	0.031[a]	0.140	0.764	0.189
STAT1	0.000[a]	0.315	0.000[a]	0.052	0.466
STAT2	0.000[a]	0.017[a]	0.000[a]	0.017[a]	0.717
STAT3	0.260	0.569	0.414	0.764	1.000
IFN-α	0.041[a]	1.000	0.077	0.604	0.499
IFN-β	0.004[a]	0.770	0.036[a]	0.566	0.604
IFN-γ	0.000[a]	0.131	0.003[a]	0.806	0.249
IL-1β	0.026[a]	0.432	0.031[a]	0.849	0.272
IL-6	0.001[a]	0.209	0.177	1.000	0.208
IL-10	0.296	0.469	0.939	0.604	0.272
IL-15	0.019[a]	0.794	0.039[a]	0.53	0.376
IL-17	0.440	0.528	0.286	0.723	1.000
TGF-β	0.430	0.508	0.396	0.978	0.678
TNF-α	0.004[a]	0.432	0.346	0.309	0.405
CXCL10	0.000[a]	0.396	0.000[a]	0.441	0.263
CCL8	0.000[a]	0.177	0.000[a]	0.46	0.071

[a]Indicates significance level of $P \leq 0.05$. In the first three columns, the second group of the comparison is significantly higher in all cases (e.g. for G1 versus G2, G2 levels are higher). In the FIP columns, the value of the 'present' group is in both cases higher than in the 'absent' group.

of other aetiologies was observed in the MLNs of two of the 30 G1− cats and none of the G1+ animals. All G1 samples were also negative for FCoV antigen by immunohistochemistry.

Association between Key Pathological Findings and Relative Viral Load in Mesenteric Lymph Nodes of Cats with Feline Infectious Peritonitis

The MLNs were available for histological examination in 28 of the 30 cats with FIP. In 21 cases (75%), these exhibited the typical pyogranulomatous lesions, with or without associated serosal lesions on the lymph node capsule (e.g. serofibrinous to granulomatous serositis). All samples with typical pyogranulomatous lesions also showed FCoV antigen in lesional macrophages (Figs. 2a, b). Seven MLNs had no typical lesions; among these was only one case (G2.19) in which FCoV antigen was detected, in low numbers of macrophages within the marginal sinus, suggesting an early lesion (Figs. 2c, d). There was no significant difference in FCoV load found between MLNs with and without lesions, although those with lesions had a tendency to higher FCoV levels (Fig. 1).

Of the 30 cats with FIP, 22 exhibited effusions (Table 1C). These were not associated with a higher relative FCoV load in the MLNs in comparison with the cats without effusion ($n = 6$; data not available for two cats).

Association between Feline Infectious Peritonitis and Feline Coronavirus Status, Disease Features, Viral Load and Gene Expression of Immune Mediators

In order to evaluate the effect of FCoV infection and FIP on target gene transcription, G1 and G2 were first compared with each other before comparisons between all three groups (G1+, G1− and G2). The assessed target genes are described below according to their positions in immune signalling pathways as first line receptors, inflammatory mediators or signal transducers. Detailed results are provided in Table 3.

Toll-like Receptors: Relative TLR2, 4 and 8 gene transcription levels were significantly higher in G2 than G1. Within G1 there was no difference between virus-positive and virus-negative MLNs for these TLRs; however, TLR9 gene expression, although not elevated in G2, was significantly higher in G1+ than in G1− (Fig. 3).

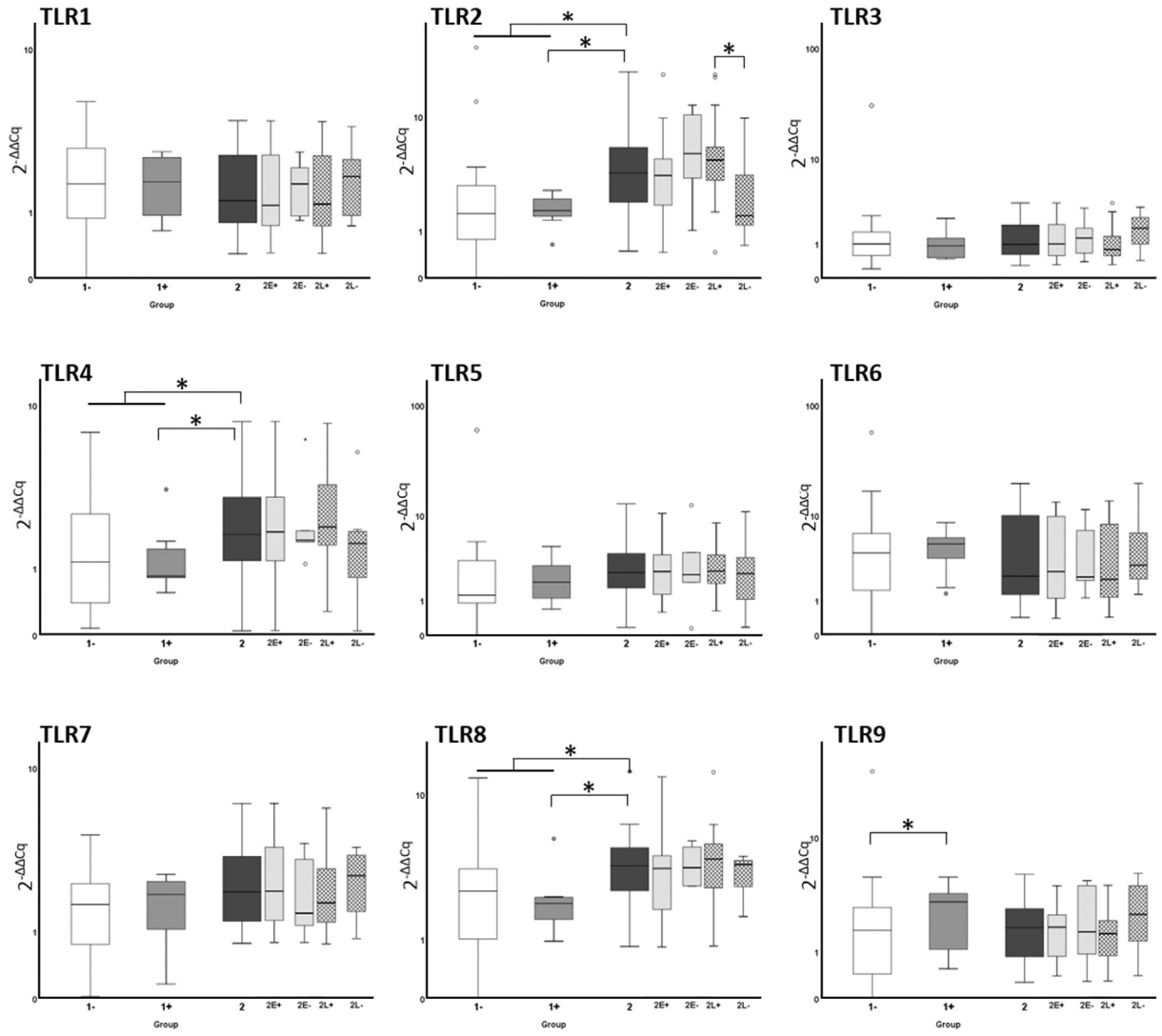

Fig. 3. Boxplots of relative levels of TLR gene expression in each group. The amount of target was calculated by $2^{-\Delta\Delta Cq}$, using fGAPDH as the internal reference gene and expressed as an n fold difference relative to the G1 mean as a calibrator. The boxes depict the median and interquartile (IQ) range with whiskers extending to the highest and lowest values, which are within 1.5 × the IQ range. Outliers beyond this are individually marked. * marks significant differences between individual groups ($P \leq 0.05$) or, where joined by a bar, between G1 as a whole and G2. 2E+, 2E−, L2+ and L2− represent relative gene expression levels among MLNs of cats with and without effusions/lesions.

In G2 cats, gene transcription levels were compared between MLNs with and without FIP lesions, and in relation to the presence of effusions. A significant difference was found only for TLR2 (higher expression in MLNs with lesions) (Fig. 3, Table 3); in contrast, TLR2 expression appeared slightly lower in cats with effusions (Fig. 3). A possible trend not reaching significance was for a slightly higher TLR4 expression level in MLNs with lesions, while TLR3 and 9 gene expression levels were slightly lower (Fig. 3). Investigating this further, we found that TLR3 gene expression levels in G2 MLNs without lesions were also slightly higher than levels in G1 (which were similar to those in G2 MLNs with lesions), suggesting a potential negative regulation of TLR3 by FCoV (Fig. 3).

Cytokines and Chemokines: Relative IL-1β, IL-6, IL-15, TNF-α, IFN-α, -β, -γ, CCL8 and CXCL10 gene transcription levels were all significantly higher in G2 compared with G1 (Fig. 4). None of these showed any significant difference between G1+ and G1−. For most cytokines, G1+ and G1− clustered together; however, for IL-6, TNF-α and IFN-γ, G1+ appeared to cluster slightly between the other two groups (G1− and G2), suggesting a possible intermediate stage (Fig. 4). Between groups, the fold

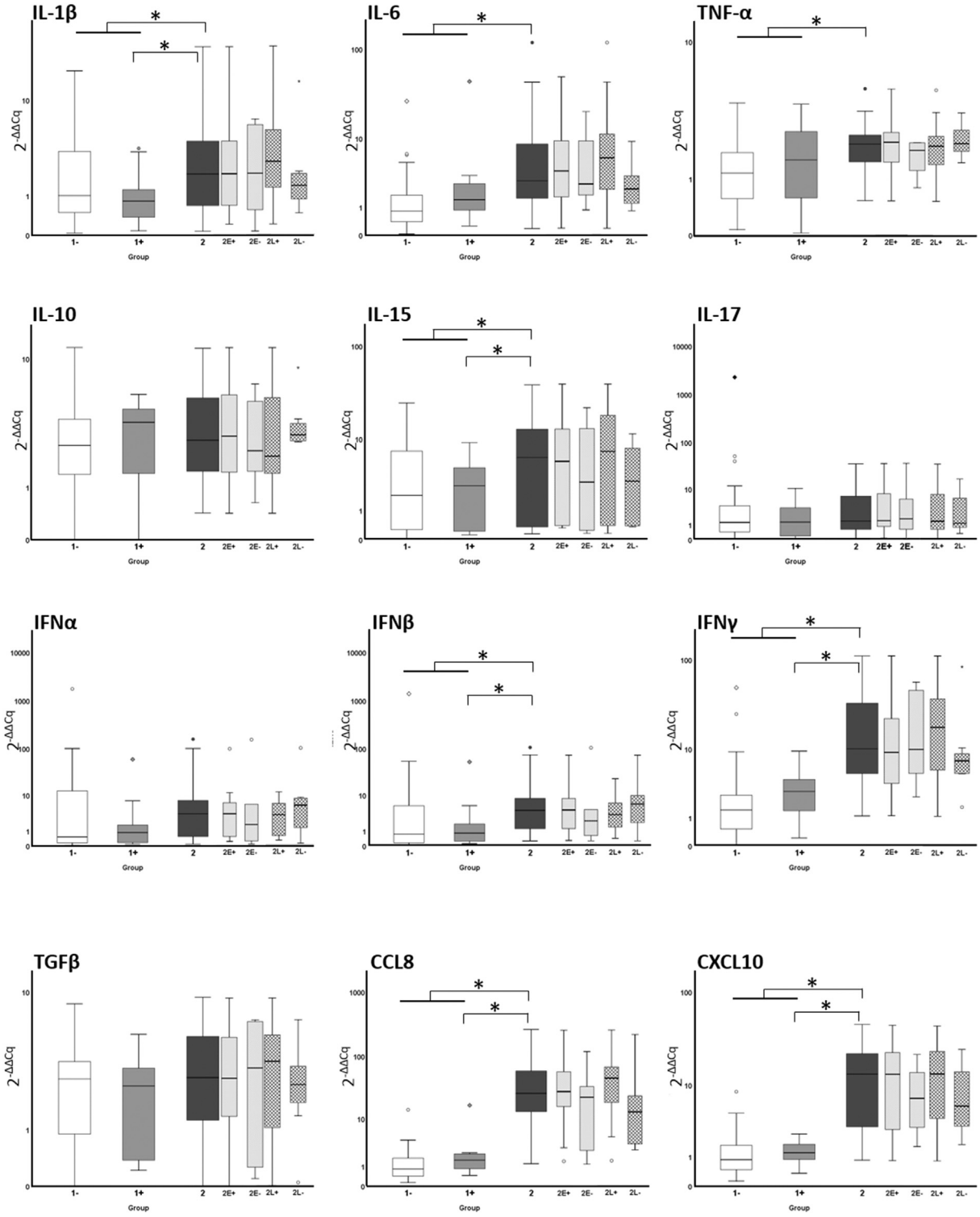

Fig. 4. Boxplots of relative levels of cytokine and chemokine gene expression in each group. The amount of target was calculated by $2^{-\Delta\Delta Cq}$, using fGAPDH as the internal reference gene and expressed as an n fold difference relative to the G1 mean as a calibrator. The boxes depict the median and interquartile (IQ) range with whiskers extending to the highest and lowest values, which are within 1.5 × the IQ range. Outliers beyond this are individually marked. * marks significant differences between individual groups ($P \leq 0.05$) or, where joined by a bar, between G1 as a whole and G2. 2E+, 2E−, 2L+ and 2L− represent relative gene expression levels among MLNs of cats with and without effusions/lesions.

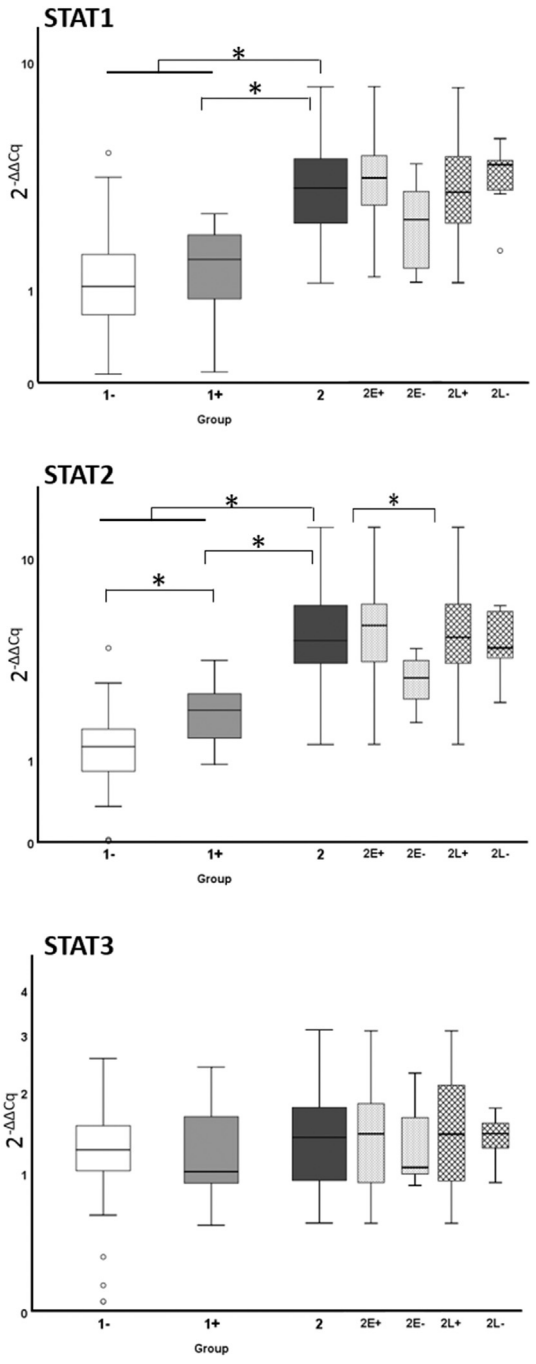

Fig. 5. Boxplots of relative levels of STAT gene expression in each group. The amount of target was calculated by $2^{-\Delta\Delta Cq}$, using fGAPDH as the internal reference gene and expressed as an n fold difference relative to the G1 mean as a calibrator. The boxes depict the median and interquartile (IQ) range with whiskers extending to the highest and lowest values, which are within 1.5 × the IQ range. Outliers beyond this are individually marked. * marks significant differences between individual groups ($P \leq 0.05$) or, where joined by a bar, between G1 as a whole and G2. 2E+, 2E−, 2L+ and 2L− represent relative gene expression levels among MLNs of cats with and without effusions/lesions.

differences in the chemokine gene expression levels (CXCL10 and CCL8) were mainly in the range of 10−100×, while those for the pyrogenic cytokines (IL-1β, IL-6 and TNF-α) rarely exceeded 10×. IL-10, IL-17 and TGF-β gene transcription levels showed no intergroup differences (Fig. 4, Table 3).

For IL-1β, IL-6, IFN-γ and CCL8, a possible trend towards increased transcription (not reaching significance) was observed in G2 MLNs with lesions compared with those without (Fig. 4).

Signal Transducers and Activators of Transcription: STAT1 and 2 gene expression levels were significantly higher in G2 than G1. For both transcription factors, gene expression levels were also higher in G1+ than in G1−, significantly so for STAT2. STAT3 gene expression levels were similar across all groups (Fig. 5).

In G2, STAT2 gene expression levels were significantly higher in cats with effusions (Fig. 5, Table 3). For STAT1, there was an insignificant trend to be higher with effusions (Fig. 5).

Correlation of Target Immune Mediators and Feline Coronavirus Load in Cats with Feline Infectious Peritonitis

The majority of gene targets elevated in G2 also showed significant positive correlation with relative viral load (Supplementary Table 1). These included TLR2 and 4, the cytokines IL-1β, IL-6, together with STAT2, CXCL10, CCL8, IFN-β and IFN-γ ($P \leq 0.01$). TLR8 and IFN-α gene expression showed weaker correlation ($P \leq 0.05$), while STAT1, TGF-β, and TNF-α gene expression showed no correlation, and TLR9 a weak, although significant, negative correlation (Table 4).

Expression of genes encoding IL-6, IL-17 and STAT3, a 'holy trinity' of autoimmunity (Camporeale and Poli, 2012), was significantly correlated despite the latter two not showing any correlation with FCoV.

Partial S Gene Sequencing

Of the 40 cats shown by RT-qPCR to carry FCoV in their MLNs, 38 had analysable S gene sequences following conventional PCR. From the remaining two cats (G1+ cats 1 and 6) it was not possible to obtain samples of sufficient quality even after repeated attempts (Table 1B).

Of the 30 cats with FIP, one was infected with FCoV serotype 2 for which the previously described S gene sequence characterization is not applicable (Herrewegh *et al.*, 1998; Barker *et al.*, 2017). Twenty-six MLN samples contained virus that encoded leucine (M1048L) (cDNA sequence TTG,

Table 4
Summary of Spearman's rank one-tailed correlation results within the FIP group, showing immune mediators with significant results

	FCoV	*TLR2*	*TLR4*	*TLR8*	*TLR9*	*STAT1*	*STAT2*	*STAT3*	*IFN-α*	*IFN-β*	*IFN-γ*	*IL-1β*	*IL-6*	*IL-15*	*IL-17*	*TGF-β*	*TNF-α*	*CXCL10*	*CCL8*
FCoV	●	↑↑	↑↑	↑	↑		↑↑		↑	↑↑	↑↑	↑↑	↑↑	↑				↑↑	↑↑
TLR2	↑↑	●	↑↑	↑↑			↑	↑↑		↑↑	↑↑	↑↑	↑↑					↑↑	↑↑
TLR4	↑↑	↑↑	●	↑↑		↑	↑↑	↑↑		↑	↑↑	↑↑	↑↑	↑	↑↑			↑↑	↑↑
TLR8	↑	↑↑	↑↑	●				↑↑				↑↑	↑↑					↑	↑
TLR9	↓				●	↑↑	↑	↑↑								↑↑	↑		
STAT1			↑		↑↑	●	↑↑	↑↑				↑	↑	↑	↑		↑↑	↑↑	↑
STAT2	↑↑	↑	↑↑		↑	↑↑	●	↑↑		↑	↑	↑↑	↑↑	↑↑	↑		↑↑	↑↑	↑↑
STAT3		↑↑	↑↑	↑↑	↑↑	↑↑	↑↑	●		↑		↑↑	↑↑		↑↑	↑	↑↑	↑↑	↑↑
IFN-α	↑							↑	●	↑↑	↑↑	↑	↑		↑		↑		↑
IFN-β	↑↑	↑↑	↑				↑	↑	↑↑	●	↑↑		↑		↑		↑↑	↑	↑↑
IFN-γ	↑↑	↑↑	↑↑				↑	↑	↑↑	↑↑	●	↑↑	↑↑		↑		↑	↑↑	↑↑
IL-1β	↑↑	↑↑	↑↑	↑↑		↑	↑↑	↑↑	↑		↑↑	●	↑↑		↑↑	↑	↑↑	↑↑	↑↑
IL-6	↑↑	↑↑	↑↑	↑↑		↑	↑↑	↑↑	↑	↑	↑↑	↑↑	●		↑		↑↑	↑↑	↑↑
IL-15	↑		↑			↑	↑↑							●				↑↑	↑
IL-17			↑↑			↑	↑	↑↑	↑	↑	↑	↑↑	↑		●		↑		
TGF-β					↑↑			↑				↑				●	↑		
TNF-α					↑	↑↑	↑↑	↑↑	↑	↑↑	↑	↑↑	↑↑		↑↑	↑	●	↑	↑
CXCL10	↑↑	↑↑	↑↑	↑		↑↑	↑↑	↑↑		↑	↑↑	↑↑	↑↑	↑↑			↑	●	↑↑
CCL8	↑↑	↑↑	↑↑	↑		↑	↑↑	↑↑	↑	↑↑	↑↑	↑↑	↑↑	↑			↑	↑↑	●

↑↑, positive correlation at a significance level of $P \leq 0.01$; ↑, positive correlation at a significance level $P \leq 0.05$; ↓, negative correlation at a significance level of $P \leq 0.05$.

CTG or TTA). The remaining three cats encoded methionine at codon 1,048 (cDNA sequence ATG). The results are shown in Table 1C. Of the eight sequences obtained from the G1+ cats, all encoded leucine (M1048L). Of the three cases encoding methionine at codon 1,048, two encoded alanine at codon 1,050 (S1050A), while the third encoded serine (Table 1B).

The small methionine group size ($n = 3$), including only one cat that carried the 'enteric' virus (M1048, S1050), was not considered valid for statistical comparison with the leucine group, 'systemic' virus. Instead, individual cases were plotted, revealing the methionine group to fall within the range of the leucine group for every target, including FCoV load (Fig. 1).

Discussion

As predicted from previous studies, the results of the present investigation confirm the complex effect of FCoV on the immune system in association with FIP. The disease is caused by an exaggerated immune response to FCoV, but it is well known that cats can also carry FCoV systemically without developing FIP (Meli *et al.*, 2004). Here we have assessed some of the key mediators of the innate immune response, focussing on the MLN, the most likely first site of infection beyond the intestine and one of the main sites of viral persistence in experimentally infected healthy animals (Kipar *et al.*, 2010). By comparing FCoV-positive, lesion-free MLNs from cats affected by diseases other than FIP with both FCoV-negative cats without FIP and cats with FIP, we aimed to separate the direct viral effects from the host effects contributing to FIP in a natural setting.

FIP presents as a spectrum of disease with variable duration rather than as a discrete clinical picture; as such the pathological features also vary. This was reflected by variation in organ involvement and presence of effusions in our case cohort. We therefore also wanted to assess whether the inflammatory mediator production in the MLNs showed any correlation with the form of disease. Although vascular permeability is, to a large extent, cytokine mediated (Takano *et al.*, 2011), and we found upregulation of cytokine genes with a role in vascular permeability in the FIP cases, the inflammatory mediator gene expression profile of the MLNs differed only minimally between cats with and without effusions. This suggests that the MLN is unlikely to make a large systemic contribution to vascular permeability. Similarly, Safi *et al.* (2017) evaluated inflammatory mediators within peripheral blood mononuclear cells of FIP cats with and without effusions and found little consistent pattern to distinguish those with effusions from those without. Both studies therefore provide further, although indirect, support that vascular endothelial growth factor, which was previously shown to correlate with the degree of effusion in FIP, is key to this phenomenon (Takano *et al.*, 2011). Interestingly, the presence or absence of histological FIP lesions was not correlated with many significant differences between mediator gene expression. Alongside this, and surprisingly, although FCoV levels appeared higher in association with lesions, they were not significantly so. This may partly explain the lack of significant differences in mediator gene expression. Additionally, it cannot be entirely excluded that the area of the MLN sampled for RNA extraction was not within an FIP lesion and vice versa. An alternative explanation for the lack of significant differences between gene expression for most mediators in MLNs, while many exhibit higher overall levels in FIP, would be that systemic stimulation to upregulate inflammatory mediators is more relevant than local or lesion-specific stimulation. Finally, as trends were occasionally observed when cases with and without effusions and MLN lesions were compared, the lack of significance may also be due to the small group sizes once subgroups were created, which was a limitation of this study.

The MLNs of cats without FIP had significantly lower viral loads than their counterparts from cats with FIP. This confirms previous findings in natural infection, where cats with FIP were reported to carry higher viral loads in haemopoietic and lymphoid tissues, including MLNs, than asymptomatic FCoV-infected cats (Kipar *et al.*, 2006a). Without the disease, however, the presence or absence of FCoV in the MLN seems not to influence the transcription level of most of our target immune mediators. This would indicate that, in the main, the host response has a greater influence than any direct viral effect. Still, there were exceptions. Even among those mediators not attaining significance, IFN-γ, IL-6 and TNF-α showed a trend towards higher gene expression levels in FCoV-positive MLNs. This suggests at least a modest direct viral effect; it may have been masked by low group numbers, requiring a larger sample size to confirm or refute. Another study limitation was the composition of the groups. As all were field cases it was not possible to control for confounding factors (e.g. ensuring control cases were free of any inflammatory processes, that FIP cases were at similar disease stages, and that cats were initially subject to the same FCoV infection pressures).

Inflammatory cytokines have been previously studied in FIP, with conflicting results, possibly dependent on variations in disease form between animals

included in the different studies and/or the type of sample/organ evaluated. TNF-α gene transcription, for example, was found to be decreased in the MLNs of cats with FIP compared with FCoV-free specific pathogen-free cats, while IL-1β gene expression was elevated (Kipar *et al.*, 2006b). In the present study, gene expression for all three pyrogenic cytokines (IL-1β, IL-6 and TNF-α) was upregulated in the MLNs in FIP, as well as that for IL-15 (a stimulator of lymphocyte proliferation). We also found significantly higher transcription levels for the monocyte-recruiting chemokines CXCL10 and CCL8, which have both been found to be upregulated in Crandell–Rees feline kidney cells after *in vitro* FCoV infection (Harun *et al.*, 2013), indicating a mechanism of monocyte recruitment as a direct viral effect. Our results confirm their relevance *in vivo*, with recruitment of monocytes as the infected cell type being a potential amplifying step that is worthy of further investigation. The increase in inflammatory cytokine gene transcription supports the observation that an overexuberant inflammatory response is a key factor in the development and progression of FIP. Expression of the gene encoding the anti-inflammatory cytokine IL-10 was, in contrast, not upregulated in FIP, implying there was no local brake on the inflammatory process. This is in line with previous findings, where IL-10 expression was higher in the spleen of healthy FCoV-infected cats, but not in the MLN (Kipar *et al.*, 2006b). Gene expression for the interferons was also higher in FIP, IFN-γ being one of the cytokines to show an intermediate level in infected asymptomatic cats in our study. These type I and II interferons have major antiviral roles in the innate immune system. IFN-γ in particular has been of interest in FIP, as levels of this potentially protective cytokine tend to be low in the peripheral blood of diseased animals and host gene polymorphisms have been identified that may contribute to resistance against the disease (Gelain *et al.*, 2006; Hsieh and Chueh, 2014). Similarly to the apparent lack of impact of mediator levels on the presence of lesions or effusions in FIP, this suggests that MLN IFN production has a more local effect.

TLRs have been used for targeted therapy against a number of diseases in human medicine, both with adjuvants and inhibitors; however, veterinary medicine lags behind in this respect (Hennessy *et al.*, 2010; Klingemann, 2018). Here we identified increased gene expression levels of TLRs 2, 4, 8 and 9 with FIP and FCoV infection, respectively, indicating a possible role for these molecules in FIP and hence identifying them as potential targets for FIP control. Assessment at the protein level would be a useful avenue for further investigations; however, this is particularly challenging in feline studies owing to the lack of availability of appropriate antibodies. In most mammals, TLRs 2 and 4 are located on the cell membranes, while TLRs 8 and 9 are found in intracytoplasmic vesicles, most commonly in professional antigen presenting cells (Lester and Li, 2014). TLR2, together with TLRs 1, 6 and 10, comprise the TLR1 family (Roach *et al.*, 2005). These latter three receptors arose through evolutionary gene duplication (Hughes and Piontkivska, 2008; Hennessy *et al.*, 2010). TLR2 is able to signal as a heterodimer with any of its co-family members in order to allow a wider range of antigen recognition. It is typically responsible for detecting bacterial and fungal components (Beutler, 2009). TLR2 has been linked to detection of the SARS-CoV S protein *in vitro* (Dosch *et al.*, 2009); its upregulation in FIP could indicate that the FCoV S protein is also able to act as a ligand.

TLR4 classically detects lipopolysaccharide; however, one study linked it to protection against murine coronavirus, as TLR4-deficient mice were found to exhibit greater susceptibility to murine hepatitis virus infection. The precise mechanism was not established in that case, but it involved inflammatory cell influx in the TLR4-deficient mice (Khanolkar *et al.*, 2009). No such protective effect was observed in our study, despite upregulation of TLR4 gene expression in the MLNs in association with FIP, although its individual effect in this case cannot be separated from the mediator milieu.

TLR9 gene expression was not elevated in the MLNs of cats with FIP, but was instead increased in the FCoV-positive MLNs of cats without FIP. Considering that a previous *in vitro* study found reduced viral replication when TLR9 was stimulated with a synthetic CpG ligand prior to FCoV infection (Robert-Tissot *et al.*, 2012), the increased gene expression in FCoV-infected cats without FIP could indicate that TLR9 has a protective effect, which may even have helped prevent the development of disease. Stimulation by co-infectious agents could therefore also be hypothesized to be protective against FIP. Along these lines, co-infection must also be considered a possible alternative explanation for the raised TLR2 and 4 gene expression levels, as these TLRs are more typically associated with bacterial infections. Enteric coronavirus infection or the generalized inflammatory state induced by FIP may have increased the permeability of the intestinal barrier to microorganisms. The resulting TLR stimulation would therefore not be virus induced. A third alternative is the upregulation of TLR2 and 4 by endogenous ligand

stimulation, reported as a response to alarmin release from damaged cells (van Beijnum *et al*., 2008). This alternative also fits with upregulation of TLR2 gene expression in lesional MLNs compared with non-lesional MLNs in FIP.

From their known ligands, TLRs 3, 7 and 8 would be predicted to be triggered in infection by FCoV as it is a ssRNA virus (triggering TLRs 7 and 8), possessing a double-stranded RNA intermediate replicating phase (triggering TLR3) (Arpaia and Barton, 2011). That no upregulation occurs for TLR3 and TLR7 with FIP suggests either the lack of an appropriate trigger (TLR7 and 8 are known to show differing, if overlapping, specificity, and dsRNA intermediate replicates are a minority of the viral RNA present; Jensen and Thomsen, 2012), or that the virus is able to inhibit TLR transcription. SARS-CoV is known to inhibit both TLR3 and 7 signalling via papain-like protease activity (PLpro) (Li *et al*., 2016). This mechanism may also contribute in FCoV infection, but would be expected to affect the signalling pathways rather than the TLR mRNA levels directly. In cats with FIP, we observed slightly lower TLR3 gene transcription in MLNs with typical FIP lesions, as compared with MLNs without lesions, down to the levels seen in MLNs from cats without FIP. This could indicate a general systemic stimulus to upregulate TLR3 in FIP, which is counteracted locally by viral inhibition of TLR3. Prior stimulation of TLR3 has also been shown *in vitro* to contribute to defence against murine coronavirus via type I interferon induction (Mazaleuskaya *et al*., 2012), so is another potential avenue for future FIP research. A larger sample population, in particular with larger numbers of systemically infected cats without FIP, might have revealed significant intergroup differences for TLR3.

The STAT transcription factors are a key part of the antiviral pathways, mediating many downstream IFN effects (Aaronson and Horvath, 2002). They have also been linked to other coronavirus infections (e.g. STAT1 knock-out mice show a markedly increased susceptibility to SARS-CoV, while avian infectious bronchitis coronavirus uses STAT1 inhibition of IFN responses) (Frieman *et al*., 2010; Kint *et al*., 2015). STAT1 and 2 gene transcription levels correlated with type II and I interferon transcription levels, respectively, in our study, while in virus-positive MLNs of cats without FIP, STAT1 and 2 levels (the latter significantly so), as well as IFN-γ levels, lay between the other two groups. This shows that the levels of IFNs and their downstream transcription factors are closely linked. Interestingly, STAT2 gene expression levels were significantly higher in the MLNs of cats with FIP and with effusions, a finding that cannot be readily explained. STAT2 has been linked to IL-6 upregulation, which itself has been linked to increased vascular permeability (Maruo *et al*., 1992; Nan *et al*., 2018); however, the IL-6 gene was not upregulated in our cohort, suggesting that responsibility lies with another pathway.

The results of our S gene codon mutation analysis add weight to recent findings that the M1058L mutation (referred to as M1048L in the present study due to re-evaluation of the reference sequence) is likely to contribute to systemic spread, but does not itself confer pathogenicity (Chang *et al*., 2012; Porter *et al*., 2014). This indicates that further host and/or viral factors are required for the development of FIP or, more precisely, the activation of virus-infected monocytes as a prerequisite to set off FIP vasculitis (Kipar and Meli, 2014). Most likely owing to the low viral RNA levels within the MLNs of cats without FIP, obtaining an adequate sequence from this group proved problematic. Other researchers experienced similar problems, often finding that FCoV RT-PCR-positive samples from cats without FIP were not amenable to sequencing (Felten *et al*., 2017b). The lack of FCoV antigen expression in these cats was not unexpected and reflects the rarity of infected cells and/or the low virus load in infected cells; this is in line with the results of a previous study that found only rare positive macrophages in the MLNs of experimentally persistently-infected cats (Kipar *et al*., 2010).

It was not possible to compare statistically the induced immune response of viruses showing S protein amino acid variations (codons 1,048 and 1,050) as only one cat had the 'enteric' form.

The future outcome of our FCoV infected cats without FIP, had they not succumbed to other diseases, is unknown, as is the contribution of yet to be defined viral factors. These cats may have remained carriers or have been demonstrating a transitional phase to later development of disease. However, based on our observations, activation of genes encoding TLRs 2, 4 and 8 in MLNs is associated with a negative outcome (i.e. FIP), while carrier animals upregulated the gene encoding TLR9. IFN-γ, and particularly STAT2 with its myriad opportunities to direct cell fate, displayed intermediate levels of upregulation in the MLNs of the carrier/transitional group, not associated with a widespread increase in mediators of inflammation.

This study is only the start of determining the extent of involvement of PRRs in FIP; the downstream effects of these transcriptional alterations must be further investigated. However, our results

reinforce the need for a balanced immune response against the virus, with the hypothesis that the moderate response in cats without FIP is part of the key to controlling the virus; when this balance is lost the animal may be at risk of succumbing to disease.

Acknowledgments

This study was supported by the 2017 *Journal of Comparative Pathology* Educational Trust and Petplan Charitable Trust Joint Research Award in Veterinary Pathology. Earlier sequencing work included in this study was supported by a project grant from The Petplan Charitable Trust (10–27) and by a project grant from the Morris Animal Foundation (#D16FE-507). The authors thank all the practitioners, owners and colleagues who helped in the acquisition of samples used in this study. We thank the technical staff of the Histology Laboratory, Institute of Veterinary Pathology, Vetsuisse Faculty, University of Zurich, for technical support.

Conflict of interest statement

The authors declare no conflicts of interest with respect to the publication of this manuscript.

Supplementary data

Supplementary data to this article can be found online at https://doi.org/10.1016/j.jcpa.2018.11.001.

References

Aaronson DS, Horvath CM (2002) A road map for those who don't know JAK–STAT. *Science*, **296**, 1653–1655.

Abbas AK, Lichtman AH, Pillai S (2017) *Cellular and Molecular Immunology*, 9th Edit., Saunders Elsevier, Philadelphia, pp. 63–65.

Arpaia N, Barton G (2011) Toll-like receptors: key players in antiviral immunity. *Current Opinion in Virology*, **1**, 447–454.

Barker EN, Stranieri A, Helps CR, Porter EL, Davidson AD *et al.* (2017) Limitations of using feline coronavirus spike protein gene mutations to diagnose feline infectious peritonitis. *Veterinary Research*, **48**, 1–14.

Beutler BA (2009) TLRs and innate immunity. *Blood*, **113**, 1399–1407.

Camporeale A, Poli V (2012) IL-6, IL-17 and STAT3: a holy trinity in auto-immunity? *Frontiers in Bioscience*, **17**, 2306–2326.

Chang H-W, Egberink HF, Halpin R, Spiro DJ, Rottier PJM (2012) Spike protein fusion peptide and feline coronavirus virulence. *Emerging Infectious Diseases*, **18**, 1089–1095.

Dean GA, Olivry T, Stanton C, Pedersen NC (2003) In vivo cytokine response to experimental feline infectious peritonitis virus infection. *Veterinary Microbiology*, **97**, 1–12.

Dewerchin HL, Cornelissen E, Nauwynck HJ (2005) Replication of feline coronaviruses in peripheral blood monocytes. *Archives of Virology*, **150**, 2483–2500.

Dosch SF, Mahajan SD, Collins AR (2009) SARS coronavirus spike protein-induced innate immune response occurs via activation of the NF-kappaB pathway in human monocyte macrophages in vitro. *Virus Research*, **142**, 19–27.

Felten S, Leutenegger CM, Balzer H-J, Pantchev N, Matiasek K *et al.* (2017a) Sensitivity and specificity of a real-time reverse transcriptase polymerase chain reaction detecting feline coronavirus mutations in effusion and serum/plasma of cats to diagnose feline infectious peritonitis. *BMC Veterinary Research*, **13**, 228.

Felten S, Weider K, Doenges S, Gruendl S, Matiasek K *et al.* (2017b) Detection of feline coronavirus spike gene mutations as a tool to diagnose feline infectious peritonitis. *Journal of Feline Medicine & Surgery*, **19**, 321–335.

Frieman MB, Chen J, Morrison TE, Whitmore A, Funkhouser W *et al.* (2010) SARS-CoV pathogenesis is regulated by a STAT1 dependent but a type I, II and III interferon receptor independent mechanism. *PLoS Pathogens*, **6**, e1000849.

Gelain ME, Meli M, Paltrinieri S (2006) Whole blood cytokine profiles in cats infected by feline coronavirus and healthy non-FCoV infected specific pathogen-free cats. *Journal of Feline Medicine & Surgery*, **8**, 389–399.

Gut M, Leutenegger CM, Huder JB, Pedersen NC, Lutz H (1999) One-tube fluorogenic reverse transcription-polymerase chain reaction for the quantitation of feline coronaviruses. *Journal of Virological Methods*, **77**, 37–46.

Harun MSR, Kuan CO, Selvarajah GT, Wei TS, Arshad SS *et al.* (2013) Transcriptional profiling of feline infectious peritonitis virus infection in CRFK cells and in PBMCs from FIP diagnosed cats. *Virology Journal*, **10**, 1–9.

Hennessy EJ, Parker AE, O'Neill LAJ (2010) Targeting Toll-like receptors: emerging therapeutics? *Nature Reviews Drug Discovery*, **9**, 293–307.

Herrewegh AAPM, Smeenk I, Horzinek MC, Rottier PJM, De Groot RJ (1998) Feline coronavirus type II strains 79-1683 and 79-1146 originate from a double recombination between feline coronavirus type I and canine coronavirus. *Journal of Virology*, **72**, 4508–4514.

Hsieh L-E, Chueh L-L (2014) Identification and genotyping of feline infectious peritonitis-associated single nucleotide polymorphisms in the feline interferon-γ gene. *Veterinary Research*, **45**, 57.

Hughes AL, Piontkivska H (2008) Functional diversification of the toll-like receptor gene family. *Immunogenetics*, **60**, 249–256.

Ignacio G, Nordone S, Howard KE, Dean GA (2005) Toll-like receptor expression in feline lymphoid tissues. *Veterinary Immunology and Immunopathology*, **106**, 229–237.

Jensen S, Thomsen AR (2012) Sensing of RNA viruses: a review of innate immune receptors involved in

recognizing RNA virus invasion. *Journal of Virology*, **86**, 2900–2910.

Khanolkar A, Hartwig SM, Haag BA, Meyerholz DK, Harty JT *et al.* (2009) Toll-like receptor 4 deficiency increases disease and mortality after mouse hepatitis virus type 1 infection of susceptible C3H mice. *Journal of Virology*, **83**, 8946–8956.

Kint J, Dickhout A, Kutter J, Maier HJ, Britton P *et al.* (2015) Infectious bronchitis coronavirus inhibits STAT1 signaling and requires accessory proteins for resistance to type I interferon activity. *Journal of Virology*, **89**, 12047–12057.

Kipar A, Baptiste K, Barth A, Reinacher M (2006a) Natural FCoV infection: cats with FIP exhibit significantly higher viral loads than healthy infected cats. *Journal of Feline Medicine & Surgery*, **8**, 69–72.

Kipar A, Bellmann S, Kremendahl J, Köhler K, Reinacher M (1998) Cellular composition, coronavirus antigen expression and production of specific antibodies in lesions in feline infectious peritonitis. *Veterinary Immunology and Immunopathology*, **65**, 243–257.

Kipar A, Koehler K, Bellmann S, Reinacher M (1999) Feline infectious peritonitis presenting as a tumour in the abdominal cavity. *Veterinary Record*, **144**, 118–122.

Kipar A, Leutenegger CM, Hetzel U, Akens MK, Mislin CN *et al.* (2001) Cytokine mRNA levels in isolated feline monocytes. *Veterinary Immunology and Immunopathology*, **78**, 305–315.

Kipar A, Meli ML (2014) Feline infectious peritonitis: still an enigma? *Veterinary Pathology*, **51**, 505–526.

Kipar A, Meli ML, Baptiste KE, Bowker LJ, Lutz H (2010) Sites of feline coronavirus persistence in healthy cats. *Journal of General Virology*, **91**, 1698–1707.

Kipar A, Meli ML, Failing K, Euler T, Gomes-Keller M *et al.* (2006b) Natural feline coronavirus infection: differences in cytokine patterns in association with the outcome of infection. *Veterinary Immunology and Immunopathology*, **112**, 141–155.

Klingemann H (2018) Immunotherapy for dogs: running behind humans. *Frontiers in Immunology*, **9**, 133.

Lester SN, Li K (2014) Toll-like receptors in antiviral innate immunity. *Journal of Molecular Biology*, **426**, 1246–1264.

Leutenegger CM, Mislin CN, Sigrist B, Ehrengruber MU, Hofmann-Lehmann R *et al.* (1999) Quantitative real-time PCR for the measurement of feline cytokine mRNA. *Veterinary Immunology and Immunopathology*, **71**, 291–305.

Li S-W, Wang C-Y, Jou Y-J, Huang S-H, Hsiao L-H *et al.* (2016) SARS coronavirus papain-like protease inhibits the TLR7 signaling pathway through removing Lys63-linked polyubiquitination of TRAF3 and TRAF6. *International Journal of Molecular Sciences*, **17**, 678.

Maruo N, Morita I, Shirao M, Murota S (1992) IL-6 increases endothelial permeability in vitro. *Endocrinology*, **131**, 710–714.

Mazaleuskaya L, Veltrop R, Ikpeze N, Martin-Garcia J, Navas-Martin S (2012) Protective role of Toll-like receptor 3-induced type I interferon in murine coronavirus infection of macrophages. *Viruses*, **4**, 901–923.

Meli M, Kipar A, Müller C, Jenal K, Gönczi E *et al.* (2004) High viral loads despite absence of clinical and pathological findings in cats experimentally infected with feline coronavirus (FCoV) type I and in naturally FCoV-infected cats. *Journal of Feline Medicine & Surgery*, **6**, 69–81.

Nan J, Wang Y, Yang J, Stark GR (2018) IRF9 and unphosphorylated STAT2 cooperate with NF-κB to drive IL6 expression. *Proceedings of the National Academy of Sciences of the USA*, **115**, 3906–3911.

Pedersen NC (1987) Virologic and immunologic aspects of feline infectious peritonitis virus infection. *Advances in Experimental Medicine & Biology*, **218**, 529–550.

Pedersen NC (2014) An update on feline infectious peritonitis: virology and immunopathogenesis. *Veterinary Journal*, **201**, 123–132.

Pedersen NC, Boyle JF (1980) Immunologic phenomena in the effusive form of feline infectious peritonitis. *American Journal of Veterinary Research*, **41**, 868–876.

Pedersen NC, Boyle JF, Floyd K, Fudge A, Barker J (1981) An enteric coronavirus infection of cats and its relationship to feline infectious peritonitis. *American Journal of Veterinary Research*, **42**, 368–377.

Pfaffl MW (2001) A new mathematical model for relative quantification in real-time RT-PCR. *Nucleic Acids Research*, **29**, e45.

Poland AM, Vennema H, Foley JE, Pedersen NC (1996) Two related strains of feline infectious peritonitis virus isolated from immunocompromised cats infected with a feline enteric coronavirus. *Journal of Clinical Microbiology*, **34**, 3180–3184.

Porter E, Tasker S, Day MJ, Harley R, Kipar A *et al.* (2014) Amino acid changes in the spike protein of feline coronavirus correlate with systemic spread of virus from the intestine and not with feline infectious peritonitis. *Veterinary Research*, **45**, 49.

Roach JC, Glusman G, Rowen L, Kaur A, Purcell MK *et al.* (2005) The evolution of vertebrate Toll-like receptors. *Proceedings of the National Academy of Sciences of the USA*, **102**, 9577–9582.

Robert-Tissot C, Rümegger VL, Cattori V, Meli ML, Riond B *et al.* (2011) The innate antiviral immune system of the cat: Molecular tools for the measurement of its state of activation. *Veterinary Immunology and Immunopathology*, **143**, 269–281.

Robert-Tissot C, Rüegger VL, Cattori V, Meli ML, Riond B *et al.* (2012) Stimulation with a class A CpG oligonucleotide enhances resistance to infection with feline viruses from five different families. *Veterinary Research*, **43**, 60.

Safi N, Haghani A, Ng SW, Selvarajah GT, Mustaffa-Kamal F *et al.* (2017) Expression profiles of immune mediators in feline coronavirus-infected cells and clinical samples of feline coronavirus-positive cats. *BMC Veterinary Research*, **13**, 92.

Taglinger K, Van Nguyen N, Helps CR, Day MJ, Foster AP (2008) Quantitative real-time RT-PCR

measurement of cytokine mRNA expression in the skin of normal cats and cats with allergic skin disease. *Veterinary Immunology and Immunopathology*, **122**, 216–230.

Takano T, Ohyama T, Kokumoto A, Satoh R, Hohdatsu T (2011) Vascular endothelial growth factor (VEGF), produced by feline infectious peritonitis (FIP) virus-infected monocytes and macrophages, induces vascular permeability and effusion in cats with FIP. *Virus Research*, **158**, 161–168.

Tekes G, Hofmann-Lehmann R, Bank-Wolf B, Maier R, Thiel H-J *et al.* (2010) Chimeric feline coronaviruses that encode type II spike protein on type I genetic background display accelerated viral growth and altered receptor usage. *Journal of Virology*, **84**, 1326–1333.

van Beijnum JR, Buurman WA, Griffioen AW (2008) Convergence and amplification of toll-like receptor (TLR) and receptor for advanced glycation end products (RAGE) signaling pathways via high mobility group B1 (HMGB1). *Angiogenesis*, **11**, 91–99.

[*Received, August 21st, 2018*
Accepted, November 5th, 2018]

Association between FIP and FCoV infection status, disease features, viral load, and mRNA levels of immune mediators

In order to keep the focus on the TLR responses and allow more space for discussion of these, the publication did not include all the mediators involved in the thesis. The matrix metalloproteinases (MMP2, 9, 13, TIMP1, 3) and colony stimulating factors (G-CSF, M-CSF, GM-CSF) were left out as it was felt that these results did not directly enhance the TLR results and that these were groups in themselves for separate discussion.

The following graphs and table are extensions of those in the preceding manuscript so only additional information will be described. This includes additional targets that were not included in the publication. All graphs are based on the same raw data as is presented in the manuscript (see page 1 of this chapter) but presented calibrated to the bone marrow mean.

Those results portrayed in the manuscript are shown with the new calibrator in Fig. 5.2.1-5.2.5.

Matrix remodelling enzymes

The direction of trends varied between enzymes. MMP2 mRNA levels were significantly higher in Group 2 cats than Group 1, and MMP13 significantly lower. MMP9 levels were not significantly altered. For the TIMPs, TIMP1 mRNA levels were significantly higher in Group 2, with no alteration between groups for TIMP3.

Colony stimulating factors

Only G-CSF showed significantly altered expression levels between groups, being higher in Group 2 than Group 1 cats. M- and GM-CSF showed no variation.

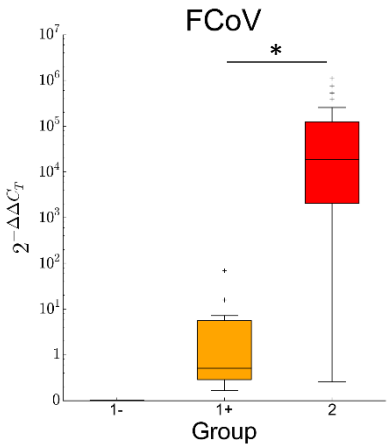

Figures 5.2.1: *Boxplots of relative mRNA levels of FCoV in each group. The amount of target was calculated by $2^{-\Delta\Delta CT}$, using fGAPDH as the internal reference gene for normalisation and expressed as an n-fold difference relative to the G1 mean of the BM samples as a calibrator. The boxes depict the median and interquartile (IQ) range with whiskers extending to the highest and lowest values which are within 1.5 x the IQ range. Outliers beyond this are individually marked. * marks significant differences between groups (p≤0.05).*

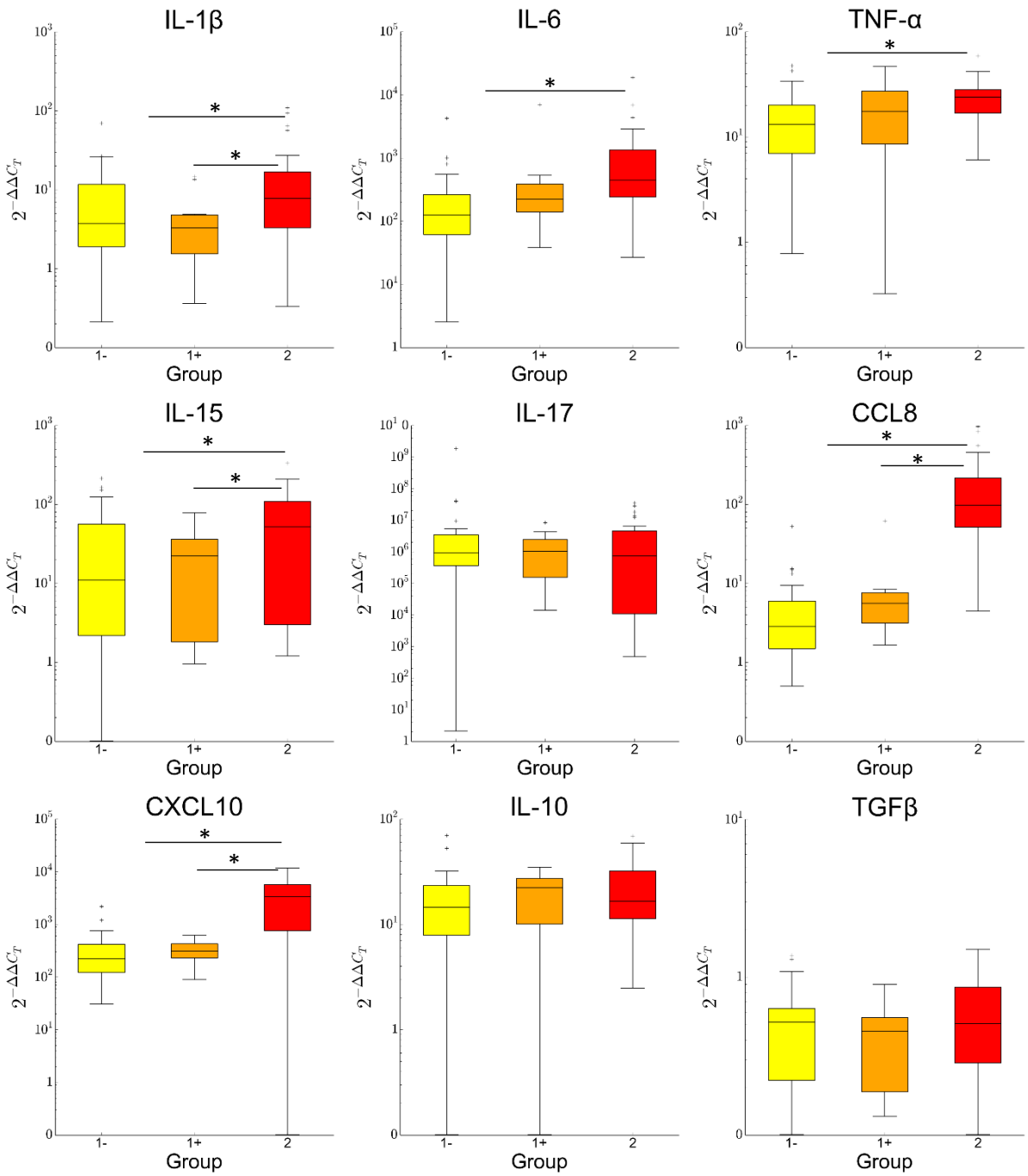

Figures 5.2.3: *Boxplots of relative mRNA levels of cytokines and chemokines in each group. The amount of target was calculated by $2^{-\Delta\Delta CT}$, using fGAPDH as the internal reference gene for normalisation and expressed as an n-fold difference relative to the G1 mean of the BM samples as a calibrator. The boxes depict the median and interquartile (IQ) range with whiskers extending to the highest and lowest values which are within 1.5 x the IQ range. Outliers beyond this are individually marked. * marks significant differences between groups (p≤0.05). Where the bar begins between G1+ and G1-, this indicates a significant difference to G1 as a whole.*

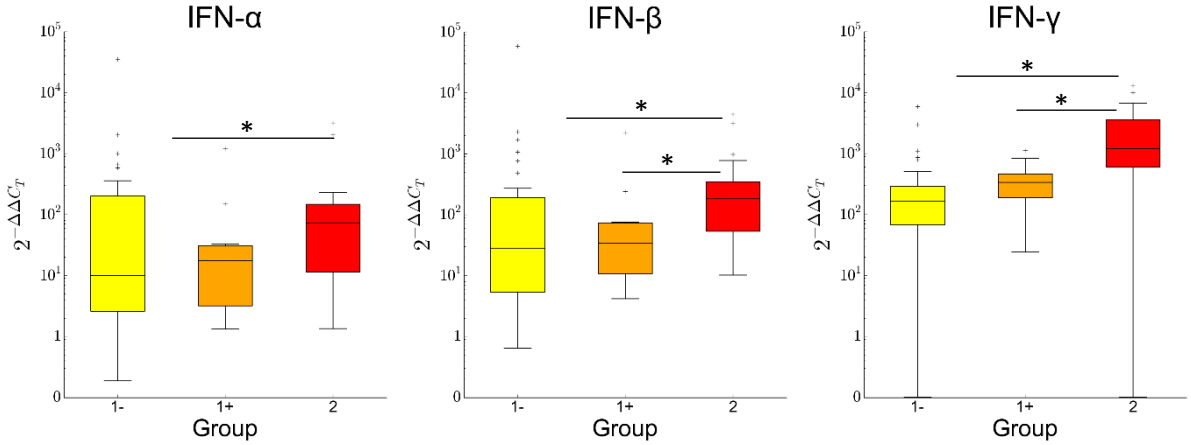

Figures 5.2.4: *Boxplots of relative mRNA levels of interferons in each group. The amount of target was calculated by $2^{-\Delta\Delta CT}$, using fGAPDH as the internal reference gene for normalisation and expressed as an n-fold difference relative to the G1 mean of the BM samples as a calibrator. The boxes depict the median and interquartile (IQ) range with whiskers extending to the highest and lowest values which are within 1.5 x the IQ range. Outliers beyond this are individually marked. * marks significant differences between groups (p≤0.05). Where the bar begins between G1+ and G1-, this indicates a significant difference to G1 as a whole.*

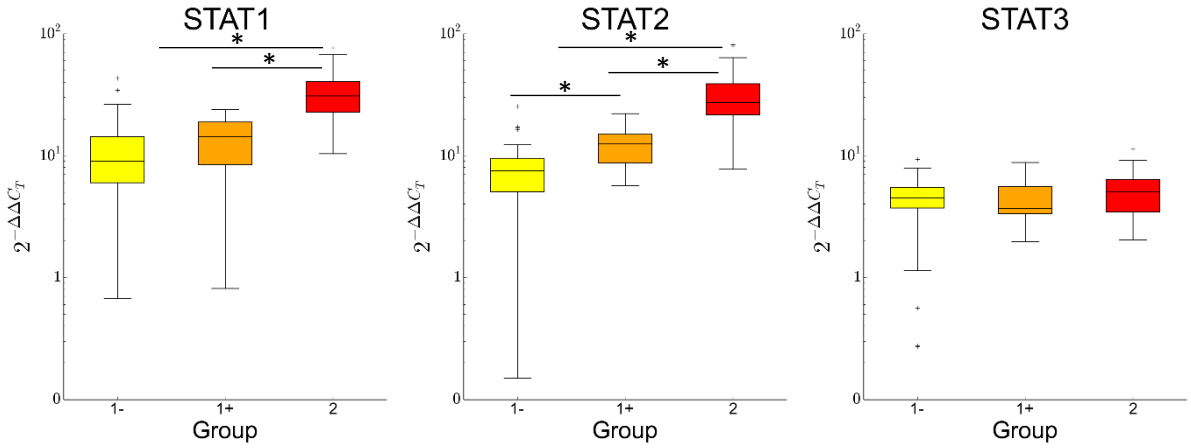

Figures 5.2.5: *Boxplots of relative mRNA levels of STATs in each group. The amount of target was calculated by $2^{-\Delta\Delta CT}$, using fGAPDH as the internal reference gene for normalisation and expressed as an n-fold difference relative to the G1 mean of the BM samples as a calibrator. The boxes depict the median and interquartile (IQ) range with whiskers extending to the highest and lowest values which are within 1.5 x the IQ range. Outliers beyond this are individually marked. * marks significant differences between groups (p≤0.05). Where the bar begins between G1+ and G1-, this indicates a significant difference to G1 as a whole.*

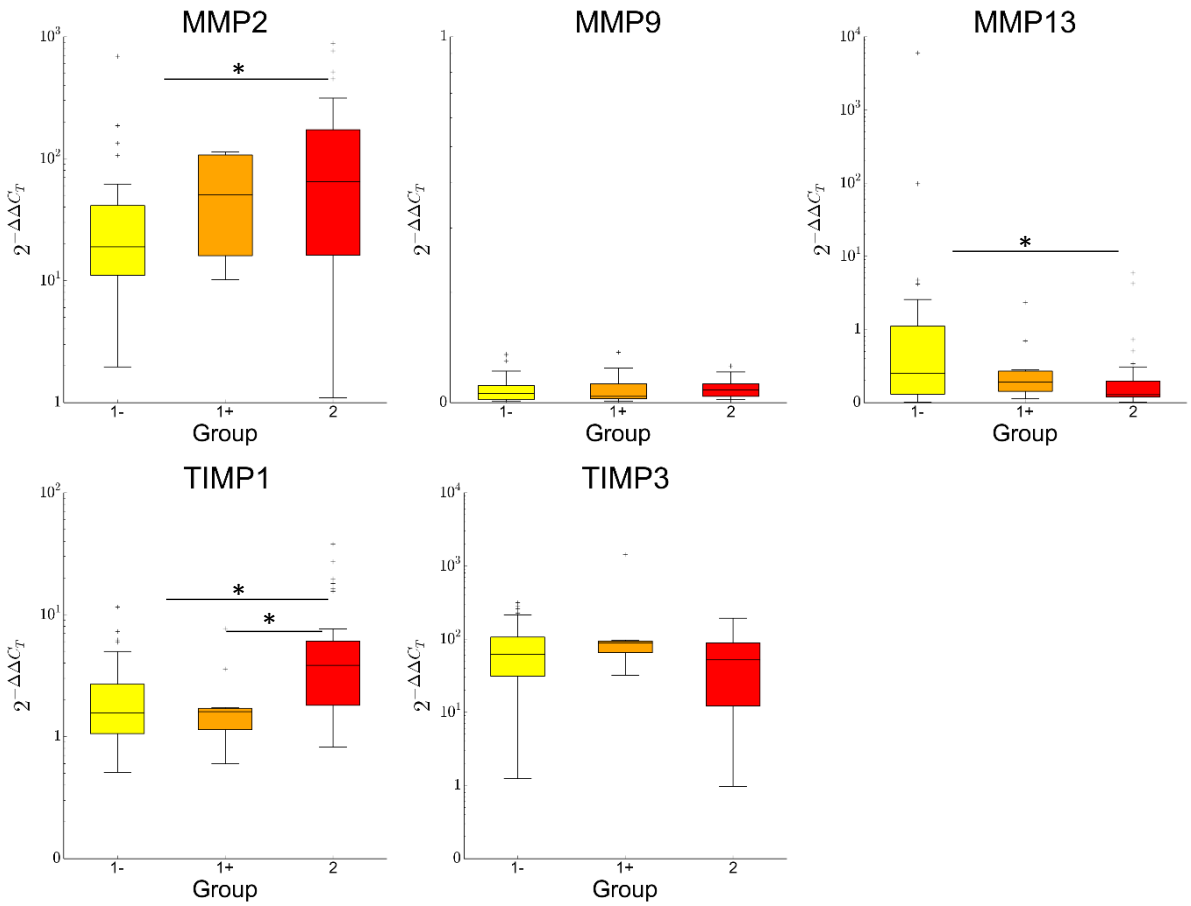

Figures 5.2.6: *Boxplots of relative mRNA levels of matrix remodelling enzymes in each group. The amount of target was calculated by $2^{-\Delta\Delta CT}$, using fGAPDH as the internal reference gene for normalisation and expressed as an n-fold difference relative to the G1 mean of the BM samples as a calibrator. The boxes depict the median and interquartile (IQ) range with whiskers extending to the highest and lowest values which are within 1.5 x the IQ range. Outliers beyond this are individually marked. * marks significant differences between groups (p≤0.05). Where the bar begins between G1+ and G1-, this indicates a significant difference to G1 as a whole.*

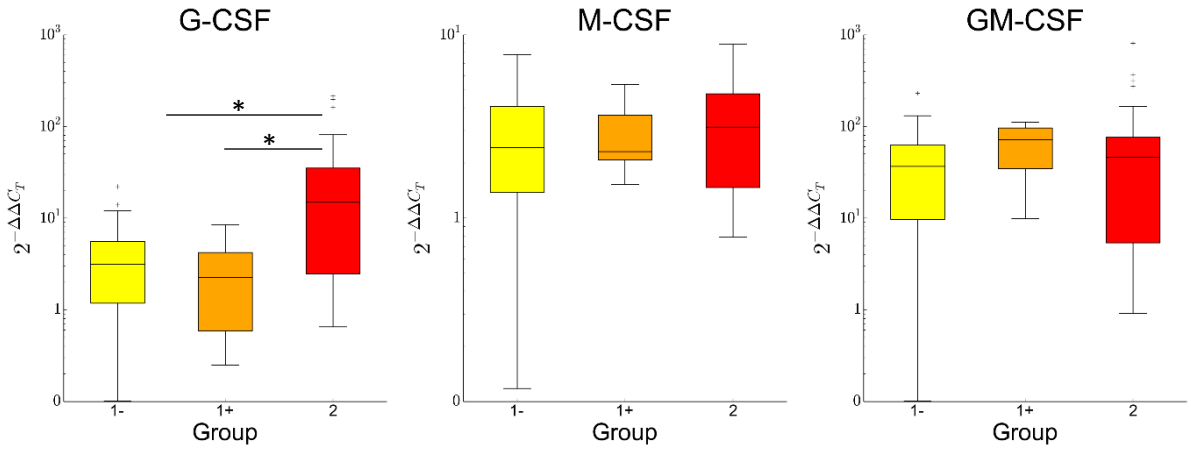

Figures 5.2.7: *Boxplots of relative mRNA levels of CSFs in each group. The amount of target was calculated by $2^{-\Delta\Delta CT}$, using fGAPDH as the internal reference gene for normalisation and expressed as an n-fold difference relative to the G1 mean of the BM samples as a calibrator. The boxes depict the median and interquartile (IQ) range with whiskers extending to the highest and lowest values which are within 1.5 x the IQ range. Outliers beyond this are individually marked. * marks significant differences between groups (p≤0.05). Where the bar begins between G1+ and G1-, this indicates a significant difference to G1 as a whole.*

Table 5.2.1: Statistical results of intergroup comparisons, with significant results (p≤0.05) highlighted in blue. The arrow indicates the direction of change of the second versus the first group of the comparison; *absent versus present.

Target	G1 vs G2		G1- vs G1+		G1+ vs G2		lesions*		effusions*	
FCoV	0.000	↑	NA		0.000	↑	0.071		0.764	
TLR1	0.610		0.914		0.794		0.533		0.643	
TLR2	0.000	↑	0.724		0.002	↑	0.048	↑	0.259	
TLR3	0.569		0.724		0.656		0.189		0.682	
TLR4	0.019	↑	0.794		0.022	↑	0.208		1.000	
TLR5	0.053		0.508		0.396		0.756		0.806	
TLR6	0.859		0.286		0.469		0.228		0.764	
TLR7	0.059		0.770		0.272		0.568		0.427	
TLR8	0.013	↑	0.246		0.015	↑	0.435		0.566	
TLR9	0.991		0.031	↑	0.140		0.189		0.764	
STAT1	0.000	↑	0.315		0.000	↑	0.466		0.052	
STAT2	0.000	↑	0.017	↑	0.000	↑	0.717		0.017	↑
STAT3	0.260		0.569		0.414		1.000		0.764	
IFN-α	0.041	↑	0.988		0.077		0.499		0.604	
IFN-β	0.004	↑	0.770		0.036	↑	0.604		0.566	
IFN-γ	0.000	↑	0.131		0.006	↑	0.272		0.764	
IL-1β	0.026	↑	0.432		0.031	↑	0.272		0.849	
IL-6	0.001	↑	0.209		0.158		0.172		0.935	
IL-10	0.296		0.469		0.914		0.376		0.427	
IL-15	0.019	↑	0.794		0.039	↑	0.376		0.530	
IL-17	0.440		0.569		0.818		0.189		1.000	
TNF-α	0.004	↑	0.432		0.346		0.405		0.309	
TGFβ	0.430		0.508		0.396		0.678		0.978	
CCL8	0.000	↑	0.177		0.000	↑	0.071		0.460	
CXCL10	0.000	↑	0.396		0.000	↑	0.376		0.566	
MMP2	0.035	↑	0.167		0.548		0.296		0.530	
MMP9	0.204		0.866		0.432		0.435		0.194	
MMP13	0.011	↓	0.432		0.187		0.376		0.365	
TIMP1	0.000	↑	0.866		0.012	↑	0.055		0.309	
TIMP3	0.117		0.569		0.095		0.090		0.336	
G-CSF	0.000	↑	0.590		0.002	↑	0.080		0.395	
M-CSF	0.476		0.747		1.000		0.756		0.460	
GM-CSF	0.921		0.125		0.363		0.717		0.604	

Correlation between relative viral load and immune mediator mRNA levels in the MLN of cats with FIP

Correlation was investigated within the FIP group in order to determine whether the mere presence of the virus in a diseased animal set off an inflammatory chain, or whether this response appeared to be directly linked to the local level of virus in the tissue. A table of correlation was presented and briefly discussed in the manuscript. This did not include either the additional mediators or the graphs

For each mediator, the result for each Group 2 cat was plotted against that cat's viral load.

From the graphs it could be seen whether a positive or negative correlation, or no trend was visible. The Spearman's rank correlation applied was therefore one-tailed. The statistical results are summarised in Table 5.2.2.

TLRs

Within the TLRs, there was positive correlation at the 0.01 level for TLR 2, 4, and 5. TLR 2 and 4 had been significantly elevated in FIP. TLR8, the third to have been significantly elevated was significant only at the $p<0.05$ level (subsequently referred to in this section as a weak correlation). TLR9 mRNA levels showed a weak negative correlation with viral load. Fig. 5.2.8.

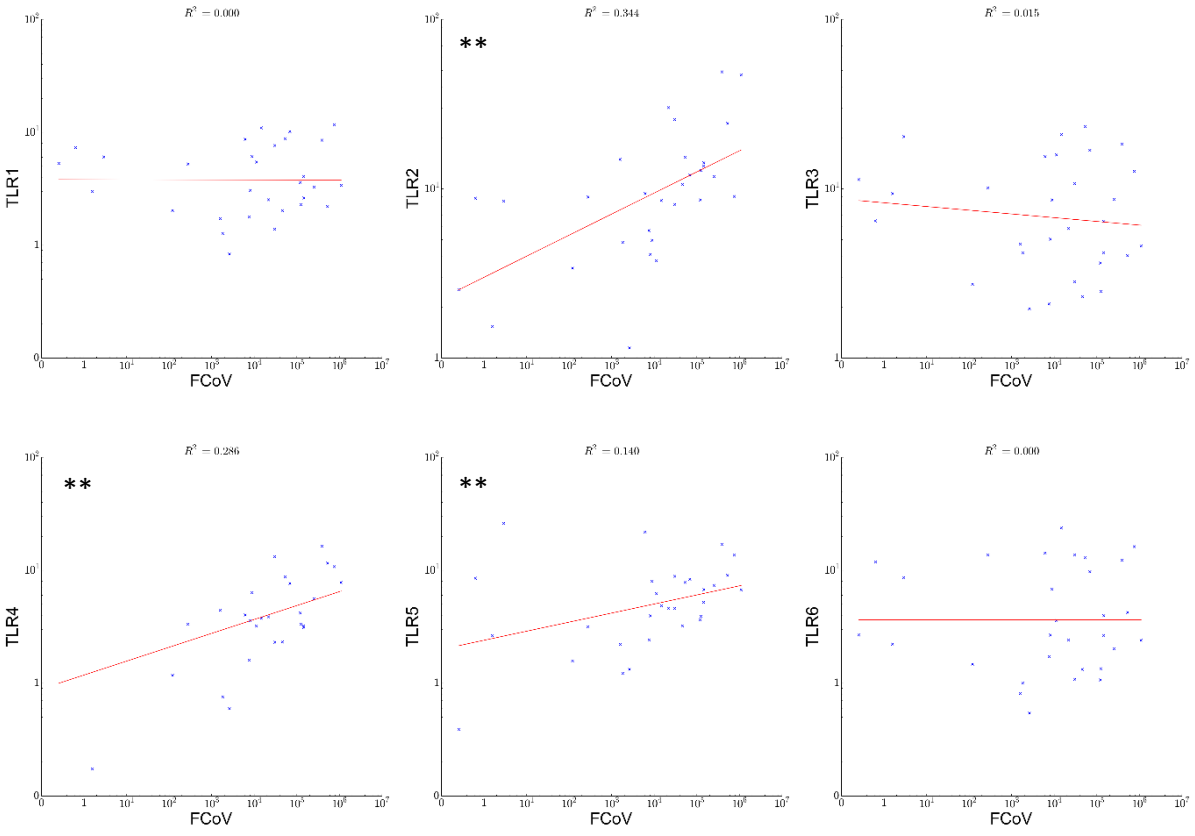

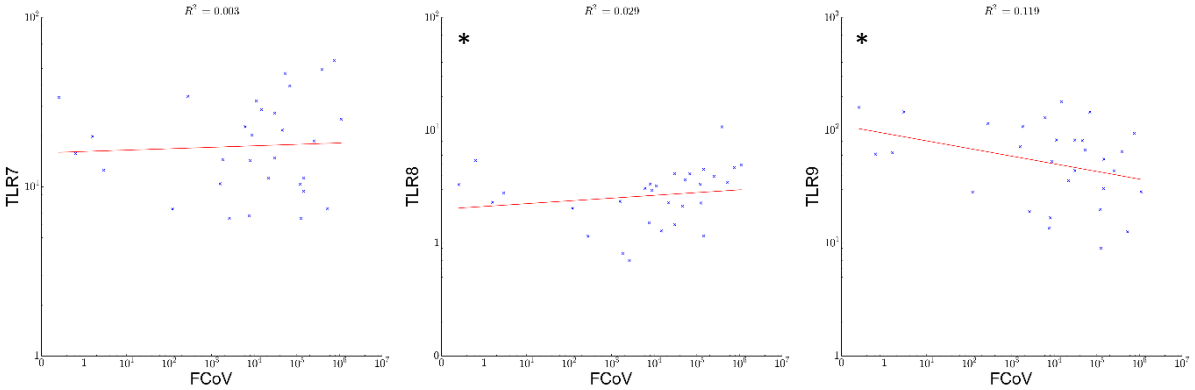

Figure 5.2.8: *Correlation between relative mRNA levels of TLRs and FCoV viral loads. Significance levels are marked by ** = p≤0.01; * = p≤0.05.*

Inflammatory cytokines and chemokines

The inflammatory cytokines IL-1β and IL-6, but not TNF-α, showed a positive correlation with viral load. All three had been significantly elevated in FIP. IL-15 was also positively correlated as were the chemokines CCL8 (which showed the strongest correlation) and CXCL10 (all at p≤0.01); Fig.5.2.9.

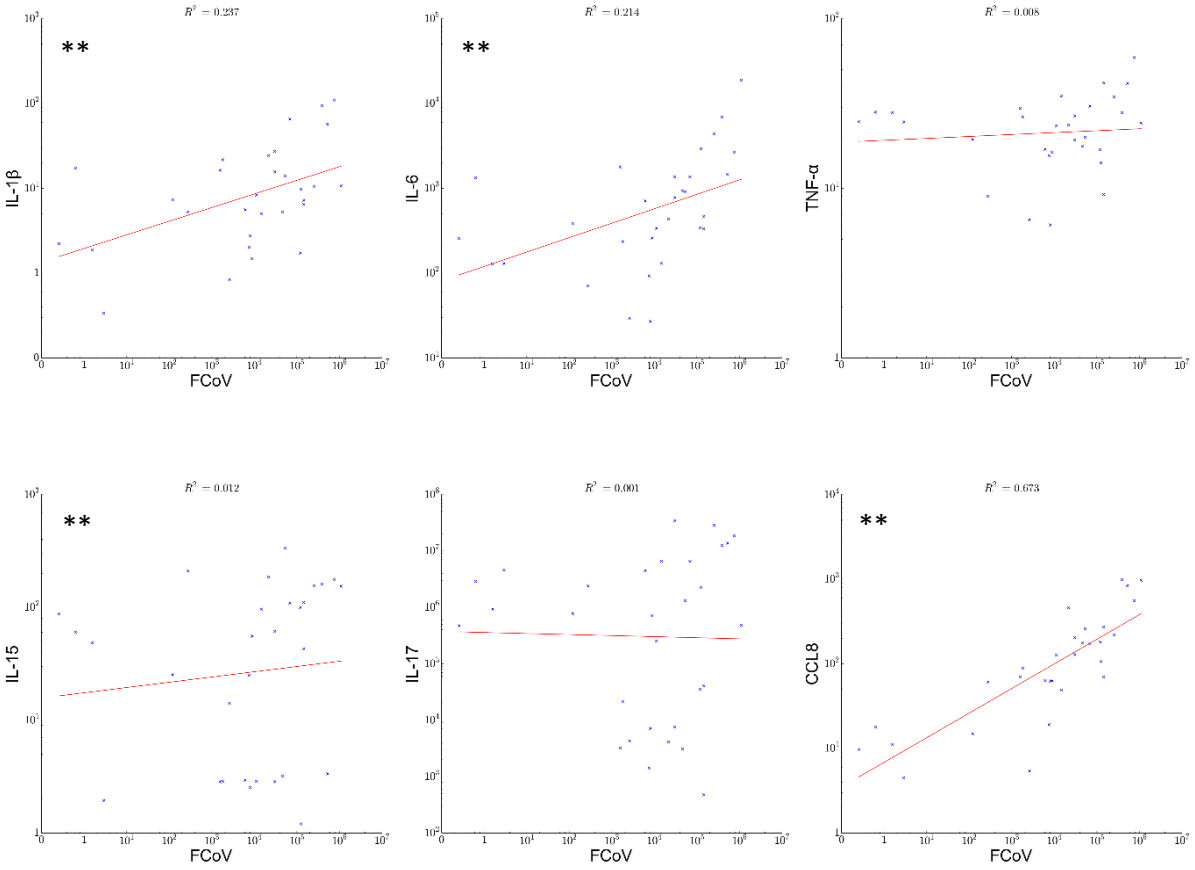

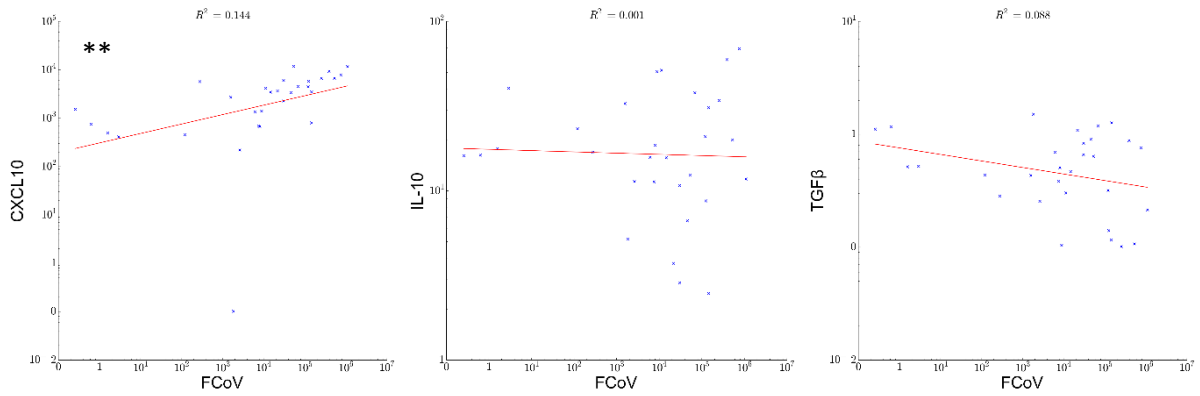

Figure 5.2.9: *Correlation between relative mRNA levels of cytokines and chemokines, and FCoV viral loads. Significance levels are marked by ** = p≤0.01; * = p≤0.05.*

Interferons

All three interferons showed positive correlation, this was only weak in the case of IFN-α. Fig. 5.2.10.

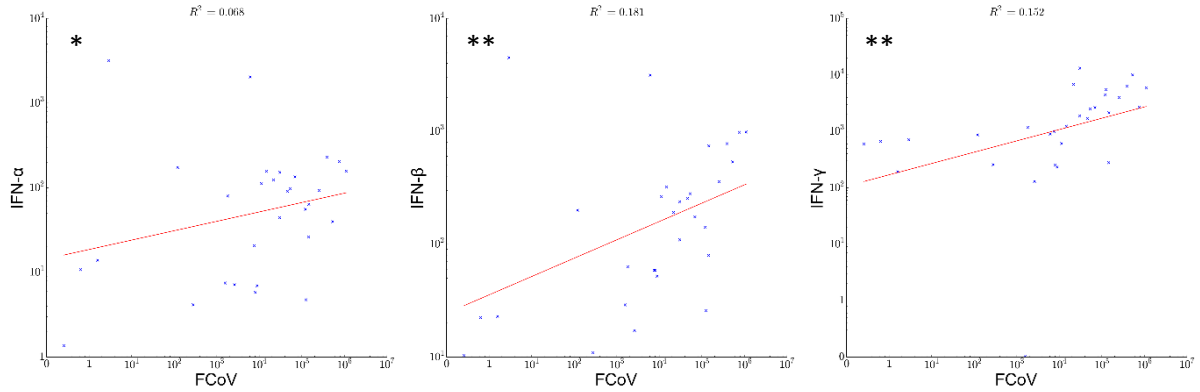

Figure 5.2.10: *Correlation between relative mRNA levels of interferons and FCoV viral loads. Significance levels are marked by ** = p≤0.01; * = p≤0.05.*

STATs

STAT2 was the only STAT to show significant correlation with viral load. Fig. 5.2.11.

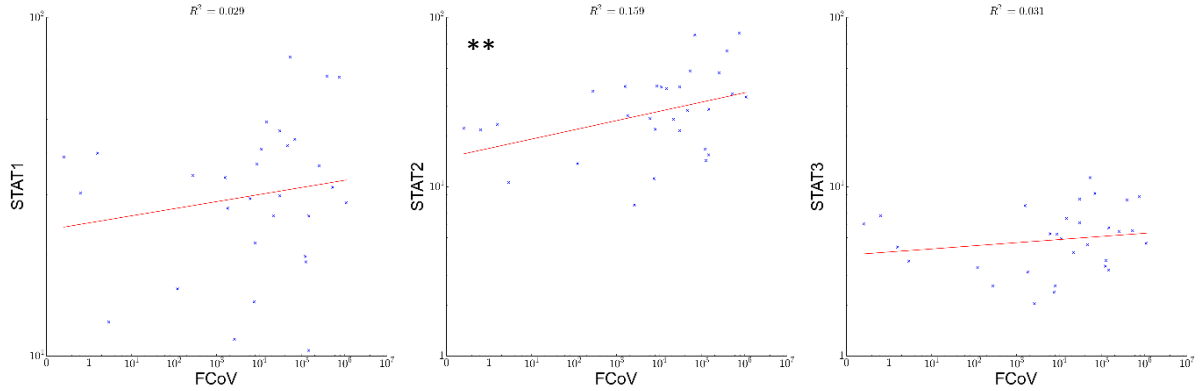

Figure 5.2.11: *Correlation between relative mRNA levels of STATs and FCoV viral loads. Significance levels are marked by ** = p≤0.01; * = p≤0.05.*

Matrix remodelling enzymes

These were one of the two groups of newly included mediators; MMP2 and TIMP1 were the only matrix remodelling enzymes to show correlation (with both being positive); both had been elevated in FIP. Fig. 5.2.12.

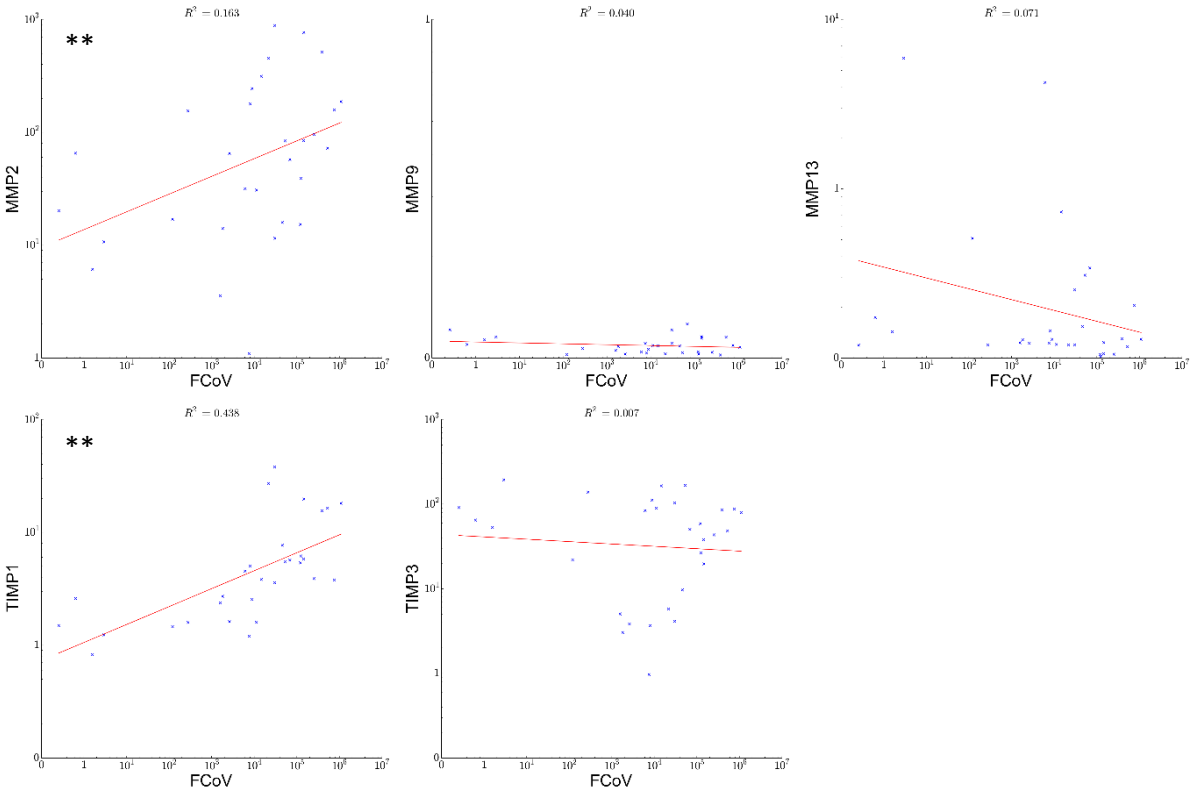

Figure 5.2.12: *Correlation between relative levels of matrix remodelling enzymes and FCoV viral loads. Significance levels are marked by ** = p≤0.01; * = p≤0.05.*

Colony stimulating factors

GM-CSF was the only CSF to show correlation with viral load, in a positive direction.

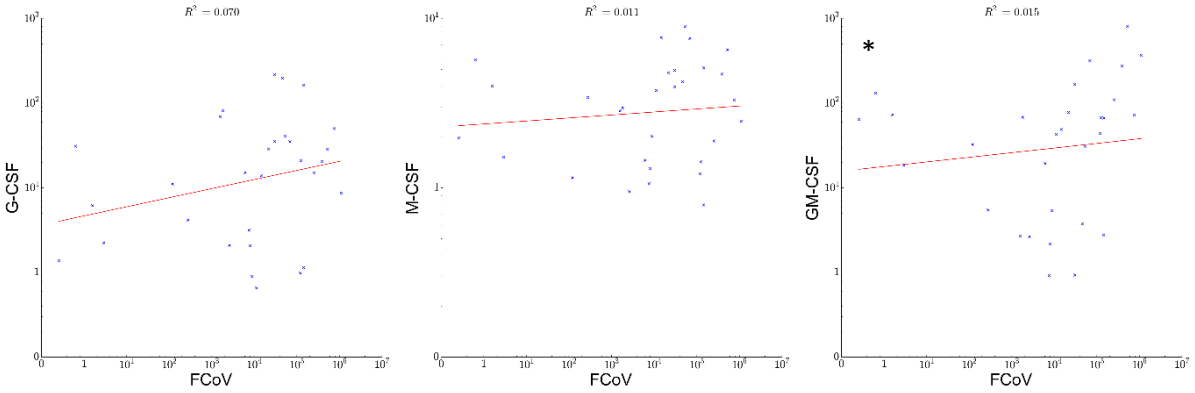

Figure 5.2.13: *Correlation between relative levels of colony stimulating factors and FCoV viral loads. Significance levels are marked by ** = p≤0.01; * = p≤0.05.*

Table 5.2.2: Summarised results of a one-tailed Spearman's rank test correalting results between FCoV viral loads and each mediator. The direction of the arrows indicates a positive or negative correlation and the number of arrows indicates the degree of significance ($p<0.01$ or $p<0.05$ respectively).

	FCoV	TLR1	TLR2	TLR3	TLR4	TLR5	TLR6	TLR7	TLR8	TLR9	STAT1	STAT2	STAT3	IFN-α	IFN-β	IFN-γ	IL-1β	IL-6	IL-10	IL-15	IL-17	TNF-α	TGFβ	MMP2	MMP9	MMP13	CXCL10	CCL8	TIMP1	TIMP3	G-CSF	M-CSF	GM-CSF
FCoV	●		↑↑		↑↑	↑↑			↑	↓		↑↑		↑	↑↑	↑↑	↑↑	↑↑		↑				↑↑			↑↑	↑↑	↑↑				↑
TLR1		●		↑↑	↑↑	↑↑	↑↑	↑↑	↑↑	↑↑	↑↑	↑	↑↑	↑	↑				↑↑	↑	↑↑			↑↑		↑↑	↑			↑↑		↑	↑
TLR2	↑↑		●		↑↑	↑↑			↑↑			↑	↑↑		↑↑	↑↑	↑↑	↑↑						↑↑			↑↑	↑↑	↑↑		↑↑	↑	↑↑
TLR3		↑↑		●	↑↑	↑↑	↑↑	↑↑	↑	↑↑	↑↑	↑↑	↑↑	↑	↑				↑↑		↑↑	↑		↑		↑↑				↑↑		↑↑	↑
TLR4	↑↑	↑↑	↑↑	↑↑	●	↑↑	↑↑	↑↑	↑↑		↑	↑↑	↑↑		↑	↑↑	↑↑	↑↑	↑	↑	↑↑			↑↑			↑↑	↑↑	↑↑	↑↑		↑	↑↑
TLR5	↑↑	↑↑	↑↑	↑↑	↑↑	●	↑↑	↑	↑↑			↑	↑↑	↑↑	↑↑	↑	↑	↑↑	↑		↑↑	↑		↑↑		↑	↑	↑	↑	↑↑		↑	↑
TLR6		↑↑		↑↑	↑↑	↑↑	●	↑↑	↑	↑↑	↑↑	↑	↑↑		↑						↑↑			↑↑		↑↑				↑↑		↑↑	↑
TLR7		↑↑		↑↑	↑↑	↑	↑↑	●	↑	↑↑	↑↑	↑↑	↑↑							↑↑	↑↑		↑	↑		↑	↑↑			↑↑		↑↑	↑
TLR8	↑	↑↑	↑↑	↑	↑↑	↑↑	↑	↑	●				↑↑				↑↑	↑↑	↑↑		↑			↑			↑	↑	↑	↑			↑↑
TLR9	↓	↑↑		↑↑			↑↑	↑↑		●	↑↑	↑	↑↑								↑	↑	↑↑		↑	↑↑				↑↑		↑	
STAT1		↑↑		↑↑	↑		↑↑	↑↑		↑↑	●	↑↑	↑↑				↑	↑		↑	↑	↑↑					↑↑	↑		↑↑	↑	↑↑	
STAT2	↑↑	↑	↑	↑↑	↑↑	↑	↑	↑↑		↑	↑↑	●	↑↑		↑		↑↑	↑↑	↑	↑↑	↑	↑↑					↑↑	↑↑			↑	↑↑	
STAT3		↑↑	↑↑	↑↑	↑↑	↑↑	↑↑	↑↑	↑↑	↑↑	↑↑	↑↑	●	↑	↑	↑	↑↑	↑↑			↑↑	↑↑	↑			↑	↑↑	↑↑	↑	↑↑	↑↑	↑↑	↑↑
IFN-α	↑	↑		↑		↑↑							↑	●	↑↑	↑↑	↑	↑			↑	↑				↑↑		↑					
IFN-β	↑↑	↑	↑↑	↑	↑	↑↑	↑					↑	↑	↑↑	●	↑↑		↑↑			↑	↑↑				↑	↑↑	↑↑	↑				
IFN-γ	↑↑		↑↑		↑↑	↑							↑	↑↑	↑↑	●	↑↑	↑↑		↑	↑	↑					↑↑	↑↑	↑↑		↑↑	↑	↑↑
IL-1β	↑↑		↑↑		↑↑	↑			↑↑		↑	↑↑	↑↑	↑		↑↑	●	↑↑			↑	↑↑	↑				↑↑	↑↑	↑↑		↑↑	↑↑	↑↑
IL-6	↑↑		↑↑		↑↑	↑↑			↑↑		↑	↑↑	↑↑	↑	↑↑	↑↑	↑↑	●			↑	↑↑					↑↑	↑↑	↑↑		↑↑	↑	↑↑
IL-10		↑↑		↑↑	↑	↑			↑↑			↑							●		↑		↓							↑	↓↓		
IL-15	↑	↑			↑			↑↑			↑	↑↑				↑				●				↑			↑↑	↑					
IL-17		↑↑		↑↑	↑↑	↑↑	↑↑	↑↑	↑	↑	↑	↑	↑↑	↑	↑	↑	↑	↑	↑		●	↑↑		↑		↑	↑			↑↑		↑	↑↑
TNF-α				↑		↑				↑	↑↑	↑↑	↑↑	↑	↑↑	↑	↑↑	↑↑			↑↑	●	↑		↑		↑	↑			↑↑	↑↑	↑↑
TGFβ								↑		↑↑			↑				↑		↓			↑	●			↑↑					↑↑	↑↑	
MMP2	↑↑	↑↑	↑↑	↑	↑↑	↑↑	↑↑	↑	↑											↑	↑			●			↑	↑↑	↑↑	↑		↑	↑
MMP9										↑												↑			●								
MMP13		↑↑		↑↑		↑	↑↑	↑		↑↑			↑	↑↑	↑						↑		↑↑			●				↑			
CXCL10	↑↑	↑	↑↑		↑↑	↑		↑↑	↑		↑↑	↑↑	↑↑		↑↑	↑↑	↑↑	↑↑		↑↑	↑	↑		↑			●	↑↑	↑↑			↑↑	↑
CCL8	↑↑		↑↑		↑↑	↑			↑		↑	↑↑	↑↑	↑	↑↑	↑↑	↑↑	↑↑		↑		↑		↑↑			↑↑	●	↑↑		↑↑	↑	↑↑
TIMP1	↑↑		↑↑		↑↑	↑			↑				↑		↑	↑↑	↑↑	↑↑						↑↑			↑↑	↑↑	●		↑	↑	↑↑
TIMP3		↑↑		↑↑	↑↑	↑↑	↑↑	↑↑	↑	↑↑	↑↑		↑↑						↑		↑↑			↑		↑				●		↑	
G-CSF			↑↑								↑	↑	↑↑			↑↑	↑↑	↑↑	↓↓			↑↑	↑↑					↑↑	↑		●	↑↑	
M-CSF		↑	↑	↑↑	↑	↑	↑↑	↑↑		↑	↑↑	↑↑	↑↑			↑	↑↑	↑			↑	↑↑	↑↑	↑			↑↑	↑	↑	↑	↑↑	●	↑↑
GM-CSF	↑	↑	↑↑	↑	↑↑	↑	↑	↑	↑↑				↑↑			↑↑	↑↑	↑↑			↑↑	↑↑		↑			↑	↑↑	↑↑				●

Relationship between the presence of specific amino acid sequences and mediator levels

Following selected S gene sequencing, comparisons between animals carrying virus with M or L at codon 1048 were described in the manuscript. With only one cat infected by a 'non-mutated enteric virus', no statistical comparisons were possible. Instead the sequencing results for the MLN from Group 2 cats were compared visually by plotting results for individual cats in columns relating to sequence within the overall group results. Only the FCoV result was portrayed graphically in the publication, therefore the remainder are displayed in full here, along with the additional mediator groups. FCoV is shown again for direct comparison with the mediators.

These results show that the 'non-pathogenic' virus levels, with M and S at the described codons, are at the upper limit of the whiskers (Fig. 5.2.14), indicating a spread of 1.5 times the interquartile range (IQR). For brevity, this cat will be referred to in this section as 'E' for enteric virus.

Results for the single E cat were near the top of the interquartile range for the significantly elevated TLRs 2, 4, and 8 (Fig. 5.2.15). It is known that these correlate with FCoV so this is compatible with the viral load.

All cytokine and chemokine levels in cat E except IL-1β and TGFβ (i.e. IL-6, IL-10, IL-15, IL-17, TNF-α, CCL8, CXCL10) are above the group interquartile range. All these targets were generally elevated in FIP except IL-10, IL-17 and TGFβ. See Fig. 5.2.16

IFNs were all expressed in the upper half (IFN-α), to upper limit (IFN-β and -γ) of the IQR by cat E (Fig. 5.2.17).

STAT expression was in the upper half (STAT1 and 3) or above the IQR (STAT2). See Fig. 5.2.17.

Cat E expressed MMPs 2 and 9, and TIMPs 1 and 3 within the IQR. MMP13 was below it. See Fig. 5.2.18.

Of the CSFs, only G-CSF was elevated in Group 2, cat E had the median G-CSF result, within range M-CSF and above range GM-CSF. See Fig. 5.2.18.

These results show that cat E had a tendency towards the extremes of the ranges, usually in the same direction as the significance of that target (i.e. the top end in targets elevated in FIP). However, reliable conclusions cannot be drawn from these results; the tendency was not always consistent, is only the result of one cat, and may relate to the high FCoV load relative to the group.

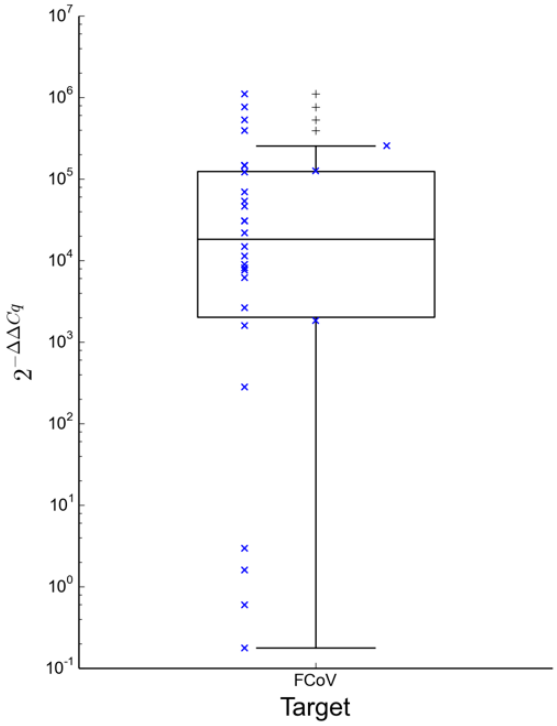

Figure 5.2.14: *Results for relative viral mRNA loads in the MLN of cats within Group 2. Columns of crosses represent from left to right: M1048L (27 cats); 1048M-S1050A (2 cats); 1048M-1050S (1 cat).*

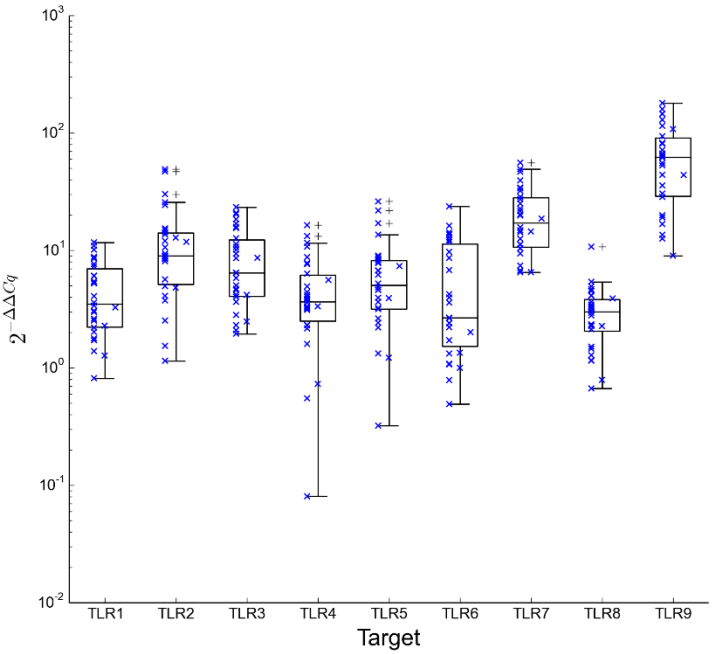

Figure 5.2.15: *Results for relative TLR mRNA levels in the MLN of cats within Group 2. Columns of crosses represent from left to right: M1048L (27 cats); 1048M-S1050A (2 cats); 1048M-1050S (1 cat).*

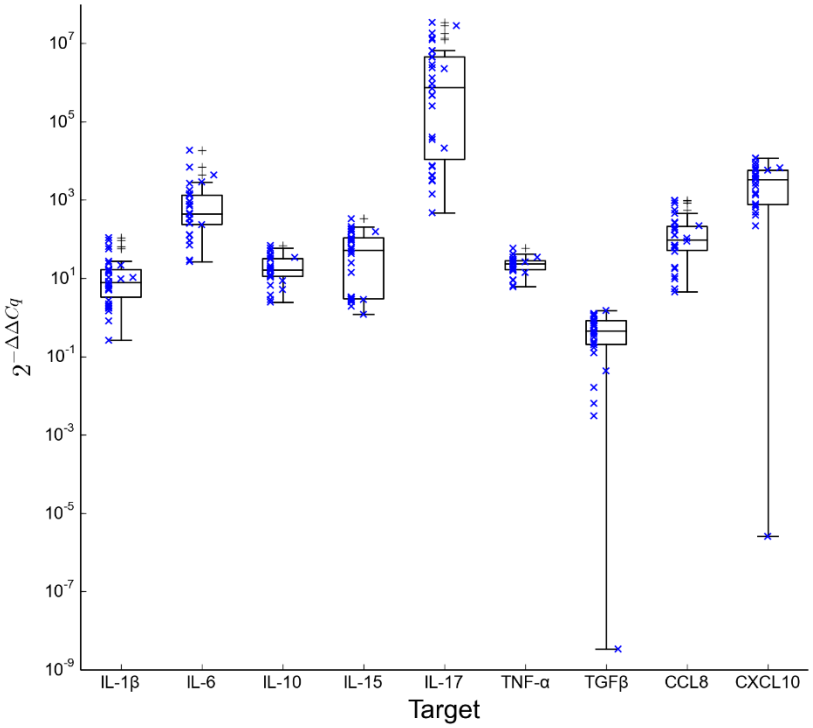

Figure 5.2.16: *Results for relative cytokine and chemokine mRNA levels in the MLN of cats within group 2. Columns of crosses represent from left to right: M1048L (27 cats); 1048M-S1050A (2 cats); 1048M-1050S (1 cat).*

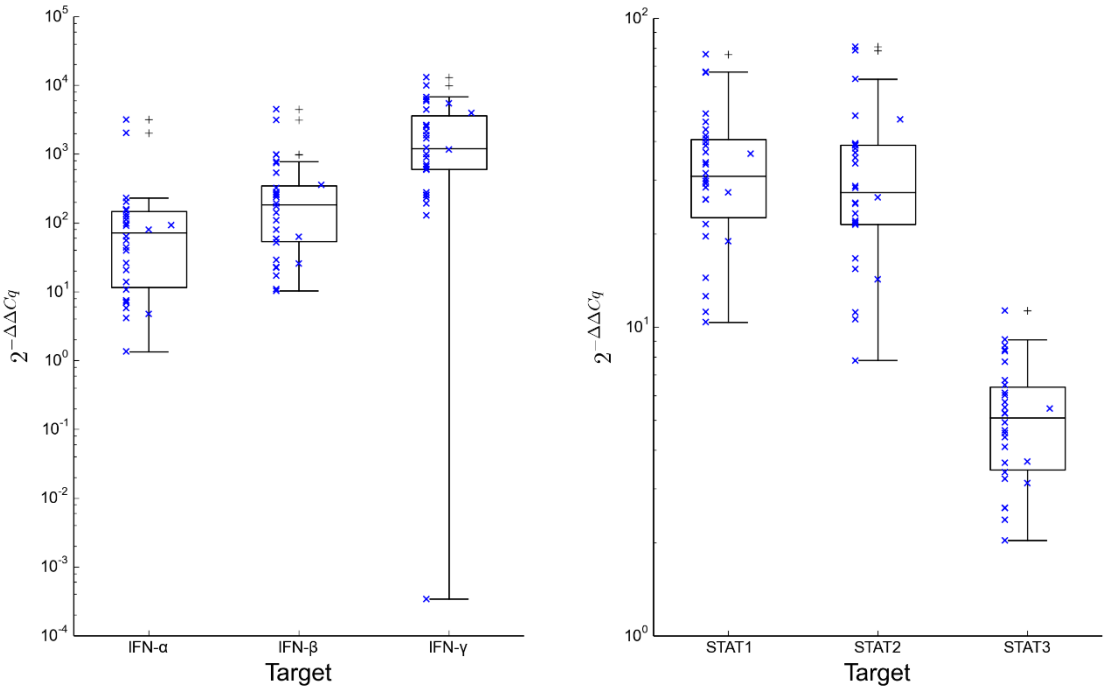

Figure 5.2.17: *Results for relative interferon (left) and STAT (right) mRNA levels in the MLN of cats within group 2. Columns of crosses represent from left to right: M1048L (27 cats); 1048M-S1050A (2 cats); 1048M-1050S (1 cat).*

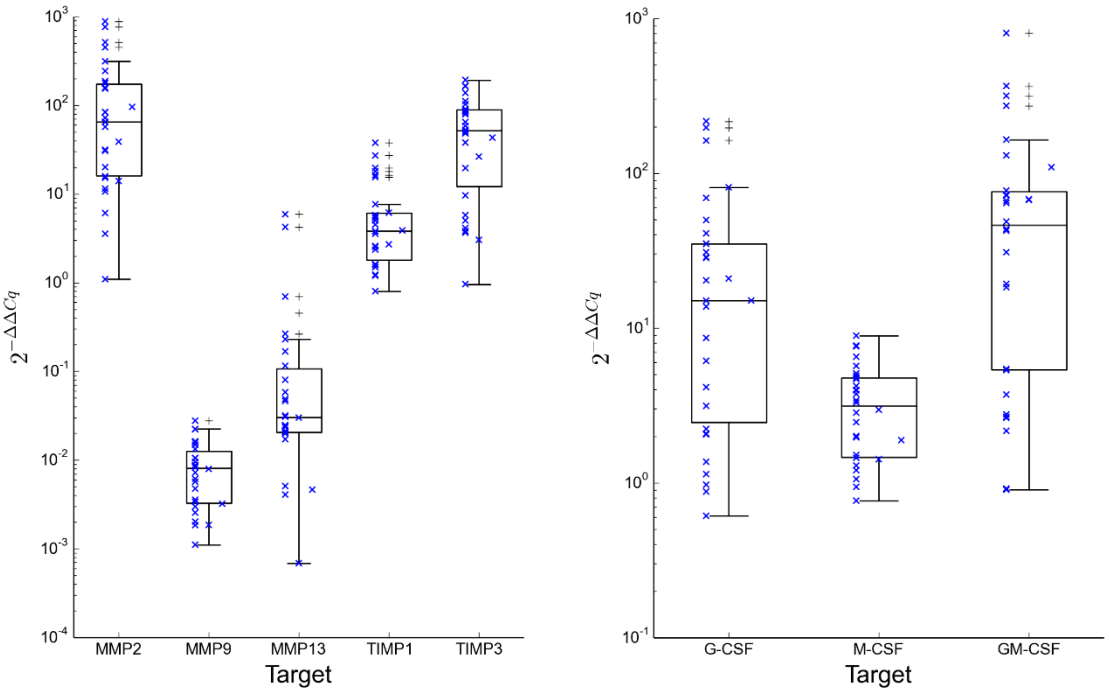

Figure 5.2.18: *Results for relative matrix remodelling enzyme (left) and colony stimulating factor (right) mRNA levels within Group 2. Columns of crosses represent from left to right: M1048L (27 cats); 1048M-S1050A (2 cats); 1048M-1050S (1 cat).*

3. Results of RT-qPCR for immune mediators on laser capture microdissection (LCM) samples

Cryoblocks made from FIP lesions of the cats sampled in Zurich were used for LCM. LCM samples were taken from the typical, macrophage-dominated FIP lesions both on the serosa (e.g. Fig. 5.3.1) and within tissues (parenchymal lesions e.g. 5.3.2). All lesion samples were assembled into a new group (Group 2+) and compared with the entire Group 2 MLN results (as presented in the previous chapter) (shown in Fig. 5.3.3-Fig. 5.3.9 and Table 5.3.1). None of the LCM samples taken included recognisable pre-existing parenchyma (e.g. a sample from hepatic serositis contained only cells from a focal inflammatory infiltrate and no hepatocytes), therefore samples were not further segregated by organ. Instead, they were subsequently further divided into those dominated by a fibrinous exudate (serositis; though the macrophage dominated regions were still targeted) and granulomatous lesions, and these two subgroups compared (Fig. 5.3.3.5.3.9 and Table 5.3.1).

Examples of the cryoblock sections are shown in Fig. 5.3.1 and 5.3.2. As a smaller investigation, and in order to exclude as far as possible the macrophage contribution within the red pulp, LCM samples of lymphoid follicles were also taken from four cats (see below for more details and Fig. 5.3.10-5.3.14).

When the term ‘bulk’ tissue is used, it refers to the organ samples taken into RNAlater in which there was no selection for region.

It was not possible to reliably compare TLR6, IL-10, IL-15, IL-17, MMP9, MMP13, IFN-β, G-CSF or GM-CSF mRNA levels owing to uneven pre-amplification (see methods section 4); these results were not included in the evaluation.

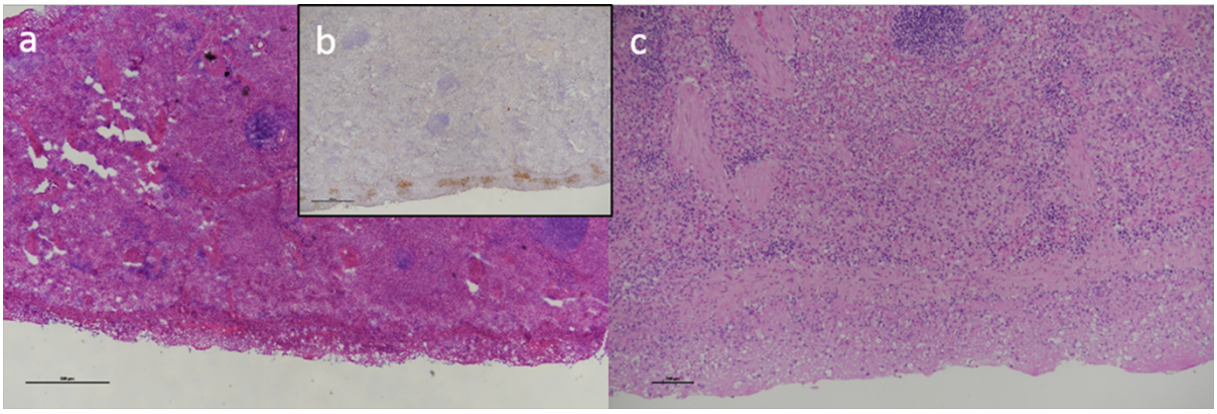

Figure 5.3.1: *Splenic serositis from case S16-0167, example of cryoblock quality stained by HE (a) and IH for FCoV (b) versus FFPE section stained by HE (c).*

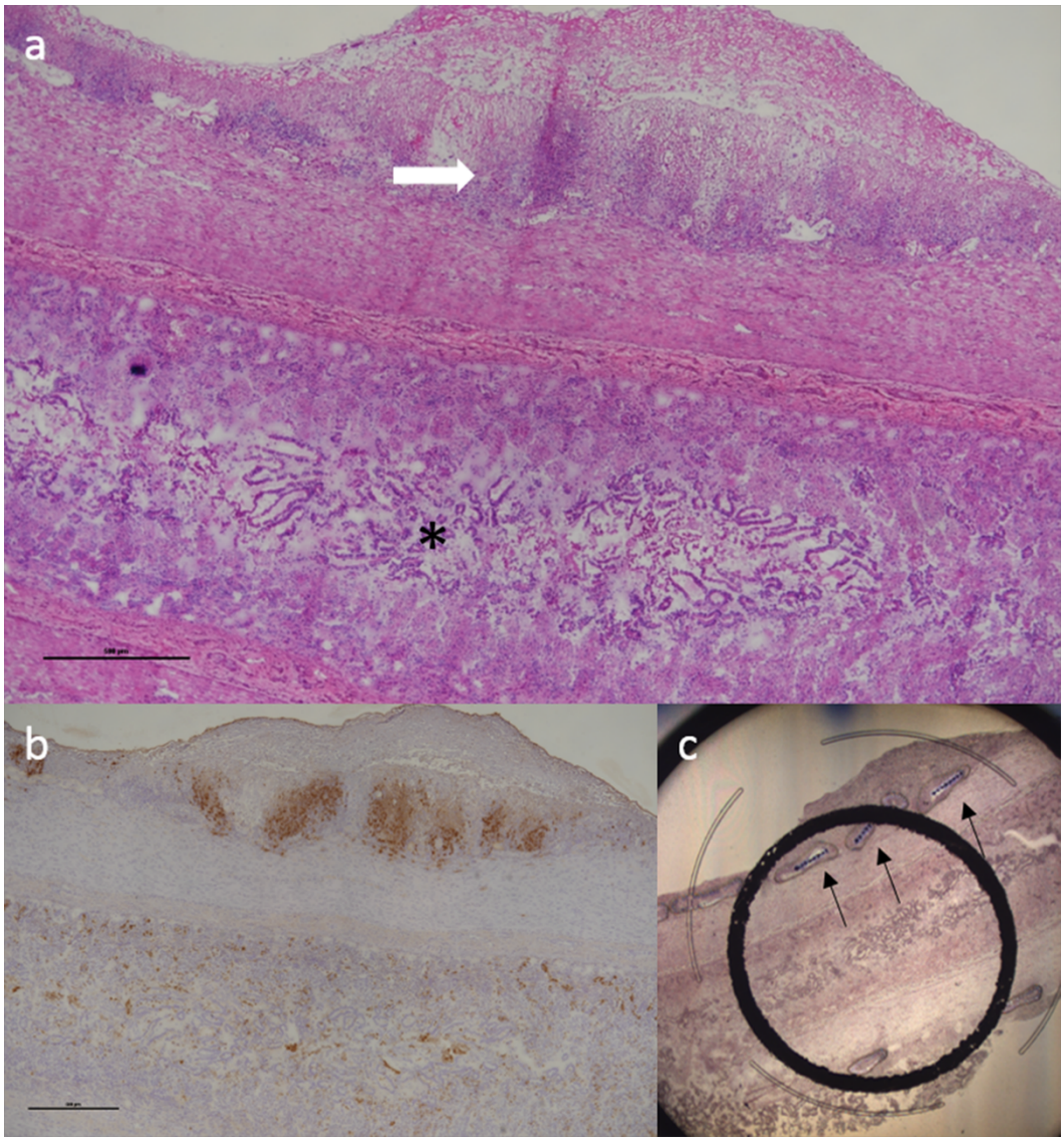

Figure 5.3.2: *Small intestine from case S17-0124; a) example HE stained cryoblock of a sampled granulomatous lesion (arrow) beneath serositis; b) FCoV IH of a consecutive section confirming concentration of FCoV infected cells in the lesions (there are also positively stained epithelial cells); c) cresyl violet stained membrane slide during LCM, the cap is overlying the slide and arrows mark the selected and laser captured areas, corresponding to lesions shown in a) and b).*

FCoV

Viral RNA levels were significantly higher in the LCM lesion samples in comparison to the bulk MLN results from Group 2 cats (Fig. 5.3.3), reinforcing that regions dominated by infected macrophages had been successfully sampled. The levels in granulomatous lesions were significantly higher than in serositis lesions, likely due to the overall higher number of macrophages, though the groups overlapped.

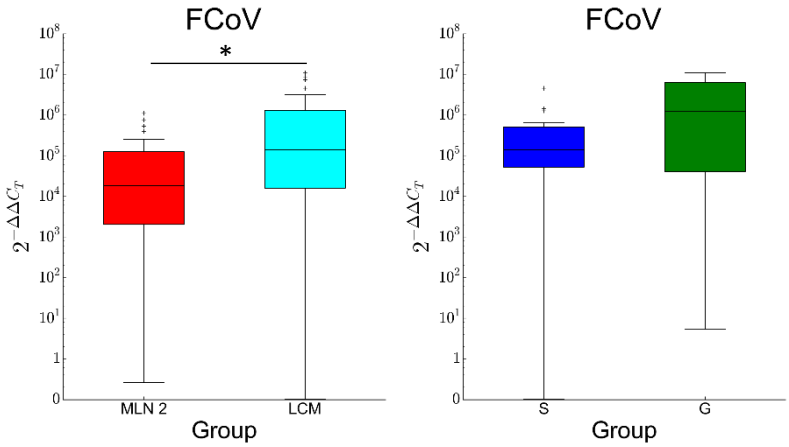

Figure 5.3.3: *Boxplots of (left) relative mRNA levels of FCoV in the FIP (Group 2) MLN samples (n=30) versus the LCM lesion samples (n=27); boxplots of (right) relative mRNA levels of FCoV between serosal lesions (n=17) and granulomatous parenchymal lesions (n=10) within the LCM lesion group. The amount of target was calculated by $2^{-\Delta\Delta CT}$, using fGAPDH as the internal reference gene for normalisation and expressed as an n-fold difference relative to the G1 mean of the BM samples as a calibrator. The boxes depict the median and interquartile (IQ) range with whiskers extending to the highest and lowest values which are within 1.5 x the IQ range. Outliers beyond this are individually marked. * marks significant differences between individual groups (p≤0.05).*

Toll-like receptors

TLR2, 4, and 8 mRNA levels were significantly higher in LCM lesion samples in comparison to the bulk MLN levels from Group 2 cats, whilst TLR1, 7, and 9 were significantly lower in lesions. TLR3 had a very mild tendency (not significant) to be lower in lesions. None of the TLRs showed any significant differences, or noticeable tendencies, between the lesion subtypes. Fig. 5.3.4.

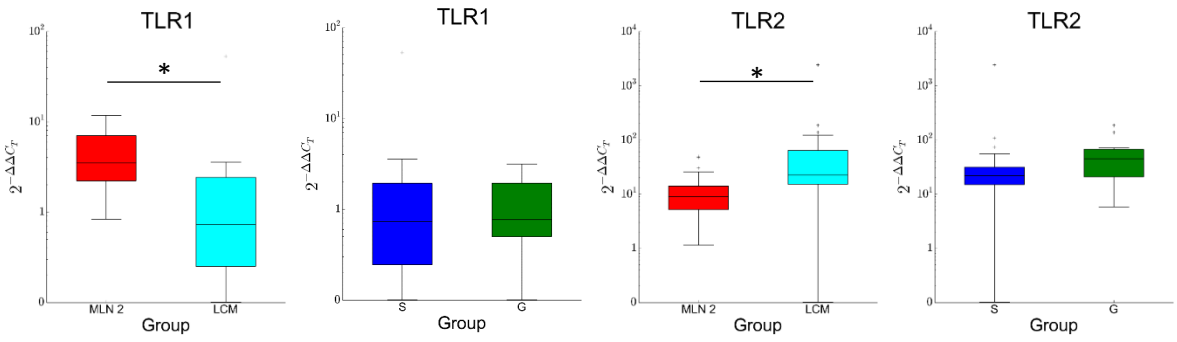

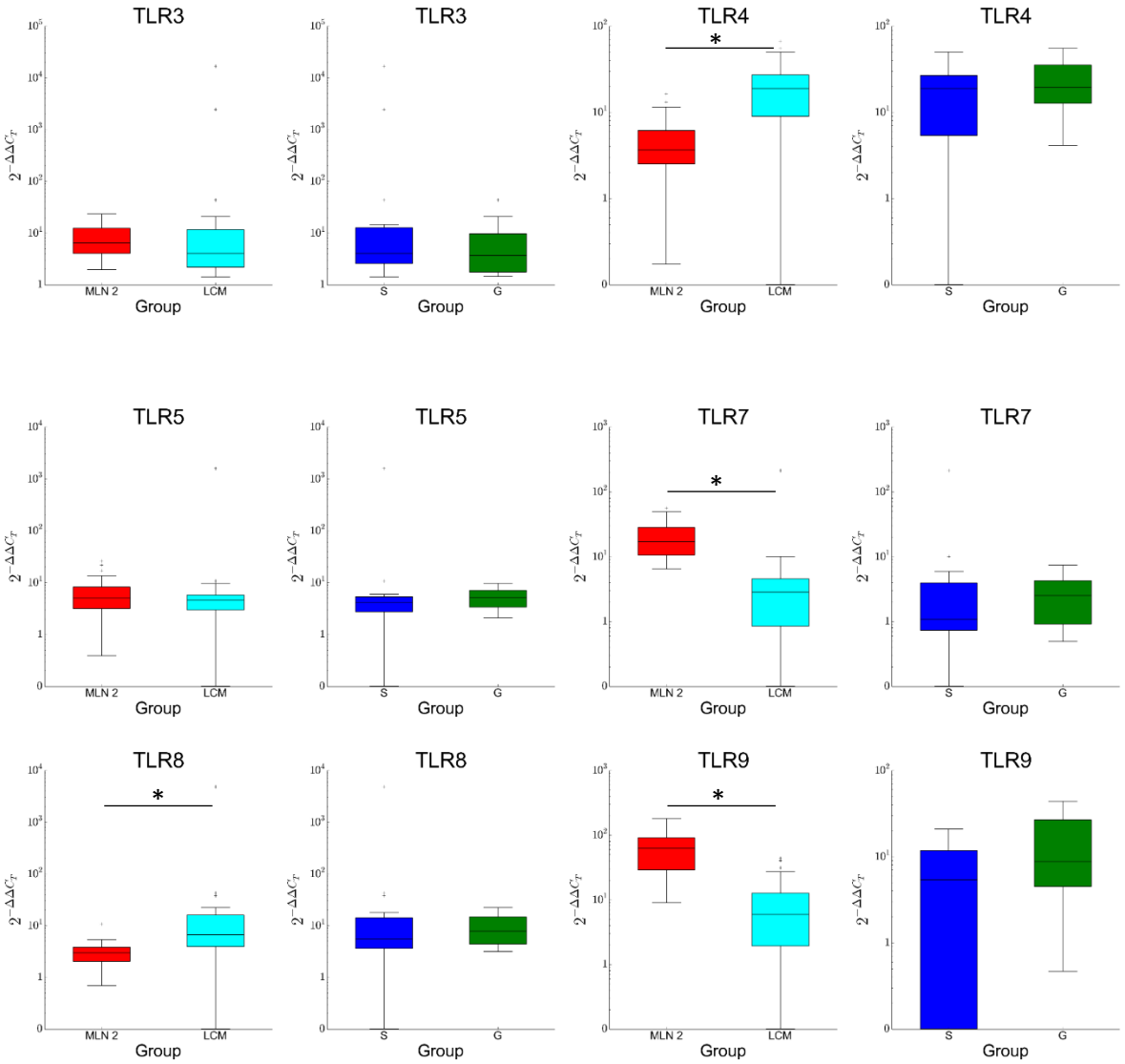

Figure 5.3.4: *Red and turquoise: Boxplots of relative TLR mRNA levels in the FIP MLN samples ((Group 2; n=30) versus the LCM lesion samples (Group 2+; n=27). Blue and green: Boxplots of relative TLR mRNA levels between serosal lesions (n=17) and granulomatous parenchymal lesions (n=10) within the LCM lesion group. The amount of target was calculated by* $2^{-\Delta\Delta CT}$*, using fGAPDH as the internal reference gene for normalisation and expressed as an n-fold difference relative to the G1 mean of the BM samples as a calibrator. The boxes depict the median and interquartile (IQ) range with whiskers extending to the highest and lowest values which are within 1.5 x the IQ range. Outliers beyond this are individually marked. * marks significant differences between individual groups (p≤0.05).*

Cytokines and chemokines

Of the interleukins, only IL-1β and IL-6 could be evaluated, with only IL-1β significantly higher in LCM lesions in comparison to the bulk MLN levels from Group 2 cats. IL-6 exhibited no difference at all between LCM samples and bulk MLN but was higher in granulomatous parenchymal lesions than in serosal lesions. TGF-β levels were significantly lower in LCM samples than in the bulk MLN and yet significantly higher in granulomatous lesions than in serosal lesions. CCL8 but not CXCL10 levels were significantly higher in LCM lesions than in the bulk MLN, neither differed between subgroups. Fig. 5.3.5

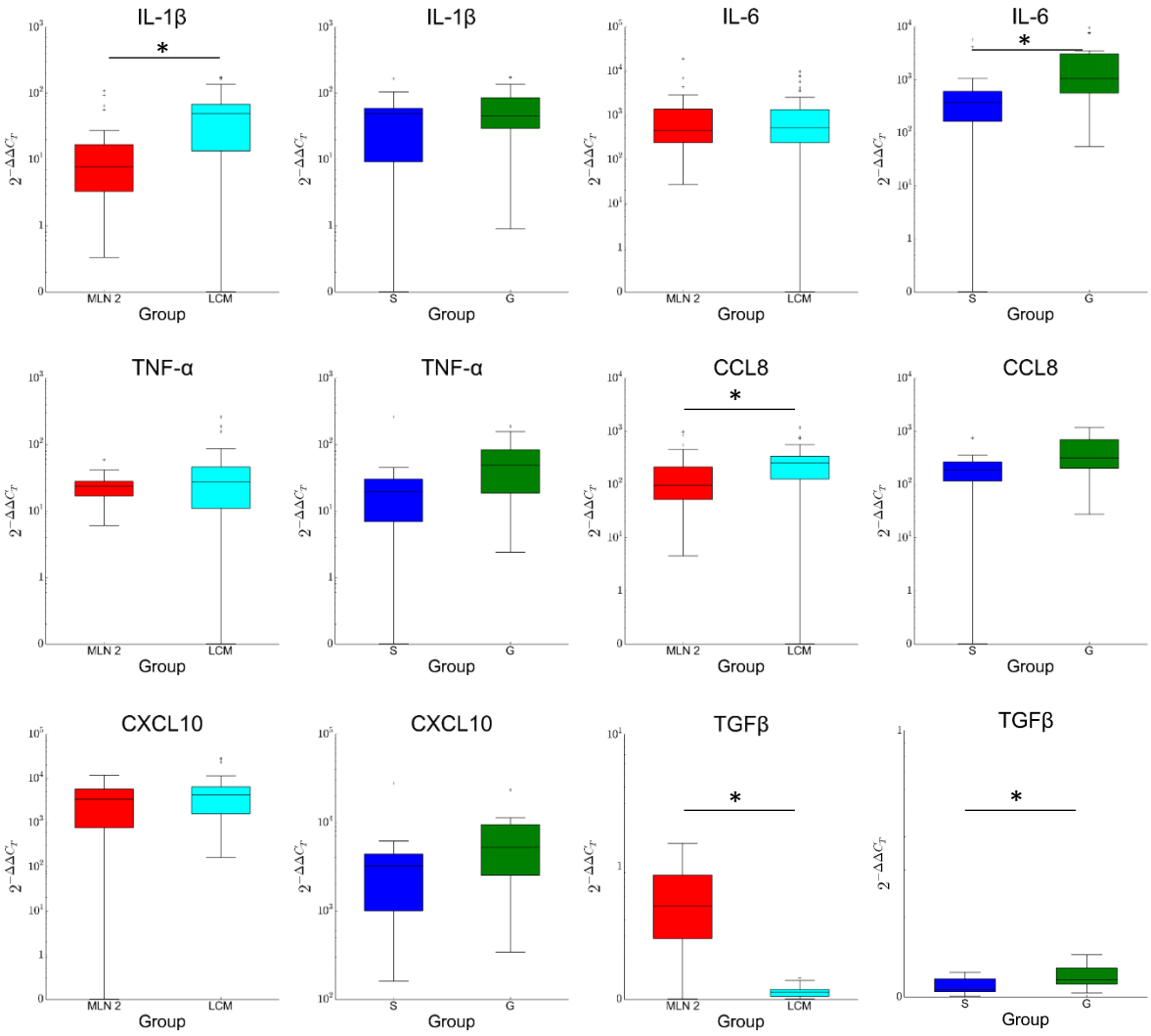

Figure 5.3.5: *Red and turquoise: Boxplots of relative cytokine and chemokine mRNA levels in the FIP MLN samples (Group 2; n=30) versus the LCM lesion samples (Group 2+; n=27). Blue and green: Boxplots of relative cytokine and chemokine mRNA levels between serosal lesions (n=17) and granulomatous parenchymal lesions (n=10) within the LCM lesion group. The amount of target was calculated by 2-ΔΔCT, using fGAPDH as the internal reference gene and expressed as an n fold difference relative to the G1 mean of the BM samples as a calibrator. The boxes depict the median and interquartile (IQ) range with whiskers extending to the highest and lowest values which are within 1.5 x the IQ range. Outliers beyond this are individually marked. * marks significant differences between individual groups (p≤0.05).*

Interferons

IFN-α and -γ were evaluated, with only the former significantly higher in LCM lesions in comparison to bulk MLN. Neither IFN showed a significant difference between granulomatous and serosal lesions. Fig. 5.3.6.

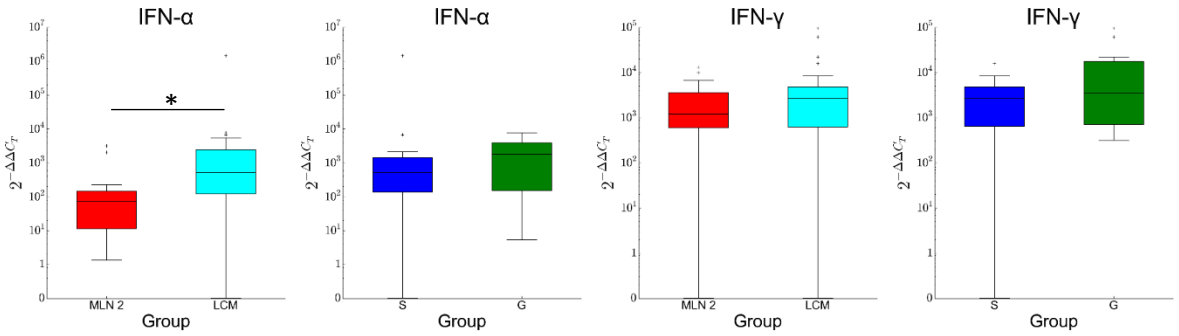

*Figure 5.3.6: Red and turquoise: Boxplots of relative interferon mRNA levels in the FIP MLN samples (Group 2; n=30) versus the LCM lesion samples (Group 2+; n=27). Blue and green: Boxplots of relative interferon mRNA levels between serosal lesions (n=17) and granulomatous parenchymal lesions (n=10) within the LCM lesion group. The amount of target was calculated by $2^{-\Delta\Delta CT}$, using fGAPDH as the internal reference gene for normalisation and expressed as an n-fold difference relative to the G1 mean of the BM samples as a calibrator. The boxes depict the median and interquartile (IQ) range with whiskers extending to the highest and lowest values which are within 1.5 x the IQ range. Outliers beyond this are individually marked. * marks significant differences between individual groups (p≤0.05).*

STATs

All three STATs were significantly lower in LCM lesions than in bulk MLN. Interestingly, none of the comparisons in previous chapters (between the control group and the FIP group for the BM, spleen, and MLN) had shown a significant difference for STAT3. STAT1 and 3 mRNA levels were significantly higher in granulomatous than serosal lesions, with STAT2 levels just failing to reach significance in the same direction. Fig. 5.3.7.

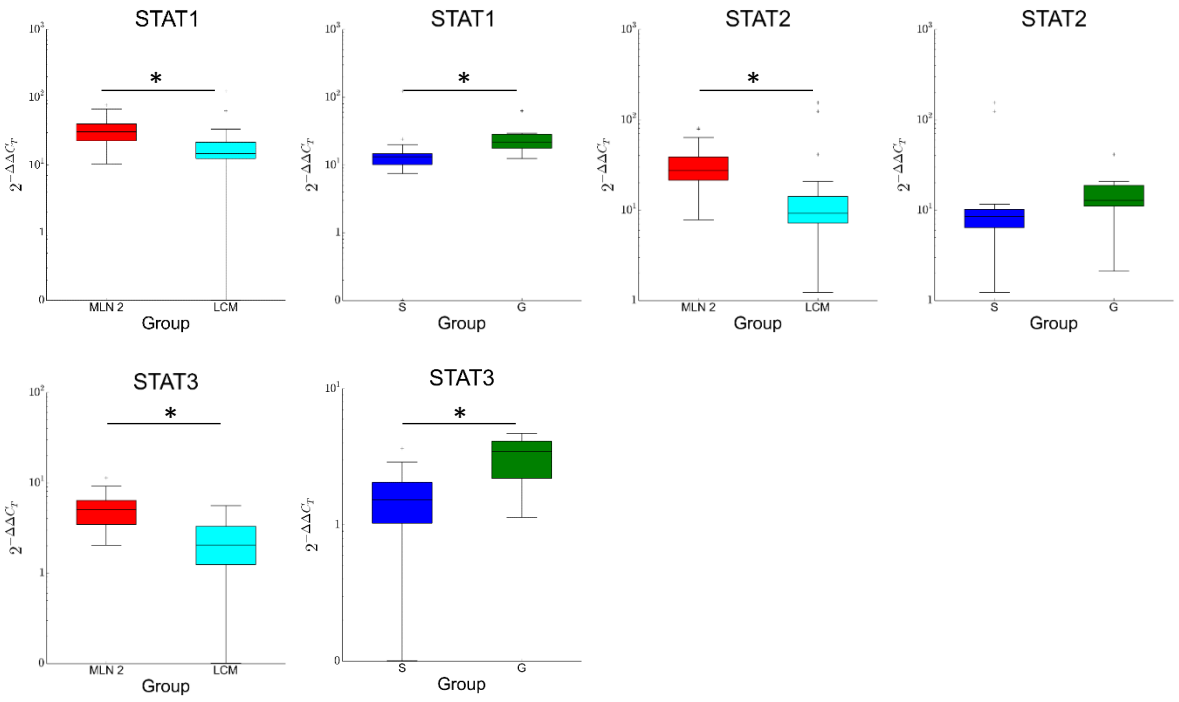

***Figure 5.3.7:** Red and turquoise: Boxplots of relative STAT mRNA levels in the FIP MLN samples (Group 2; n=30) versus the LCM lesion samples (Group 2+; n=27). Blue and green: Boxplots of relative STAT*

*mRNA levels between serosal lesions (n=17) and granulomatous parenchymal lesions (n=10) within the LCM lesion group. The amount of target was calculated by $2^{-\Delta\Delta CT}$, using fGAPDH as the internal reference gene for normalisation and expressed as an n-fold difference relative to the G1 mean of the BM samples as a calibrator. The boxes depict the median and interquartile (IQ) range with whiskers extending to the highest and lowest values which are within 1.5 x the IQ range. Outliers beyond this are individually marked. * marks significant differences between individual groups (p≤0.05).*

Matrix remodelling enzymes

Only MMP2 and the TIMPs could be evaluated, with significantly lower MMP2 and TIMP3 mRNA levels in lesions and significantly higher TIMP1 levels than in bulk MLN. Granulomatous lesions had significantly higher levels than serosal lesions for all three enzymes. Fig. 5.3.8.

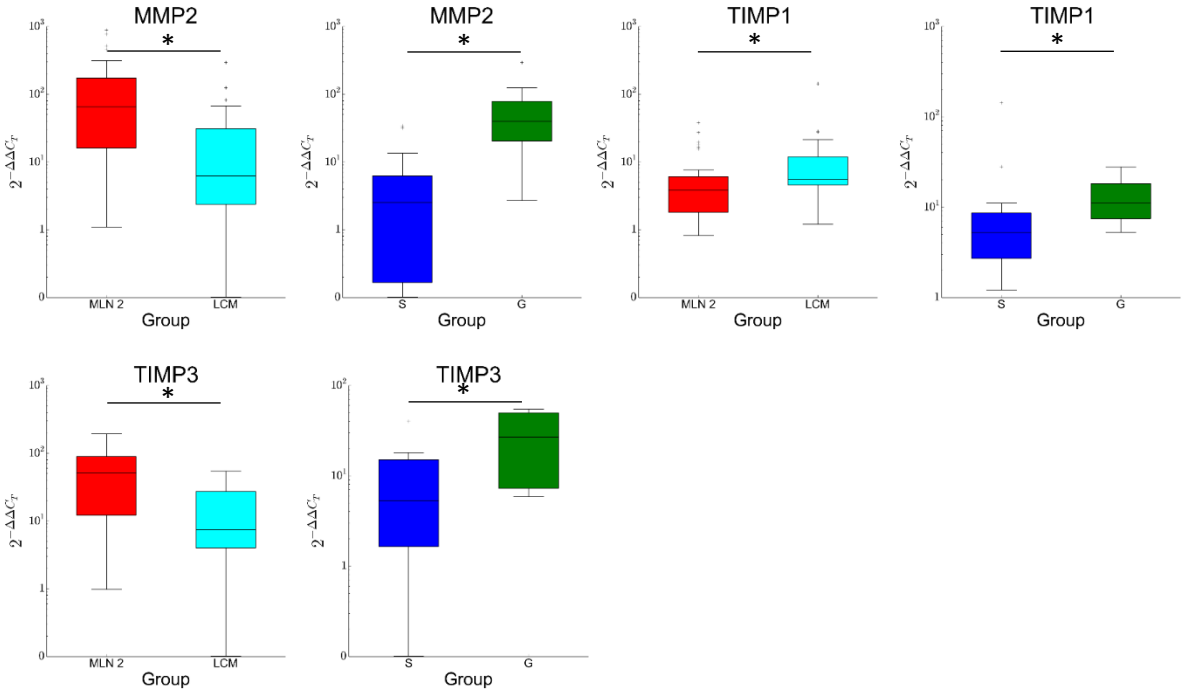

Figure 5.3.8: *Red and turquoise: Boxplots of relative matrix remodelling enzyme mRNA levels in the FIP MLN samples ((Group 2; n=30) versus the LCM lesion samples (Group 2+; n=27). Blue and green: Boxplots of relative matrix remodelling enzyme mRNA levels between serosal lesions (n=17) and granulomatous parenchymal lesions (n=10) within the LCM lesion group. The amount of target was calculated by $2^{-\Delta\Delta CT}$, using fGAPDH as the internal reference gene for normalisation and expressed as an n-fold difference relative to the G1 mean of the BM samples as a calibrator. The boxes depict the median and interquartile (IQ) range with whiskers extending to the highest and lowest values which are within 1.5 x the IQ range. Outliers beyond this are individually marked. * marks significant differences between individual groups (p≤0.05).*

Colony stimulating factors

Only M-CSF could be evaluated, this was significantly lower in LCM lesions than in bulk MLN, and significantly higher in granulomatous than in serosal lesions. Fig. 5.3.9.

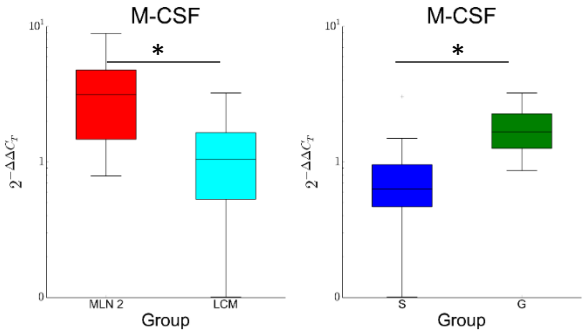

Figure 5.3.9: *Red and turquoise: Boxplots of relative M-CSF mRNA levels in the FIP MLN samples (Group 2; n=30) versus the LCM lesion samples (Group 2+; n=27). Blue and green: Boxplots of relative M-CSF mRNA levels between serosal lesions (n=17) and granulomatous parenchymal lesions (n=10) within the LCM lesion group. The amount of target was calculated by 2-ΔΔCT, using fGAPDH as the internal reference gene for normalisation and expressed as an n-fold difference relative to the G1 mean of the BM samples as a calibrator. The boxes depict the median and interquartile (IQ) range with whiskers extending to the highest and lowest values which are within 1.5 x the IQ range. Outliers beyond this are individually marked. * marks significant differences between individual groups (p≤0.05).*

Table 5.3.1: Statistical results of a Mann-Whitney comparison between MLN G2 samples and LCM lesion samples, and between serosal (S) and granulomatous (G) lesions. Significant results ($p \leq 0.05$) are highlighted in blue. ↑: increased in G2+/G. Targets written in grey could not be compared for LCM samples. The G1 vs G2 result from Chapter 2 is included for reference.

Target	G1 vs G2		G2 vs G2+		G2+: S vs G	
FCoV	0.000	↑	0.009	↑	0.223	
TLR1	0.610		0.000	↓	0.473	
TLR2	0.000	↑	0.000	↑	0.286	
TLR3	0.569		0.144		0.505	
TLR4	0.019	↑	0.000	↑	0.604	
TLR5	0.053		0.350		0.414	
TLR6	0.859					
TLR7	0.059		0.000	↓	0.639	
TLR8	0.013	↑	0.000	↑	0.749	
TLR9	0.991		0.000	↓	0.141	
STAT1	0.000	↑	0.000	↓	0.003	↑
STAT2	0.000	↑	0.000	↓	0.052	
STAT3	0.260		0.000	↓	0.003	↑
IFN-α	0.041	↑	0.002	↑	0.414	
IFN-β	0.004	↑				
IFN-γ	0.000	↑	0.225		0.537	
IL-1β	0.026	↑	0.002	↑	0.473	
IL-6	0.001	↑	0.988		0.040	↑
IL-10	0.296					
IL-15	0.019	↑				
IL-17	0.440					
TNF-α	0.004	↑	0.586		0.083	
TGFβ	0.430		0.000	↓	0.040	↑
CCL8	0.000	↑	0.003	↑	0.443	
CXCL10	0.000	↑	0.384		0.204	
MMP2	0.035	↑	0.000	↓	0.000	↑
MMP9	0.204					
MMP13	0.011	↓				
TIMP1	0.000	↑	0.046	↑	0.023	↑
TIMP3	0.117		0.001	↓	0.004	↑
G-CSF	0.000	↑				
M-CSF	0.476		0.000	↓	0.001	↑
GM-CSF	0.921					

Comparisons of selected mediator levels between organs and lesions

From all mediators examined, a selection were chosen which were of most interest based on the results of the current and previous chapters. These comprised: the TLRs upregulated in the MLN in FIP (TLR 2, 4, and 8); the TLRs with a possible viral-mediated downregulation in the MLN in FIP (TLR 3 and 7); TLR9 which was upregulated in the MLN of FCoV-infected control cats in comparison to cats without FCoV positive MLN; IFNs, the main cytokines downstream of anti-viral TLRs; the main cytokines downstream of pro-inflammatory TLR signalling (IL-1β, IL-6, TNF-α,); the chemokines with a potential role in cell recruitment to lesions (CCL8 and CXCL10); the transcription factors mediating IFN signalling (STATs).

For each of these mediators, the relative mRNA levels detected in different tissues were compared. The bone marrow, a primary haemolymphatic organ, was used as a basal level (n=10). This organ showed no lesions or immunohistologically detectable virus in any animal yet was, in all except one of the animals in this cohort, PCR positive for FCoV; suggesting this is mainly a result of virus within monocytes and indicating that animals with FIP are generally viraemic at the final stage of disease. As far as possible, splenic samples were taken from lesion free areas so that levels here mainly reflect the systemic response of this lymphatic organ (n=11). The MLN, as previously described, were of specific interest as the first site of viral spread beyond the intestine (n=8). Lymphoid follicles, free of lesions and morphologically detectable coronavirus infection, were taken by LCM from four cases, from spleen, MLN, and Peyer's patches, with the aim of largely excluding the macrophage contribution to mediator production (n=4). It was also of interest to see how similarly these various lymphoid follicles behaved in terms of mediator transcription, i.e. the importance of cell type versus anatomic location. Finally, the lesions themselves were evaluated to gain an approximation of the contribution of the infected cells themselves. These were pooled without reference to the affected organ as all excluded adjacent parenchyma (n=27). All cases from which lesion samples had been taken were included, with the number of samples available for each tissue varying (see materials and methods).

FCoV

Relative viral load was as expected, being lowest in the BM and lymphoid follicles and progressing from spleen through MLN to lesions where the highest mRNA levels were found. Fig. 5.3.10.

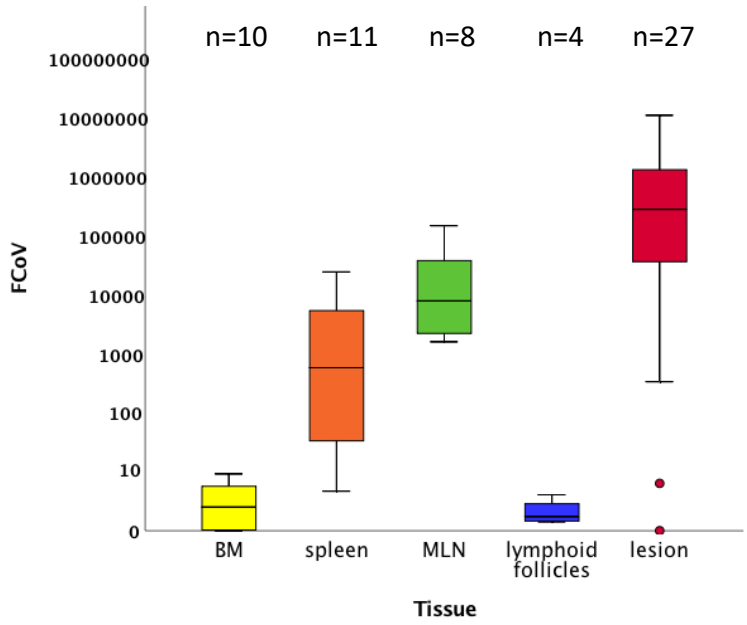

Figure 5.3.10: *Boxplots of relative FCoV mRNA levels in different tissues of cats with FIP, taken from within the LCM lesion group. The amount of target was calculated by* $2^{-\Delta\Delta CT}$*, using fGAPDH as the internal reference gene for normalisation and expressed as an n-fold difference relative to the G1 mean of the BM samples as a calibrator (depicted on the y axis). The boxes depict the median and interquartile (IQ) range with whiskers extending to the highest and lowest values which are within 1.5 x the IQ range. Outliers beyond this are individually marked.*

Toll-like receptors

The BM transcribed the lowest levels of all TLRs except TLR9. For all those elevated in FIP (TLR 2, 4, and 8), levels were highest in the lesions but there was no dominant trend between the spleen, MLN, and lymphoid follicles. TLR3 mRNA levels showed little variation between organs whilst TLR 7 and 9 levels were lowest in the lesions and highest in follicles. Fig. 5.3.11.

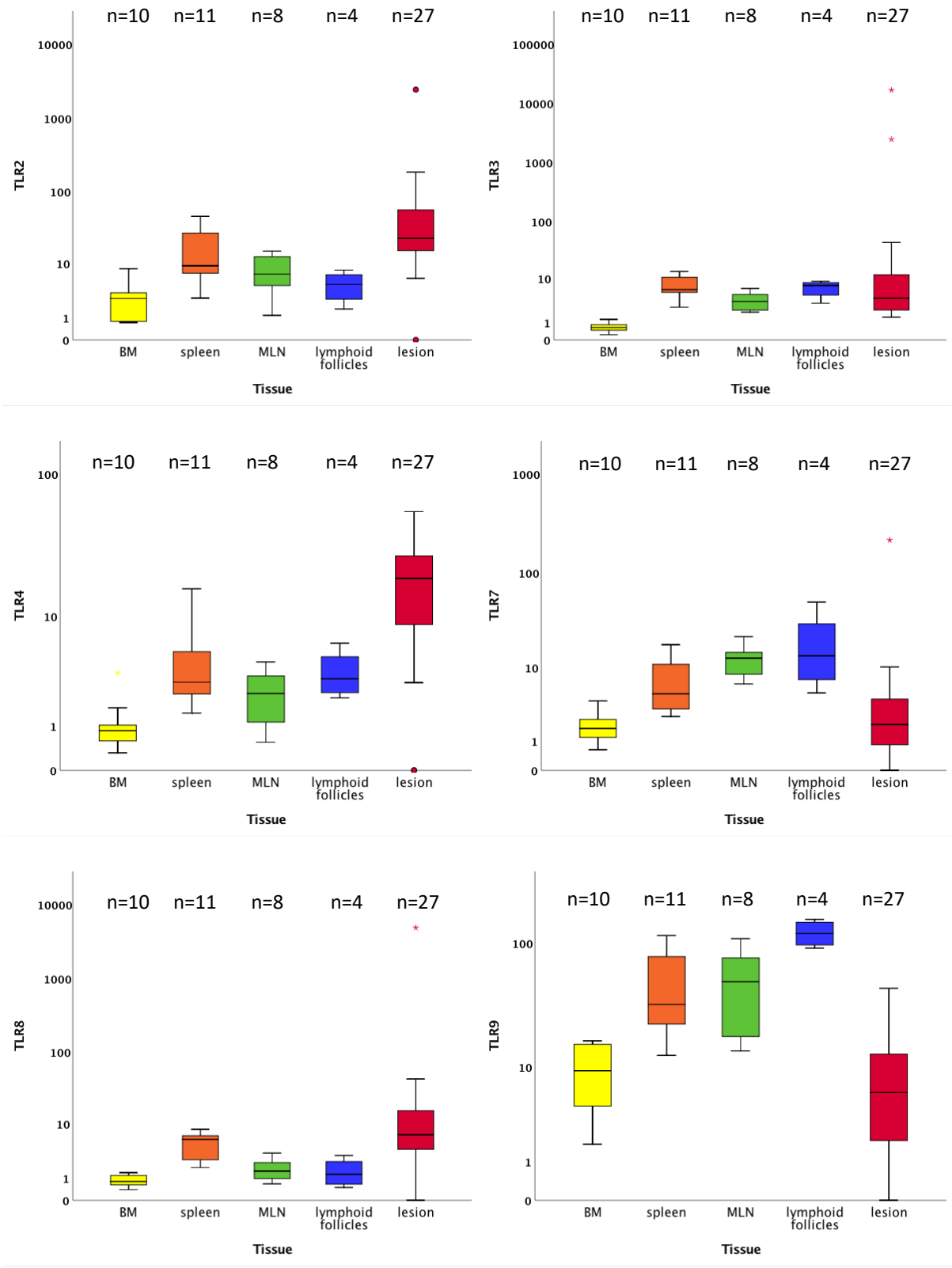

Figure 5.3.11: *Boxplots of relative TLR mRNA levels in different tissues of cats with FIP, taken from within the LCM lesion group. The amount of target was calculated by* $2^{-\Delta\Delta CT}$*, using fGAPDH as the internal reference gene for normalisation and expressed as an n-fold difference relative to the G1 mean of the BM samples as a calibrator (depicted on the y axis). The boxes depict the median and interquartile (IQ) range with whiskers extending to the highest and lowest values which are within 1.5 x the IQ range. Outliers beyond this are individually marked.*

Inflammatory cytokines and chemokines

IL-1β and IL-6 displayed very similar expression profiles but with higher basal expression of IL-1β in the BM. For both, levels decreased from spleen to MLN to lymphoid follicles, with levels in lesions similar to those in the spleen. TNF-α mRNA levels were lowest in the BM but otherwise showed little variation across tissues and lesions. The chemokines CCL8 and CXCL10 also had the lowest expression in the BM and the highest in the lesions, but whereas for CCL8 the levels within lymphoid follicles were lower than in the spleen and MLN (and similar to the BM), for CXCL10 these three tissues were all on a par, above the BM levels. Fig. 5.3.12.

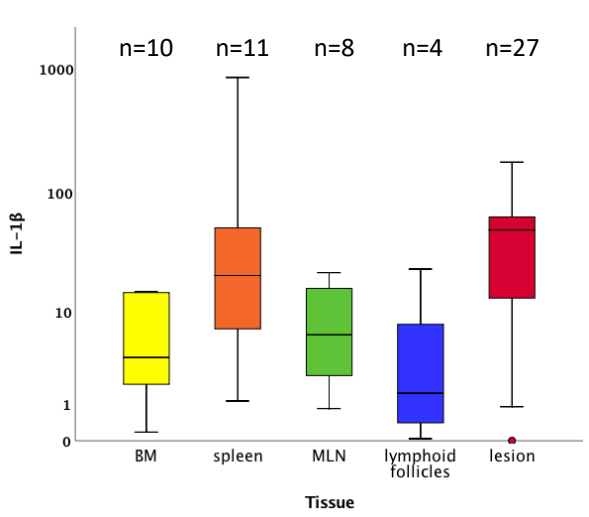

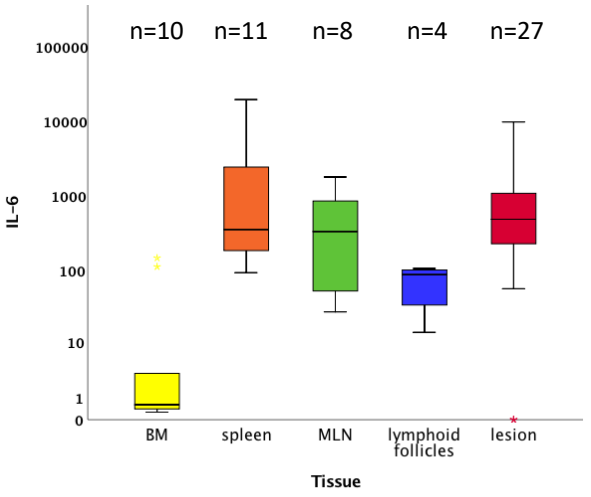

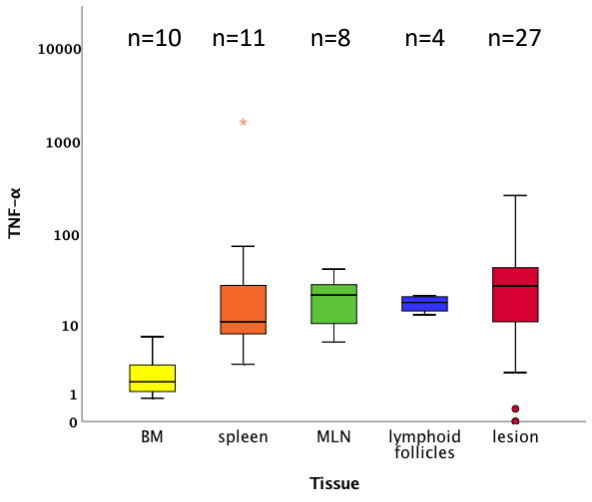

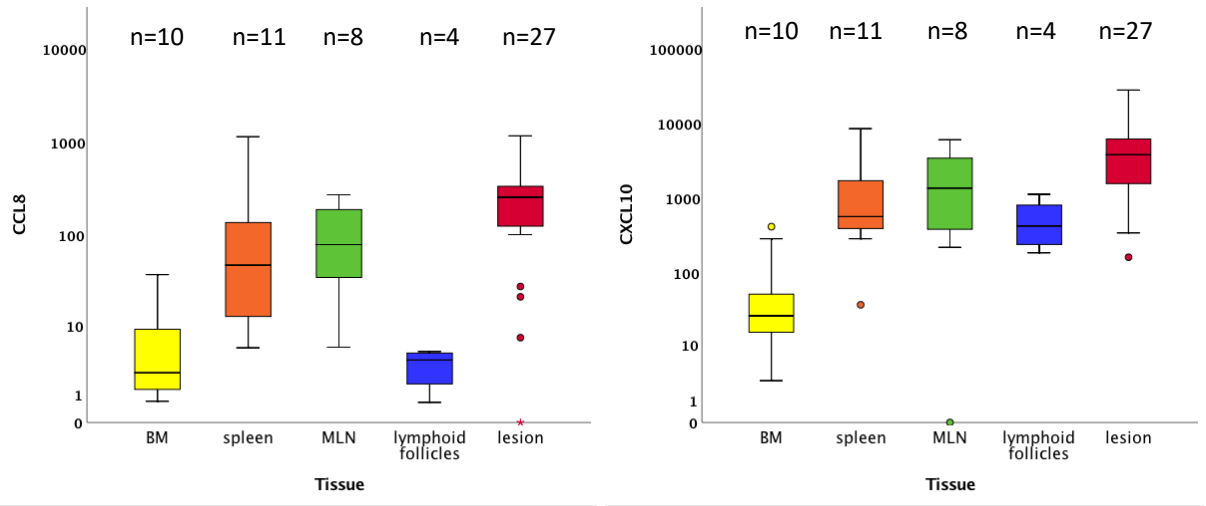

Figure 5.3.12: *Boxplots of relative inflammatory cytokine and chemokine mRNA levels in different tissues of cats with FIP, taken from within the LCM lesion group. The amount of target was calculated by $2^{-\Delta\Delta CT}$, using fGAPDH as the internal reference gene for normalisation and expressed as an n-fold difference relative to the G1 mean of the BM samples as a calibrator (depicted on the y axis). The boxes depict the median and interquartile (IQ) range with whiskers extending to the highest and lowest values which are within 1.5 x the IQ range. Outliers beyond this are individually marked.*

Interferons

IFN-α relative mRNA levels increased steadily from BM to spleen, MLN, lymphoid follicles and finally lesions. IFN-γ showed a similar progression with the exception of levels in lymphoid follicles which were very slightly below the levels of the spleen and MLN. Fig. 5.3.13.

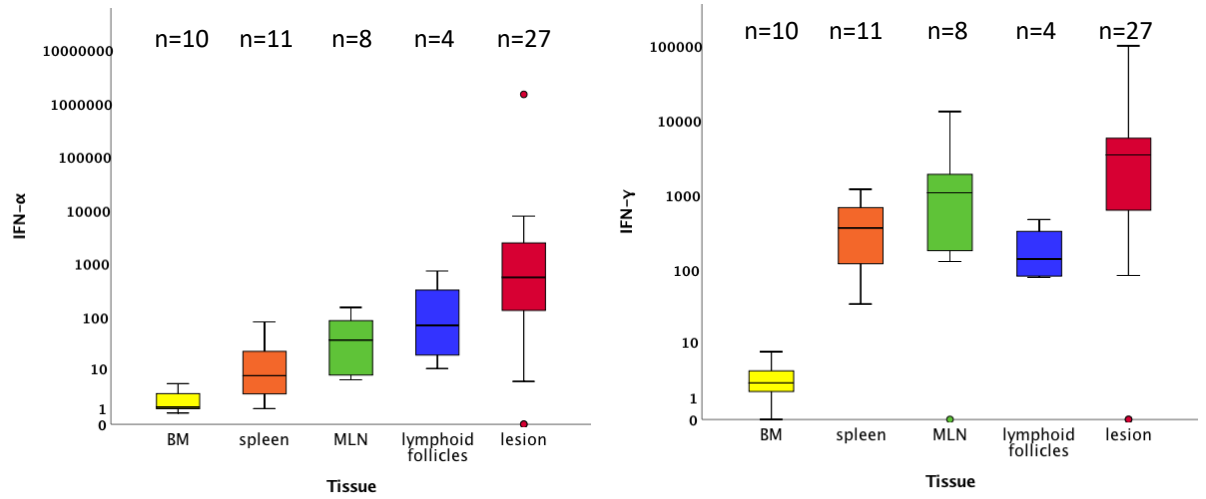

Figure 5.3.13: *Boxplots of relative interferon mRNA levels in different tissues of cats with FIP, taken from within the LCM lesion group. The amount of target was calculated by $2^{-\Delta\Delta CT}$, using fGAPDH as the internal reference gene for normalisation and expressed as an n-fold difference relative to the G1 mean of the BM samples as a calibrator (depicted on the y axis). The boxes depict the median and interquartile (IQ) range with whiskers extending to the highest and lowest values which are within 1.5 x the IQ range. Outliers beyond this are individually marked.*

STATs

For STAT1, the lowest levels were in the BM, followed by the lesions, though with overlap between lesions, spleen, MLN and lymphoid follicles. The latter three were the most similar. STAT2 mRNA levels were similar in the BM, lymphoid follicles and lesions, being higher in the spleen and MLN. Fig 5.3.14.

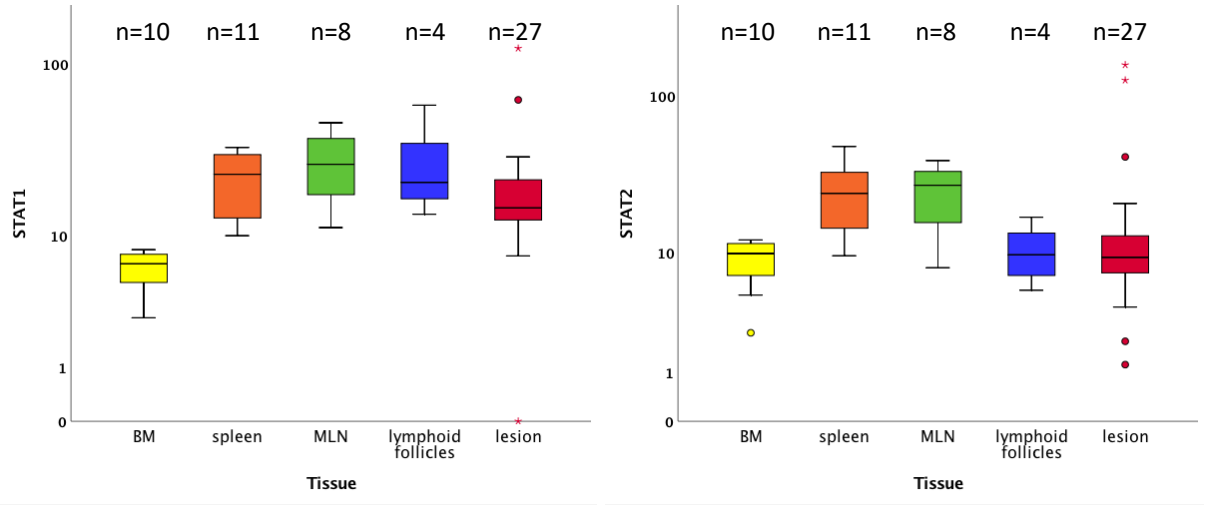

Figure 5.3.14: *Boxplots of relative STAT mRNA levels in different tissues of cats with FIP, taken from within the LCM lesion group. The amount of target was calculated by* $2^{-\Delta\Delta CT}$*, using fGAPDH as the internal reference gene for normalisation and expressed as an n-fold difference relative to the G1 mean of the BM samples as a calibrator (depicted on the y axis). The boxes depict the median and interquartile (IQ) range with whiskers extending to the highest and lowest values which are within 1.5 x the IQ range. Outliers beyond this are individually marked.*

(3). Immunohistological examination

Immunohistology (IH) was undertaken using cross-reacting antibodies against TLR8 and Iba-1 on control cat MLN to approximately characterise which cells express this receptor before progression to IF and correlation with FCoV staining.

TLR8 staining showed rare scattered cells exhibiting a strong cytoplasmic reaction. These cells had a moderate to abundant amount of cytoplasm (resembling macrophages/DC) and were most frequently found in the sinuses and medullary cords (Fig. 5.3.15). The number of TLR8 positive cells was far outweighed by the number of cells staining positively for Iba-1 (i.e. macrophages). Only very rarely were TLR8 positive cells observed within the follicles.

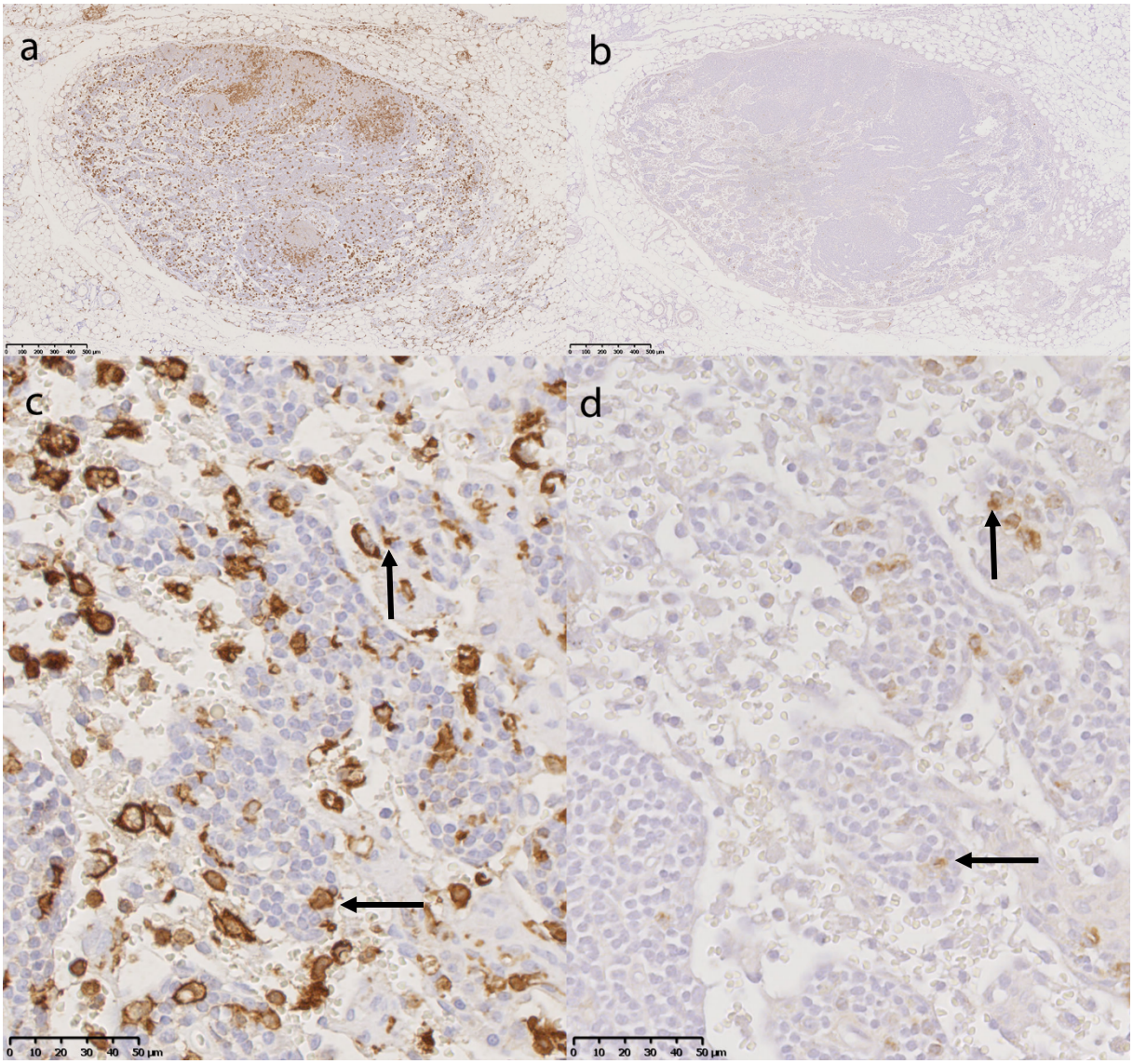

Figure 5.3.15: *a) and b) Overview of MLN stained for Iba-1 and TLR8 respectively; c) and d) close up view of medulla stained for Iba-1 and TLR8 respectively, TLR8 positive cells appear to correlate with Iba-1 positive cells as indicated by upwards and left facing arrow pair examples .*

Immunofluorescence

Sections were all double stained for TLR8 and FCoV antigen, with an Iba-1 FCoV double stain used. All regions were evaluated, with the regions of interest (ROI) used for digital image analysis those corresponding to lesions sampled by LCM for RT-qPCR. These lesions were from various organ as shown in Table 5.3.2 below. As the virus-infected cells were clearly visible and restricted to certain areas, each of these areas was carefully evaluated for the presence of TLR8 staining. Only very rare examples of cells double-stained for FCoV and TLR8 could be found, exemplified in Fig. 5.3.16, within a lymph node paracortex.

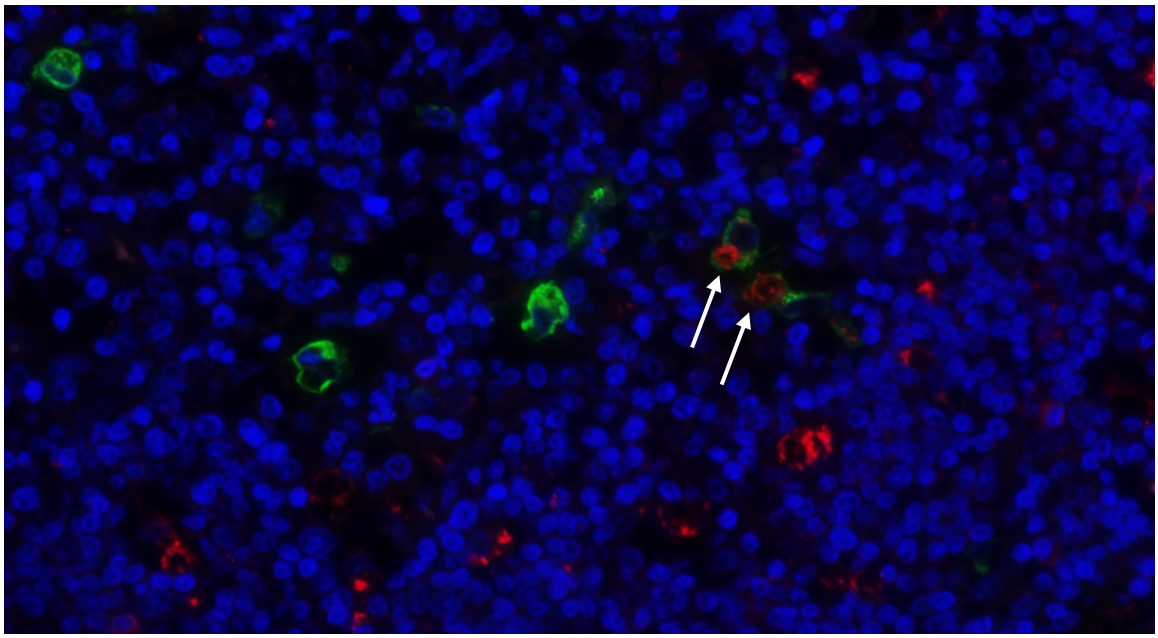

Figure 5.3.16: *S15-1842 MLN, x40: Lymph node (paracortex) showing cells double-stained (arrows) for FCoV (green) and TLR8 (red).*

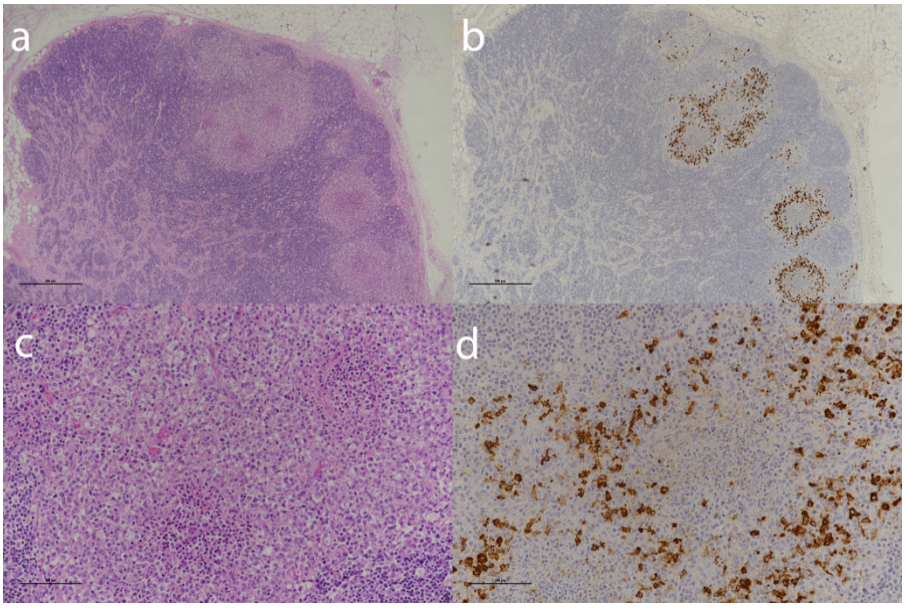

Figure 5.3.17: *S15-1539 MLN; provided as orientation for Fig. 5.3.18 below; a) and b) overview of cortical lesions with HE and IH for FCoV antigen respectively, 4x; c) and d) close up of cortical lesion with HE and FCoV IH respectively, showing central necrosis surrounded by numerous infected macrophages, x20.*

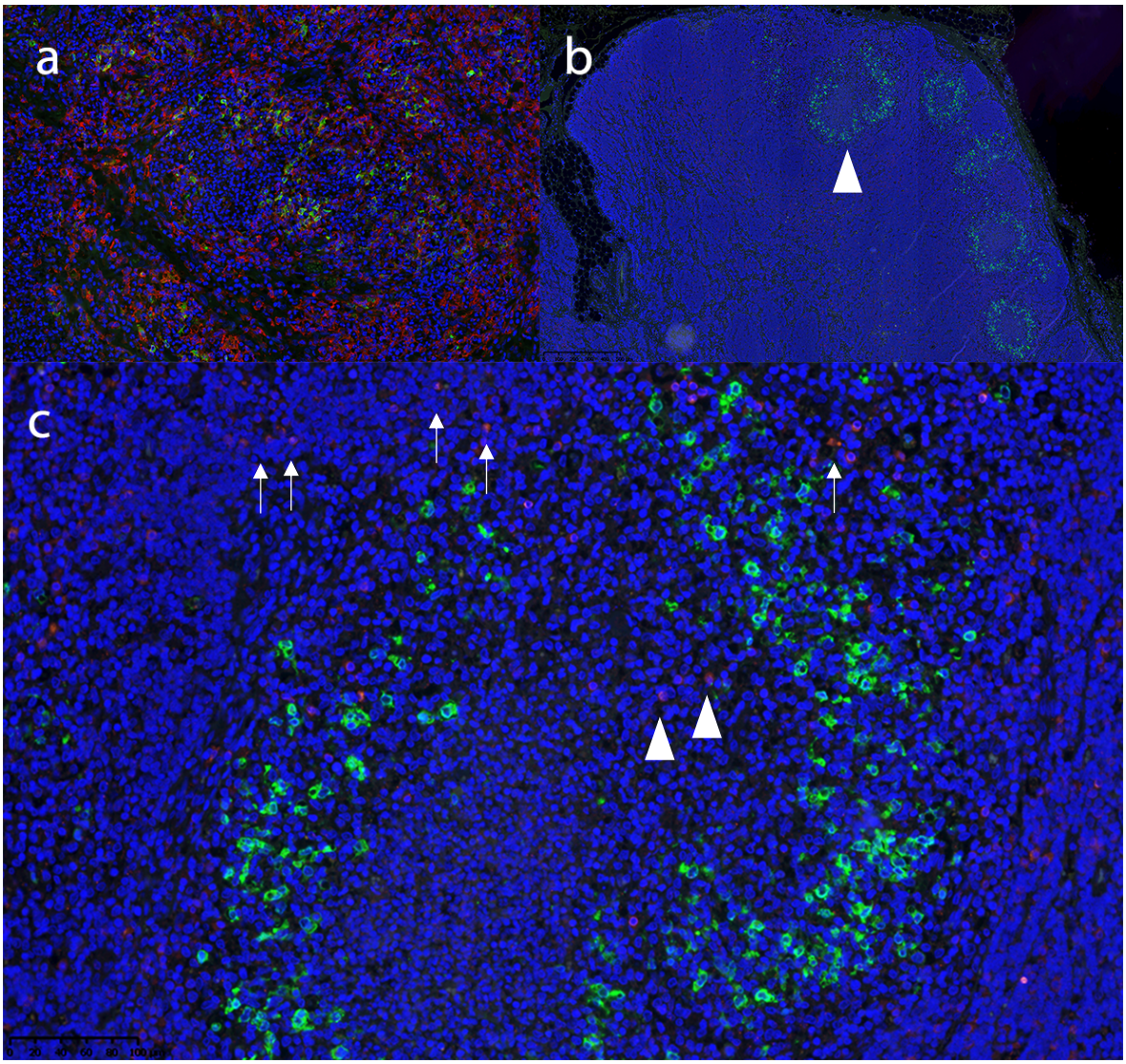

Figure 5.3.18: *S15-1539 MLN a) Iba1 (red) and FCoV (green) staining showing the frequency of macrophages within the lymph node, the scale of which is often underappreciated by HE staining; shown as a prelude to TLR8 staining 10x; b) cortical granulomatous infiltrates are prominently outlined by FCoV staining (green and arrowhead example) 5x; c) close up view of a lesion. Centrally there are very rare TLR8 positive cells (arrowheads) with increasing numbers in the surrounding tissue (arrows, staining is of lower intensity than FCoV).*

Digital Image Analysis

Following traditional evaluation of the slides it appeared clear that a high level of correlation between FCoV staining and TLR8 staining would not be observed. Slides were nevertheless processed in case digital analysis was able to offer a greater sensitivity.

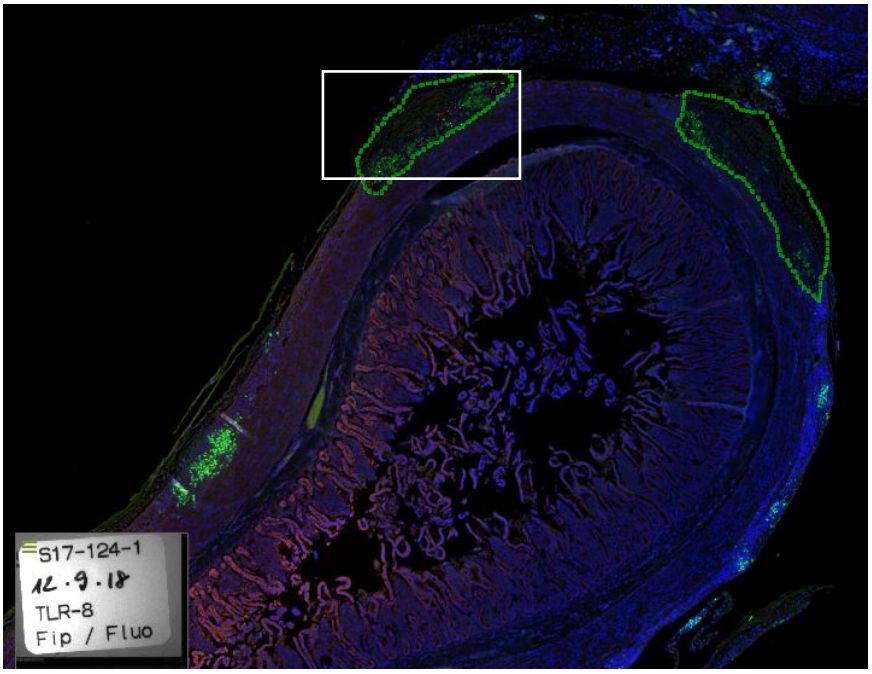

Figure 5.3.19: *Overview of small intestine (cross section) from case S17-0124, fluorescently stained for FCoV antigen (green) and TLR8 (red). Green dashed lines mark the regions of interest (ROI) selected for image analysis, the white box marks the location shown in Fig. 5.3.20 below.*

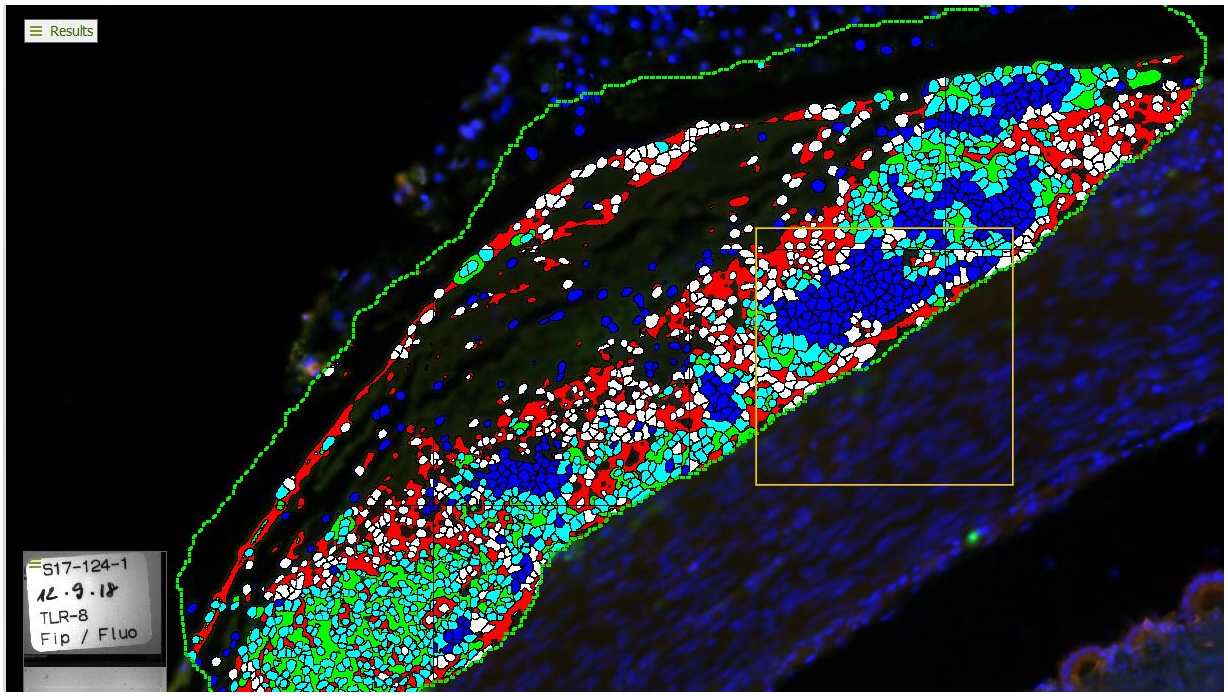

Figure 5.3.20: *Close up view of an ROI from case S17-0124 following image analysis. Red label: TLR8 staining; white: nucleus of cell expressing TLR8; green: FCoV antigen staining; turquoise: nucleus of cell infected with FCoV; blue: nucleus of cell associated with neither stain.*

The APP had also been programmed to label double stained cells yellow, however these were not detected.

The output was as follows:

Table 5.3.2: Visiopharm output of image classification combined with calculated ratios.

		Nucleus label			% of total		PCR result	
Organ	**Sample no.**	**None**	**FCoV**	**TLR8**	**FCoV**	**TLR8**	**FCoV**	**TLR8**
Spleen - serosa	106	2244	387	36	14.51069	1.349831	278161.6	3.604915
Spleen - follicles	107	14978	0	48	0	0.319446	3.066604	3.034988
Spleen - serosa	110	2306	14	97	0.57923	4.01324	52507.86	2.97885
Spleen - follicles	111	16798	0	1093	0	6.109217	27.9118	0.928768
MLN - serosa	113	13599	11	365	0.078712	2.611807	83747.15	4.69659
MLN - follicles	114	18394	9	180	0.048431	0.968627	0.422382	0.493353
Liver - serosa	115	7214	1364	218	15.50705	2.478399	134383	5.484345
Liver - serosa	134	1451	1164	680	35.32625	20.63733	4548819	2.520724
SI - granulomatous	136	2752	1318	730	27.45833	15.20833	8645755	4.183775

These results were plotted but showed no real correlation and multiple discrepancies between the IH and protein levels in the sections. With only nine results, a few discrepancies are able to distort the dataset.

This has a number of possible explanations. Firstly, owing to the lack of homogeneity of the lesions, there are often marked differences between sections even from the same block subsequent to multiple sectioning. As a consequence, the proportions of cells taken for PCR will differ from those stained by IH. This is thought to have made the greatest contribution to the occasional discrepancies. Taking the known entity of FCoV, the majority of lesions correlated approximately (e.g. no cells seen by IH in follicles, negligible qPCR levels) whereas others (e.g. case 113), appeared mismatched. The expected level of correlation for TLR8 was unknown, additionally the small range of results by RT-qPCR further complicated interpretation of discrepancies observed.

Secondly, despite multiple optimisation steps, the classification system struggles when applied to densely cellular areas (common in the lesions). As a positive staining cytoplasm is in contact with multiple nuclei, even accurate nuclear segregation cannot lead to completely accurate nuclear allocation.

Image analysis was therefore not further investigated at this stage.

4. Selected FCoV S gene Sanger sequencing

The particular S gene region of interest was sequenced based on a previous study purporting to be able to distinguish FIPV from FECV in the majority of cases [132]. The mutations in question were reported at codons 1058 and 1060 on the reference gene, however re-evaluation shows these to be at 1048 and 1050, and they will therefore be referred to subsequently as such. The previous study found that, at codon 1048, a transition from methionine to leucine (M1048L) was present in the majority of tissue samples from cats with FIP in comparison to faecal samples of healthy cats. A smaller group of cats with FIP retained this M1048 but instead had a second mutation at codon 1050, serine to alanine (S1050A).

More recent studies found the mutations to be an indicator of the virus' capacity to spread systemically instead of remaining solely enteric rather than its direct pathogenicity so these former terms will be used here to describe the mutations [91,133].

In total, there were 101 tissue samples from cats with FIP, from which 96 had had a positive RT-qPCR FCoV result. Following a second conventional PCR directed against a section of the S gene (see methods and below), adequate sequencing results were obtained from 86 of the 96. These are shown below grouped by organ, disease status and by individual cat.

From many of the Bristol cases, faecal samples had also been analysed and results were available for interpretation. This procedure was not performed on Zurich cases, as this was not the area of interest of the study.

FCoV S gene sequencing results from the bone marrow of cats with FIP

All 11 BM samples from FIP cats were from Zurich cases; of these, nine were FCoV RT-qPCR positive, and the samples were amenable to sequencing. One of these cats carried virus encoding methionine (M) at codon 1048 and serine (S) at codon 1050, corresponding to 'enteric' virus. The remaining eight encoded leucine (L) at 1048, displaying the 'systemic' M1048L mutation, as well as S1050. Table 5.4.1. No Group 1 cats were found to carry FCoV in the BM, so samples were not subjected to conventional PCR.

Table 5.4.1: Viral sequencing results from the bone marrow of cats with FIP, with the only example of 'enteric' virus highlighted.

Case no.	Sample no.	FCoV C_T	Codon 1048		Codon 1050	
S15-1738	20	38.8	CTG	Leu	TCT	Ser
S15-1809	23	31.1	TTG	Leu	TCA	Ser
S15-1539	26	30.5	TTG	Leu	TCC	Ser
S15-1728	29	39.2	TTG	Leu	TCT	Ser
S15-1094	31	-	no sequence			
S15-0983	33	32.4	ATG	Met	TCC	Ser
S15-0259	35	38.5	TTG	Leu	TCT	Ser
S15-0134	37	30.9	TTG	Leu	TCT	Ser
S15-1842	41	34.2	TTG	Leu	TCT	Ser
S16-0454	44	-	no sequence			
S17-0124	47	31.9	TTG	Leu	TCT	Ser

FCoV S gene sequencing results from the spleen of cats with FIP

All 14 Group 2 splenic samples (again, all from Zurich cases), were FCoV positive by RT-qPCR and were amenable to sequencing. There was again only one cat carrying 'enteric' virus (S15-1094) but this was not the same cat as the one found to carry 'enteric' virus in the BM (S15-0983). Cat S15-0983 had virus with M1048 in both organs however, in the spleen, the second (and less common) systemic associated mutation, from S to alanine (A) at 1050 was also present. A third cat (S15-1738) carried this second S1050A mutation; this cat carried virus with L and S respectively in the BM. Table 5.4.2.

Table 5.4.2: Summary of viral sequencing results from the spleen of cats with FIP, with the only example of 'enteric' virus highlighted.

Case no.	Sample no.	FCoV C_T	Codon 1048		Codon 1050	
H15-2389	13	33.29	TTG	Leu	TCT	Ser
S16-0167	14	20.76	TTG	Leu	TCT	Ser
S15-1368	16	29.47	CTG	Leu	TCT	Ser
S15-1738	19	29.9	ATG	Me	GCT	Ala
S15-1809	22	21.26	TTG	Leu	TCA	Ser
S15-1539	25	22.72	TTG	Leu	TCC	Ser
S15-1728	28	20.07	TTG	Leu	TCT	Ser
S15-1094	30	22.52	ATG	Met	TCC	Ser
S15-0983	32	23.32	ATG	Met	GCC	Ala
S15-0259	34	33.67	CTG	Leu	TCT	Ser
S15-0134	36	26.39	TTG	Leu	TCC	Ser
S15-1842	42	32.41	TTG	Leu	TCT	Ser
S16-0454	45	31.72	TTG	Leu	TCC	Ser
S17-0124	48	27.24	TTG	Leu	TCT	Ser

FCoV S gene sequencing results from MLN and faeces of cats with FIP

This group includes both cats from Zurich (indicated by an Sxx-xxxx case number) and Bristol.
Of the 30 cats with FIP, one was infected with FCoV serotype 2 for which the previously described S gene sequence characterisation is not applicable [91,313]. Twenty-six MLN samples contained virus that encoded leucine (M1048L) (cDNA sequence TTG, CTG, or TTA). The remaining three cats encoded methionine at codon 1048 (cDNA sequence ATG). Of these three cases, two carried S1050A, whilst the third encoded S1050.The results are shown in Table 5.4.3.
Within the faeces, a 50:50 split between 'enteric' and 'systemic' virus was observed; all the former being found in cats with M1058L in the MLN. The cat with systemic 'enteric' virus had no detectable faecal FCoV with which to compare.

Table 5.4.3: Summary of viral sequencing results from the MLN of cats with FIP, and from faecal samples of the same cats, with 'enteric' virus highlighted. Bases in lower case indicate a mixed sequencing result (sample 75); neg: negative; ND: not done.

Case no.	Sample no.	MLN				Faeces			
		codon 1048		codon 1050		codon 1048		codon 1050	
S16-0167	15	TTG	Leu	TCT	Ser	ND			
S15-1368	17	CTG	Leu	TCT	Ser	ND			
S15-1738	18	ATG	Met	GCT	Ala	ND			
S15-1809	21	TTG	Leu	TCA	Ser	ND			
S15-1539	24	TTG	Leu	TCC	Ser	ND			
S15-1728	27	TTG	Leu	TCT	Ser	ND			
S15-1842	43	TTG	Leu	TCT	Ser	ND			
S16-0454	46	TTG	Leu	TCC	Ser	ND			
S17-0124	49	TTG	Leu	TCT	Ser	ND			
30	56	TTG	Leu	ND	-	ND			
31	57	TTG	Leu	ND	-	ATG	Met	TCC	Ser
32	58	TTG	Leu	ND	-	ATG	Met	TCC	Ser
37	59	TTG	Leu	ND	-	ATG	Met	TCC	Ser
42	61	TTG	Leu	ND	-	ATG	Met	TCC	Ser
93	72	CTG	Leu	TCC	Ser	CTT	Leu	TCC	Ser
94	73	TTG	Leu	TCC	Ser	TTG	Leu	TCC	Ser
96	74	TTG	Leu	TCT	Ser	neg			
100	75	c/tTG	Leu	TCT	Ser	neg			
101	76	TTG	Leu	TCC	Ser	TCT	Leu	TCC	Ser
103	78	ATG	Met	TCC	Ser	neg			
121	83	ATG	Met	GCC	Ala	ND			
122	84	TTG	Leu	TCC	Ser	ND			
127	88	TTA	Leu	TCA	Ser	neg			
128	89	TTG	Leu	TCC	Ser	ATG	Met	TCC	Ser
131	90	TTG	Leu	TCC	Ser	TTG	Leu	TCC	Ser
142	96	CTG	Leu	TCT	Ser	neg			
146	98	FCoV Type II				neg			
43	150	TTG	Leu	TCC	Ser	neg			
46	151	TTG	Leu	ND	-	TTG	Leu	ND	-
50	152	TTG	Leu	ND	-	neg			

FCoV S gene sequencing results from MLN and faeces of cats without FIP

From the 10 cats in Group 1+, it was possible to obtain a usable sequence from eight of the MLN samples. All of these eight encoded leucine (M1048L). The quality of the remaining two was not high enough to reliably interpret in the region of interest even after repeated attempts. These cases are shown in Table 5.4.4 together with those G1- cases from which faecal virus was sequenced (20 cases). The Zurich cases and four untested Bristol cases have not been included. These results show that, where measurable, all of the non FIP cats with detectable virus in the MLN were carrying the 'systemic' form. Codon 1050 could not always be sequenced, where analysable it was a serine amino acid, consistent with the original publication findings that this remains unchanged in virus expressing leucine [132].

Table 5.4.4: Summary of viral sequencing results from the MLN, and from faecal samples of the same cats, with 'enteric' virus highlighted in blue. Neg: negative; ND: not done.

Case no.	Sample no.	FCoV C_T	Group	MLN				Faeces			
				codon 1048		codon 1050		codon 1048		codon 1050	
54	63	-	1-					neg			
56	64	-	1-					neg			
63	65	-	1-					neg			
80	66	-	1-					ATG	Met	TCC	Ser
84	67	-	1-					neg			
87	68	-	1-					neg			
89	69	-	1-					neg			
91	71	-	1-					neg			
115	79	-	1-					not possible to sequence			
116	80	-	1-					neg			
118	81	-	1-					neg			
119	82	-	1-					neg			
126	87	-	1-					ATG	Met	TCC	Ser
136	93	-	1-					neg			
141	95	-	1-					neg			
143	97	-	1-					neg			
59	154	-	1-					ATG	Met	TCC	Ser
72	156	-	1-					neg			
104	160	-	1-					neg			
105	161	-	1-					neg			
38	60	39.8	1+	not possible to sequence				ATG	Met	TCC	Ser
51	62	37.81	1+	TTG	Leu	ND	-	neg			
102	77	39.30	1+	CTG	Leu	ND	-	neg			
125	86	29.21	1+	CTG	Leu	TCC	Ser	neg			
132	91	37.60	1+	TTG	Leu	TCT	Ser	neg			
135	92	36.38	1+	not possible to sequence				ND			
149	99	37.00	1+	TTG	Leu	ND	-	neg			
156	101	34.88	1+	TTG	Leu	TCT	Ser	ND			
69	155	38.50	1+	CTG	Leu	ND	-	ATG	Met	TCC	Ser
78	158	39.84	1+	CTG	Leu	ND	-	ATG	Met	TCC	Ser

FCoV S gene sequencing results from LCM samples of cats with FIP

Finally, the viral RNA obtained from the LCM samples was also subjected to Sanger sequencing. These should therefore contain virus capable of inducing lesions and not just of becoming systemic. The success rate was lower owing to the exponentially reduced sample size, however 26 of 32 RT-qPCR positive samples were possible to sequence. All comprised 'systemic' virus with three (from two cats) exhibiting the S1050A rather than M1048L.

Table 5.5.5: Summary of viral sequencing results from LCM samples. The generally lower C_T values than in the tables above are following pre-amplification of samples. SI, small intestine; S, serositis; PP, Peyer's patches; A arteries; F, follicles; G, granulomatous lesions; LI, large intestine; M, sinus macrophages; LPC, subcapsular lymphoplasmacytic inflammation.

Case no.	Sample no.	Organ	FCoV C_T	codon 1048		codon 1050	
S15-1842	102	SI (S)	11.87	TTG	Leu	TCT	Ser
S15-1842	103	SI (PP)	30.90	TTG	Leu	TCA	Ser
S15-1842	104	SI (A)	-	sequencing not attempted			
S15-1842	105	liver (S)	14.21	TTG	Leu	TCT	Ser
S15-1809	106	spleen (S)	16.35	TTG	Leu	TCA	Ser
S15-1809	107	spleen (F)	31.81	TTG	Leu	TCA	Ser
S15-1809	108	spleen (A)	26.06	TTG	Leu	TCA	Ser
S15-1738	109	spleen (F)	31.42	not possible to sequence			
S15-1738	110	spleen (S)	14.93	ATG	Met	GCT	Ala
S15-1738	111	spleen (A)	34.40	TTG	Leu	TCT	Ser
S15-1738	112	MLN (G)	31.43	TTG	Leu	TCT	Ser
S15-1738	113	MLN (S)	15.02	ATG	Met	GCT	Ala
S15-1738	114	MLN (F)	32.06	TTG	Leu	TCT	Ser
S15-1728	115	liver (S)	18.31	TTG	Leu	TCT	Ser
S15-0983	116	MLN (S)	23.35	ATG	Met	GCC	Ala
S15-1539	117	MLN (G)	15.94	TTG	Leu	TCC	Ser
S15-1728	118	MLN (G)	19.17	TTG	Leu	TCT	Ser
S16-0167	119	MLN (G)	12.26	TTG	Leu	TCT	Ser
S16-0454	120	MLN (G)	20.83	TTG	Leu	TCC	Ser
S17-0124	121	MLN (G)	15.41	TTG	Leu	TCT	Ser
S15-0134	122	LI (S)	15.49	TTG	Leu	TCC	Ser
S15-0259	123	MLN (G)	20.46	TTG	Leu	TCT	Ser
S15-0259	124	spleen (S)	-	sequencing not attempted			
S15-0259	125	liver (S)	21.01	not possible to sequence			
S15-1728	126	MLN (M)	27.94	TTG	Leu	TCT	Ser
S15-1738	127	liver (LPC)	-	sequencing not attempted			
S15-1738	128	liver (S)	31.96	not possible to sequence			
S15-1809	129	kidney (S)	23.49	not possible to sequence			
S15-1809	130	omentum (G)	14.27	TTG	Leu	TCA	Ser
S16-0167	131	spleen (S)	17.55	TTG	Leu	TCT	Ser
S16-0167	132	omentum (G)	17.00	not possible to sequence			
S16-0454	133	liver (S)	28.36	not possible to sequence			
S17-0124	134	liver (S)	13.67	TTG	Leu	TCT	Ser
S17-0124	135	spleen (S)	28.68	not possible to sequence			
S17-0124	136	SI (G)	13.80	TTG	Leu	TCT	Ser
S15-1842	137	SI (S)	16.78	TTG	Leu	TCT	Ser

Comparison of the S gene sequence within different organs of individual cats

In order to evaluate the level of viral variation within individual cats, sequences derived from different samples from each cat were compared. The amplified sequence is a 153 bp stretch of the S gene (reference sequence FCoV C1Je), with the codons of interest 1048 and 1050 at bp 94-96 and 100-103, as labelled in the images. Images are centred on these codons, highlighted in red and salmon pink respectively. The sequences have been quality trimmed so do not all cover the entire amplified region. A dot indicates a base match with the reference sequence.

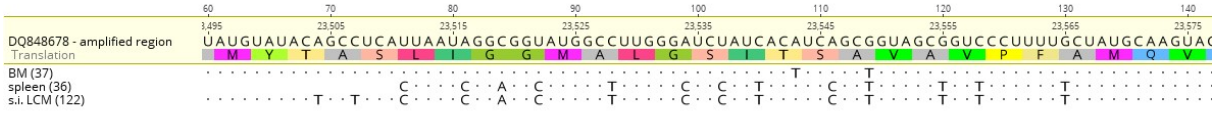

Figure 5.4.6: *S15-0134. The spleen and small intestinal lesion samples are identical, differing from the virus within the BM sample which is closer to the reference gene.*

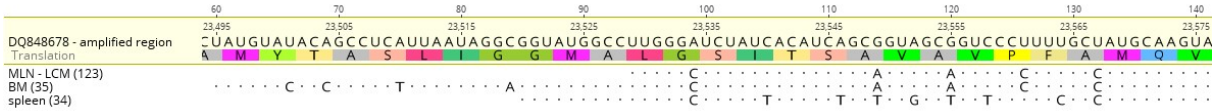

Figure 5.4.7: *S15-0259. The sequence derived from the spleen differs from that from the MLN and bone marrow at six visible sites. There are no amino acid variations.*

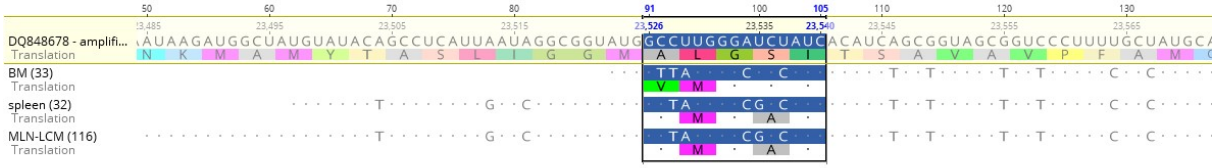

Figure 5.4.8: *S15-0983. Spleen and MLN are identical in this region whilst the BM sequence differs only slightly, this cat carried virus encoding methionine at codon 1048 in all evaluated organs, in the bone marrow only was there an S1050, encoding 'enteric' virus.*

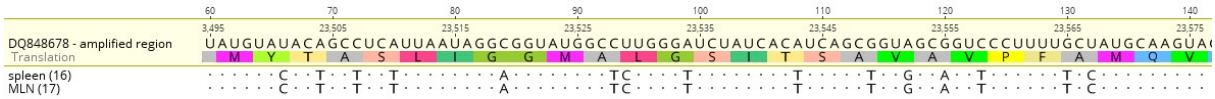

Figure 5.4.9: *S15-1368. Virus from both organs, i.e. spleen and MLN, was identical in this region, and identical in amino acid sequence to the reference.*

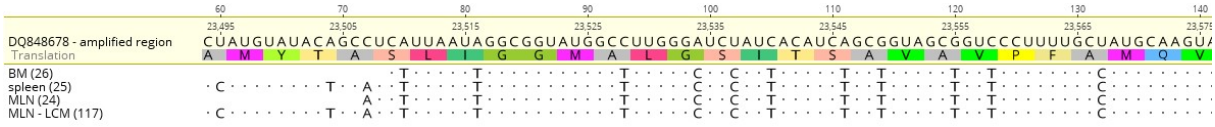

Figure 5.4.10: *S15-1539. In all samples from this cat, the virus was identical in the sequenced region, differing from the reference sequence at 14 bases (almost 10%) yet having no alterations in the amino acid sequence.*

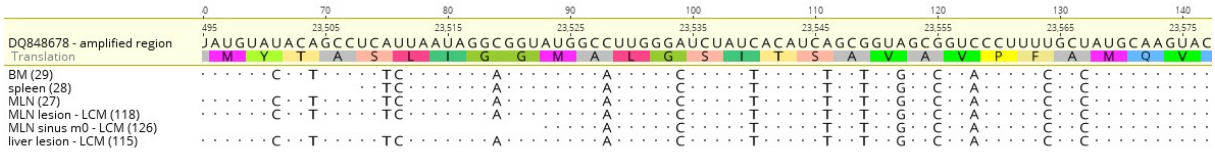

Figure 5.4.11: *S15-1728. Numerous base mutations are shared by virus in all organs, there are no amino acid changes.*

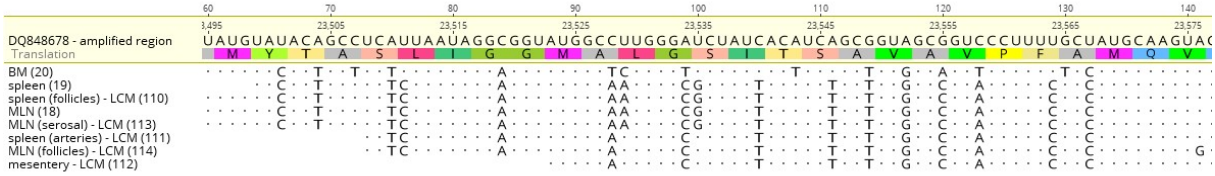

Figure 5.4.12: *S15-1738. The bone marrow sample exhibits 10 SNPs from all other samples, whilst the remaining seven samples split into two groups. These two groups differ at only two bases but these are within codons 1048 and 1050, causing a leucine/methionine switch at the former and a serine/alanine at the latter. All remain consistent with 'systemic' virus.*

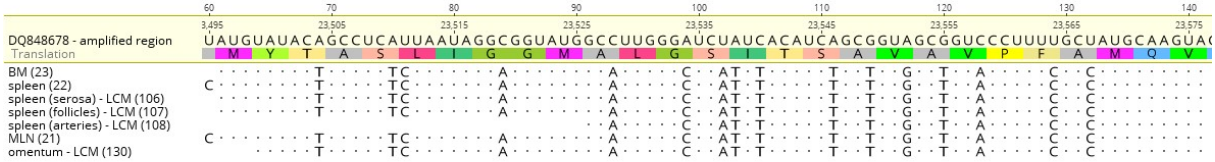

Figure 5.4.13: *S15-1809. There were no variations between organs and only one amino acid difference, I1051F, from the reference.*

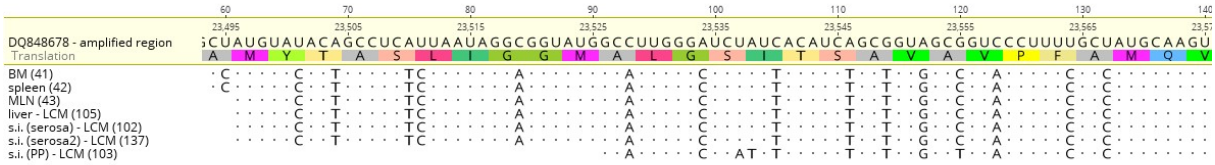

Figure 5.4.14: *S15-1842. Only the virus extracted from the small intestinal Peyer's patches (PP) differed from the others, leading to an amino acid alteration I1051F as for Fig. 4.8.*

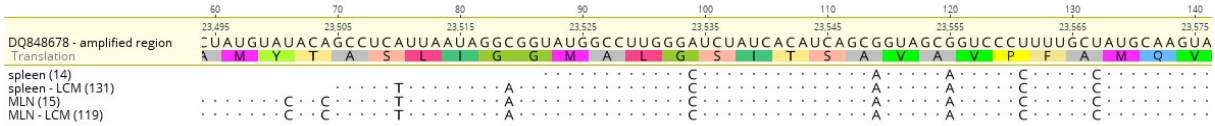

Figure 5.4.15: *S16-0167. There are no viral variations and no amino acid variations.*

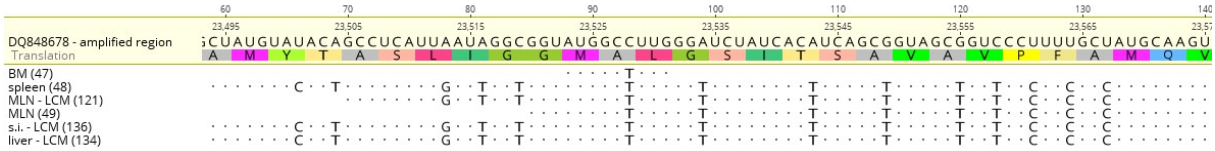

Figure 5.4.16: *S17-0124. There are no viral variations and no amino acid variations.*

These results show that despite frequent variation from the reference sequence, virus within an individual shows very little variation in this genomic region.

5. Results of RNA-Seq by NGS

The overall output from the sequencing run is first displayed, followed by the results of pairwise comparisons between groups, comparisons with the RT-qPCR results from earlier chapters, and then comparisons with other published datasets. For simplicity, groups were inputted as 1-3, therefore G1 indicates G1- (control cats with FCoV RT-qPCR negative MLN), whilst G3 is equivalent to G1+ (control cats with FCoV positive MLN). G2 remains cats with FIP.
Figures 5.5.1 – 5.5.5 show the overall quality and clustering of all samples.

Count Statistics

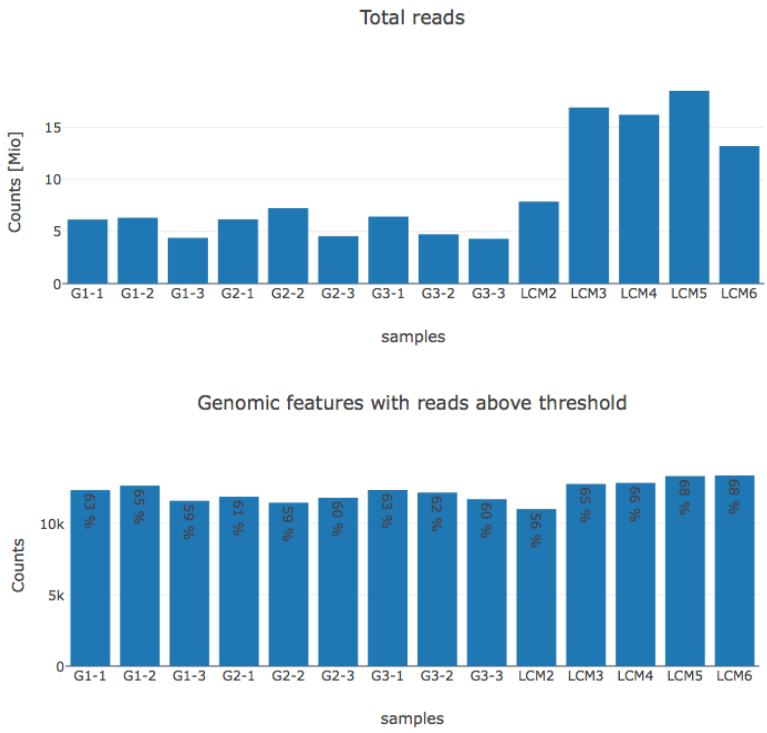

Figure 5.5.1: *LCM samples take up a greater proportion of reads than the bulk MLN samples (top) but reads above threshold are at a consistent proportion (bottom). NB: LCM1 failed the pre-sequencing quality control and was not included in the sequencing run.*

Quality Control

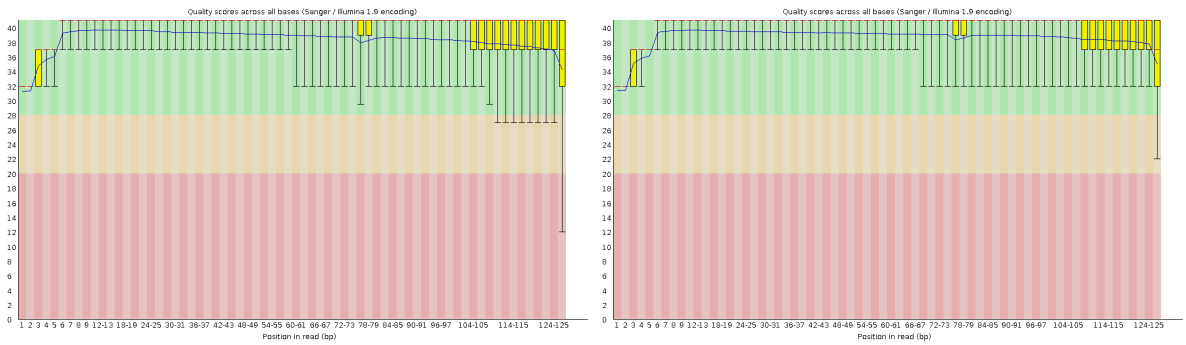

Figure 5.5.2: *Representative LCM (left) and bulk MLN (right) quality score across all bases showing almost all reads remaining within the high quality >28 score zone.*

Sample Clustering

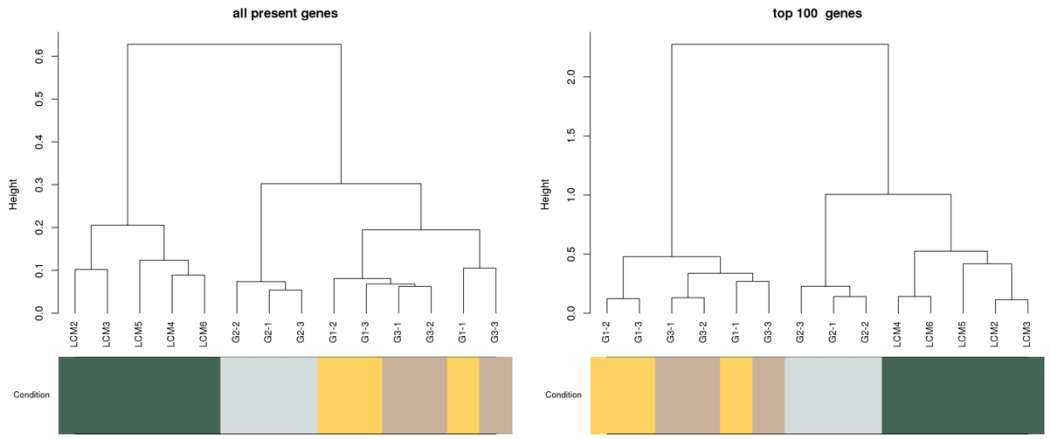

Figure 5.5.3: *Sample clustering using all genes (left) or the top 100 differentially expressed genes (right). In both cases, LCM samples (dark green) and G2 samples (pale blue) cluster in their groups, and closest to each other. All nine bulk MLN samples (G1-G3) cluster but G1 (brown) and G3 (yellow) are intermingled.*

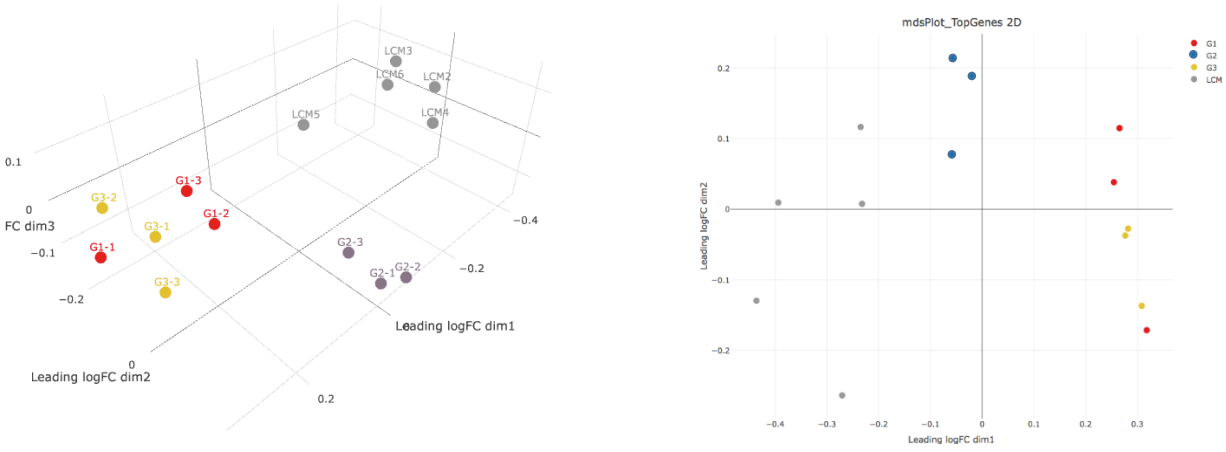

Figure 5.5.4: *3D (left) and 2D (right) clustering of the top genes again shows grouping of the FIP samples away from the non FIP groups. The non FIP groups do not segregate.*

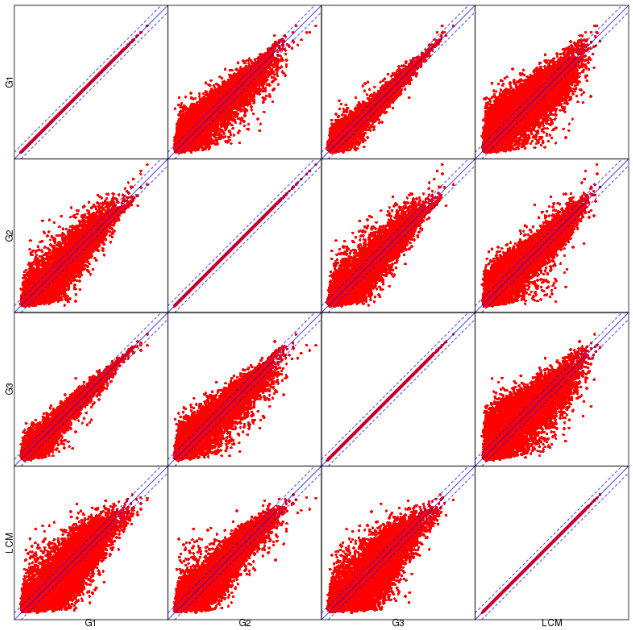

Figure 5.5.5: *Group average pairs, showing high similarity within groups (top left to bottom right diagonal row), and the smallest variability between groups G1 and G3 (i.e. G1-, G1+).*

Pairwise comparisons

Cats without FIP or detectable FCoV in the MLN versus cats with FIP (G1(-) over G2)

Number of significants by p-value and fold-change

	#significants	FDR	fc >= 1	fc >= 1.5	fc >= 2	fc >= 3	fc >= 4	fc >= 8	fc >= 10
p < 0.1	4150	0.301700	4150	4007	2342	1006	585	181	124
p < 0.05	2907	0.215400	2907	2902	2078	959	568	179	123
p < 0.01	1224	0.102300	1224	1224	1184	718	438	138	96
p < 0.001	313	0.039970	313	313	313	293	223	93	65
p < 1e-04	89	0.013500	89	89	89	89	88	55	41
p < 1e-05	25	0.004357	25	25	25	25	25	24	21

Figure 5.5.6: *Overview of results ordered by significance and fold change. FDR = false discovery rate (0.1 means 10% could be expected to not be truly differentially expressed), fc = fold change. Out of 19493 possible features, 12533 were above the threshold.*

To evaluate the level of variation within each group, each sample was compared to its group mean (example in Fig. 5.5.7). Those marked as significant (red) apply to the group comparisons above, therefore when the red genes are close to the central line it means they are very similarly expressed by all samples in the group. Within each pair, individual samples were compared to the mean of the opposite group (example in Fig. 5.5.8), in these graphs, a clearing of the red genes along the central line shows that group differences are notable.

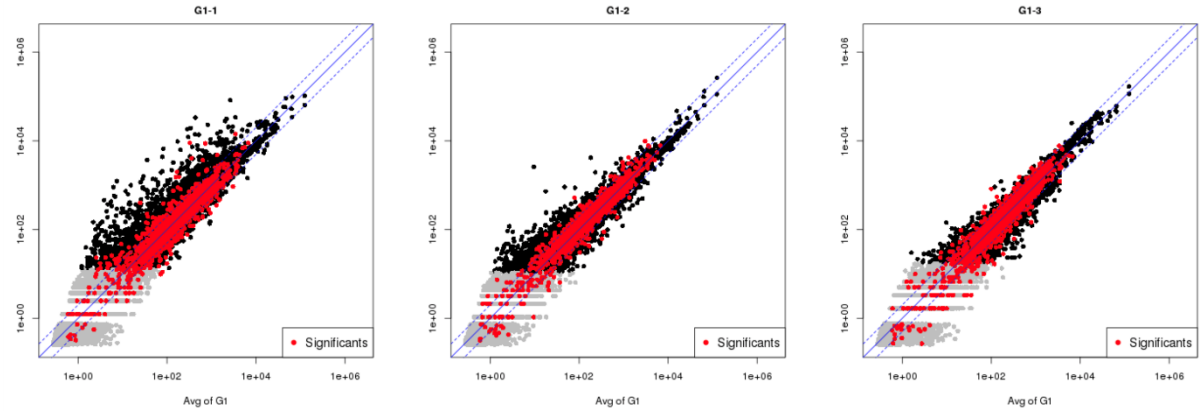

Figure 5.5.7: *Intragroup comparisons using G1 as an example. Individual G1 samples vs G1 mean.*

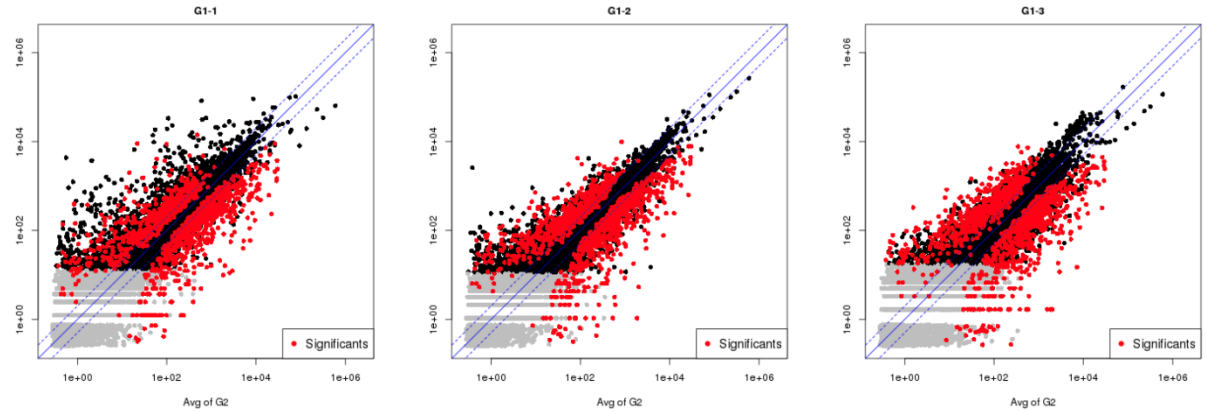

Figure 5.5.8: *Intergroup comparisons using individual G1 vs the G2 mean as an example.*

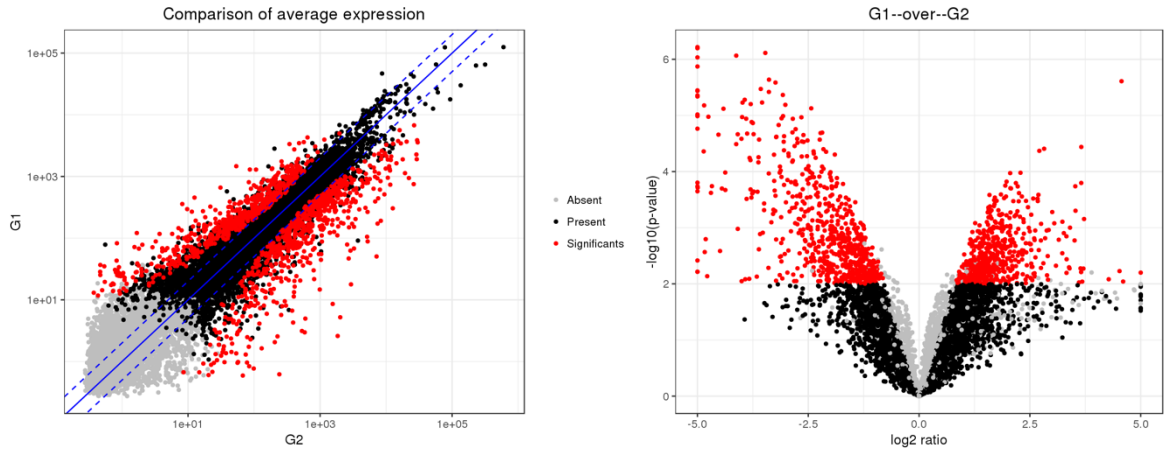

Figure 5.5.9: *Comparison between average group expressions (left), with significant values indicated together with their fold change log ratio (right). A negative log ratio indicates a higher expression in G2.*

All differentially expressed genes are displayed graphically in Fig. 5.5.9. Of the top 20 differentially expressed individual genes by fold change, all except one were higher in FIP. Tables 5.5.1 and 5.5.2 below show the top 20 up and down regulated genes. The term ‘upregulated’ in the software

generated charts relates to the group name as they were compared (with all comparisons being in numerical order i.e. 1 vs 2, 1 vs 3), rather than to a direction of a biological process.
The mapping software was unable to name five of the top 20 upregulated genes. Comparison of individual identifiers with the UniProt website http://UniProt.org was able to name two further genes, with the remainder being predicted (remaining unnamed but having a predicted protein function). This programme was also used to summarise the main functions of these genes [314].
The second gene on the list had a fold change of greater than 100 but was unnamed. The identifier was therefore put into the STRING consortium website https://string-db.org to search for predicted networks involving the gene and hence predict its function from the surrounding genes. Fig. 5.5.10 shows the resulting network. In this case, the most informative functional enrichments in this network were shown as KEGG pathways https://www.genome.jp/kegg/pathway.html. These are presented in Table 5.5.3.

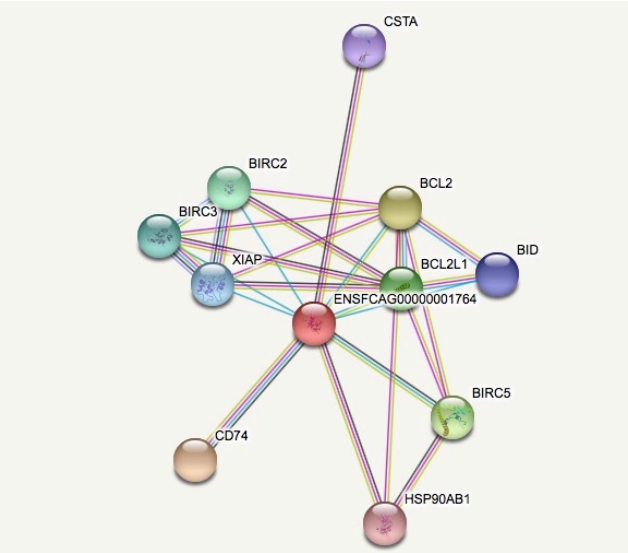

Figure 5.5.10: *Predicted gene associations of ENSFCAG00000001764, the second most upregulated gene detected in G2 compared with G1.*

Table 5.5.1: The top 20 upregulated genes in G2 compared to G1(-) by fold change.

Identifier	Gene	Protein	p	log2 Ratio	fc	Function
^010436	ACOD1	aconitate decarboxylase 1	4E-06	-6.9	117.87	defence response
^001764			1E-05	-6.7	102.25	U.P.; predicted apoptosis regulation
^013594	CCL8	C-C motif chemokine ligand 8	1E-06	-6.6	96.94	cell signalling
^018779	IFIT3	interferon induced protein with tetratricopeptide repeats 3	1E-05	-6.5	87.67	response to IFN-α
^025965	SAA2*	Serum amyloid A protein	0.0002	-6.2	71.56	acute phase response, chemotaxis
^025002	SAA1	Serum amyloid A protein	0.0002	-5.9	59.92	acute phase response, chemotaxis
^000708	RSAD2	radical S-adenosyl methionine domain-containing protein 2	4E-06	-5.9	58.44	predicted ↑regulation of TLR7 and 9 signalling
^029623			0.0038	-5.6	49.32	U.P.; predicted involvement in Ag and Ig R binding
^030236	SFRP2	secreted frizzled related protein 2	2E-05	-5.4	43.68	apoptosis regulation (both ↑ and ↓ cited)
^031821	IRF7	interferon regulatory factor 7	5E-06	-5.3	40.64	regulates IFN transcription
^005933	IFIT1*	interferon induced protein with tetratricopeptide repeats 1	6E-07	-5.3	39.18	predicted response to IFN-α
^011708	IFIT2	interferon induced protein with tetratricopeptide repeats 2	9E-07	-5.3	38.32	response to IFN-α
^003362	ISG15	interferon stimulated gene 15	4E-06	-5.2	38.03	response to Type I, reg of Type II, viral defence
^000645	C5	complement C5	6E-07	-5.2	37.98	↑ chemokine secretion, ↓ macrophage chemotaxis
^008365	CXCL9	C-X-C motif chemokine ligand 9	0.0002	-5.1	34.80	cell signalling
^025088			0.0061	-5.1	33.54	U.P.; predicted involvement in immune response and Ig production
^029292	IGKV4-1*	Immunoglobulin kappa variable 4-1	0.0061	-5.0	32.31	antibody response
^009503	CXCL10	C-X-C motif chemokine ligand 10	0.0002	-5.0	31.89	cell signalling
^007076	CLEC4D	C-type lectin domain family 4 member D	4E-05	-4.9	29.04	Ig receptor binding
^027331			7E-06	-4.8	28.82	U.P.; predicted role in phagocytosis

Key: The colour of the fold change (fc) indicates the cluster to which the gene belongs (see below); ^ indicates the prefix ENSFCAG00000; *: name derived from UniProt search; a negative log ratio indicates upregulation in G2; U.P.: unclassified protein; Ag: antigen; R: receptor; Ig: immunoglobulin

Table 5.5.2: The top 20 downregulated genes in G2 compared to G1(-) by fold change.

Identifier	Gene	Protein	p	log2 Ratio	fc	Function
^006464	CIDEA	cell death-inducing DFFA-like effector A	0.006317	6.3	77.39	apoptosis
^022678	LIPE	lipase E, hormone sensitive type	0.00909	4.6	24.32	metabolism and catabolism
^001359	CLEC10A	C-type lectin domain containing 10A	2.46E-06	4.6	23.70	not described
^026891	S100A1	S100 calcium binding protein A1	0.005927	4.5	22.98	angiogenesis and NOS activity
^021944	APCDD1	APC down-regulated 1	0.008284	4.3	19.40	↓Wnt signalling
^002851	SLC22A1	solute carrier family 22 member 1	0.006278	3.9	14.85	U.P.: neurotransmitter transport
^030063	FADS6	fatty acid desaturase 6	0.0007	3.7	13.20	lipid metabolism
^007290	STAB2	stabilin 2	0.00535	3.7	13.06	cell adhesion
^001421	SORBS1	sorbin and SH3 domain containing 1	0.009127	3.7	12.82	actin filament organisation
^006864	GPC3	glypican 3	3.64E-05	3.7	12.64	signal transduction regulation
^014026	MARCO	macrophage receptor with collagenous structure	0.00016	3.7	12.62	apoptotic cell clearance
^019173	SCART1	scavenger receptor family member expressed on T-cells 1	0.006174	3.7	12.61	scavenger receptor activity
^008518	LPIN1	lipin 1	0.005304	3.6	12.49	metabolism, catabolism, and transcription
^006231	PPARG	peroxisome proliferator activated receptor gamma	0.009438	3.6	12.19	myriad, most cell proliferation
^028966	TIMP4	TIMP metallopeptidase inhibitor 4	0.000499	3.5	11.54	MMP inhibition
^030062	RBP7	retinol binding protein 7	0.000183	3.5	11.50	retinoid binding
^023768	IGHE	immunoglobulin heavy constant epsilon	0.001687	3.5	11.38	Ag and Ig binding
^001602	CLEC4G	C-type lectin domain family 4 member G	0.000998	3.4	10.59	negative T cell regulation
^024268	CD36	CD36 molecule	0.005317	3.4	10.51	lipoprotein binding
^010296	GYG2	glycogenin 2	0.005071	3.4	10.43	transferase activity

Key: The colour of the fold change (fc) indicates the cluster to which the gene belongs (see below, black: no cluster); ^ indicates the prefix ENSFCAG00000; U.P.: unclassified protein; Ag: antigen; Ig: immunoglobulin

Table 5.5.3: KEGG pathways predicted to be enriched in the STRING predicted network associated with the unnamed gene ENSFCAG00000001764. The gene count is out of the 11 in the network.

ID	Pathway description	Gene count	fdr
4210	Apoptosis	6	1.70E-10
4064	NF-kappa B signalling pathway	5	4.48E-08
4621	NOD-like receptor signalling pathway	3	0.000104
4612	Antigen processing and presentation	3	0.000109
4510	Focal adhesion	4	0.000114
4120	Ubiquitin mediated proteolysis	3	0.00139
4151	PI3K-Akt signalling pathway	3	0.0145
4668	TNF signalling pathway	2	0.0262

A 'colorectal cancer' pathway as well as 'tuberculosis' were also mildly enriched and are not shown here. These names relate to manually drawn pathway maps allocated by the software, representing current knowledge of molecular interactions, reactions, and relationships in different functions and conditions. Of the genes in this network, none showed significant differential expression at the 0.01 level, and only BCL2-like protein 1 showed significant differential expression at the 0.05 level, being upregulated in FIP. Except for CSTA and BIRC5, there was insignificant upregulation found. This network was therefore not further analysed. The apoptosis regulator BCL2 could not be identified within the database.

The data was then analysed by cluster analysis. An automated function generates the six most distinct clusters by expression values. The clusters are defined based on the two groups in the comparison, with the scheme displayed as applying to all. This shows that in this analysis, G3 clusters with G1 and LCM with G2.

All clusters (shown on the y axis as different coloured bands) appear differentially expressed between G1 and G2. However, at this stage the cluster generation process is only associated with the expression values. The next stage of GO (gene ontology) analysis evaluates the genes in each cluster which may or may not result in significantly enriched categories.

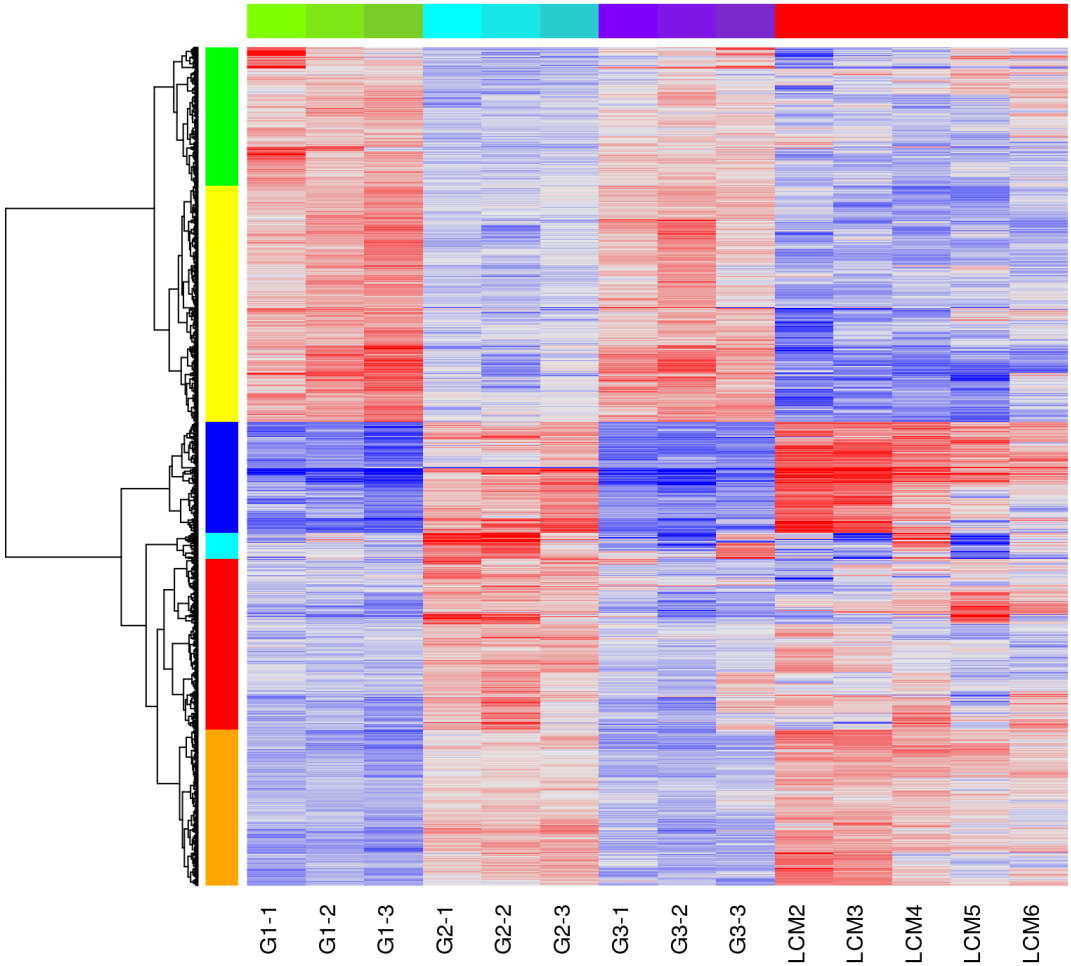

Figure 5.5.11: *Cluster plot comparing G1(-) and G2; colours on the y axis represent GO (gene ontology) category feature clusters, with each individual sample marked on the x axis. The chart colour intensity indicates comparative up or down regulation (blue -; red +).*

Ontology is split into three classes; **BP** (biological process), **MF** (molecular function), and **CC** (cellular component). Here the focus was on the former two. Each cluster containing significantly enriched categories is listed below (Tables 5.5.4 – 5.5.7). The yellow and green clusters were lower in G2 than G1- but the green cluster produced no significant categories and the yellow only three, which are instead listed subsequently. These two categories were also those containing the top downregulated genes in FIP.

The individual genes contributing to these cluster results are far greater in number than the GO categories they can be associated with. They were filtered from the overall results chart using a $p \leq 0.01$ cut off. There were found to be 249 differentially expressed red cluster genes, 228 orange, 162 blue and 38 cyan cluster genes. All except two blue genes were upregulated in G2 compared to G1-.

Table 5.5.4: Red feature cluster of GO categories in G1- vs G2, ranked by probability (p), where N shows the number of significant genes (p<0.01) within the total number of genes in the category.

Class	Rank	Term	ID	p	N
BP	1	collagen fibril organization	GO:0030199	1.95e-8	8/24
BP	2	collagen biosynthetic process	GO:0032964	0.0000369	3/4

Table 5.5.5: Orange feature cluster of GO categories in G1- vs G2, ranked by probability (p), where N shows the number of significant genes (p<0.01) within the total number of genes in the category.

Class	Rank	Term	ID	p	N
BP	1	interferon-gamma-mediated signalling pathway	GO:0060333	0.0000291	3/4
BP	2	negative regulation of viral release from host cell	GO:1902187	0.0000422	4/11
BP	3	positive regulation of calcium ion transport into cytosol	GO:0010524	0.0000718	3/5
CC	1	death-inducing signalling complex	GO:0031264	0.0000234	3/4

Table 5.5.6: cyan feature cluster of GO categories in G1- vs G2, ranked by probability (p), where N shows the number of significant genes (p<0.01) within the total number of genes in the category. '.' represents a 'child' term of the term above it.

Class	Rank	Term	ID	p	N
BP	1	immunoglobulin production	GO:0002377	5.01e-17	10/45
BP	2	phagocytosis, recognition	GO:0006910	1.61e-11	7/38
BP	3	positive regulation of B cell activation	GO:0050871	1.96e-11	7/39
BP	4	phagocytosis, engulfment	GO:0006911	3.42e-11	7/42
BP	5	immune response	GO:0006955	3.03e-10	10/203
BP	6	.innate immune response	GO:0045087	2.04e-7	7/142
BP	7	defense response to bacterium	GO:0042742	1.43e-9	7/70
MF	1	immunoglobulin receptor binding	GO:0034987	1.29e-12	7/37
MF	2	antigen binding	GO:0003823	3.35e-12	7/42

Table 5.5.7: Blue feature cluster of GO categories in G1- vs G2, ranked by probability (p), where N shows the number of significant genes (p<0.01) within the total number of genes in the category. './..' represent 'child' terms of the term above.

Class	Rank	Term	ID	p	N
BP	1	immune response	GO:0006955	2.11e-14	22/203
BP	2	.innate immune response	GO:0045087	5.4e-9	14/142
BP	3	chemotaxis	GO:0006935	7.17e-13	13/60
BP	4	response to virus	GO:0009615	2.55e-12	12/52
BP	5	.defense response to virus	GO:0051607	2.89e-18	17/63
BP	6	chemokine-mediated signalling pathway	GO:0070098	8.35e-12	11/44
BP	7	G-protein coupled receptor signalling pathway	GO:0007186	2.78e-9	17/212
BP	8	response to lipopolysaccharide	GO:0032496	1.21e-7	10/82
BP	9	.cellular response to lipopolysaccharide	GO:0071222	4.29e-11	12/65
BP	10	. .lipopolysaccharide-mediated signalling pathway	GO:0031663	0.00000119	6/27
BP	11	positive regulation of cAMP-mediated signalling	GO:0043950	1.5e-7	4/5
BP	12	positive regulation of chemokine production	GO:0032722	1.71e-7	5/11
BP	13	negative regulation of viral genome replication	GO:0045071	3.17e-7	6/22
BP	14	positive regulation of interleukin-8 production	GO:0032757	0.00000153	5/16
BP	15	positive regulation of cAMP metabolic process	GO:0030816	0.00000233	3/3
BP	16	defense response	GO:0006952	0.00000519	5/20
BP	17	.inflammatory response	GO:0006954	6.67e-21	25/150
BP	18	.innate immune response	GO:0045087	5.4e-9	14/142
BP	19	cellular response to interleukin-1	GO:0071347	0.00000984	6/38
BP	20	positive regulation of gene expression	GO:0010628	0.0000141	12/200
BP	21	positive regulation of interferon-alpha production	GO:0032727	0.0000452	3/6
BP	22	interleukin-1 beta secretion	GO:0050702	0.0000452	3/6
BP	23	.positive regulation of interleukin-1 beta secretion	GO:0050718	0.00000932	4/11
BP	24	cellular response to lipoteichoic acid	GO:0071223	0.0000452	3/6
BP	25	positive regulation of ERK1 and ERK2 cascade	GO:0070374	0.0000505	8/99
BP	26	positive regulation of interleukin-6 production	GO:0032755	0.0000506	5/31
BP	27	regulation of cytokine secretion	GO:0050707	0.0000783	3/7
BP	28	.positive regulation of cytokine secretion	GO:0050715	0.0000804	4/18
BP	29	positive regulation of nitric oxide biosynthetic process	GO:0045429	0.0000804	4/18
MF	1	cytokine activity	GO:0005125	5.34e-16	16/67
MF	2	.chemokine activity	GO:0008009	5.64e-13	10/25
MF	3	CCR chemokine receptor binding	GO:0048020	3.04e-8	6/15
MF	4	double-stranded RNA binding	GO:0003725	0.00000191	7/43
MF	5	CXCR3 chemokine receptor binding	GO:0048248	0.00000269	3/3
MF	6	carbohydrate binding	GO:0030246	0.00000274	8/64
MF	7	lipopolysaccharide binding	GO:0001530	0.000033	4/14
MF	8	interleukin-1 receptor binding	GO:0005149	0.0000521	3/6

Within the individually upregulated genes in G2, the blue cluster is highly overrepresented and is the also the largest cluster to be generated. Blue, cyan and orange clusters all centre on the immune response and particularly the anti-viral response, with involvement of both innate and adaptive factors. The red cluster is far smaller and involves matrix synthesis.
The downregulated genes fall within green or yellow; of these the only BP GO term produced was peptidyl-tyrosine autophosphorylation in the yellow cluster (not shown in tabular from).
The biological process (BP) class contained the highest number of GO categories of interest; an enrichment diagram was created (Fig. 5.5.12) showing which categories were of most significance and how heavily they were represented amongst differentially expressed genes.

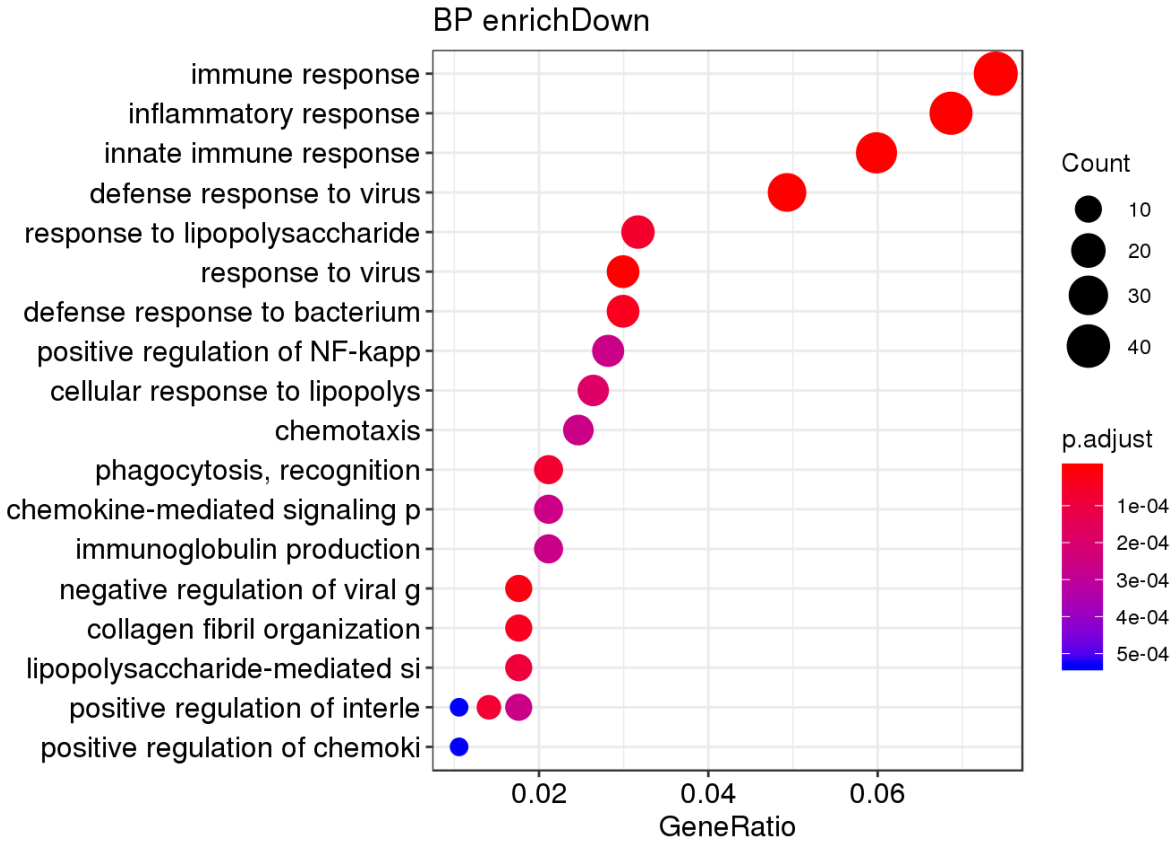

Figure 5.5.12: *Enriched biological process categories which are upregulated in G2 vs G1.*

In total, 1775 GO categories were identified from which at least one significantly upregulated gene in G2 was present. 125 of these had a p value ≤0.01 and the list can be further narrowed by FDR to a top 30 with an FDR <0.01. Those shown below are those significant when also selected by clustered genes (Table 5.5.8).

Table 5.5.8: significant BP categories in G1- versus G2 which are also enriched by cluster

Rank	Term	ID	p	N
1	inflammatory response	GO:0006954	8.44e-17	39/150
2	immune response	GO:0006955	3.64e-13	42/203
3	.innate immune response	GO:0045087	7.68e-12	34/142
4	. .response to interferon-gamma	GO:0034341	0.00000363	6/9
5	response to virus	GO:0009615	1.44e-8	17/52
6	.defence response to virus	GO:0051607	1.44e-17	28/63
7	. . . .positive regulation of defence response to virus by host	GO:0002230	0.0000622	6/13
8	negative regulation of viral genome replication	GO:0045071	4.02e-7	10/22
9	collagen fibril organization	GO:0030199	7.22e-7	10/24
10	chemokine-mediated signalling pathway	GO:0070098	9.72e-7	12/44
11	response to lipopolysaccharide	GO:0032496	0.00000104	18/82
12	.cellular response to lipopolysaccharide	GO:0071222	0.00000643	15/65
13	. .lipopolysaccharide-mediated signalling pathway	GO:0031663	0.00000279	10/27
14	positive regulation of interleukin-8 production	GO:0032757	0.00000138	8/16
15	defence response to bacterium	GO:0042742	0.00000157	17/70
16	chemotaxis	GO:0006935	0.00000184	14/60
17	positive regulation of interleukin-6 production	GO:0032755	0.00000353	10/31
18	phagocytosis, recognition	GO:0006910	0.00000652	12/38
19	positive regulation of NF-kappaB transcription factor activity	GO:0051092	0.0000068	16/77
20	positive regulation of chemokine production	GO:0032722	0.0000083	6/11
21	positive regulation of interleukin-1 beta secretion	GO:0050718	0.0000108	6/11
22	G-protein coupled receptor signalling pathway	GO:0007186	0.0000132	26/212
23	immunoglobulin production	GO:0002377	0.0000403	12/45
24	positive regulation of cAMP-mediated signalling	GO:0043950	0.0000504	4/5
25	negative regulation of endopeptidase activity	GO:0010951	0.0000588	12/53
26	positive regulation of type I interferon production	GO:0032481	0.0000687	6/12
27	positive regulation of interleukin-5 production	GO:0032754	0.0000703	4/6
28	endoplasmic reticulum unfolded protein response	GO:0030968	0.0000989	10/39

Cats without FIP but with detectable FCoV in the MLN versus cats with FIP [G2 vs G3 (G2 vs G1+)]

Number of significants by p-value and fold-change

	#significants	FDR	fc >= 1	fc >= 1.5	fc >= 2	fc >= 3	fc >= 4	fc >= 8	fc >= 10
p < 0.1	4671	0.266700	4671	4155	2120	888	494	163	112
p < 0.05	3453	0.180500	3453	3377	2014	873	487	163	112
p < 0.01	1766	0.070500	1766	1766	1526	770	441	150	103
p < 0.001	605	0.020580	605	605	605	463	316	117	78
p < 1e-04	221	0.005638	221	221	221	219	195	89	59
p < 1e-05	67	0.001860	67	67	67	67	67	40	23

Figure 5.5.13: *Results summary ordered by significance and fold change, where FDR = false discovery rate and fc = fold change. 12472/19493 features had counts above the threshold.*

Genes designated 'upregulated' by the software in this comparison are higher in G2 than G3 (G1+).

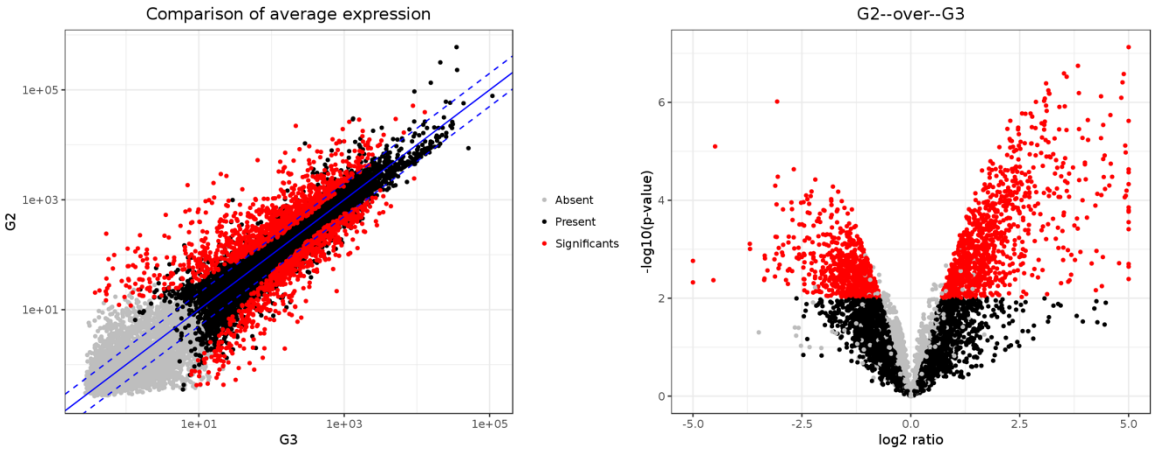

Figure 5.5.14: *Comparison between average group expressions (left), with significant values indicated together with their fold change log ratio (right). A negative log ratio indicates a higher expression in G2.*

The 20 top up and down regulated genes are shown in Table 5.5.9 and 5.5.10, together with significant clusters and the most significantly upregulated GO categories from all clusters.

Table 5.5.9: The top 20 genes by fold change which were higher in G2 than G3 (G1+).

Identifier	Gene	Protein	p	log2 Ratio	fc	Function
^029292	IGKV4-1	Immunoglobulin kappa variable 4-1	0.00016	7.7	208.51	Ig R binding
^024010			0.00014	5.9	58.81	U.P.: Ag and Ig R binding
^025088			0.002266	5.7	52.06	U.P.: Ig production
^029623			0.001997	5.6	47.34	U.P.: Ag and Ig R binding
^026111			0.004063	5.2	36.28	U.P.: Ig production
^001764			4.68E-05	6.3	77.98	unknown
^025965	SAA2	serum amyloid A protein	0.00028	6.2	72.91	acute phase response
^013594	CCL8	C-C motif chemokine ligand 8	7.44E-08	6.1	67.56	cell signalling and chemotaxis
^025002	SAA1	Serum amyloid A protein Amyloid protein A	0.00039	6.0	66.21	acute phase response
^010436	ACOD1	aconitate decarboxylase 1	0.000171	5.9	59.06	defence response
^014062	S100A12	S100 calcium binding protein A12	2.39E-06	5.3	40.25	innate immune response, many
^003199	S100A9	S100 calcium binding protein A9	2.33E-05	5.2	36.81	innate immune response, many
^001290	S100A8	S100 calcium binding protein A8	2.68E-05	5.0	32.67	innate immune response, many
^018779	IFIT3	interferon induced protein with tetratricopeptide repeats 3	6.36E-05	5.0	30.95	response to IFN-α
^009575	IL1RN	interleukin 1 receptor antagonist	8.07E-05	4.9	30.59	negative regulation of IL-1
^031821	IRF7	interferon regulatory factor 7	1.06E-05	4.9	30.53	regulates IFN transcription
^007076	CLEC4D	C-type lectin domain family 4 member D	7.63E-06	4.9	30.32	Ig R binding
^028244	AQP9	aquaporin 9	8.68E-05	4.9	30.09	response to cAMP
^000708	RSAD2	radical S-adenosyl methionine domain containing 2	2.64E-07	4.9	29.61	predicted ↑regulation of TLR7 and 9 signalling
^024242			3.90E-07	4.9	29.04	U.P.: response to biotic stimuli

Key: The colour of the fold change (fc) indicates the cluster to which the gene belongs (see below; yellow, cyan, orange); ^ indicates the prefix ENSFCAG00000; function derived from UniProt search; U.P.: unclassified protein; Ag: antigen; R: receptor; Ig: immunoglobulin

Table 5.5.10: The top 20 genes by fold change which were lower in G2 than G3 (G1+).

Identifier	Gene	Protein	p	log2 Ratio	fc	Function
^023768	IGHE	immunoglobulin heavy constant epsilon	0.004754	-6.7	104.33	Ig binding
^028847	HBA1	Globin C1	0.001727	-5.0	32.85	haemoglobin subunit
^030143			0.004289	-4.5	23.12	U.P. haem binding
^006464	CIDEA	cell death-inducing DFFA-like effector A	7.95E-06	-4.5	22.50	apoptosis
^011920	FRMPD1	FERM and PDZ domain containing 1	0.000775	-3.7	12.95	G protein couple R signalling
^013351	PLIN1	perilipin 1	0.000986	-3.7	12.91	lipid metabolism*
^004411	CELA1	chymotrypsin like elastase family member 1	0.004254	-3.4	10.31	protease
^013832	FCAMR	Fc fragment of IgA and IgM receptor	0.003971	-3.4	10.26	Ig binding
^012336	MYCBPAP	MYCBP associated protein	0.001349	-3.4	10.22	spermatogenesis
^004058	VPREB3	V-set pre-B cell surrogate light chain 3	0.001538	-3.3	10.18	Ig production and response
^006286	PLIN4	perilipin 4	0.002712	-3.3	9.78	lipid transport and metabolism
^005424	LYZ	lysozyme	0.001605	-3.1	8.75	defence against bacteria
^000419	PCK1	phosphoenolpyruvate carboxykinase 1	0.003607	-3.1	8.68	cellular metabolism
^014052	GZMK	granzyme K	5.04E-05	-3.1	8.64	cell defence
^004909	PLA2G2D	phospholipase A2 group IID	0.000556	-3.1	8.59	cellular metabolism
^019173	SCART1	scavenger receptor family member expressed on T-cells 1	0.001236	-3.1	8.48	scavenger receptor activity
^004635	DGAT2	diacylglycerol O-acyltransferase 2	0.000121	-3.1	8.46	lipid metabolism
^001089	CPNE5	copine 5	0.000561	-3.1	8.44	dendrite extension
^006864	GPC3	glypican 3	9.63E-07	-3.1	8.39	signal transduction regulation
^027632			3.30E-05	-3.1	8.30	unknown

Key: The colour of the fold change indicates the cluster to which the gene belongs (see below); ^ indicates the prefix ENSFCAG00000; function derived from UniProt; a negative log ratio indicates upregulation in G2; U.P.: unclassified protein; R: receptor; Ig: immunoglobulin

Seven of the top 20 genes higher in G2 than in G1 were also amongst the top 20 higher in G2 than G3. Three of the top 20 genes which are lower in G1 or G3 than G2 also overlapped.

Cluster analysis results for G2 versus G3 are shown below. With reference to individual genes, there are 58 in the red cluster, all lower in FIP; 201 in yellow, all upregulated; 321 in orange all upregulated; 625 in green, all downregulated; 370 in blue, all upregulated; 191 in cyan with all except one upregulated in FIP.

In keeping with these findings, the top 20 upregulated individual genes come from clusters yellow, orange and cyan and the bottom regulated from red and green. By far the largest cluster was the cyan cluster, this is also where over half of the individual upregulated genes came from.

Those lower in FIP largely involve cellular metabolism, and those upregulated the immune system with an emphasis on viral defence and cytokine signalling.

Table 5.5.11: Red feature cluster of GO categories, ranked by probability (p), where N shows the number of significant genes within the total number of genes in the category.

Class	Rank	Term	ID	p	N
BP	1	lipid storage	GO:0019915	2.36e-8	5/19
BP	2	low-density lipoprotein particle clearance	GO:0034383	6E-06	3/8
BP	3	negative regulation of lipid catabolic process	GO:0050995	9E-06	3/9
BP	4	triglyceride biosynthetic process	GO:0019432	1E-05	3/10
MF	1	lipid binding	GO:0008289	5E-06	5/50

Table 5.5.12: Yellow feature cluster of GO categories, ranked by probability (p), where N shows the number of significant genes within the total number of genes in the category. '.' indicates that the term is a 'child' term of the term above.

Class	Rank	Term	ID	p	N
BP	1	immunoglobulin production	GO:0002377	3.33e-9	10/47
BP	2	phagocytosis, recognition	GO:0006910	5.86e-9	9/37
BP	3	positive regulation of B cell activation	GO:0050871	7.57e-9	9/38
BP	4	defense response to bacterium	GO:0042742	1.15e-8	11/68
BP	5	phagocytosis, engulfment	GO:0006911	1.23e-8	9/40
BP	6	B cell receptor signalling pathway	GO:0050853	2.41e-8	10/57
BP	7	proteolysis	GO:0006508	1.36e-7	20/307
BP	8	complement activation	GO:0006956	4.25E-05	3/5
BP	9	.complement activation, classical pathway	GO:0006958	1.92e-9	9/33
MF	1	immunoglobulin receptor binding	GO:0034987	2.04e-9	9/36
MF	2	antigen binding	GO:0003823	7.11e-9	9/41
MF	3	extracellular matrix binding	GO:0050840	9.28E-06	5/20
MF	4	peptidase activity	GO:0008233	1.14E-05	12/174
MF	5	insulin-like growth factor binding	GO:0005520	4.37E-05	4/14

Table 5.5.13: Orange feature cluster of GO categories, ranked by probability (p), where N shows the number of significant genes within the total number of genes in the category. '.' indicates that the term is a 'child' term of the term above.

Class	Rank	Term	ID	p	N
BP	1	cell adhesion	GO:0007155	7.49e-7	18/168
BP	2	.cell adhesion mediated by integrin	GO:0033627	0.000016	5/13
BP	3	cytokine-mediated signalling pathway	GO:0019221	0.0000441	10/77

Table 5.5.14: Green feature cluster of GO categories, ranked by probability (p), where N shows the number of significant genes within the total number of genes in the category. '.' indicates that the term is a 'child' term of the term above.

Class	Rank	Term	ID	p	N
BP	1	peptidyl-tyrosine autophosphorylation	GO:0038083	0.0000394	9/37
BP	2	sulfate transport	GO:0008272	0.0000668	4/6
BP	3	.sulfate transmembrane transport	GO:1902358	0.0000231	4/5
MF	1	sulfate transmembrane transporter activity	GO:0015116	0.0000227	4/5
MF	2	non-membrane spanning protein tyrosine kinase activity	GO:0004715	0.0000475	9/38
MF	3	calcium ion binding	GO:0005509	0.0000953	32/336

Table 5.5.15: Blue feature cluster of GO categories, ranked by probability (p), where N shows the number of significant genes within the total number of genes in the category. '.' indicates that the term is a 'child' term of the term above.

Class	Rank	Term	ID	p	N
BP	1	ATP hydrolysis coupled proton transport	GO:0015991	0.00000125	7/19
BP	2	signal transduction	GO:0007165	0.00000182	40/561
BP	3	response to lipopolysaccharide	GO:0032496	0.0000116	12/82
BP	4	inflammatory response	GO:0006954	0.0000246	16/149
BP	5	defence response to virus	GO:0051607	0.0000304	10/63
MF	1	signal transducer activity	GO:0004871	9.14e-8	23/201
MF	2	proton transmembrane transporter activity	GO:0015078	0.0000815	6/24
MF	3	.proton-transporting ATPase activity, rotational mechanism	GO:0046961	2.12e-8	7/12

Table 5.5.16: Cyan feature cluster of GO categories, ranked by probability (p), where N shows the number of significant genes within the total number of genes in the category. './..' indicates that the term is a 'child' term of the term above.

Class	Rank	Term	ID	p	N
BP	1	immune response	GO:0006955	1.05e-13	23/205
BP	2	.innate immune response	GO:0045087	4.41e-8	14/141
BP	3	chemotaxis	GO:0006935	2.47e-13	14/59
BP	4	response to virus	GO:0009615	1.93e-11	12/52
BP	5	.defense response to virus	GO:0051607	2.02e-18	18/63
BP	6	chemokine-mediated signalling pathway	GO:0070098	4.07e-11	11/43
BP	7	G-protein coupled receptor signalling pathway	GO:0007186	6.99e-11	20/206
BP	8	cellular response to interleukin-1	GO:0071347	8.59e-8	8/37
BP	9	positive regulation of cAMP-mediated signalling	GO:0043950	2.98e-7	4/5
BP	10	defense response	GO:0006952	4.6e-7	6/20
BP	11	.inflammatory response	GO:0006954	1.72e-21	27/149
BP	12	.innate immune response	GO:0045087	4.41e-8	14/141
BP	13	response to lipopolysaccharide	GO:0032496	5.94e-7	10/82
BP	14	.cellular response to lipopolysaccharide	GO:0071222	1.04e-12	14/65
BP	15	. .lipopolysaccharide-mediated signalling pathway	GO:0031663	0.00000321	6/27
BP	16	negative regulation of viral genome replication	GO:0045071	8.63e-7	6/22
BP	17	interleukin-1 beta secretion	GO:0050702	8.83e-7	4/6
BP	18	.positive regulation of interleukin-1 beta secretion	GO:0050718	0.0000183	4/11
BP	19	positive regulation of interleukin-8 production	GO:0032757	0.00000353	5/16
BP	20	positive regulation of cAMP metabolic process	GO:0030816	0.00000389	3/3
BP	21	positive regulation of interleukin-6 production	GO:0032755	0.00000618	6/30
BP	22	positive regulation of gene expression	GO:0010628	0.0000163	13/200
BP	23	positive regulation of chemokine production	GO:0032722	0.0000183	4/11
BP	24	cellular response to tumor necrosis factor	GO:0071356	0.0000206	7/54
BP	25	regulation of cell proliferation	GO:0042127	0.0000448	11/160
BP	26	positive regulation of interferon-alpha production	GO:0032727	0.000075	3/6
BP	27	cellular response to lipoteichoic acid	GO:0071223	0.000075	3/6
MF	1	cytokine activity	GO:0005125	2.22e-17	18/68
MF	2	.chemokine activity	GO:0008009	6.95e-14	11/25
MF	3	CCR chemokine receptor binding	GO:0048020	8.54e-8	6/15
MF	4	carbohydrate binding	GO:0030246	0.00000112	9/65
MF	5	CXCR3 chemokine receptor binding	GO:0048248	0.00000452	3/3
MF	6	double-stranded RNA binding	GO:0003725	0.00000602	7/43
MF	7	lipopolysaccharide binding	GO:0001530	0.0000649	4/14
MF	8	interleukin-1 receptor binding	GO:0005149	0.0000872	3/6

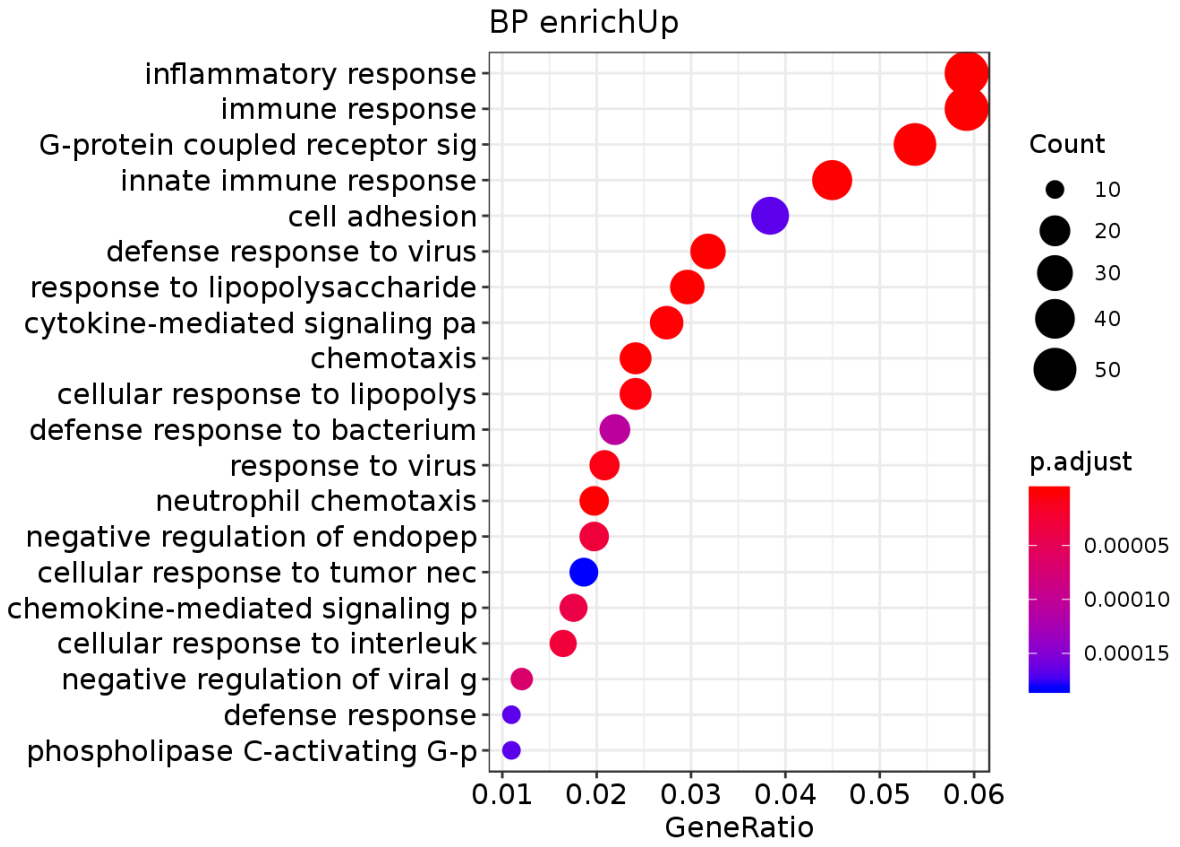

Figure 5.5.15: *Hypergeometric over-representation test applied to BP categories of G2 vs G3 (G1+) (G2 higher)*

Table 5.5.17: Table of significantly enriched BP GO categories taken from the overall gene set, containing only those upregulated in FIP and cluster restricted.

Rank	Term	ID	p	N
1	immune response	GO:0006955	4.08e-13	54/205
2	.innate immune response	GO:0045087	2.12e-11	41/141
3	. .response to interferon-gamma	GO:0034341	5.5E-06	7/10
4	response to lipopolysaccharide	GO:0032496	2.13e-9	27/82
5	.cellular response to lipopolysaccharide	GO:0071222	4.89e-8	22/65
6	chemotaxis	GO:0006935	2.34e-9	22/59
7	response to virus	GO:0009615	1.55e-7	19/52
8	.defense response to virus	GO:0051607	5.41e-14	29/63
9	cellular response to interleukin-1	GO:0071347	2.85e-7	15/37
10	signal transduction	GO:0007165	2.86e-7	86/561
11	.G-protein coupled receptor signalling pathway	GO:0007186	2.75e-11	49/206
12	. .phospholipase C-activating G-protein coupled receptor signalling pathway	GO:0007200	1.4E-06	10/20
13	negative regulation of viral genome replication	GO:0045071	1.8E-06	11/22
14	cell adhesion	GO:0007155	2.8E-06	35/168
15	.cell adhesion mediated by integrin	GO:0033627	6.9E-05	7/13
16	cellular response to tumor necrosis factor	GO:0071356	3.2E-06	17/54
17	defense response	GO:0006952	3.9E-06	10/20
18	.inflammatory response	GO:0006954	3.38e-20	54/149
19	. .regulation of inflammatory response	GO:0050727	8E-05	13/42
20	. . .positive regulation of inflammatory response	GO:0050729	5.3E-05	10/26
21	.innate immune response	GO:0045087	2.12e-11	41/141
22	. .response to interferon-gamma	GO:0034341	5.5E-06	7/10
23	positive regulation of interleukin-6 production	GO:0032755	5.2E-06	12/30
24	positive regulation of chemokine production	GO:0032722	1.1E-05	7/11
25	proteolysis	GO:0006508	1.2E-05	52/307
26	endodermal cell differentiation	GO:0035987	1.8E-05	10/23
27	positive regulation of NF-kappaB transcription factor activity	GO:0051092	1.9E-05	20/78
28	positive regulation of vascular endothelial growth factor production	GO:0010575	4.5E-05	8/17
29	vacuolar acidification	GO:0007035	5.8E-05	6/9

Control cats without FIP: those without FCoV detected in the MLN versus those with [G1 over G3 (G1- over G1+)]

Number of significants by p-value and fold-change

	#significants	FDR	fc >= 1	fc >= 1.5	fc >= 2	fc >= 3	fc >= 4	fc >= 8	fc >= 10
p < 0.1	910	0.9996	910	899	550	210	87	28	16
p < 0.05	449	0.9996	449	449	357	134	59	24	14
p < 0.01	112	0.9996	112	112	111	58	19	8	5
p < 0.001	7	0.9996	7	7	7	7	3	2	2
p < 1e-04	0	NA	0	0	0	0	0	0	0
p < 1e-05	0	NA	0	0	0	0	0	0	0

Figure 5.5.16: *Results summary ordered by significance and fold change, where FDR = false discovery rate and fc = fold change. There were 12496/19493 features above threshold.*

The overview immediately shows a much lower number (approximately 10%) of significantly differentially expressed genes in G1 vs G3 compared to G1 vs G2 or G2 vs G3. The FDR values are also far higher (at least 0.9996) implying a low confidence level of individual results.

At a standard p value and fold change of <0.01 and >2, 111 genes were found to be significant. This is in comparison to 1184 with the same criteria in G1 vs G2. These were displayed graphically and owing to their low numbers in this comparison, outliers of particular interest are marked individually (Fig. 5.5.17).

The term 'Upregulated' in the computer-generated charts refers to G1-. Tables have been labelled to convey this as higher or lower.

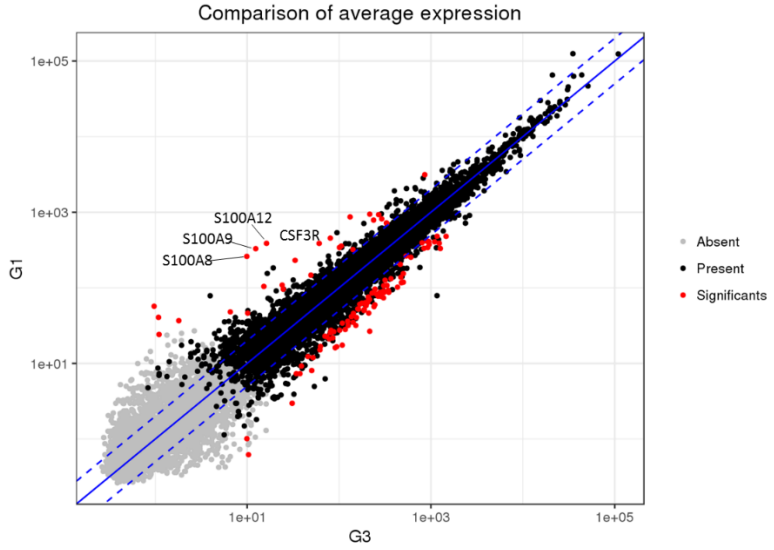

Figure 5.5.17: *Comparison of average expression between G1(-) and G3(G1+). Each dot represents a gene, those closest to the line are the most similarly expressed between groups, with significantly different genes (p <0.01) highlighted in red.*

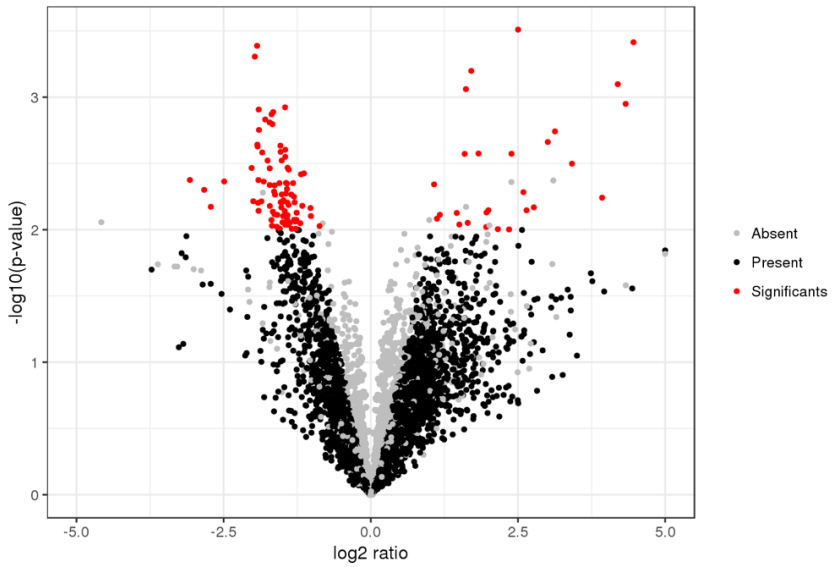

Figure 5.5.18: *Log fold changes between G1- and G1+, clearly showing (together with Fig. 5.5.17 above) that differentially expressed genes are more commonly higher in G1+ (G3) than G1- (G1); left side of the chart.*

Owing to the lower numbers of significant genes in this comparison, and the high FDR, only the top 10 in each direction are shown (Fig. 5.5.18 and 5.5.19). There were also fewer significant clusters identified, in this case red and orange (Table 5.5.20 and 5.5.21). Orange cluster genes were all higher in G1- whilst red cluster genes were higher in G1+.

The five genes with a fold change >10 at $p<0.01$ included the three S100 genes A8, A9, A12 (shown in Fig. 5.5.17), with A8 and A12 being the two genes also significant at the $p<0.001$ level. These were lower in G1+ and all in the orange cluster. The other two top five genes were not annotated.

Table 5.5.18: The top 10 genes by fold change which were higher in G3 than G1 (G1+ than G1-).

Identifier	Gene	Protein	p	log2 Ratio	fc	Function
^009774	MEF2B	myocyte enhancer factor 2B	0.0067	-2.7	6.58	↑transcription
^008534	LMO7	LIM domain 7	0.0043	-2.5	5.62	regulation of signalling
^018226	EAF2	ELL associated factor 2	0.0005	-2.0	3.92	negative regulation of cell growth
^003525	CENPE	centromere protein E	0.0004	-1.9	3.82	mitosis
^027527	CENPF	centromere protein F	0.0024	-1.9	3.79	mitosis
^028154			0.0061	-1.9	3.63	not found
^014712	RAD51	RAD51 recombinase	0.003	-1.8	3.37	DNA repair protein
^022606	DCK	deoxycytidine kinase	0.0016	-1.7	3.29	U.P: ATP binding
^001898	TPX2	TPX2, microtubule nucleation factor	0.0013	-1.7	3.22	mitosis
^010116	TNFRSF17	TNF receptor superfamily member 17	0.0093	-1.7	3.20	B cell maturation

Table 5.5.19: The top 10 genes by fold change which were lower in G3 than G1 (G1+ than G1-).

Identifier	Gene	Protein	p	log2 Ratio	fc	Function
^014062	S100A12	S100 calcium binding protein A12	0.00038	4.5	22.0	innate immune response, many
^003199	S100A9	S100 calcium binding protein A9	0.00112	4.3	20.1	innate immune response, many
^001290	S100A8	S100 calcium binding protein A8	0.0008	4.2	18.3	innate immune response, many
^023329			0.00574	3.9	15.2	U.P.: Ig binding
^024010			0.00317	3.4	10.7	U.P: Ag and Ig R binding
^000859			0.00181	3.1	8.7	U.P: peptidase inhibitor
^015790	MMP8	matrix metallopeptidase 8	0.00218	3.0	8.0	endopeptidase
^013269	CSF3R	colony stimulating factor 3 receptor	0.00679	2.8	6.8	neutrophil differentiation and chemotaxis
^029292	IGKV4-1	Immunoglobulin kappa variable 4-1	0.00714	2.6	6.3	Ig production
^024242			0.00521	2.6	6.0	U.P.: response to biotic stimulus

Key: The colour of the fold change (fc) indicates the cluster to which the gene belongs (see below; yellow, cyan, green, red); ^ indicates the prefix ENSFCAG00000; function derived from UniProt; U.P.: unclassified protein; R: receptor; Ig: immunoglobulin

Table 5.5.20: Significant GO categories within the red feature cluster of G1 vs G3. BP: biological process; MF: molecular function; Term: description of GO category; ID: identification of GO category; p: probability; N: number of genes from the category.

Class	Rank	Term	ID	p	N
BP	1	regulation of G2/M transition of mitotic cell cycle	GO:0010389	0.0000019	3/10
BP	2	mitotic chromosome condensation	GO:0007076	2.61E-06	3/11
BP	3	microtubule-based movement	GO:0007018	9.98E-06	4/53
BP	4	mitotic metaphase plate congression	GO:0007080	0.0000621	3/30
BP	5	activation of protein kinase activity	GO:0032147	0.000083	3/33
MF	1	ATP binding	GO:0005524	0.0000119	11/991
MF	2	motor activity	GO:0003774	0.000019	4/64
MF	3	.microtubule motor activity	GO:0003777	8.91E-06	4/53

Table 5.5.21: Significant GO categories within the orange feature cluster of G1 vs G3. BP: biological process; MF: molecular function; Term: description of GO category; ID: identification of GO category; p: probability; N: number of genes from the category.

Class	Rank	Term	ID	p	N
BP	1	neutrophil chemotaxis	GO:0030593	0.00000223	3/35
MF	1	RAGE receptor binding	GO:0050786	5.1e-9	3/6
MF	2	calcium ion binding	GO:0005509	0.0000516	4/335

Comparing to the complete gene differential expression charts, there are 33 genes in the red cluster, which are higher in G1+ and all relate to cell cycle functions.

The orange cluster (Table 5.5.21) consists of only eight genes, of which all are lower in G3 (G1+) than G1(-).

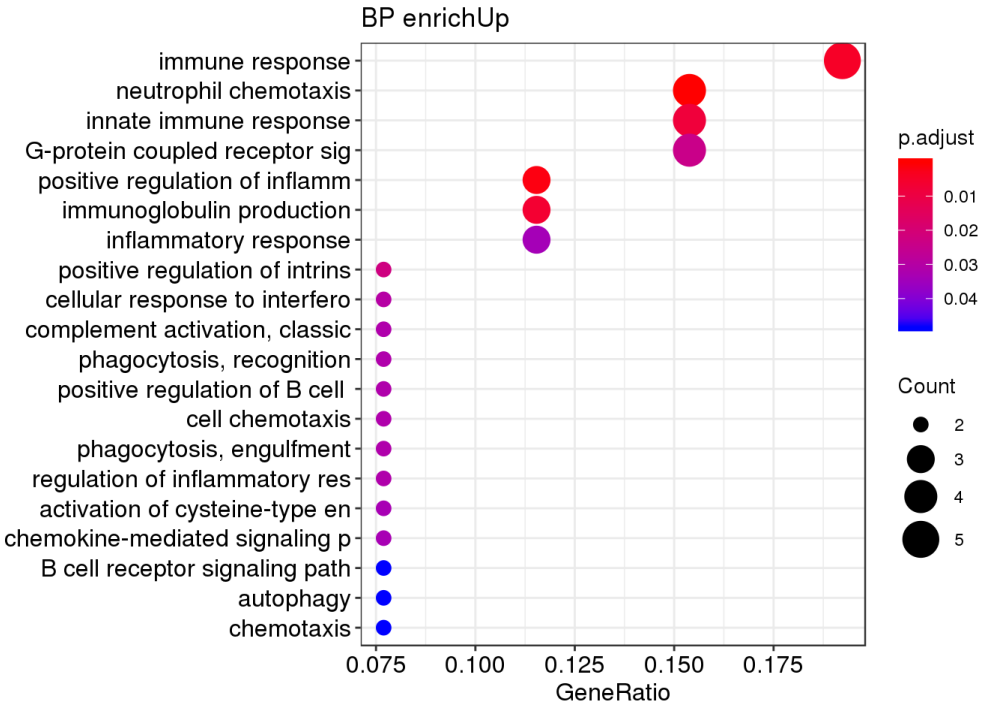

Figure 5.5.19: *BP (biological process) enrichment showing downregulated GO categories in G1+. The gene ratio (x axis) indicates what proportion of genes from a GO category (y axis) are present in the dataset, with the colour and size indicating the significance level and absolute gene count.*

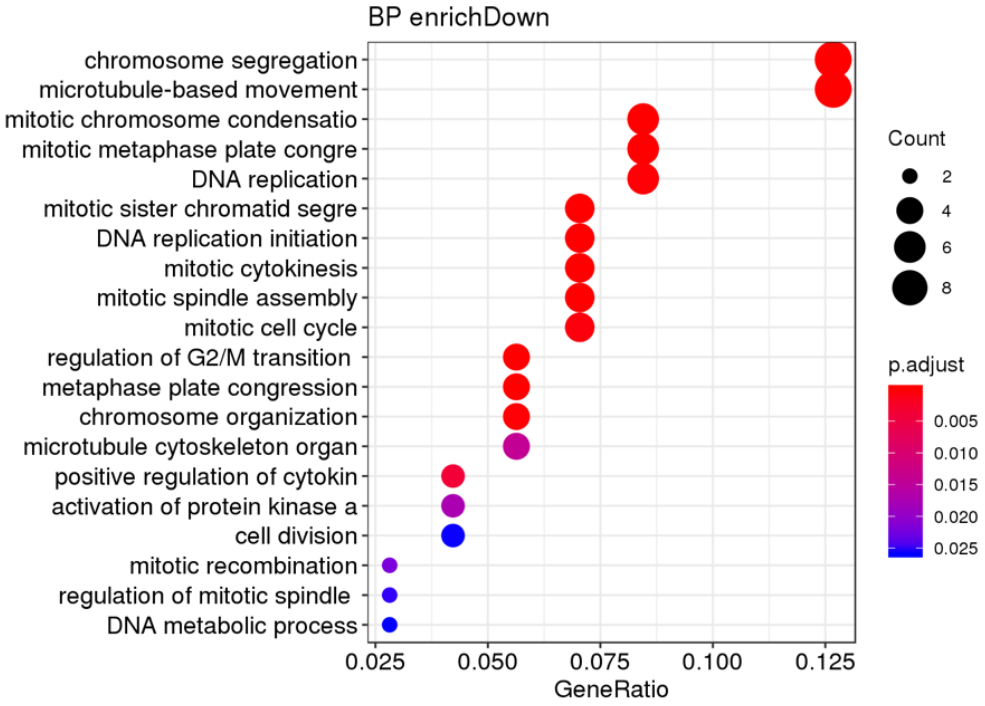

Figure 5.5.20: *BP enrichment showing GO categories which are upregulated in G1+.*

The BP terms labelled as 'enriched down' (meaning lower in G3 (G1+); Fig. 5.5.20 and Table 5.5.19) were entered into the online tool REViGO (reduce and visualise gene ontology). This uses a clustering algorithm to assess and visually display the semantic similarity of GO terms after filtering the terms for redundancy [315]. Fig. 5.5.21.

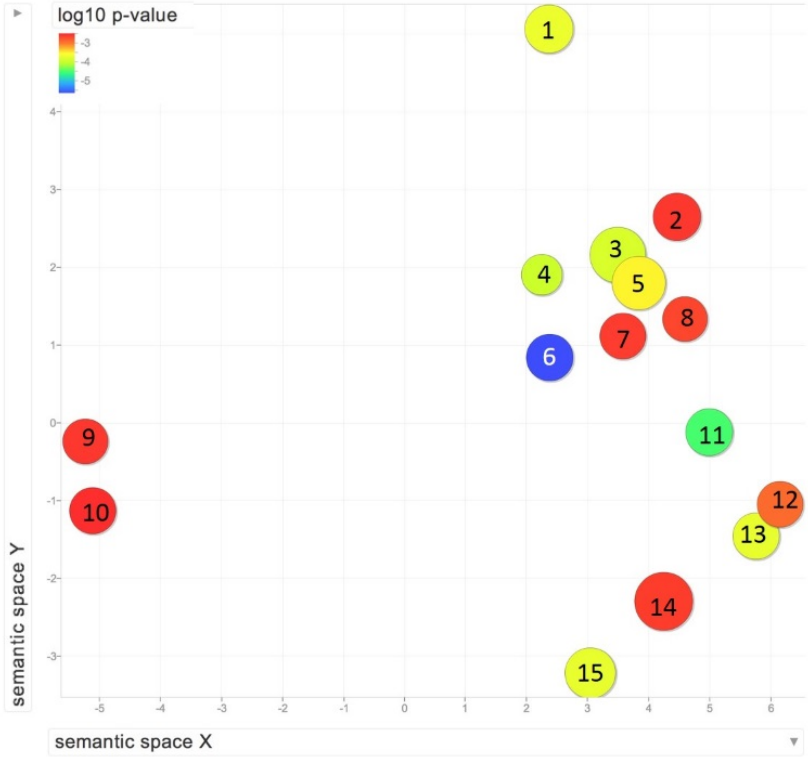

Figure 5.5.21: *REViGO generated scatterplot summarising significantly enriched GO categories in G1 vs G3.*

1. Immunoglobulin production
2. Positive regulation of B cell activation
3. Immune response
4. Leukocyte migration involved in inflammation
5. Innate immune response
6. Neutrophil chemotaxis
7. Cellular response to IFN-γ
8. Complement activation, classical pathway
9. Phagocytosis, recognition
10. Phagocytosis, engulfment
11. Positive regulation of inflammatory response
12. Positive regulation of intrinsic apoptotic pathway
13. Positive regulation of JAK-STAT cascade
14. G protein coupled receptor signalling
15. xenobiotic metabolic process

This shows that most of the terms which are lower in G3 (G1+) cluster together or form sub clusters, reinforcing the significance of the findings.

Table 5.5.21: Up-enriched Biological Process categories in G1(-) compared to G3 (G1+) (i.e. lower in G1+).

GO ID	P value	fdr	Count	Size	Term	Gene Names
GO:0030593	0.000	0.01	4	35	neutrophil chemotaxis	S100A8; S100A9; CSF3R; CCL24
GO:0050729	0.000	0.07	3	24	positive regulation of inflammatory response	S100A8; S100A9; CCL24
GO:0002523	0.000	0.13	2	6	leukocyte migration involved in inflammatory response	S100A8; S100A9
GO:0006955	0.000	0.13	5	196	immune response	; CCL24; ; ;
GO:0046427	0.000	0.13	2	8	positive regulation of JAK-STAT cascade	KIT; CYP1B1
GO:0006805	0.000	0.13	2	8	xenobiotic metabolic process	S100A12; CYP1B1
GO:0002377	0.000	0.13	3	48	immunoglobulin production	; ;
GO:0045087	0.000	0.17	4	136	innate immune response	S100A8; S100A9; ;
GO:2001244	0.001	0.60	2	21	positive regulation of intrinsic apoptotic signaling pathway	S100A8; S100A9
GO:0006958	0.002	0.83	2	32	complement activation, classical pathway	;
GO:0007186	0.002	0.83	4	200	G-protein coupled receptor signaling pathway	ADGRD2; ; CCL24; ADGRL4
GO:0071346	0.003	0.83	2	28	cellular response to interferon-gamma	CCL24; MRC1
GO:0050871	0.003	0.83	2	35	positive regulation of B cell activation	;
GO:0006910	0.003	0.83	2	35	phagocytosis, recognition	;
GO:0006911	0.003	0.91	2	38	phagocytosis, engulfment	;
GO:0050727	0.004	1.00	2	38	regulation of inflammatory response	S100A8; S100A9
GO:0060326	0.004	1.00	2	36	cell chemotaxis	KIT;
GO:0006919	0.005	1.00	2	42	activation of cysteine-type endopeptidase activity involved in apoptotic	S100A8; S100A9
GO:0070098	0.006	1.00	2	42	chemokine-mediated signaling pathway	; CCL24
GO:0006954	0.007	1.00	3	141	inflammatory response	KIT; ; CCL24
GO:0006027	0.007	1.00	1	3	glycosaminoglycan catabolic process	LYVE1
GO:0050853	0.007	1.00	2	56	B cell receptor signaling pathway	;
GO:0071603	0.008	1.00	1	3	endothelial cell-cell adhesion	CYP1B1
GO:0006914	0.008	1.00	2	57	autophagy	S100A8; S100A9
GO:0018119	0.009	1.00	1	3	peptidyl-cysteine S-nitrosylation	S100A8
GO:0032642	0.009	1.00	1	3	regulation of chemokine production	
GO:0061304	0.009	1.00	1	4	retinal blood vessel morphogenesis	CYP1B1

There are 28 categories with a p value <0.001, of which only the first eight have an FDR below 0.2. The first two categories carry the most weight and these also have an FDR below 0.1. The same five genes (S100A8, S100A9, S100A12, CCL24, CSF3R) are responsible for almost all the pathway enrichments detected so that this reflects the breadth of functions of these genes rather than a breadth of pathways.

There are also nine up-enriched MF categories however these are highly overlapping as they again comprise the same key genes.

The counts for these five genes were extracted from the bulk MLN dataset to plot the levels in each group as had been done by RT-qPCR (Fig. 5.5.22). The three S100 genes are all significantly downregulated in G1+ compared to either G1- or G2. The same can be said of CSF3R whilst CCL24 only shows a significant difference in the current comparison.

For all genes except CCL24 which was lower in G2 than G1+, levels in cats with FIP were closer to levels in cats without disease or virus. Only CCL24 showed a significant difference between G1- and G2 ($p=0.006379$).

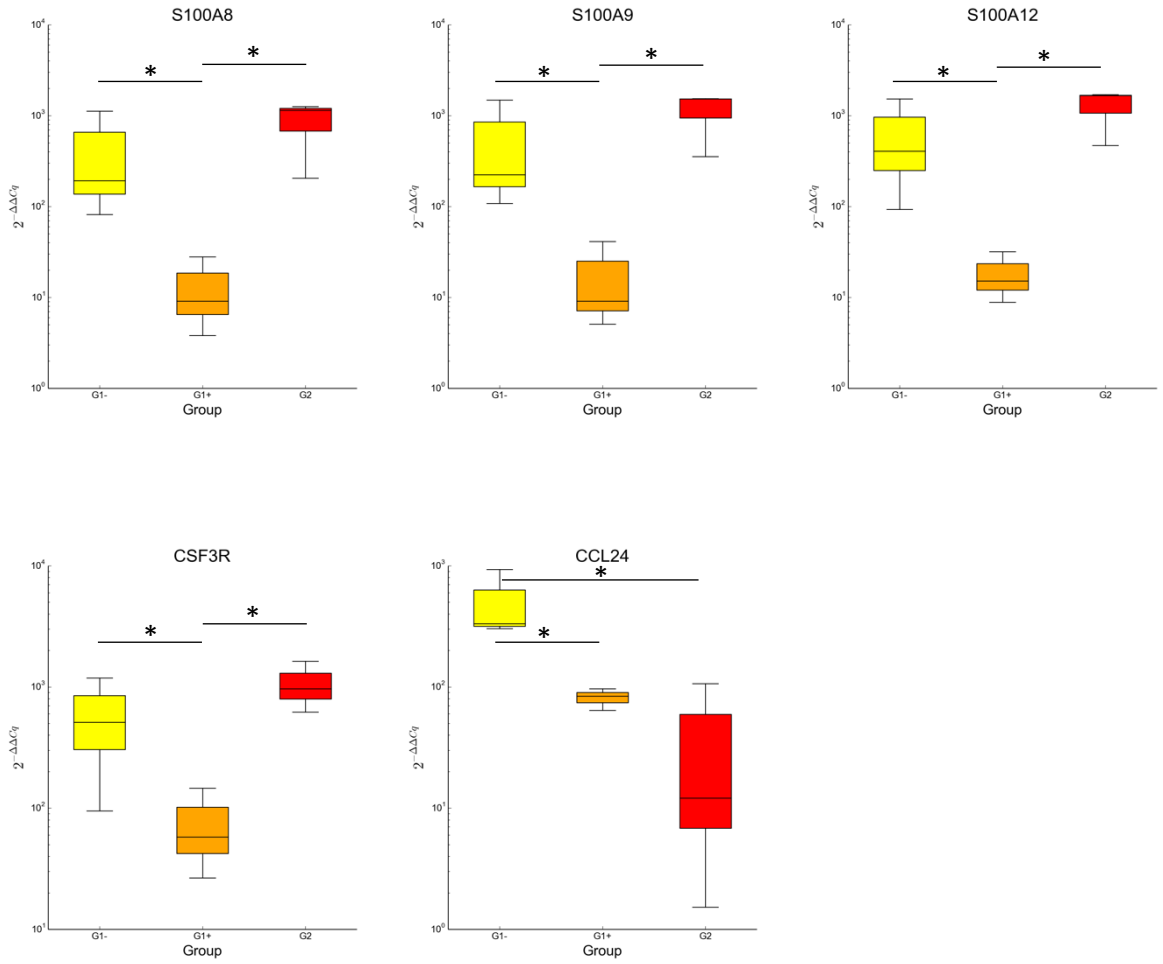

Figure 5.5.22: *Box plots showing the distribution across all three groups of the five most downregulated genes in G1+ vs G1-.*

Comparison between NGS and RT-qPCR results on the MLN (Chapter 3)

As the thousands of genes cannot feasibly be listed here, those targeted and investigated by RT-qPCR were extracted from the results.

The genes used for RT-qPCR have been tabulated for each pairwise comparison (Table 5.5.22), allowing comparison between the two methods. The sample populations were of course not identical, with the NGS cases being a small subset of the PCR cases.

Within G1 vs G2 there was disagreement for six targets between the two methods (PCR vs NGS) in terms of significant versus non-significant results, the significant result always being in PCR. These were IL-6, IFN-α, TNF-α, IL-15, MMP13, and TIMP1. Of the cytokines, all except IFN-α would be significant also by NGS if the probability threshold had been set at 0.05; IFN-α was close to this threshold. The matrix remodelling enzymes showed no agreement.

There was no agreement with the RT-qPCR positive G1+ vs G1- cases but all PCR significant targets in G1+ vs G2 were also significant by NGS. In this last comparison NGS also marked IL-6, STAT3, M-CSF, and MMP2 as significant.

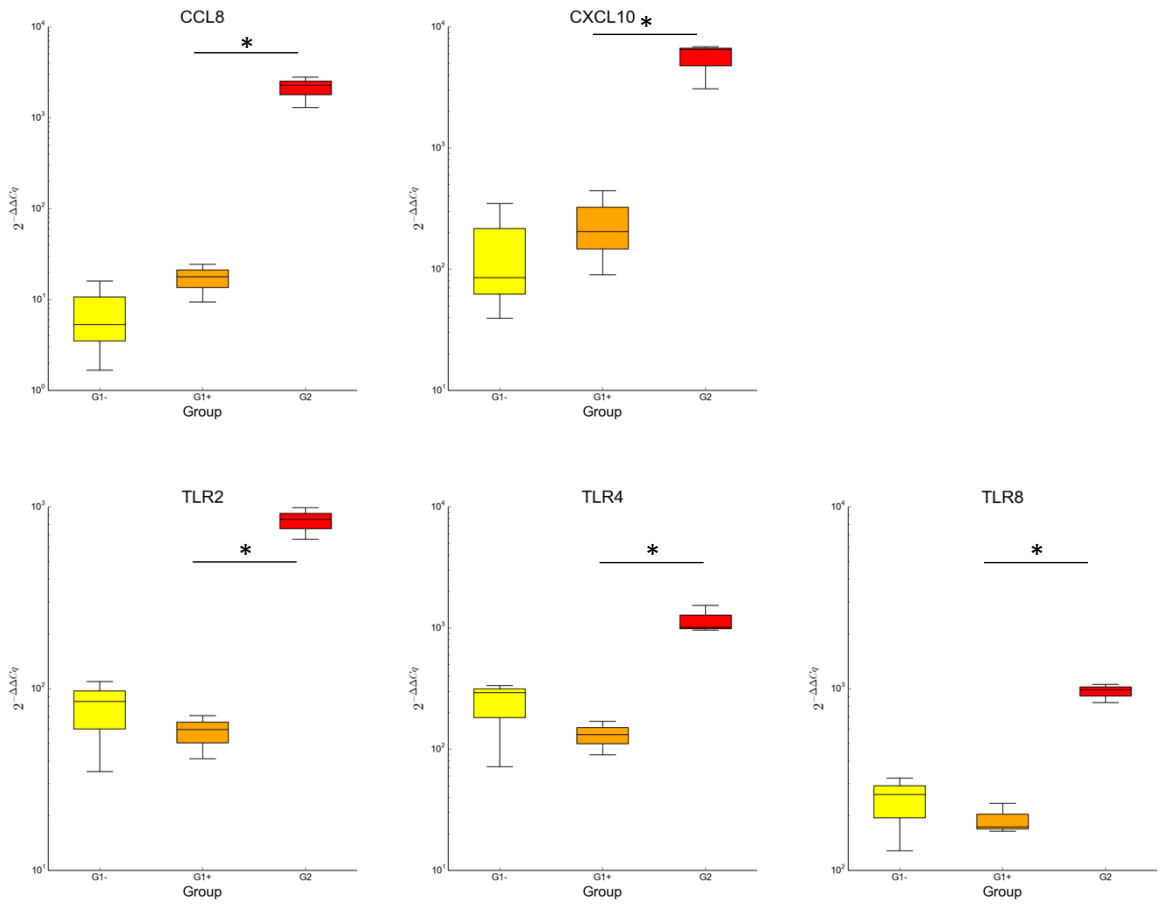

Figure 5.5.23: *Selected box plots from genes used in RT-qPCR, showing the significant TLRs and the chemokines (CCL8 and CXCL10 were the only genes from the panel to be in the top 20 fold change list).*

These box plots all show the same (and significant) trends as in RT-qPCR but with a more prominent increase in cats with FIP that, unlike in RT-qPCR, shows no overlap.

Table 5.5.22: Comparison of significance levels between RT-qPCR results and NGS results for each target. Targets marked with an asterisk did not reach the required threshold level for number of reads in NGS; results have still been presented but must be interpreted with caution. Blue shading indicates significance, this was set at p≤0.05 for PCR and a stricter p≤0.01 for NGS. The arrows indicate the change in the second group of each comparison relative to the first. N/A indicates that the sequences were not available in the database used.

	G1 vs G2			G1- vs G1+			G1+ vs G2		
Target	**RT-qPCR**		**NGS**	**RT-qPCR**		**NGS**	**RT-qPCR**		**NGS**
FCoV	0.000	↑		0.000	↑		0.000	↑	
TLR1	0.610		0.225	0.914		0.754	0.794		0.203
TLR2	0.000	↑	0.000	0.724		0.460	0.002	↑	0.000
TLR3	0.569		0.242	0.724		0.771	0.656		0.124
TLR4	0.019	↑	0.002	0.794		0.161	0.022	↑	0.000
TLR5	0.053		N/A	0.508		N/A	0.396		N/A
TLR6	0.859		0.315	0.286		0.774	0.469		0.184
TLR7	0.059		N/A	0.770		N/A	0.272		N/A
TLR8	0.013	↑	0.000	0.246		0.483	0.015	↑	0.000
TLR9	0.991		N/A	0.031	↑	N/A	0.140		N/A
STAT1	0.000	↑	0.001	0.315		0.046	0.000	↑	0.007
STAT2	0.000	↑	0.000	0.017	↑	0.157	0.000	↑	0.001
STAT3	0.260		0.363	0.569		0.313	0.414		0.009
IFN-α*	0.041	↑	0.063	0.988		1.000	0.077		0.057
IFN-β*	0.004	↑	0.008	0.770		1.000	0.036	↑	0.006
IFN-γ	0.000	↑	0.000	0.131		0.048	0.006	↑	0.001
IL-1β	0.026	↑	0.000	0.432		0.251	0.031	↑	0.000
IL-6	0.001	↑	0.037	0.209		0.467	0.158		0.001
IL-10	0.296		0.529	0.469		0.767	0.914		0.712
IL-15	0.019	↑	0.042	0.794		0.515	0.039	↑	0.000
IL-17*	0.440		0.327	0.569		0.437	0.818		0.098
TNF-α	0.004	↑	0.031	0.432		0.592	0.346		0.018
TGFβ	0.430		0.720	0.508		0.585	0.396		0.267
CCL8	0.000	↑	0.000	0.177		0.211	0.000	↑	0.000
CXCL10	0.000	↑	0.000	0.396		0.413	0.000	↑	0.000
MMP2	0.035	↑	0.003	0.167		0.813	0.548		0.003
MMP9	0.204		0.270	0.866		0.228	0.432		0.845
MMP13*	0.011	↓	0.420	0.432		0.979	0.187		0.367
TIMP1	0.000	↑	0.367	0.866		0.030	0.012	↑	0.000
TIMP3	0.117		0.040	0.569		0.032	0.095		0.525
G-CSF*	0.000	↑	0.003	0.590		0.704	0.002	↑	0.003
M-CSF	0.476		0.626	0.747		0.085	1.000		0.002
GM-CSF*	0.921		0.047	0.125		0.999	0.363		0.035

G2 versus LCM (bulk MLN from cats with FIP versus LCM MLN lesions from cats with FIP).

The final pairwise comparison was between G2 and LCM lesion samples, as had been done by PCR (see Chapter 4). The numbers of differentially expressed genes at each cutoff, and the distribution of these genes is shown in Fig. 5.5.24.

Number of significants by p-value and fold-change

	#significants	FDR	fc >= 1	fc >= 1.5	fc >= 2	fc >= 3	fc >= 4	fc >= 8	fc >= 10
p < 0.1	5097	0.253000	5097	4986	3552	1464	697	130	92
p < 0.05	3947	0.163300	3947	3940	3061	1363	677	130	92
p < 0.01	2202	0.058370	2202	2202	2054	1063	568	118	86
p < 0.001	928	0.013760	928	928	928	682	401	95	69
p < 1e-04	333	0.003807	333	333	333	325	245	73	55
p < 1e-05	113	0.001124	113	113	113	113	111	48	36

Figure 5.5.24: *There are over 2000 genes significant at the standard p<0.01, fc >2 cut off. 12900/19493 features were above the threshold.*

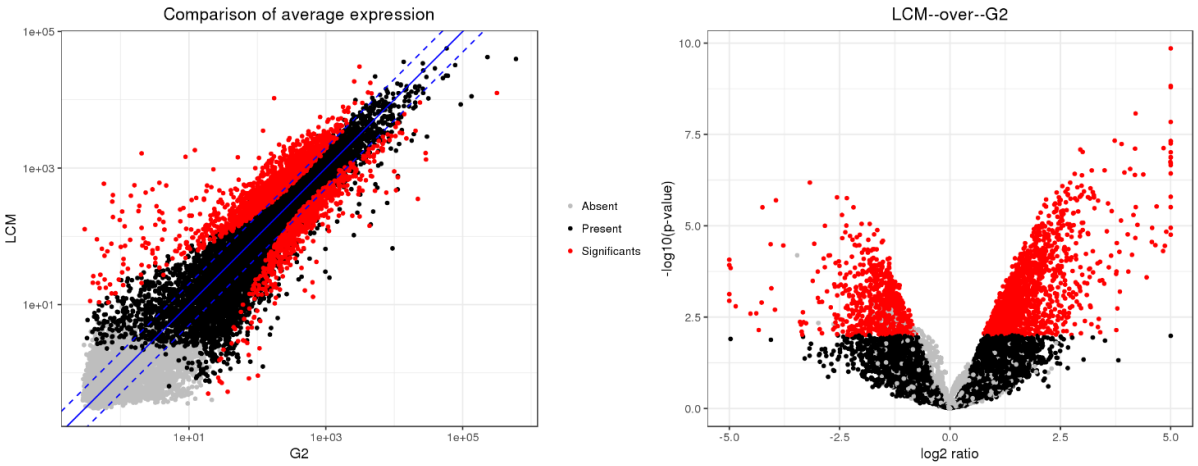

Figure 5.5.25: *Comparison between average group expressions (left), with significant values indicated together with their fold change log ratio (right). A negative log ratio indicates a higher expression in G2.*

The top dysregulated genes between LCM lesions and bulk MLN from FIP cats appeared highly related therefore only the top 10 in each direction are presented (Table 5.5.23 and 5.5.24).

Table 5.5.23: The top 10 genes by fold change which were higher in LCM lesion samples than in G2 bulk MLN samples.

Identifier	Gene	Protein	p	log2 Ratio	fc	Function
^028590			1.49E-09	7.6	197.54	unknown
^025213	HIST1H2AC	histone cluster 1 H2A family member C	3.70E-07	6.9	117.78	chromatin silencing
^003805	HIST1H1E	histone cluster 1 H1 family member E	1.40E-10	6.6	95.74	chromatin silencing
^028991			5.58E-08	6.6	95.01	unknown
^024806	HIST2H2AC	histone cluster 2 H2A family member C	4.86E-08	6.1	67.84	chromatin silencing
^032075	ND6	NADH-ubiquinone oxidoreductase chain 6	1.61E-06	6.0	64.45	redox reactions
^006079	HIST1H1B	histone cluster 1 H1 family member B	1.32E-07	6.0	63.91	chromatin silencing
^028667	HIST2H2AB	histone cluster 2 H2A family member B	1.44E-08	5.8	57.28	chromatin silencing
^031347			1.36E-07	5.8	56.14	unknown
^024303	HIST1H2BB	histone cluster 1 H2B family member B	1.93E-07	5.8	53.85	chromatin silencing

Table 5.5.24: The top 10 genes by fold change which were lower in LCM lesion samples than in G2 bulk MLN samples.

Identifier	Gene	Protein	pValue	log2 Ratio	fc	Function
^029292	IGKV4-1*	immunoglobulin kappa variable 4-1	8.50E-05	-6.4	87.00	Ig production
^027582			0.001134	-6.1	70.52	U.P.: Ig production
^027673			0.0007427	-5.2	37.90	U.P.: Ig production
^029623			0.0001193	-5.1	35.16	U.P.: Ag and Ig R binding
^022825	IGHV6-1	immunoglobulin heavy variable 6-1	0.0001432	-5.0	31.34	Ig production
^024837			0.001598	-4.9	28.94	U.P.: Ig production
^000390			0.002542	-4.5	22.96	U.P.: Ig production
^030776			0.002492	-4.4	20.95	U.P.: Ig production
^025144			0.007137	-4.3	20.15	unknown
^022386			0.001261	-4.3	19.27	unknown

Key: The colour of the fold change (fc) indicates the cluster to which the gene belongs (see below, orange, cyan, blue); ^ indicates the prefix ENSFCAG00000; function derived from UniProt; U.P.: unclassified protein; Ig: immunoglobulin; Ag: antigen; R: receptor

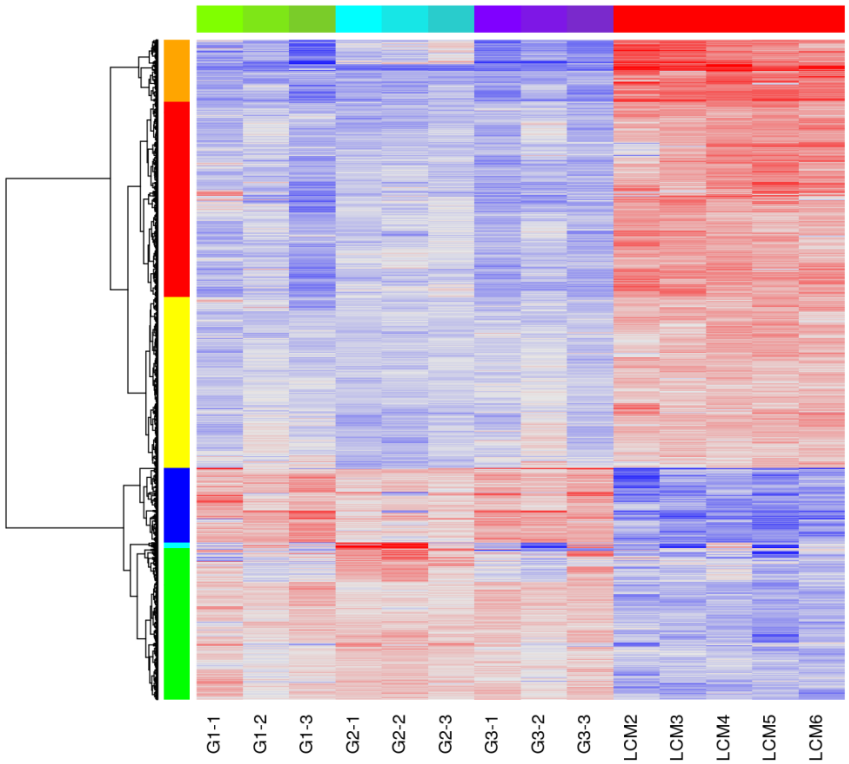

Figure 5.5.26: *Cluster plot comparing G2 and LCM; colours on the y axis represent GO (gene ontology) category feature clusters, with each individual sample marked on the x axis. The chart colour intensity indicates comparative up or down regulation (blue -; red +).*

The cluster analysis shows a generally distinct segregation of LCM samples from all other samples with orange, red and yellow higher in LCM lesion samples, and blue, cyan and green lower in LCM lesion samples. The cluster GO categories are shown below.
Red contains 590 genes, orange contains 189, yellow 519 genes, all higher in LCM samples. The top 10 higher genes all grouped in the orange cluster. Green contains 459, blue 226 and cyan 17 genes, all lower in LCM samples

Table 5.5.25: Significant GO categories within the orange feature cluster. BP, biological process; MF, molecular function; Term, description of GO category; ID, identification of GO category; p, probability; N, number of genes from the category.

Class	Rank	Term	ID	p	N
BP	1	nucleosome assembly	GO:0006334	8.63e-36	29/74
BP	2	DNA-templated transcription, initiation	GO:0006352	2.75e-12	10/29
BP	3	chromatin silencing	GO:0006342	4.17e-8	7/26
BP	4	nucleosome positioning	GO:0016584	0.000085	3/7
BP	5	protein heterotetramerization	GO:0051290	0.0000895	4/18
MF	1	protein heterodimerization activity	GO:0046982	2.18e-23	35/274
MF	2	DNA binding	GO:0003677	2.69e-21	52/790
MF	3	histone binding	GO:0042393	1.26e-11	15/98

Table 5.5.26: Significant GO categories within the red feature cluster. BP, biological process; MF, molecular function; Term, description of GO category; ID, identification of GO category; p, probability; N, number of genes from the category.

Class	Rank	Term	ID	p	N
BP	1	microtubule-based movement	GO:0007018	8.46E-06	12/57
BP	2	epidermal growth factor receptor signalling pathway	GO:0007173	1.03E-05	8/25
MF	1	microtubule motor activity	GO:0003777	6.23E-05	11/58
MF	2	microtubule binding	GO:0008017	7.26E-05	19/151

Table 5.5.27: Significant GO categories within the yellow feature cluster. BP, biological process; MF, molecular function; Term, description of GO category; ID, identification of GO category; p, probability; N, number of genes from the category.

Class	Rank	Term	ID	p	N
BP	1	chromatin remodeling	GO:0006338	3E-05	10/54
MF	1	immunoglobulin receptor binding	GO:0034987	2.45e-9	4/36
MF	2	antigen binding	GO:0003823	4.21e-9	4/41

Table 5.5.28: Significant GO categories within the blue feature cluster. BP, biological process; MF, molecular function; Term, description of GO category; ID, identification of GO category; p, probability; N, number of genes from the category.

Class	Rank	Term	ID	p	N
BP	1	translation	GO:0006412	1.04e-11	22/203
BP	2	chemokine-mediated signalling pathway	GO:0070098	9.4E-05	6/42
MF	1	structural constituent of ribosome	GO:0003735	3.26E-13	21/152

Table 5.5.29: Significant GO categories within the cyan feature cluster. BP, biological process; MF, molecular function; Term, description of GO category; ID, identification of GO category; p, probability; N, number of genes from the category.

Class	Rank	Term	ID	p	N
BP	1	immunoglobulin production	GO:0002377	2.25e-23	11/43
BP	2	immune response	GO:0006955	1.39e-15	11/200
BP	3	.innate immune response	GO:0045087	0.0000764	4/143
BP	4	phagocytosis, recognition	GO:0006910	3.76e-7	4/38
BP	5	positive regulation of B cell activation	GO:0050871	3.76e-7	4/38
BP	6	phagocytosis, engulfment	GO:0006911	5.14e-7	4/41
BP	7	defense response to bacterium	GO:0042742	0.00000427	4/69
MF	1	immunoglobulin receptor binding	GO:0034987	2.45e-9	4/36
MF	2	antigen binding	GO:0003823	4.21e-9	4/41

Table 5.5.30: Significant GO categories within the green feature cluster. BP, biological process; Term, description of GO category; ID, identification of GO category; p, probability; N, number of genes from the category.

Class	Rank	Term	ID	p	N
BP	1	protein N-linked glycosylation	GO:0006487	7.56e-8	9/23
BP	2	carbohydrate metabolic process	GO:0005975	2.87E-05	14/102

Comparison with results of selected publications on the transcriptome in feline coronavirus infection

One of the publications which had contributed to our original list of PCR mediators (CCL8 and CXCL10) was that of Harun et al. who evaluated the transcriptome of FCoV infected CRFK cells compared to controls [242]. The current G1(-) vs G2 dataset was compared against their list of top up and down regulated genes to assess the similarities.

Of their top 20 upregulated genes, 16 could be identified. Of these, 12 were significantly upregulated also in the current dataset ($p \leq 0.01$). In addition to CCL8 and CXCL10, these were RSAD2, SLAMF7, AFT3, IFI35, TRIM25, MX1, CD274, PHF11, HERC5, DTX3L. The first three were also in the top 20 upregulated of our data.

13 of their top 17 downregulated genes could be identified, of which only two were significant in our dataset but were in fact upregulated.

An *in vitro* transcriptome study looking at peritoneal macrophages after experimental infection of cats with a virulent cat-passaged strain of FCoV was published after our data was acquired [168]. Therefore, their main findings were also compared briefly to determine how cell specific the changes are. They found upregulation of 18 pathways in FIP, including apoptosis, TLR signalling and JAK-STAT signalling. These were also upregulated in our FIP group (in the MLN intergroup comparison rather than the MLN - LCM comparison). Others were against specific but unlikely of relevance infectious diseases e.g. trypanosomiasis; these were not compared with our results.

Only three pathways were downregulated, all involved in cellular metabolism, also consistent with our findings [168].

Evaluation of the feline coronavirus transcriptome within infected samples

A secondary aim had been to compare viral sequences between G3 (G1+) and G2. Levels of the viral reads in G1+, already known to be low from PCR, were drowned out by the host reads in the software calculations and did not reach a read threshold required to be allocated to a gene. However, manual extraction of matching sequences to the genes from the dataset allowed intergroup comparisons.

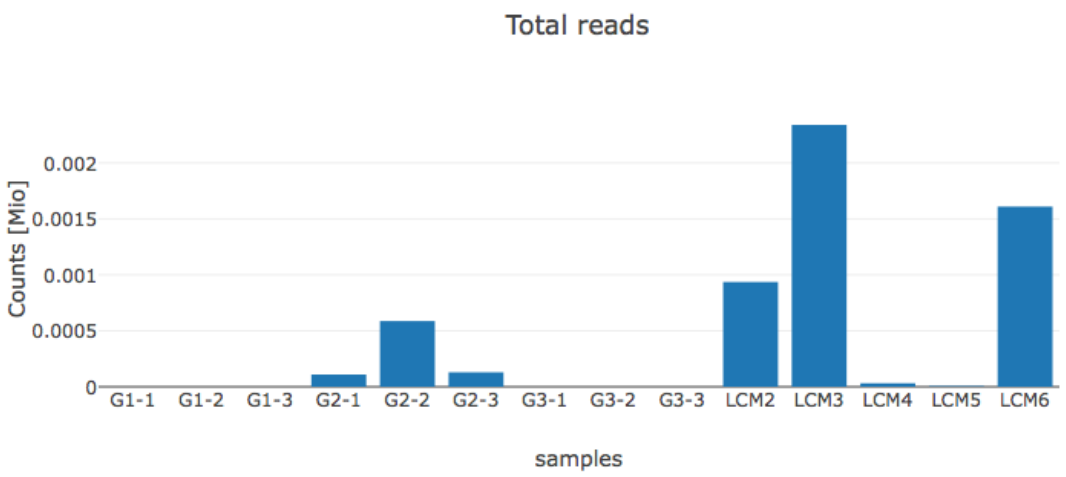

Figure 5.5.26: *Total reads allocated to a reference FIPV gene sequence (DQ848678) for each sample, using an automated approach. It can be seen that two out of the three G2 samples had barely detectable levels, and none of the G3 (G1+) samples. Virus was also not detected from one LCM sample.*

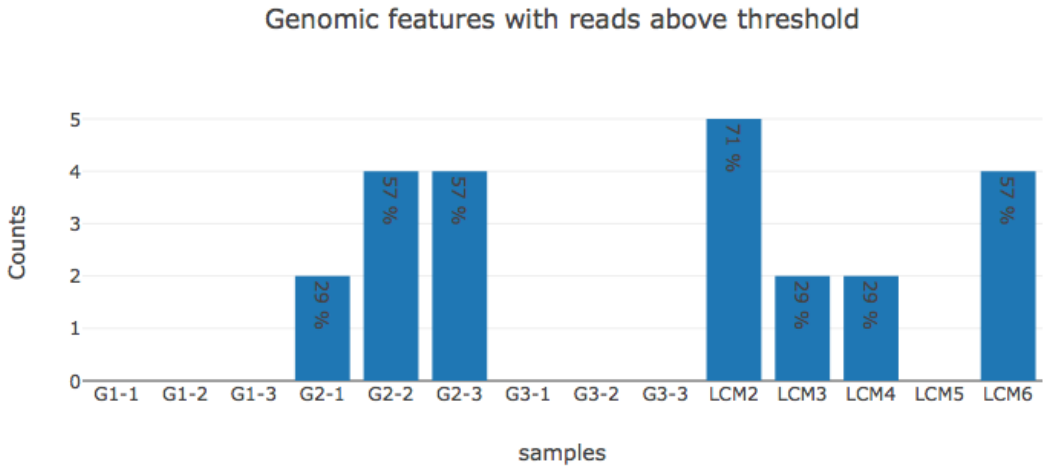

Figure 5.5.27: *Proportion of genomic feature reads above threshold for each sample.*

The primary aim had been a comparison between FCoV infected cats with and without disease; this was therefore not possible using the pre-programmed applications. Instead, by searching the raw data for specific sequences it was possible to obtain a count of reads mapping to the individual viral mRNA sequences of polyprotein 1ab and the structural proteins. These are shown in the graphs below (Fig. 5.5.28). The same statistical comparisons cannot be applied to individually extracted data as to the bulk data therefore an ANOVA test was applied, this tests the premise that not all results are the same. Of the seven individual viral mRNA coding regions, a significant difference was only found between G2 and G3 (G1+) for the envelope and membrane coding genes.

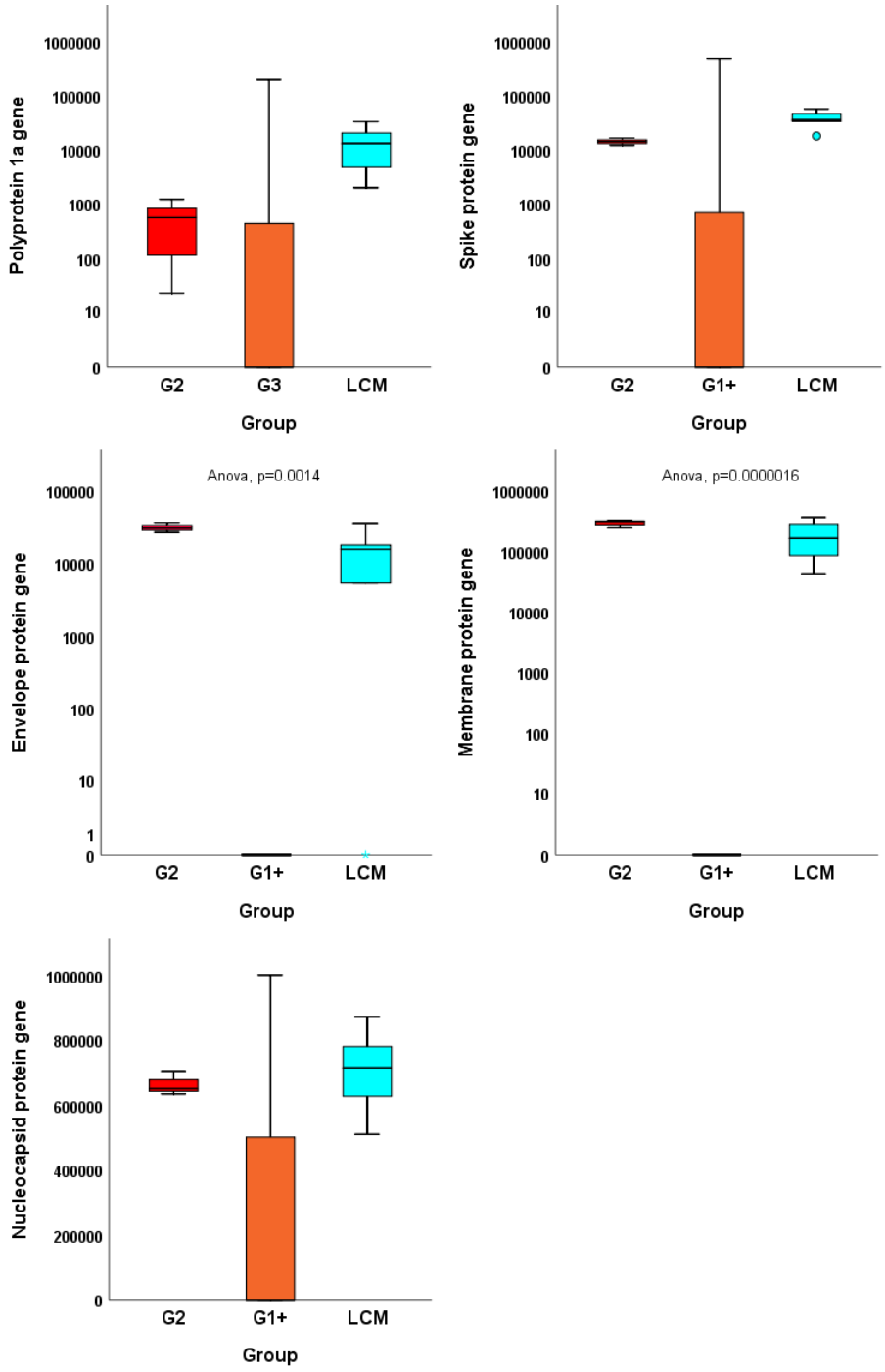

Figure 5.5.28: *Direct expression values of FCoV gene segments across the viral positive groups.*

The expression values from each gene were compared by ANOVA across all groups. Significant differences, once corrected for by the number of genes compared, were only found for the membrane and envelope genes, for which cats with FIP had significantly higher levels than infected cats without FIP. These are direct counts, and are not normalised to viral level, therefore higher counts from the FIP groups would be automatically expected for all genes. The fact that only two genes are affected may be significant and is discussed.

Discussion

Despite decades of research, the precise pathogenesis of FIP remains unclear. Much of what is understood has been assumed from piecing together information gleaned from various studies. It is so far known that an enteric coronavirus gains access to the systemic circulation, via monocyte infection, and that this stage may occur in the majority of infected cats with no ill effect [316]. The susceptibility of an individual host to FIP is then somehow combined with as yet incompletely characterised gain of virulence mutations within the virus, leading to monocyte/macrophage activation, with development of typical lesions and non-specific inflammatory clinical signs. Both the pathological and clinical features of FIP, including vasculitis, increased vascular permeability, recruitment of leukocytes to expanding lesion sites, fever etc., indicate an inflammatory cytokine-mediated disease [32,42,317]. However, the source of these cytokines remains to be fully elucidated. Levels in the blood of cats with FIP have not been shown to be markedly elevated, nor have those so far studied in haemolymphatic tissues [47,48,134].

Studies so far have generally been directed at the cytokines themselves, the effector molecules of inflammatory pathways. The present study chose here to focus predominantly on molecules upstream of these effectors, in particular the Toll-like receptors (TLRs) and the STATs which have not been studied before in FIP. Anti-viral cytokines, pro- and anti-inflammatory cytokines as well as molecules with a role in cell recruitment and tissue remodelling were also of vital importance to determine. TLRs are the most important of the pattern recognition receptors (PRRs) of the innate immune system [179]. PRRs recognise conserved motifs not associated with self and induce, in an ideal model, a targeted and balanced immune response [318]. They are also crucial to the link between the innate and adaptive immune system, being able to present antigen to specific lymphocytes [164]. STATs are a family of transcription factors which are able to influence a vast array of downstream cellular processes critical for the inflammatory response, including directing leukocyte differentiation [319].

In evaluating these mediators, the two areas the present study most wished to explore were the immune profile within the lesions themselves, and the relationship between FCoV infection status and FIP disease status within the MLN in terms of immune mediator expression. The MLN is of particular interest as the first site of spread beyond the intestine. To this end tissues and lesions from cats with FIP were compared with tissues from control cats (with and without detectable FCoV in the MLN).

The lesions of FIP, particularly the pathognomonic pyogranulomatous vasculitis, contain a concentrated population of virus-infected macrophages, all with the potential to secrete and respond to pro-inflammatory cytokines and exert positive feedback on one another with an ensuing cascade effect. The nature of the lesions also gives a direct communication with the circulation, hypothetically contributing to clinical signs such as biphasic fever [320]. It was predicted that the inflammatory mediator production in these local microcosms would far outweigh the systemic response.

Secondarily, certain aspects of the virus were looked at in order to try to disentangle the virus' contribution to disease from that of the host.

Various complementary methods have been used, beginning with RNA expression analysis by RT-qPCR in BM, spleen, and MLN, before laser capture microdissection (LCM) of lesions. Finally, a

transcriptome wide approach was applied to both MLN and lesion samples to attempt to place the PCR results more accurately in the context of cellular pathways as a whole. Comparative BM and spleen analyses were performed between uninfected control cases (cats without FIP) and cats with FIP, as none of the control cats tested positive by RT-qPCR for FCoV. From the larger cohort of cases for which MLN were available, it was possible to split the control group into virus positive and virus negative cases.

With regards to the host response, firstly the effect of virus in the absence of disease is discussed, before comparison with haematopoietic tissues in the disease state, and finally with tissues from specific lesions. The viral aspects are discussed separately.

FCoV infection, even in the absence of disease, is associated with immunomodulatory changes

In the first instance, mediator expression was compared between control cases with FCoV positive and negative MLN, first by RT-qPCR and then by NGS.

The current state of knowledge on FCoV does not as yet allow distinction between the mystical non-pathogenic and pathogenic viruses. As our cases were all natural infections we therefore cannot say whether infected cats without FIP were resistant to developing disease or were infected with a non-pathogenic virus that nonetheless spread from the intestine. Results are also a snapshot in time and it cannot be excluded that control cats with and without virus may have interchanged between these groups in the past or would do so in the future.

Only TLR9 and STAT2 showed a significant increase in expression by RT-qPCR in the infected MLN. IL-6, STAT1, and IFN-γ showed tendencies (not reaching significance) to be higher in the infected MLN, with levels below that of cats with FIP. These subtle changes indicate a mild upregulation from basal levels of pro-inflammatory, antiviral, and signalling molecules associated with the virus, suggesting a modulated and controlled response and explaining the lack of observed lesions.

The precise ligand of TLR9 in the FCoV infected MLN is unclear, however the increase in virus-positive MLN of control cats compared to uninfected MLN suggests a potentially protective effect of TLR9, which may even have helped prevent the development of disease in these animals. Stimulation by co-infectious agents could therefore be hypothesised to be protective against FIP. There is debate in the literature as to the precise ligand requirements of TLR9 for signalling and varying synthetic ligands have induced different effects, triggering either type I IFN or pro-inflammatory cytokines [167,198]. The initial belief was that the receptor is stimulated by CpGs, specifically the unmethylated CpGs which largely distinguish host from microbial DNA [181]. The unmethylated CpGs of bacteria are also found in mammalian mitochondria, released following cell damage such as may be induced by viral infection and resulting in upregulated TLR9 signalling (Bao et al., 2016). TLR9 was found to mediate a protective effect on enterovirus infected mice by responding to endogenous danger-associated molecular patterns (DAMPs); the enterovirus itself had no effect on TLR9 levels [321]. Morphologically there was no evidence of cell damage within the FCoV-infected MLN, and also no upregulation of TLR9 in association with the lesions in FIP, leaving the trigger for TLR9 in our cases unknown.

When comparing between control groups by NGS, the number of differentially expressed genes was only a fraction (~10%) of those differentially expressed when comparing between control groups and FIP. TLR9 and STAT2, significantly higher in infected MLN by PCR were not significantly higher in the NGS comparison (most likely due to the samples being only subgroups, added to an initial small effect). IFN-γ and STAT1 had shown less than significant elevation in infected MLN by PCR. These reached significance by NGS only at the $p<0.05$ level; as a standard, the more stringent $p<0.01$ was used for NGS.

The majority of differentially expressed genes were higher in the FCoV-infected MLN, and most of these related to cell cycle regulation with no direct link to inflammatory responses. This is likely to reflect macrophage proliferation and provides an mRNA correlate to the morphological findings of previous studies in which healthy FCoV-infected cats exhibited histiocytosis and macrophage activation in the MLN [46].

A very small number of genes showed a significantly lower expression in infected MLN, together with a high fold change. Five of these genes stand out in particular; S100A8, S100A9, S100A12, CSF3R, and IGKV4-1. These genes had many overlapping features and functions all linked to the immune response. Cluster analysis of NGS data groups up or down regulated genes by function, determining differential expression of these functional groups (gene ontology [GO] categories) as opposed to just of individual genes. The GO categories with significantly lower gene expression in infected MLN of control cats were dominated by immune regulatory functions. These included neutrophil chemotaxis (the top category), RAGE receptor binding, phagocytosis, immunoglobulin production, response to IFN-γ, and positive regulation of the JAK-STAT cascade. The genes most frequently involved in those functions were the three S100 calcium-binding proteins (A8, A9, A12). S100 proteins are involved in diverse functions including regulation of apoptosis, DNA repair, migration, differentiation and inflammation [322]. Apoptosis induction is part of the host's armoury of defence against viruses, along with inhibition of cell protein synthesis (to block the mechanisms hijacked by the viruses) and induction of type I IFN [256]. The S100 family, otherwise known as calgranulins, includes more than 20 proteins. Three of these, A8, A9, and A12 (i.e., the same three found to be decreased in FCoV-infected MLN of control cats) have been specifically linked to innate immune functions owing to their expression by phagocytes at sites of inflammation [323,324]. A8 and A9 can be detected in granulocytes, monocytes and early macrophages, whilst S100A12 is more specific to granulocytes [324].

These S100 proteins have many roles in innate immunity and are amongst the DAMPs to be released from damaged cells and trigger an inflammatory response. DAMPs are host proteins which typically have a normal intracellular role separate to their extracellular role in danger signalling [325]. S100A9 stimulates neutrophil migration both *in vitro* and *in vivo* [322], helping explain the lower S100A9 levels in infected MLN of control cats.

RAGE (receptor for advanced glycation end products) binding was one of the processes found to be downregulated in infected MLN of control cats. RAGE is another PRR and recognises DAMPs. There is crossover between the endogenous ligands of RAGE and those of TLR4, which include the S100 proteins [326–328]. RAGE is able to bind S100A12 alone or the heterodimers S100A8/A9 [324,326].

The influence of the three S100 genes led to statistical downregulation of the terms associated with the RAGE-binding process, but the RAGE gene itself (aka AGER) did not differ between control

groups. The MLN of cats with FIP, in contrast to FCoV-infected MLN of cats without FIP, had levels of S100A8, 9, and 12 levels much closer to those of the uninfected control group MLN (slightly above though not significantly so). Calprotectin is a tetramer of S100A8 and A9 and can induce pro-inflammatory cytokine production in monocytes and macrophages as well as being involved with neutrophil and monocyte migration, as shown by the downregulated GO categories [322]. The antibody against calprotectin is used as an immunohistological myelomonocytic marker, identifying recently-blood derived macrophages (in addition to neutrophils which are easily morphologically distinguished) [329]. This will be returned to with discussion of the FIP cases.

CSF3R was another of the five closely linked genes significantly lower in infected than uninfected control cat MLN. It is the receptor for G-CSF, a key regulator of neutrophil chemotaxis as well as neutrophil differentiation and survival [330]. G-CSF mRNA has previously been shown to be induced in FIP and to reduce neutrophil apoptosis along with TNF-α and GM-CSF [331]. G-CSF and TNF-α but not GM-CSF were also upregulated in FIP MLN in our study, this may help provide a renewable supply of neutrophils towards the formation of FIP lesions. Consequently, a reduction in G-CSF signalling associated with reduced CSF3R in infected control cat MLN may reduce the opportunity for lesion development by limiting the number of cells (i.e. monocytes) required for both FCoV replication and initiation of lesions. The current results parallel previous results of our group, when it was observed that the lowest transcription levels of G-CSF (i.e. the ligand rather than the receptor) in the MLN were seen in infected cats without FIP [48].

The fifth gene to stand out as lower in infected control MLN was IGKV4-1, this gene is responsible for part of the antigen recognition binding site of the antibody. Somatic hypermutations in the variable (V) region of the Ig gene confer B cells with the ability to recognise a plethora of different antigens from a single original genome sequence [332]. Its reduction links with the lower levels of pathways involved in adaptive immunity in the infected controls (e.g. B cell receptor signalling, immunoglobulin production).

It cannot be said for sure whether FCoV-infected cats show pathway downregulation or have inherently lower expression levels of certain genes than uninfected cats. This would ideally be evaluated by a prospective study to determine whether constitutively transcribed levels in an individual can predict susceptibility to subsequent development of FIP. What we can see is that infected MLN of control cats showed a lower level of expression of a number of inflammatory genes. The enriched pathways expressed at lower levels included immunoglobulin production, phagocytosis and complement activation, all common immune response processes which in FIP seemingly contribute to the pathogenesis rather than being beneficial [22,25,333]. The phenomenon of antibody dependant enhancement is frequently observed in experimental cases, and complement deposition is found in vasculitis [25,333–335]. The latter is only a small part of the story of vasculitis pathogenesis as the lesions, and their predisposition to veins, do not fit the profile of a type III (immune complex mediated) hypersensitivity reaction [42]. The mediator profile in the infected cats supports original theories that mounting a humoral response has a detrimental effect in the case of FIP [22,320], and that by downregulating these mechanisms infected cats may avert disease.

In cats with FIP, these same five genes were transcribed in the MLN at levels similar to the uninfected controls. This leads to the hypothesis that they are in some way a protective response by the host which may contribute to dampening down the inflammatory response by negative

regulation of these proteins. Whether this is an active downregulation or whether low basal expression is linked to resistance to development of FIP is not clear at this stage. Another possibility is that the non-pathogenic FCoV variants repress these genes to help them avoid triggering the host immune response. Coronaviruses are known to use various methods of host gene suppression including altering ubiquitination as discussed later. Controlled experimental infections with viruses of known pathogenicity would be required to make this distinction.

FIP is associated with extensive changes in the immune profile of the MLN, far beyond those induced by the presence of FCoV

The results discussed above show that the presence of virus has a small but potentially crucial effect on the immune system in the absence of disease. When applying the same selected RT-qPCR immune mediator panel to the MLN of cats with FIP and comparing to control groups, significant differences were evident for almost all of the mediators. These results prompted a deeper look into changes in the transcriptome by means of NGS. This revealed over 1000 differentially expressed genes between FIP and control groups (with each control group compared independently), vastly more than between the two control groups themselves. These genes contributed to a multitude of enriched differentially regulated pathways. FIP cats very clearly clustered away from both of the control groups and were unsurprisingly seen to be more similar to the LCM lesion group by cluster analysis.

Looking first by RT-qPCR at a combined control group, mediators with altered expression levels almost exclusively showed an upregulation in FIP. Significantly higher mRNA levels were found for TLR 2, 4, and 8, the pyrogenic cytokines (IL-1β, IL-6, TNF-α), the chemokines CCL8 and CXCL10, the transcription factors STAT1 and 2, and the interferons IFN-α, -β, -γ. The changes amongst the matrix remodelling enzyme (MMPs and TIMPs) responses were mixed, with MMP13 the only downregulated mediator observed.

The TLRs that can be expected to respond to viruses are TLR3 (dsRNA), 7 (ssRNA), and 8 (ssRNA), of which only TLR8 was significantly elevated in FIP. This result was confirmed by NGS. TLR8 is often overlooked, or grouped with TLR7 in functional studies [336]. This may be as humans but not mice or rats detect ssRNA through TLR8 and therefore many experimental (and hence rodent based) studies have ignored it. It is thought that in mice the protein, though present, may be non-functional, and therefore lack downstream signalling ability [181,337]. The results of the present study show that in cats the response also clearly differs between TLR 7 and 8, at least at the transcriptional level.

TLR8 was the only TLR for which a reliable immunohistological and immunofluorescent protocol could be established. It is reportedly broadly expressed by both conventional DCs and macrophages in mice [181] and in the present study positive cells in the MLN were most commonly of macrophage/dendritic cell morphology. Consecutive sections of MLN stained for the macrophage marker Iba-1 also supported this observation, though the frequency of Iba-1 positive cells far exceeded that of TLR8 in both control and FIP MLN.

Immunofluorescence double staining with FCoV antibody was then used, with the expectation of localising TLR8 expression to infected cells. Contrary to those expectations, only exceedingly rare examples of co-expressing cells could be found despite plentiful cells positive for each marker.

This leads to two main questions; what then is the trigger for TLR8 expression (supposedly ssRNA; the most likely culprit to respond to FCoV [184]), and why do infected cells not appear to upregulate TLR8 protein expression? Identifying the precise cell subtype expressing each marker would be an informative next step. In theory, flow cytometry would allow simultaneous evaluation of infection status, TLR expression, and cell marker co-expression triple immunofluorescence combined with confocal microscopy would be another possible, though more limited, modality. In practice, feline macrophage/DC characterisation studies unfortunately lag behind those of many other species meaning that antibody cross-reactivity is as ever an issue [188,338]. TLRs, in contrast to other PRRs, detect presented, processed antigen without the requirement that the cell itself is infected. This would explain the presence of TLR8 in uninfected cells but not the inverse lack of TLR8 in infected cells. The advancements of single cell analysis make *in vitro* assessment on an individual cell level a viable option for future investigation, comparing responses in infected and adjacent uninfected cells. It would also allow determination of whether the downstream TLR8 signalling pathway is activated.

In attempting to define the involved cell types there is much confusion in the literature as to the classification and ontogeny of the various members of the mononuclear phagocyte system (MPS). The MPS includes monocytes, macrophages, and dendritic cells, each with their own multiple subsets; a recent publication attempts to classify these to provide a replicable nomenclature across species [339]. As a result of this confusion, the three cell types have often been used interchangeably, further complicated by the many supposedly unique markers that have been shown to overlap [339]. To my knowledge, the susceptibility of different macrophage/DC subsets to FCoV infection has not been assessed in detail (once again due in no small part to antibody availability), although at least some members of the DC family are reported to be susceptible *in vitro* [340,341]. In learning more about the subtype restrictions of the virus, we may also glean further clues to the cell surface receptors it utilises; currently still unknown for serotype I.

TLR 3 and 7 were predicted to be elevated in FIP, in response to dsRNA replicative intermediates and the ssRNA viral genome respectively [93,169]. There was instead a less than significant downregulation, leading to the suspicion that viral inhibition may be occurring (discussed in more detail below).

As with all virus detecting TLRs, TLR3 induces downstream production of the antiviral type I interferons [164]. It does this via the adaptor proteins TRAM/TRIF and the interferon regulatory transcription factor (IRF) 3, being the only TLR not to signal via the predominantly inflammatory Myd88 branch [169]. TLR4, unlike the remaining TLRs, is also able to utilise this alternative branch but to do this it must first be trafficked to endosomes from its usual cell surface location [181]. This partly explains the overlap of TLR4 with TLR3 in its ability to induce an anti-viral response in addition to its more stereotypical pro-inflammatory cytokine response. TLR3 can, however induce a greater anti-viral response than TLR4 *in vitro* [342]. The upregulation of TLR4 and not 3 in FIP MLN may partly explain the ineffective response to FCoV that is likely a relevant component of FIP pathogenesis.

TLR3$^{-/-}$ mice have been used to demonstrate the importance of this TLR signalling pathway in various viral infections. In experimental infections of mice with West Nile and influenza virus (+ssRNA and -ssRNA viruses respectively), the presence of the TLR increased the severity of disease [203,343]. On the other hand, TLR3 signalling is reported to have a protective role *in vivo* against

infection with the murine hepatitis virus (MHV), also a coronavirus [175], and *in vitro* against influenza virus infection of human epithelial cells [344].

A separate study found mice with intact TLR3 have milder disease in response to SARS-CoV but that it is the adaptor protein TRIF rather than TLR3 itself which is most integral to this response; $TLR3^{-/-}$ mice are still partially protected if TLR4 is intact (and hence able to signal via TRIF) [176]. The authors suggest that balanced activation of TRIF/Myd88 pathways is important [176]. In our FIP cases, Myd88 was significantly upregulated in FIP cat MLN whilst IRF3 (part of the TRIF pathway) was significantly downregulated, pushing the balance towards pro-inflammatory Myd88 signalling.

Although the virus specific TLRs described above appeared not to be making a large contribution in our study, TLR 2 and 4 (classically recognising bacterial ligands) were found by both methods to be significantly upregulated in FIP.

TLR2 has the widest range of ligands of the TLRs, partly owing to its ability to form heterodimers [201]. It does this with other family members, namely TLR 1, 6, or 10 [345]. Another feature of heterodimer ligand recognition is the ability of different pairings to inhibit or enhance signalling [346]. It would require more intricate downstream analysis to determine if there is signal inhibition or enhancement in FIP.

In addition to its traditional bacterial ligands, TLR2 can recognise both viral proteins and endogenous ligands from damaged cells to promote inflammation and repair [170]. This is a potential link to one of the function clusters shown by NGS to be upregulated in FIP; the 'reparative response to cell damage'. The TLR trigger in the present study is unknown, and a combination of ligands may be involved. In contrast to exogenous ligands, endogenous stimulators of TLR2 and 4 are not known to induce adaptive immunity [164]. As adaptive immune system pathways are upregulated in the present study, this suggests that exogenous ligands are involved, either with or without additional endogenous ligands.

Experimentally, it is difficult to precisely determine contribution of different TLRs even in genetically engineered mice owing to the level of overlap between the pathways. Examples of virus detection by TLR2 include the RNA viruses respiratory syncytial and measles virus as well as SARS-CoV, with TLR2 thought to be responsible for mediating the response to the SARS-CoV S protein [174,347,348]. Most of these examples demonstrate a beneficial effect of TLR2 signalling but in some cases a TLR2 deficiency reduces the pathogenic effects of the virus. For example, $TLR2^{-/-}$ mice were relatively spared from herpes simplex virus-induced encephalitis [349]. The authors' theory was that TLR2 induces too great a pro-inflammatory response and insufficient IFN.

TLR4 deficient mice are more susceptible to MHV-1 induced respiratory disease than are mice with an intact TLR4, as they exhibit increased inflammation and morbidity [350,351]. Conflicting examples include mouse mammary tumour virus activates TLR4, leading to production of the anti-inflammatory cytokine IL-10 and allowing the virus to become persistent, whilst respiratory syncytial virus also activates TLR4 but instead induces IL-6 which is protective in this case [352].

TLR agonists have been explored as vaccine adjuvants, e.g. TLR4 agonists as adjuvants in antiviral vaccines to induce Th1 responses [180]. The future with regards FIP vaccination is unclear as so far triggering adaptive immunity has proven unsuccessful (with enhancement of disease rather than immunity) [22,24,25]. The problem in this disease is not in how to help the immune system to recognise the virus but rather how to temper its response. As the virus itself apparently does little to the

host cells directly [42], perhaps investigating how to induce immune tolerance would be a more profitable direction.

A number of the related genes (GO categories) found to be upregulated in FIP refer to the LPS response. As this response is mediated heavily by TLR4 [172] it cannot yet be said if the upregulation is merely an overlap labelling of the TLR upregulation or represents a separate trigger. This would link to the possibility discussed in the manuscript that co-infections from a deficient intestinal barrier in FIP may contribute to the TLR response.

TLRs 2, 4, and 9 can also all be triggered by another endogenous ligand/alarmin, high mobility group box (HMGB)1 which is released from the nucleus in response to cell damage [353]. Although TLR 2 and 4 were elevated in the FIP MLN, TLR9 was not. This is despite the presence of MLN lesions in most animals, which therefore does not support this mechanism of action in FIP.

Correlation was assessed within the FIP group between FCoV viral loads and mediator mRNA levels in the MLN, as well as between individual mediators. It showed that the majority of mediators significantly upregulated in FIP were also correlated with FCoV levels. The exceptions were TNF-α, STAT1, and G-CSF. This suggests that either these non-correlating mediators have a more binary on/off response than a proportional response, or that their induction depends more on other mediators than on the virus itself. *In vitro*, TNF-α mRNA expression has been shown to be induced in macrophages in response to pathogenic FCoV [240]. That study compared TNF-α in infected and uninfected cells but did not attempt to differentiate responses to different viral levels [240]. It is possible that once a certain virus threshold is crossed, TNF-α production is triggered. It is therefore still difficult to definitively separate viral from disease effects as the FCoV positive MLN of cats without FIP also had much lower virus levels and would consequently be expected to express lower levels of mediators.

Within the panel of mediators, certain molecules might also be expected to correlate with each other and not just with virus levels. The STATs for example are triggered by their corresponding interferons [286] but showed almost no correlation to them. This is a reminder of the extra levels of regulation involved, or it is possible that levels at a single time point do not correspond owing to negative feedback loops preventing both rising inexorably together [287]. The lack of correlation in the MLN may also indicate that these signalling pathways have systemic rather than only local triggers such that the local mRNA levels do not need to be directly linked. TLR 2 and 4 ligand binding should lead to inflammatory cytokine production [169]; in the present study both these TLRs correlated with the inflammatory cytokines IL-1β and IL-6. As with the FCoV comparison, TNF-α levels were once again independent. One interesting observed correlation was between IL-6, IL-17, and STAT3. All three correlated to each other though only the former was upregulated in the MLN in FIP in the present study. In the case of STAT3 this was unexpected, as it is known to be activated by the pro-inflammatory cytokine IL-6 [286] which was itself elevated. The triad have been referred to as a "holy trinity of auto-immunity" [236]; part of the reason for our interest in these mediators. Whilst not of course an auto-immune disease per se, it is most likely the over-reaction of the host immune response which leads to development and maintenance of the lesions in FIP [42,354]. In the absence of upregulation of all three, however, their role is unlikely to be a prominent one.

Following the finding of lower S100A8, A9, and A12 transcription (see above) in infected control cat MLN than in uninfected controls, levels were assessed in a pairwise comparison between uninfected control MLN and cats with FIP. Levels were slightly higher in FIP but not to any significant degree. There was also no significant difference between the lesion samples and the bulk MLN of cats with FIP. Calprotectin protein (a tetramer of S100A8/A9) has been shown to be expressed at high levels within acute FIP lesions, with lower levels in more advanced lesions [62]. Immunohistologically it is a marker of blood-derived macrophages, so this reflects the presence of these cells in the early lesions which then degenerate or differentiate in older lesions. Its expression has also been shown to increase in the BM and spleen of cats with FIP but not in the MLN, reflecting an influx of monocytes in the former organs, with proliferation of local macrophages in the MLN [48]. The MLN findings in that study fit our S100 gene findings, that A8, A9, and A12 are not upregulated in the MLN in FIP compared to uninfected MLN (S100 levels were not available for BM or spleen). However, the previous study found no difference in calprotectin protein expression between infected and uninfected control cats. In the present study there was also no difference observed in the lesions compared with the bulk MLN in FIP. This may reflect the varying chronicities of our cases or may mean that formation of this tetramer protein is not the final destination of most of the expressed mRNA.

Another of the effects of these three S100 proteins is induction of increased vascular permeability, frequently a key feature of FIP. Not all of the FIP cases used for MLN NGS had effusions, which may also relate to the lack of significant difference to uninfected controls. Therefore, comparison of specific S100 levels between cases with and without effusions/vasculitis warrants further investigation. A larger cohort of cases would help to determine whether the small increase in the MLN observed in cats with FIP over uninfected controls could reach significance.

S100A12 has been used as a biomarker of inflammatory diseases, e.g. Familial Mediterranean Fever [355]. Based on the current results it seems unlikely that it would be a suitable marker in FIP. To date, inflammatory markers tested in FIP identify predominantly non-specific inflammation without being diagnostic [356,357].

Amongst the markers of inflammation tested in FIP are the serum amyloid A (SAA) proteins [284,356]. These are acute phase proteins, two of which were amongst the top ten genes upregulated in FIP MLN compared to uninfected control MLN in this study. SAA proteins are pattern recognition molecules classically produced by the liver and are used diagnostically in many species as an indicator of systemic inflammation [358,359]. SAA can bind bacterial surfaces and hence act as an opsonin, or bind the complement protein C1q where it can activate the classical complement pathway [201]. SAA was shown to be upregulated in the serum of cats with FIP [284,356] but this is not a specific finding. The specificity of another acute phase serum protein α1-acid glycoprotein (AGP) is reported to be higher [356,357,360]. However, this could not be identified in the present data.

The genes which were most upregulated in the MLN of cats with FIP were all involved in the immune response including in interferon response pathways (such as IRF7 and ISG15), the prototypical antiviral defence [254]. Additionally there were genes involved in the humoral immune response, known to be detrimental in FIP, and in apoptosis, also a feature of FIP [23,25,46,63,240]. Surprisingly, one of the top ten upregulated genes had a predicted role in upregulation of TLR 7 and 9; however, neither TLR was upregulated in FIP MLN by either PCR or NGS. When applying cluster analysis to the FIP versus uninfected control MLN comparison, all enriched categories could

be linked to known processes observed in cats with FIP, and often also directly to the PCR results. These were directly immune response related categories such as chemokine mediated signalling, IL-1β and IL-6 production, phagocytosis and immunoglobulin production. The categories included 'viral defence', 'negative regulation of viral replication', and 'interferon gamma signalling' but these were heavily outnumbered by those involved in humoral immunity and in pro-inflammatory cytokine responses.

As mentioned briefly in the introduction, TLRs are only one of the groups of PRRs, albeit arguably the most important. Other categories include the retinoic acid-inducible gene I (RIG-I) like receptors (RLRs) [163]. TLRs and RLRs are the main host responders to RNA virus infection [361]. Other PRRs include MDA5 and NOD [203]. Not all of these could be identified in the current dataset. NOD1 was detected and was not significantly altered but neither MDA5 nor its alias IFIH1 was identified. Unlike the TLRs which are membrane bound but cell type restricted, RLRs are free within the cytoplasm and expressed by all cells; they require the cell to be infected by the virus to activate their signalling pathways [203]. RIG-I is one of the principal responders to viral dsRNA [362]. As dsRNA only occurs as a replication intermediate of FCoV, a large effect would not be expected, similarly to the situation in TLR3 which appeared in our study to respond very little to FCoV infection in the MLN (with or without FIP). RIG-I, under its alias DDX58, was however present and upregulated over 15 fold in the current NGS dataset in MLN of cats with FIP versus uninfected MLN of control cats. It was also upregulated (to a much lesser extent) in FCoV-infected control MLN compared to uninfected control cats. RIG-I may therefore play a more significant role than the TLRs, with TLR 2, 4, and 8 upregulation being in the 4-10 fold range in FIP vs uninfected MLN. The fact that elevation of RIG-I can only be from infected cells shows a direct role of the virus. Considering that TLRs respond to presented virus and do not require a cell to be infected, and that infected control MLN showed no TLR upregulation in the present study, one can assume a very confined, restricted response in the MLN to FCoV infection, with infected cells responding to the presence of virus but not signalling to amplify the response.

Interestingly, despite this potentially beneficial RIG-I upregulation in infected MLN of cats without FIP over uninfected, comparing RIG-I in MLN LCM lesion samples versus bulk MLN there was no significant difference found. As the proportion of infected cells is markedly higher in the lesions, this suggests that heavily infected cells are failing to further upregulate their response, or may have reached a plateau.

Another gene family of interest had one member amongst the top 20 upregulated genes in FIP compared to both control group MLN, and two members in the top 20 downregulated in FIP. This is the C-type lectin family, a group of cell membrane proteins that have a wide range of immune functions including cell adhesion and pathogen detection; as PRRs, they are found on the surface of macrophages [201,363]. One of the C-type lectins is DC-SIGN, identified as an FCoV co-receptor [101]. Family members can also help deliver pathogens to lysosomes [363]. CLEC4D (aka CLECSF8) was the upregulated C-lectin. It can be expressed by neutrophils and monocytes and can be upregulated by IL-6, TNF-α, and IFN-γ [364]. It has been shown to be a phagocytic receptor but there is scant further information published [364]. The downregulated CLEC4G is also known as LSECtin and has been shown *in vitro* to interact with the SARS CoV spike protein to enhance infection [365]. The second top 20 downregulated C-type lectin, CLEC10A, has thus far only been implicated in filovirus infection [366]. The significance that downregulation of transcription of these proteins could have in

the feline immune system, and in FCoV infection in particular, is unknown. If both proteins are able to act as co-receptors then downregulation may represent a protective attempt by the host. Conversely, the upregulation of CLEC4D, as a phagocytic receptor, may contribute to virus uptake. The implications on cell function of the regulation discrepancies are unknown. However, the observed expression profile may represent a general macrophage activation or be a response to a specific stimulus.

Downregulated genes and pathways in FIP were dominated by those involved in cellular metabolism. This is consistent with the downstream effects of the antiviral response, i.e. shutting down cell protein synthesis in an attempt to deny the virus access to replication machinery [256].

Unsurprisingly, given the minimal differences between the two control groups, the comparison of MLN from cats with FIP with infected control MLN overlapped heavily with the comparison to uninfected control MLN. However, some interesting differences stood out in terms of enriched GO categories: 'positive regulation of vascular endothelial growth factor production' and 'vacuolar acidification' were both only significantly elevated in FIP MLN versus FCoV-infected control MLN and not in FIP versus uninfected controls. For these pathways to be affected indicates that the associated genes must be lower in infected control MLN than in uninfected MLN. This is another example of a downregulated/inherently lower inflammatory response in infected control MLN.

Vascular endothelial growth factor (VEGF; corresponding to VEGFA) has been previously shown to correlate with the degree of effusion in FIP [367]. By NGS, the mRNA for genes VEGFA-D were all detected in our study, of which only VEGFD was significantly differentially expressed between FIP and the uninfected control MLN, though in fact lower in FIP. The pathway was however significantly up-enriched in FIP compared to the infected control MLN. This lack of alteration in VEGF itself may also be explained by only two of the three cats with FIP having had effusions. Therefore, it would be worth evaluating the transcription of this cytokine by RT-qPCR in more cases, which was not done as part of the present study.

Vacuolar acidification is a critical step in active TLR function of the intracellular TLR 3, 7, 8, and 9 [178]. Drugs which block this are able to also block TLR function [368]. Such drugs have in fact already been trialled in FIP, with limited success but without specific reference to their mode of action [369]. Whether the underlying premise is false, or these drugs are ineffectual owing to their specificity, could be better assessed by simultaneous TLR pathway evaluation. The lack of efficacy of these drugs suggests important parallel roles for TLRs which don't require vacuolar acidification (e.g. TLR 2 and 4), supporting the hypothesis of excessive overactivation of pro-inflammatory pathways.

Regulation of pathogen recognition pathways and possible viral interference

Evaluation of the transcriptome gives us an important insight into cell activity following viral infection, especially the activities and direction of differentiation of cells. However, it does not give us a three dimensional view of the complete cellular processes owing to the complex layers of fine-tuning and alterations possible between gene transcription and formation of a functional protein.

The PRRs are a powerful tool of the innate defence system and correspondingly require tight regulation to minimise the chances of over-activation [370]. This occurs at many levels, through transcriptional, post-transcriptional, translational and post-translational regulation [370]. Much of

the latter is in the form of post-translational modifications (PTMs). Of these PTMs, the best understood are phosphorylation, ubiquitination, methylation, and acetylation yet there are many other methods which are only slowly beginning to be understood [371]. Defects in any of these modification processes can be responsible for inflammatory diseases [372]. A number of molecules and regulators downstream to PRRs were also found to be amongst significantly upregulated genes in the present NGS study. These downstream molecules are frequently the targets for modification but the receptors themselves may also be involved [373]. Examples of direct receptor targeting include TLR4 and RIG-I [372]. TLRs addiitonally require chaperoning to their final destination (e.g. the plasma or endosomal membrane) and blocking of these chaperones can prevent TLRs functioning [374]. This reinforces the fact that evaluation of TLR levels themselves is only one aspect in determining their end effect. The amino acid sequence of signalling molecules also has a crucial impact on their function. For example, once TLR2 has bound its ligand, it requires phosphorylation for formation of a signalling complex; small changes in the amino acid sequence can alter phosphorylation and completely abrogate their signalling ability [372]. This is not specific to TLR2 and is another example of the fact that the detection of a TLR, even if at the protein level, does not necessarily equate to its ability to signal. Alternatively, small changes may markedly alter the receptor specificity such that almost identical TLRs between species respond differently to the same ligand e.g. TLR4 in horses and man [375]. A follow up to the present study is therefore planned in which variant calling on the results we have thus far obtained will be applied, to attempt to identify any sequence differences in the TLRs between the groups of cats.

The effects on function of variations in STAT mRNA levels are particularly difficult to interpret. As transcription factors, their location is of course paramount, as well as being dependant on their phosphorylation status; the active protein is nuclear and phosphorylated [319]. The active form lasts a few hours before decaying by being exported from the nucleus, dephosphorylated, or SOCS (suppressor of cytokine signalling) suppressed but it can also be recycled so a reduced rate of decay would have the same effect as an increase in mRNA template [319]. SOCS3 was upregulated in the MLN of cats with FIP so may have led to reduced downstream signalling of JAK-STAT pathways.

It had been hoped that IH for STAT2 would allow cell location to be assessed and not only an upregulation but an increased nuclear translocation to be observed. This was unfortunately not possible at this time owing to a lack of antibody cross-reactivity and is instead a potential subject for future study.

Another major post-translational method in addition to phosphorylation is ubiquitination which therefore has an important role in intracellular events. Protein degradation is as critical as protein translation to the maintenance of cell homeostasis [376]. TLR4 and RIG-I are partially regulated by ubiquitin modifications [372]. Ubiquitination is a three step process involving enzymes which activate (E1), conjugate (E2), and ligate (E3) ubiquitin to a protein [377]. Differing ubiquitin protein linkages lead to different outcomes, with proteasomal degradation the most well-known of these. Regulation of intracellular immune signals is, however also a function of ubiquitination. The TRIM (tripartite motif-containing) protein family is an important part of this process. It comprises over 70 members with E3 ubiquitin ligase activity [378]. The family is highly conserved amongst metazoans and its members are expressed in response to interferons, having a broad function in innate

immunity [378,379]. TRIM genes arise from a common ancestral gene but have then evolved independently in different species [378].

Several TRIM family members are reported to exhibit anti-viral activity; one such example is TRIM25 [377], which was found to be upregulated in the FIP MLN. TRIM25 is induced by type I and II IFN and one of its important roles in innate immunity is in RIG-I signalling. After recognition of viral dsRNA, RIG-I requires ubiquitin modifications in order to initiate an antiviral signalling cascade, in the form of K63-linked polyubiquitin chains mediated by TRIM25 [380,381]. This leads, via IRF3 and NF-κB, to predominantly type I IFN and inflammatory cytokine production respectively [377]. The ubiquitin specific protease USP15 helps promote TRIM25 activity and hence RIG-I signalling[382]. Interestingly, it is upregulated in FIP MLN versus controls.

Targeting TRIMs is one of the many viral evasion strategies which have been discovered. A number of viruses have been reported to target TRIM25 specifically, including influenza virus and SARS-CoV. Known to downregulate type I IFN, one of the methods SARS-CoV and MERS-CoV use is interaction of their N protein with TRIM25 [183,383]. This interferes with TRIM25 ubiquitination of RIG-I and hence downregulates RIG-I signalling. This mechanism, i.e. targeting the protein's function, can of course not be evaluated by TRIM RT-qPCR.

TRIM21 is another family member that was found upregulated in FIP MLN compared to controls. This enzyme can degrade IRFs (3, 5, and 7) and thus reduce the IFN response [384]. The present study indeed found IRF3 to be significantly downregulated in FIP MLN, but not IRF 5 or 7. TRIM21 can also detect intracellular, antibody-opsonised virus which it targets for ubiquitination and degradation [384]. Subsequently, the viral nucleic acid is released to be detected by PRRs in the cytoplasm. So far this has only been identified as a relevant mechanism for non-enveloped viruses [384], however the effect of TRIM21 levels on IFN would be an interesting *in vitro* experiment in FCoV infection.

Viruses commonly use the tactic of degrading host signalling components of viral detection pathways. They may use their own proteases to cleave these components or they may hijack the host proteasome degradation pathway [180]. TLR3 is a frequent target as it can be involved in both RNA and DNA virus infections [180]. Classical swine fever virus N protein induces IRF3 degradation [385] whilst enterovirus 3C cleaves IRF7 [386]. SARS-CoV encodes a papain-like protease (PLpro) through which it is able to inhibit both TLR 3 and 7 signalling [113]. The main function of the viral PLpro is the cleavage of specific ORF1ab proteins to form their individual nsps [93]. In the host cell, however, the enzyme interferes with TLR pathways by inactivating pathway regulators [113]. This particular function of the FCoV PLpro has not been studied but could contribute to the lack of expected upregulation of TLR 3 and 7 in response to their ligands (ds and ssRNA respectively). As this inactivation is at the protein level it cannot be directly concluded that this would cause the observed difference at the mRNA level. A similar mechanism can lead to inhibition of type I IFN in SARS-CoV infection via physical interaction of PLpro with STING (stimulator of interferon genes, aka TMRM173) complexes [114]. The STING gene itself was significantly upregulated (though less than 3 fold) in FIP MLN but the myriad potential downstream responses require further evaluation.

Assuming that the TLR inflammatory signalling pathways remain intact, the major downstream cytokines would be IL-1β, IL-6, and TNF-α. These were all upregulated in the MLN in FIP, as were GO terms involved in positive regulation of IL-1 and IL-6 responses. Within these pathways there are again myriad possibilities for interference and inhibition which are also areas for investigation

in FCoV infection. Though not elucidating protein levels, RNA-Seq does allow us to simultaneously assess the levels of many of these regulators and thus predict their possible effects. IL-6 should signal through STAT3, which was not found to be upregulated in the present study. Though the activation status of STAT3 is unknown this could suggest the presence of IL-6 decoy receptors interfering with signalling. Gp130 is a subunit of the IL-6 receptor and is critical for signal transduction when present on the cell membrane [216]. In its soluble form it acts as a buffer by binding IL-6 and preventing its action [216]. Levels of gp130 (IL6ST) mRNA were not significantly altered in FIP but the relative distribution of the protein between membrane bound and soluble forms cannot be determined from the present data. This would be an interesting area of investigation, in particular as the soluble form could potentially be a treatment avenue [226]. One of the functions of IL-6 is to promote B cell survival [216]. Its upregulation, though mild, may help explain some of the upregulated clusters related to B cell function in the RNA-Seq analysis.

The virus induces a local inflammatory response, more prominent than the systemic effects

The present study confirms findings of previous studies that investigated the haemolymphatic tissues in cats with and without FIP, suggesting that BM and spleen behave very differently to the MLN, and differently to each other in response to FCoV infection [48,293].

FCoV levels in the haematopoietic tissues studied here are up to 100,000 times lower in the BM than in the MLN, levels in the spleen range between the other two organs. The BM is a primary haematopoietic organ with little direct role in the immune response, and has not been reported to be affected by FIP lesions. Virus present here can therefore be assumed to originate from circulating monocytes and indicated that the majority of animals were viraemic at the time of death [316]. These current findings are in agreement with a previous study comparing viral load between haematopoietic tissues and between cats with and without FIP [55]. Mediator levels in the BM can therefore be assumed to give an approximate indication of the inflammatory response and or activation status in circulating cells.

The spleen meanwhile is a sentinel organ of the immune system. Serosal lesions were frequently observed in the cats with FIP but were avoided for RT-qPCR. Parenchymal lesions were only occasionally observed which is in agreement with previous findings [44]. Mediator levels in the spleen will therefore predominantly represent the systemic immune response to the circulating virus.

The MLN has a gatekeeper role against enteric pathogens [291]. Accordingly, it also had a far higher FCoV level regardless of the presence or absence of lesions in the present study and was additionally a very frequent site of virus specific lesions. Mediator levels in the MLN will therefore be more representative of local viral effects.

Within control cats, (representing constitutive expression) mediator levels in the BM were all lower than in the spleen. Although the significant mediators varied between BM and spleen, trends were the same for almost all mediators. Only G-CSF and GM-CSF differed.

M-CSF mRNA levels were significantly lower (downregulated) in both BM and spleen of FIP cats, while G-CSF was significantly decreased only in the BM with no trend in the spleen, and GM-CSF showed an upward trend in the BM and downward trend in the spleen. This apparently random

pattern goes against a previous finding of increased M-CSF transcription in the BM of cats with FIP, but supports the same study's finding of decreased M-CSF in the spleen in FIP [48]. As the CSFs are growth factors for granulocytes and macrophages, the primary cells involved in FIP lesions, an increase in FIP had been expected across the board, in particular of the less constitutive and more reactive G-CSF [268]. Whereas M-CSF is produced ubiquitously, GM-CSF is produced mainly by activated leukocytes [268]. The upward trend of GM-CSF therefore fits with an increase in activated monocytes in the BM, as previously observed [44]. As the primary site of haematopoiesis, the increase in GM-CSF in the BM fits to its role, promoting maturation and differentiation of granulocytes and macrophages [387]. GM-CSF levels are also reported to rise following IL-1β stimulation and the cytokine is also involved in promoting inflammation, e.g. by positive feedback to IL-1β stimulation [268]. As both GM-CSF and IL-1β were elevated in the BM in the current study, this suggests a local or even autocrine effect [270].

The three TLRs significantly upregulated in both MLN and lesions in FIP were TLR 2, 4, and 8. None of these were significantly elevated in the BM and only TLR2 was significantly elevated in the spleen in FIP.

This finding reinforces that cells outwith the lesions contribute to PRR upregulation (with upregulation in organs without lesions) but that within lesions the response to virus is enhanced. Comparison of results between tissues must be interpreted with a greater level of caution than those within tissues as GAPDH levels can vary between organs [303].

There was only a minimal inflammatory cytokine response by both BM and spleen in FIP; generally slight upward trends were observed for the three pyrogenic cytokines (IL-1β, IL-6, TNF-α) but only IL-1β transcription in the BM was significantly elevated which could reflect a general monocyte activation. These findings are similar to those of a previous study by our group where no significant alterations in mRNA levels were found in either the BM or spleen for the inflammatory cytokines [48].

The interferons were similar, an upward trend in all reached significance for IFN-β in both organs and for IFN-γ in the spleen. IFN-γ mRNA has previously been found to be decreased in PBMCs in cats with FIP, and the protein in the blood [134,259]. Separately, effusion levels of the IFN-γ protein were higher than serum levels, suggesting a local, i.e. lesional rather than a systemic primary source [258].

The significantly lower transcription of the anti-inflammatory cytokine TGF-β in FIP in BM and spleen indicates that although these organs made a low direct contribution to inflammatory cytokine production, there was also no systemic application of this particular brake on inflammation [245]. Potentially this may lead to a similar end result of increased inflammation by reducing negative feedback on pro-inflammatory cytokines. Although an effect can never be predicted from a single cytokine this suggests that part of the contribution of the BM and spleen to systemic inflammation may be permissive rather than active by decreasing the inhibition of inflammatory mediators. This would require study of the wider transcriptome.

The overall impression is that in the absence of lesions, haemolymphatic tissues make only a modest individual contribution to systemic cytokine production. We have also observed inflammatory cytokine production by the heart and liver (unpublished data), suggesting that multiple organs make a small contribution, topping up the more significant input of lesions and tissues local to lesions to create a systemic inflammatory environment.

Infected cells within the lesions appear to make a greater contribution to inflammation than to anti-viral defence

Specific regions were micro-dissected from tissues with FIP lesions, and non-lesional tissues from FIP cases. Lesions were additionally categorised into serositis or granulomatous parenchymal lesions [44]. In most cases the distinction between serosal and parenchymatous lesions was clear histologically, fitting the two described presentations [257]. Mediator levels were statistically compared with levels within the MLN of cats with FIP, and graphically between BM, spleen, MLN, lesions and lymphoid follicles from four cats. Statistical analysis was not performed on the latter comparisons owing to the small 'lymphoid follicle' group size.

It had been hypothesised that the mediator patterns observed in the FIP MLN would be exaggerated in the lesions themselves, correlating with the highest density of infected cells. This was largely the case but with a few notable exceptions.

The TLRs elevated in the lesions (TLR2, 4, and 8) corresponded with those elevated in the MLN of FIP cats versus control cats. This was despite a lack of significance found for TLR4 and 8 when comparing between bulk MLN with and without lesions in FIP. This discrepancy has a number of possible explanations. It may relate to small subgroup sizes (the 'non-lesion' subgroup of FIP cats had only seven animals), potentially poor correlation between the tissue samples for PCR and for histological examination, or it may be that in the bulk MLN the lesions were diluted within the sample and did not dominate the transcriptome as they did in the LCM samples. The cell types present in each sample are of course also an important factor. The present results provide clues but no simple answer as to the main source of these TLRs. Cells belonging to the mononuclear phagocyte system are the most common source, but both B and T lymphocytes in felines have been found capable at least of mRNA transcription of TLR 2, 4, and 8 [164,165]. This was determined by cell sorting prior to PCR; other researchers have called into question the accuracy of using PCR with cell sorting methods as a very low level of cell contamination could lead to false positives [388].

Levels of mediators within lymphoid follicles, were generally very similar across a range of origins (MLN, spleen, and small intestinal BALT), consistent with a cell type/function specific more than an organ specific response. These follicles could reasonably be expected to have markedly different (and lower) expression patterns than the other tissues, being dominated by B cells. Though a far purer population than an overall organ sample, the follicles will still of course contain other cell types such as follicular dendritic cells (FDC) and tingible body macrophages as well as a small T cell portion [389], either of which may contribute to the TLR levels observed. Studies on the contribution of B cells to TLR production in mice and humans have shown great variability both between and within species depending on B cell subsets, with subsets in our cats remaining unknown [390].

TLR 7 and 9 transcription levels, unaltered in FIP vs non FIP bulk MLN, were both significantly lower in the LCM samples. This may be a true viral inhibition or be related to the cell type present in each case. In humans, TLR7 and 9 are often said to be exclusively plasmacytoid dendritic cell (pDC) derived whereas in mice there is significant overlap in TLR expression between DC subsets [181,338,391]. pDCS are prototypic anti-viral DCs [185]. If they exist in the cat (which is so far not known) and are roughly comparable, they would be expected to be found within T cell zones and surrounding high endothelial venules[185], i.e. not within the sampled follicles. Despite this, the

lymphoid follicles in the present study had the highest levels of both TLR 7 and 9 (above bulk MLN as well as above levels in the lesions), the antithesis of the expected result. This suggests another cell type is likely to be responsible. As the elevated levels in follicles indicate the cell type in question should also be concentrated there, the two main suspects are the B cells themselves and the FDC. Going against the commonly held consensus of pDC specificity, human B cells have been shown capable of intrinsic TLR 7 and 9 signalling, contributing to a mechanism implicated in autoimmunity in which the cells respond to self nucleic acids [392]. Similarly, FDC have also been shown to respond to TLR ligands (at least for TLR 4 and 7) which can themselves also contribute to B cell activation [393,394]. The FDC is in fact not of DC origin but from perivascular precursors [395]. In the absence of appropriate antibodies, either for immunohistology or preferably multi-channel FACS analysis, it was not possible to investigate our cases further at this timepoint.

Further evidence that there is an alternative/additional cell type to pDCs responsible for TLR 7 and 9 production in cats is provided by the IFN levels in various tissues. Though all cell types are capable of type I IFN production, by far the most prolific in mice and humans are usually the pDCs, known as the professional IFN-α/β producing cells [185]. IFN-α levels were higher in the lymphoid follicles than in the bulk MLN (though not exceeding the lesion levels), correlating with levels of TLR 7 and 9. This is despite the negligible viral levels in the follicles so is not a direct viral effect. This correlation supports the role of these two TLRs as the main type I IFN inducers but leaves open the question of cell source. The lack of upregulation of TLR 7 and 9 in lymph nodes or lesions in FIP is also a possible explanation for the poor ability of the host to combat the virus.

By NGS, IFN-α, -β, and -γ all showed an upregulation in FIP compared to control cats but this was minimal; this only reached significance for IFN-γ and then only at a $p<0.05$ level.

So far, the existence and distribution of pDCs has not been investigated in the cat, again partly owing to the availability of antibodies. A human study evaluated their density in reactive LN due to different aetiologies [396]. Two of the defined aetiological subgroups in that study could be apposite with FIP; viral and granulomatous, but these were at opposite ends of the spectrum. 'Granulomatous' lesions contained the highest levels of pDCs and 'viral' the lowest [396]. This appears rather counterintuitive when considering that the pDCs dominant function is anti-viral.

Returning to receptive cell types for FCoV, one of the viral co-receptors has been identified as DC-SIGN (dendritic cell (DC)-specific ICAM-3-grabbing nonintegrin/CD209) [101,340]. When characterised, pDCs in other species (mice, humans, and swine) are reported not to have DC-SIGN [188]. Their existence in cats is unknown, if the same is true as in other species this may mean they are unlikely to be infected. This would help explain why the levels of pDC specific TLRs would not necessarily correlate to areas dominated by infected cells. MHV for example is however able to infect both DCs and pDCs [397,398].

TLR3 was tendentially but not significantly lower in the lesion group than in the bulk MLN. For TLR7, the difference was significant. This supports the theory of a possible viral inhibition of TLR3 and 7 as observed in SARS and discussed above [113]. Targeted experimental investigations would be required to confirm this mechanism, in which protein levels and downstream effects should also be taken into consideration.

All three studied STATs showed lower transcription levels in the lesions than in bulk MLN from cats with FIP, the opposite of what had been expected. As they are downstream of cytokines

including the interferons, IL-6 and IL-10 this suggests reduced cytokine signalling and loss of positive feedback [319]. Nonetheless, IFN-α was upregulated in the lesions, however neither IFN-γ nor IL-6 were (IFN-β and IL-10 could not be assessed in the lesions). This may be as whilst most cells can produce IFN-α, T cells are the main source of IFN-γ (and lesions were macrophage dominant) [399]. It also explains the lower levels of IFN-γ found in B cell dominated lymphoid follicles than in bulk MLN.

IL-1β was the only inflammatory cytokine that was significantly higher in the lesions than in the bulk MLN. This was unexpected as although macrophages are a main source of IL-1β they are also main sources of TNF-α which should be upregulated by FCoV infection [204,240]. However, a previous study observed that TNF-α expression appears to switch from macrophage-dominant in uninfected lymph nodes to lymphocyte-dominant following FCoV infection (including within the follicles) [47].

Transcription of the anti-inflammatory TGF-β was significantly lower in lesions than bulk MLN but slightly higher in granulomatous than serosal lesions. TGF-β can be produced by many parenchymal and leukocyte cell types and is produced as an inactive form so gene levels do not necessarily correlate with levels of active protein [245]. Nevertheless, comparing mRNA levels with cell types present suggests that within the lesions, macrophages are the main source, but that they are not the main contributors in lymphatic tissue.

Comparing within the LCM sample group between granulomatous and serosal lesions, when a significant difference was observed the target level was always higher in the granulomatous lesions. The simplest explanation is the relative proportion of macrophages. Areas which were macrophage dominant were selected, however serosal lesions more often contained admixed neutrophils and fibrin. As neutrophils are far less productive sources of cytokines, this may reflect a dilution of the macrophage response [400].

The levels of the only assessable matrix remodelling enzyme in the lesions (MMP2) were lower in lesions than in FIP bulk MLN but were higher in granulomatous than in serosal lesions, suggesting, logically, that there was a greater degree of destruction of the pre-existing parenchyma taking place in the granulomatous lesions. These lesions may also contain a greater proportion of recently blood-derived macrophages, which may use MMPs to break down the basement membrane during extravasation [42]. This is not necessary in serosal lesions which instead consist of effused cells without a developed tissue matrix to infiltrate. The serosal lesions within the lesion group may have cancelled out any difference between granulomatous lesions and MLN. MMPs and TIMPs showed variable expression patterns between the organs studied with no clear shift in balance to favour either proteolysis or inhibition. Taken together the findings suggest that matrix remodelling is not a prominent feature in FIP which is also supported by the histological features of FIP in general; even in chronic lesions, fibrosis is not observed [29,44].

The aim had been to take endothelial cells from regions of vasculitis but this proved impossible from the available samples. These either lacked vasculitis or vessels were effaced such that isolation of pure endothelial cells was not viable. This can never be predicted before histological examination of tissues so continued case recruitment, and luck, would be required to obtain these samples. With the advancement of FFPE RNA extraction techniques this partially removes one of the obstacles in future sample collection (though fresh cases are still a logistical problem) [401].

However the quality is still far below that of fresh frozen samples so the methods should not be combined in analysis.

Possible epigenetic effects of feline coronavirus

The comparison of RNA-Seq data between micro-dissected lesion samples and bulk MLN of cats with FIP is the most difficult to attribute significance to as here distinctly different cell populations were compared; a lymphocyte dominated versus a macrophage dominated population. This comparison was part of an attempt to determine which processes the virus can affect regardless of cell type.

There was a very apparent segregation between the two groups by cluster analysis. This included the whole transcriptome as results were not filtered prior to analysis, and hence many genes without a role in immunity. In fact there appeared to be surprisingly few immune system associated genes upregulated in the lesions compared to the bulk MLN. The main genes found to be more highly expressed in the lesions were all histone proteins, responsible for chromatin packaging. The top 10 genes alone included six histone (H) cluster genes from clusters 1 and 2, with both 2A and 2B members. H2A and 2B are two of the four histone molecules involved in forming a core around which DNA is wrapped [402]. H1 is a linker protein which helps compact the chromatin [402]. When closed, the chromatin is not transcriptionally active [403].

Histone modifications are one of the methods of epigenetic regulation, i.e. any modification which alters a phenotype without any alteration to the genotype [404]. Modifications include amongst others, acetylation, methylation, and phosphorylation of histones, as well as nucleosome positioning, and regulatory RNAs [403,405]. These alterations may serve to either repress or activate transcription. Epigenetic alterations are one of the key methods by which a transcriptional response can be tailored to a specific stimulus [403]. The promoters of key primary response genes such as IFN often contain regions which are resistant to modification, so that the initial response is less flexible. Their downstream genes however, such as interferon stimulated genes (ISGs), often require remodelling of their promotion sites to allow transcription [403]. Indeed, expression levels of IFN and ISG have been correlated with disease outcome [403], and specific histone modifications have been inversely correlated with ISG levels which regulates the IFN response [406]. Crucially, the location of the modification is of more importance than the type in determining outcome; for example methylation may cause either repression (as in the previous example) or activation [403]. In another study, macrophages were found to have a huge increase in histone acetylation at TLR promoter regions following LPS stimulation [407]. Not only do these processes occur as part of normal cell regulation of transcription but they are also frequently bidirectional in viral infection. As well as a virus using host machinery for its own replication, it may utilise epigenetic methods to dysregulate the host immune system and/or to direct cellular function towards viral replication [405]. DNA viruses more commonly influence host epigenetics but there are also examples of RNA viruses, including coronaviruses. Both SARS-CoV and MERS-CoV have been found to interfere with the host IFN response; the latter causes a downregulation of IFN responsive genes associated with antigen presentation, suggesting it is able to evade the immune response in this way [408].

Cell culture experiments showed that MHV can enhance its own infectivity through epigenetic modifications affecting cell receptor expression; these modifications led to increased levels of persistent infection [409]. This susceptibility was passed down to the next generation as cells were passaged [409].

In the present study, the normal ratio of histone transcription between a lymph node population and a macrophage dominated population is unknown therefore the possible interpretations are at this stage hypothetical. It cannot be excluded that the differences represent constitutive cell type associated factors. However the results raise fascinating questions regarding the potential impact of FCoV infection on the host epigenome. One hypothesis could be that the virus induces alterations in histone packaging which then contribute to an ineffectual response. The next logical step to investigate this further would be to conduct *in vitro* infection studies with chromatin immunoprecipitation (ChIp) analysis [410]. ChIp can also be combined with deep sequencing to simultaneously elucidate both the epigenome and transcriptome (ChIp-seq). Although the host genome of cats with and without FIP has been compared to try to identify host factors involved in susceptibility to disease, and the transcriptome has been evaluated in specific settings, the epigenome has not been studied to date [75,168,411,412]. Epigenome-wide association studies (EWAS) can provide a way to study epigenetic variants associated with disease outcomes [413]. However, once again application of methods which are routine in other species can be challenging in the cat, with this method also relying on antibodies of appropriate specificity.

The genes found at lower levels in the lesions than the bulk MLN were unfortunately poorly annotated, it could only be established that the majority are involved with antibody production. The simplest explanation is the paucity of B cells (or more specifically plasma cells) within the lesion samples in comparison to the MLN. When in the future more information is available to characterise these proteins further, the possibility that they are macrophage expressed proteins assisting antibody function can be investigated. In this scenario this would suggest viral-induced downregulation in the lesions. This potentially fits with the above described downregulation of host cell antigen presentation by MERS-CoV infected cells but is thought to be a far less likely explanation at this stage.

Looking beyond the viral spike protein

Of all the viral mutations postulated to be key to the pathogenesis of FIP, the spike protein mutations have come the most tantalisingly close to date. The finding of so called 'FIP causing' and hence 'diagnostic' mutations has sparked much debate since being identified in a comparison between tissue samples from cats with FIP and faeces of FCoV infected healthy cats [132]. This study found that the vast majority of tissue samples contained virus with one of two amino acid alterations (at codons 1048 and 1050) [132]. Later studies also compared tissue samples of FCoV infected healthy cats and found that the viral mutations could also be identified in these samples, suggesting they were linked to systemic spread rather than pathogenicity [91,133]. Nevertheless these mutations are often suggested as tools for use in a diagnostic setting [414–416]. For this reason we first targeted this mutation site to investigate, comparing a selected region of the S gene between FCoV infected control cats and cats with FIP.

We found the 'systemic' mutations present in all FCoV infected cats without FIP, and found cats without FIP which lacked the mutation. This confirmed earlier studies that the codon 1048 and 1050 mutations are neither specific to FIP nor always present in cats with FIP [91,133]. They added further support to the hypothesis of these previous studies that the mutations are associated with the virus' ability to spread systemically but not with its virulence [91,133].

Three cats carried virus associated with the 'enteric' form (in BM, spleen, and MLN). Of these three cats, additional organs (spleen and MLN) were available from the cat with 'enteric' virus in the BM, and these carried the 'systemic' mutation.

From another cat, virus from seven different sites was available to sequence. All except one of the obtained sequences were identical, this was from lesion free Peyer's patches and thereby the closest site to purely enteric (intestinal epithelial) virus. This site carried the 'systemic' mutation but results suggest that additional mutations (two bases within the sequenced region) occurred before further spread.

All samples taken from lesions did in fact carry the mutated form regardless of the presence of virus in other organs from the same animal. Whilst this warrants further analysis it is of little diagnostic advantage as the benefit of a 'definitive' PCR over lesion sampling is in allowing testing of low invasiveness on easy to access samples. It can also never be possible to ensure that all virus types present in an individual infected animal are sampled so the risk of false positives and negatives remains.

FCoV is reported to frequently exist as quasispecies, one theory holds that these overwhelm the immune system of a compromised individual [417]. A study on blood samples found limited quasispecies in the N protein, but a high level in the S protein [119]. Many cats in our study showed a surprising lack of 'within host' viral variation at the nucleotide level within the S gene region sequenced; six cats showed no variations at all. This is possibly as our population consisted almost exclusively of client-owned pet cats which were hence less prone to FCoV co-infections than cattery animals. The degree of viral mutations observed at the genetic level (in this study often around 10% from the reference sequence even over only a small 150bp stretch) in comparison with the rare mutations at the protein level shows that selection pressure rarely favours mutations. Alongside this, the tendency of the virus to vary between organs brings great difficulties in interpretation. When viruses with varying protein sequences are present within the same organ or different organs of the same cat, it cannot be easily determined which, or if all, are responsible for disease. The same was found by Borschensky and Reinacher [125] who looked at the FCoV 3c and 7b genes and found multiple sequences within individuals.

A secondary aim of NGS was to compare the viral transcriptome between cats with and without FIP. However, as the library preparation protocol was chosen to suit the primary aim of analysing host mRNA differential expression, rather than preferentially amplifying virus, the number of viral reads was not amenable to the automated analysis programmes. Nonetheless, it could be compared by analysis of the raw data. The genes coding for the virus polyprotein1ab and the structural proteins were compared between the FCoV positive groups. The virus from FIP cats appeared similar whether or not bulk MLN or lesion was evaluated. Between cats with FIP and the infected control cats, the only significantly differentially expressed genes were the envelope and membrane protein genes. At this stage, the small group sizes mean that these results must be interpreted with a high degree of caution and require further validation. Howeve, they have

fascinating implications and could potentially indicate a difference in relative gene transcription between virulent and non-virulent virus. The E and M proteins have not been previously linked with FCoV pathogenesis, with studies tending to focus on viral mutations. The functions of the E protein vary between coronaviruses [93]. Some coronaviruses, including the closely related TGEV have been found to require E and M but not N for formation of the virion envelope, though this may vary with the propagation system [93,418,419]. This particular property has apparently not yet been investigated in FCoV. Thus, increased levels of these proteins may allow an increased rate of virion formation and go some way to explaining the higher viral titres observed in cats with FIP than infected cats without, both in this and a previous study [55]. The E protein has also been implicated in viral egress from cells, altering the host secretory pathways to benefit the virus [419]. A SARS-CoV E protein deletion was able to replicate but was attenuated in culture. It also caused a lower level of pulmonary inflammation in hamsters though this may be more directly linked to the lower viral load [420]. Another possible explanation for the reduced inflammation, and potentially of high impact in FIP, is decreased activation of NF-κB in infected cells by E gene knock out viruses [419].

The M protein is involved in viral assembly [93] but studies on its potential involvement in immune modulation have provided conflicting results. The SARS-CoV M protein has been variably found to induce IFN-β and to inhibit its production [347,421]. To be of relevance in the scenario of FIP, the latter effect would be more important.

Summarising the transcriptome approach

A number of previous studies have looked at the transcriptome in FCoV (FIPV) infected CRFK cells *in vitro,* and a recent study looked at peritoneal macrophages from experimentally infected cats *in vivo* [168,241,242,251,411]. Despite the differing cell populations (with CRFK cells far removed from macrophages), our results showed a surprisingly high overlap with previous *in vitro* findings of other groups but of course not complete. This is despite the huge biological difference between an artificially propagated, experimentally infected, culture-adapted cell type and a natural infection of a living organism with all the different cell types and interactions taking place within an organ. It demonstrates how preserved the effects induced by FCoV are and supports the use of *in vitro* experiments for more specific cell manipulations (e.g. gene knockouts or protein antagonists). However, the differences highlight how crucial it is that *in vitro* work is validated *in vivo,* e.g. the lack of TLR induction in CRFK cells [167] compared to that observed in our study render knock out studies with this method irrelevant. In comparing our results with those of Harun et al. who used a CRFK infection system, agreement for upregulated genes was far higher than for downregulated genes [412]. This suggests that whilst many cells may have a similar initial response to infection and upregulate first line defence genes, their downstream responses e.g. downregulation of metabolism are more cell-type specific.

One previous transcriptomic study specifically looked at apoptosis regulation in FIP [251] as this feature is observed histologically in lymphatic tissues in FIP and is known to be virus induced [46,63,240]. Their results reinforce how important correlation with the pathological picture is as, based on gene expression only, the effect on apoptosis could not easily be predicted; up and downregulated genes within an apoptosis cluster were evenly detected [411].

The S100 protein genes for example were not identified by any previous group as being of interest but this also fits with the lack of an 'intermediate' group (infected animals without FIP) in the *in vitro* experiments [168,242,411].

It is of course well known that protein levels cannot be directly extrapolated from mRNA levels. The precise figure varies with the biological system being tested, but it can be that only approximately 40% of protein variation can be directly explained by mRNA levels [422,423]. A far more positive finding for NGS interpretation was that when considering only differentially expressed genes, the correlation was much improved [424]. As already partly discussed there are a wealth of post-transcriptional modifications possible before even contemplating functional alterations though molecular interactions and post-translational modifications. Nevertheless, knowledge gleaned from other models can be used to predict the validity of results, as discussed.

An *in vitro* study on human cell lines assessed correlation between mRNA and protein levels in detail. The authors found that whilst there was overall poor correlation, for any given RNA the ratio was actually very reliable so that application of a correction factor could accurately predict one from the other [425]. This was within an experimental rather than *in vivo* situation but is nevertheless a promising option for the future.

One restriction of working with feline samples is the level of gene annotation so far available. Although this has expanded greatly in recent years, annotations are still a long way behind those of e.g. the human or mouse genome. This also links to the lack of available cross-reacting antibodies with which to confirm translation. It is hoped that, as databases are continuously updated, repeat analysis of this dataset will offer further insight in the future.

A common assumption in FIP is that there is an insignificant anti-viral interferon response. Here it was hypothesised that the balance between interferons and pro-inflammatory cytokines is swung in favour of the latter, with resulting damage to the host. Our results support what can be observed both clinically and pathologically, i.e. that the inflammatory upregulation occurring is too widespread and non-specific. Anti-viral pathways are upregulated, but this appears outweighed by the extensive involvement of the adaptive immune system and inflammatory cytokines, causing the severe damage observed which may therefore be a bystander effect.

Outlook and perspectives

As tends to be the case with FIP, each new discovery leads to further questions.

Returning to the original aims of the project, it has not been possible to address all of these but instead, additional channels have been opened and partially explored. This has shed light on exciting avenues for further study. Many of these were discussed above but will be summarised again here.

The first hypothesis was that a distinct state might exist in the MLN of FCoV infected cats which do not develop FIP. The results provide support for this theory but until more is known of the viral factors involved, the distinction between a resistant host and a non-pathogenic virus remains obscure in natural infections.

The results also support a skewing of involved pathways, weighted towards pro-inflammatory at the expense of more targeted anti-viral responses.

We have identified which TLRs are most likely to be involved in the host response to FCoV but have also found that results are distinct between organs and cannot be extrapolated from one to another. The present results also supported the hypothesis of an inadequate response by viral specific cytokines. Using RT-qPCR, no one TLR showed a clear cut off between animals with and without FIP but a possible extension of this would be to use machine learning to determine whether the panel of results together can predict disease status.

The primary aims of this study were all directed towards increasing understanding of the host immune response rather than of the virus. Nevertheless it goes without saying that viral factors cannot be ignored if we are to one day fully unravel the pathogenesis of this elusive disease. During the course of this project, discovering more precisely where the current gaps in our understanding lay helped to suggest future areas of study.

The secondary aim of NGS, to evaluate the viral sequence and transcriptome between cats with and without FIP has been partially successful but would benefit from deeper investigation of increased sample numbers. With this as the primary aim of a project, the sequencing methods could be tailored to the virus making this investigation more likely to yield significant results. So far investigations into viral sequence have focussed on those mutations which make a difference to the protein sequence. By simultaneously comparing viral genomic and amino acid sequences with the viral transcriptome it can be determined if nucleotide alterations affect the transcribed levels of any genes (and hence replication competence), without alterations in the protein. This potential difference relates to the multiple triplets coding for a particular amino acid and would represent a highly significant mutation which may also easily slip under the radar. Ribosomal profiling could be another useful tool to study viral gene expression and compare pathogenic and non-pathogenic viruses.

The transcriptome approach provides a more informative way to assess the host response in *in vitro* treatment trials without resorting to animal experiments at too early a stage.

Whilst every attempt has been made to extract the most relevant and salient results from the sequencing data, the wealth of information provided by this technique means that there are still many avenues which can be explored in greater depth, even before increasing the sample size for greater statistical power. This will include variant calling in an attempt to uncover any potential functional alterations in proteins.

References

1. Holzworth, J. Some important disorders of cats. *Cornell Vet.* **53,** 157–160 (1963).
2. Bonaduce, A. Sulla pleurite infettiva del gatto. *Nuova Vet* **21,** 32–36 (1942).
3. Ward, J. M. Morphogenesis of a virus in cats with experimental feline infectious peritonitis. *Virology* **41,** 191–194 (1970).
4. Ward, J. M., Munn, R. J., Gribble, D. H. & Dungworth, D. L. An observation of feline infectious peritonitis. *Vet. Rec.* **83,** 416–417 (1968).
5. Vennema, H., Poland, A., Foley, J. & Pedersen, N. C. Feline infectious peritonitis viruses arise by mutation from endemic feline enteric coronaviruses. *Virology* **243,** 150–157 (1998).
6. Stephenson, N., Swift, P., Moeller, R. B., Worth, S. J. & Foley, J. Feline infectious peritonitis in a mountain lion (Puma concolor), California, USA. *J. Wildl. Dis.* **49,** 408–412 (2013).
7. Van Rensburg, I. B. & Silkstone, M. A. Concomitant feline infectious peritonitis and toxoplasmosis in a cheetah (Acinonyx jubatus). *J. S. Afr. Vet. Assoc.* **55,** 205–207 (1984).
8. Heeney, J. L. *et al.* Prevalence and implications of feline coronavirus infections of captive and free-ranging cheetahs (Acinonyx jubatus). *J. Virol.* **64,** 1964–1972 (1990).
9. Mwase, M. *et al.* Positive immunolabelling for feline infectious peritonitis in an african lion (Panthera leo) with bilateral panuveitis. *J. Comp. Pathol.* **152,** 265–268 (2015).
10. Pesteanu-Somogyi, L. D., Radzai, C. & Pressler, B. M. Prevalence of feline infectious peritonitis in specific cat breeds. *J. Feline Med. Surg.* **8,** 1–5 (2006).
11. Rohrbach, B. W. *et al.* Epidemiology of feline infectious peritonitis among cats examined at veterinary medical teaching hospitals. *J. Am. Vet. Med. Assoc.* **218,** 1111–1115 (2001).
12. Pedersen, N. C., Boyle, J. F. & Floyd, K. Infection studies in kittens, using feline infectious peritonitis virus propagated in cell culture. *Am. J. Vet. Res.* **42,** 363–367 (1981).
13. Stoddart, M. E., Gaskell, R. M., Harbour, D. A. & Pearson, G. R. The sites of early viral replication in feline infectious peritonitis. *Vet. Microbiol.* **18,** 259–271 (1988).
14. Wang, Y.-T., Su, B.-L., Hsieh, L.-E. & Chueh, L.-L. An outbreak of feline infectious peritonitis in a Taiwanese shelter: epidemiologic and molecular evidence for horizontal transmission of a novel type II feline coronavirus. *Vet. Res.* **44,** 57 (2013).
15. Barker, E. N. *et al.* Phylogenetic analysis of feline coronavirus strains in an epizootic outbreak of feline infectious peritonitis. *J. Vet. Intern. Med.* **27,** 445–450 (2013).
16. Addie, D. D., Toth, S., Herrewegh, A. A. & Jarrett, O. Feline coronavirus in the intestinal contents of cats with feline infectious peritonitis. *Vet. Rec.* **139,** 522–523 (1996).
17. Stoddart, M. E., Gaskell, R. M., Harbour, D. A. & Gaskell, C. J. Virus shedding and immune responses in cats inoculated with cell culture-adapted feline infectious peritonitis virus. *Vet. Microbiol.* **16,** 145–158 (1988).
18. Pedersen, N. C. Virologic and immunologic aspects of feline infectious peritonitis virus infection. *Adv. Exp. Med. Biol.* **218,** 529–550 (1987).
19. Cave, T. A., Golder, M. C., Simpson, J. & Addie, D. D. Risk factors for feline coronavirus seropositivity in cats relinquished to a UK rescue charity. *J. Feline Med. Surg.* **6,** 53–58 (2004).
20. Addie, D. D. & Jarrett, O. A study of naturally occurring feline coronavirus infections in kittens. *Vet. Rec.* **130,** 133–137 (1992).
21. Addie, D. D., Toth, S., Murray, G. D. & Jarrett, O. Risk of feline infectious peritonitis in cats naturally infected with feline coronavirus. *Am. J. Vet. Res.* **56,** 429–434 (1995).
22. Pedersen, N. C. & Boyle, J. F. Immunologic phenomena in the effusive form of feline infectious peritonitis. *Am. J. Vet. Res.* **41,** 868–876 (1980).
23. Pedersen, N. C. & Black, J. W. Attempted immunization of cats against feline infectious peritonitis, using avirulent live virus or sublethal amounts of virulent virus. *Am. J. Vet. Res.* **44,** 229–234 (1983).
24. Kiss, I., Poland, A. M. & Pedersen, N. C. Disease outcome and cytokine responses in cats immunized with an avirulent feline infectious peritonitis virus (FIPV)-UCD1 and challenge-exposed with virulent FIPV-UCD8. *J. Feline Med. Surg.* **6,** 89–97 (2004).
25. Olsen, C. W., Corapi, W. V, Ngichabe, C. K., Baines, J. D. & Scott, F. W. Monoclonal antibodies to the spike protein of feline infectious peritonitis virus mediate antibody-dependent enhancement of infection of feline macrophages. *J. Virol.* **66,** 956–965 (1992).
26. Pedersen, N. C., Boyle, J. F., Floyd, K., Fudge, A. & Barker, J. An enteric coronavirus infection of cats and its relationship to feline infectious peritonitis. *Am. J. Vet. Res.* **42,** 368–377 (1981).
27. Uzal, F. A., Plattner, B. L. & Hostetter, J. M. in *Jubb, Kennedy, and Palmer's Pathology of Domestic Animals* (ed. Maxie, G. M.) 146–147 (Elsevier, 2016).
28. Kipar, A. *et al.* Fatal enteritis associated with coronavirus infection in cats. *J. Comp. Pathol.* **119,** 1–14

(1998).
29. Kipar, A. & Meli, M. L. Feline infectious peritonitis: still an enigma? *Vet. Pathol.* **51,** 505–526 (2014).
30. Pedersen, N. C. A review of feline infectious peritonitis virus infection: 1963-2008. *J. Feline Med. Surg.* **11,** 225–258 (2009).
31. Riemer, F., Kuehner, K. A., Ritz, S., Sauter-Louis, C. & Hartmann, K. Clinical and laboratory features of cats with feline infectious peritonitis – a retrospective study of 231 confirmed cases (2000–2010). *J. Feline Med. Surg.* **18,** 348–356 (2016).
32. Tasker, S. Diagnosis of feline infectious peritonitis: Update on evidence supporting available tests. *J. Feline Med. Surg.* **20,** 228–243 (2018).
33. Foley, J. E. & Leutenegger, C. A review of coronavirus infection in the central nervous system of cats and mice. *J. Vet. Intern. Med.* **15,** 438–444 (2001).
34. Sigurdardóttir, O. G., Kolbjørnsen, O. & Lutz, H. Orchitis in a cat associated with coronavirus infection. *J. Comp. Pathol.* **124,** 219–222 (2001).
35. Kipar, A., Koehler, K., Bellmann, S. & Reinacher, M. Feline infectious peritonitis presenting as a tumour in the abdominal cavity. *Vet. Rec.* **144,** 118–122 (1999).
36. Bauer, B. S., Kerr, M. E., Sandmeyer, L. S. & Grahn, B. H. Positive immunostaining for feline infectious peritonitis (FIP) in a Sphinx cat with cutaneous lesions and bilateral panuveitis. *Vet. Ophthalmol.* **16,** 160–163 (2013).
37. Cannon, M. J., Silkstone, M. A. & Kipar, A. Cutaneous lesions associated with coronavirus-induced vasculitis in a cat with feline infectious peritonitis and concurrent feline immunodeficiency virus infection. *J. Feline Med. Surg.* **7,** 233–236 (2005).
38. Declercq, J., De Bosschere, H., Schwarzkopf, I. & Declercq, L. Papular cutaneous lesions in a cat associated with feline infectious peritonitis. *Vet. Dermatol.* **19,** 255–258 (2008).
39. Garner, M., Ramsell, K., Morera, N. & Juan-Sallés, C. Clinicopathologic features of a systemic coronavirus-associated disease resembling feline infectious peritonitis in the domestic ferret (Mustela putorius). *Vet. Pathol.* **45,** 236–246 (2008).
40. Wolfe, L. G. & Griesemer, R. A. Feline infectious peritonitis. *Pathol. Vet.* **3,** 255–70 (1966).
41. Montali, R. J. & Strandberg, J. D. Extraperitoneal Lesions in Feline Infectious Peritonitis. *Vet. Pathol.* **9,** 109–121 (1972).
42. Kipar, A. *et al.* Morphologic features and development of granulomatous vasculitis in feline infectious peritonitis. *Vet. Pathol.* **42,** 321–330 (2005).
43. Paltrinieri, S., Cammarata Parodi, M., Cammarata, G. & Mambretti, M. Type IV hypersensitivity in the pathogenesis of FIPV-induced lesions. *J. Vet. Med.* **45,** 151–159 (1998).
44. Kipar, A., Bellmann, S., Kremendahl, J., Köhler, K. & Reinacher, M. Cellular composition, coronavirus antigen expression and production of specific antibodies in lesions in feline infectious peritonitis. *Vet. Immunol. Immunopathol.* **65,** 243–257 (1998).
45. Paltrinieri, S., Grieco, V., Comazzi, S. & Cammarata Parodi, M. Laboratory profiles in cats with different pathological and immunohistochemical findings due to feline infectious peritonitis (FIP). *J. Feline Med. Surg.* **3,** 149–159 (2001).
46. Kipar, A., Köhler, K., Leukert, W. & Reinacher, M. A comparison of lymphatic tissues from cats with spontaneous feline infectious peritonitis (FIP), cats with FIP virus infection but no FIP, and cats with no infection. *J. Comp. Pathol.* **125,** 182–191 (2001).
47. Dean, G. A., Olivry, T., Stanton, C. & Pedersen, N. C. In vivo cytokine response to experimental feline infectious peritonitis virus infection. *Vet. Microbiol.* **97,** 1–12 (2003).
48. Kipar, A. *et al.* Natural feline coronavirus infection: differences in cytokine patterns in association with the outcome of infection. *Vet. Immunol. Immunopathol.* **112,** 141–155 (2006).
49. Meli, M. L. *et al.* Samples with high virus load cause a trend toward lower signal in feline coronavirus antibody tests. *J. Feline Med. Surg.* **15,** 295–299 (2013).
50. Hartmann, K. *et al.* Comparison of different tests to diagnose feline infectious peritonitis. *J. Vet. Intern. Med.* **17,** 781–790 (2003).
51. Gunn-Moore, D. A., Gruffydd-Jones, T. J. & Harbour, D. A. Detection of feline coronaviruses by culture and reverse transcriptase-polymerase chain reaction of blood samples from healthy cats and cats with clinical feline infectious peritonitis. *Vet. Microbiol.* **62,** 193–205 (1998).
52. Felten, S. *et al.* Investigation into the utility of an immunocytochemical assay in body cavity effusions for diagnosis of feline infectious peritonitis. *J. Feline Med. Surg.* **19,** 410–418 (2017).
53. Litster, A., Pogranichniy, R. & Lin T-L. Diagnostic utility of a direct immunofluorescence test to detect feline coronavirus antigen in macrophages in effusive feline infectious peritonitis. *Vet. J.* 362–366 (2013). at <http://www.ncbi.nlm.nih.gov/pubmed/24076123>
54. Meli, M. *et al.* High viral loads despite absence of clinical and pathological findings in cats experimentally

infected with feline coronavirus (FCoV) type I and in naturally FCoV-infected cats. *J. Feline Med. Surg.* **6,** 69–81 (2004).
55. Kipar, A., Baptiste, K., Barth, A. & Reinacher, M. Natural FCoV infection: Cats with FIP exhibit significantly higher viral loads than healthy infected cats. *J. Feline Med. Surg.* **8,** 69–72 (2006).
56. Pedersen, N. C. An update on feline infectious peritonitis: Diagnostics and therapeutics. *Vet. J.* **201,** 133–141 (2014).
57. Paltrinieri, S., Parodi, M. C. & Cammarata, G. In vivo diagnosis of feline infectious peritonitis by comparison of protein content, cytology, and direct immunofluorescence test on peritoneal and pleural effusions. *J. Vet. Diagnostic Investig.* **11,** 358–361 (1999).
58. Leeflang, M. M. G., Rutjes, A. W. S., Reitsma, J. B., Hooft, L. & Bossuyt, P. M. M. Variation of a test's sensitivity and specificity with disease prevalence. *Can. Med. Assoc. J.* **185,** E537-544 (2013).
59. Giordano, A., Paltrinieri, S., Bertazzolo, W., Milesi, E. & Parodi, M. Sensitivity of Tru-cut and fine needle aspiration biopsies of liver and kidney for diagnosis of feline infectious peritonitis. *Vet. Clin. Pathol. A* **34,** 368–374 (2005).
60. Doenges, S. J., Weber, K., Dorsch, R., Fux, R. & Hartmann, K. Comparison of real-time reverse transcriptase polymerase chain reaction of peripheral blood mononuclear cells, serum and cell-free body cavity effusion for the diagnosis of feline infectious peritonitis. *J. Feline Med. Surg.* (2016). doi:10.1177/1098612X15625354
61. Sparkes, A. H., Gruffydd-Jones, T. J. & Harbour, D. A. Feline infectious peritonitis: a review of clinicopathological changes in 65 cases, and a critical assessment of their diagnostic value. *Vet. Rec.* **129,** 209–212 (1991).
62. Paltrinieri, S., Parodi Cammarata, M., Cammarata, G. & Comazzi, S. Some aspects of humoral and cellular immunity in naturally occurring feline infectious peritonitis. *Vet. Immunol. Immunopathol.* **65,** 205–220 (1998).
63. Haagmans, B. L., Egberink, H. F. & Horzinek, M. C. Apoptosis and T-cell depletion during feline infectious peritonitis. *J. Virol.* **70,** 8977–8983 (1996).
64. Takano, T. *et al.* A 'possible' involvement of TNF-alpha in apoptosis induction in peripheral blood lymphocytes of cats with feline infectious peritonitis. *Vet. Microbiol.* **119,** 121–131 (2007).
65. Paltrinieri, S., Ponti, W., Comazzi, S., Giordano, A. & Poli, G. Shifts in circulating lymphocyte subsets in cats with feline infectious peritonitis (FIP): pathogenic role and diagnostic relevance. *Vet. Immunol. Immunopathol.* **96,** 141–148 (2003).
66. Paltrinieri, S., Rossi, G. & Giordano, a. Relationship between rate of infection and markers of inflammation/immunity in Holy Birman cats with feline coronavirus. *Res. Vet. Sci.* **97,** 263–270 (2014).
67. Stoddart, C. A. & Scott, F. W. Intrinsic resistance of feline peritoneal macrophages to coronavirus infection correlates with in vivo virulence . Intrinsic Resistance of Feline Peritoneal Macrophages to Coronavirus Infection Correlates with In Vivo Virulence. *J. Virol.* **63,** 436–440 (1989).
68. Dewerchin, H. L., Cornelissen, E. & Nauwynck, H. J. Replication of feline coronaviruses in peripheral blood monocytes. *Arch. Virol.* **150,** 2483–2500 (2005).
69. Tekes, G. *et al.* Chimeric feline coronaviruses that encode type II spike protein on type I genetic background display accelerated viral growth and altered receptor usage. *J. Virol.* **84,** 1326–1333 (2010).
70. Pedersen, N. C., Liu, H., Gandolfi, B. & Lyons, L. A. The influence of age and genetics on natural resistance to experimentally induced feline infectious peritonitis. *Vet. Immunol. Immunopathol.* **162,** 33–40 (2014).
71. Pedersen, N. C., Liu, H., Durden, M. & Lyons, L. A. Natural resistance to experimental feline infectious peritonitis virus infection is decreased rather than increased by positive genetic selection. *Vet. Immunol. Immunopathol.* **171,** 17–20 (2016).
72. Foley, J. E. & Pedersen, N. C. The inheritance of susceptibility to feline infectious peritonitis in purebred catteries. *Feline Pract.* **24,** 14–22 (1996).
73. Kennedy, M., Boedeker, N., Gibbs, P. & Kania, S. Deletions in the 7a ORF of feline coronavirus associated with an epidemic of feline infectious peritonitis. *Vet. Microbiol.* **81,** 227–234 (2001).
74. Golovko, L. *et al.* Genetic susceptibility to feline infectious peritonitis in Birman cats. *Virus Res.* **175,** 58–63 (2013).
75. Wang, Y.-T., Hsieh, L.-E., Dai, Y.-R. & Chueh, L.-L. Polymorphisms in the feline TNFA and CD209 genes are associated with the outcome of feline coronavirus infection. *Vet. Res.* **45,** 123 (2014).
76. Hsieh, L.-E. & Chueh, L.-L. Identification and genotyping of feline infectious peritonitis-associated single nucleotide polymorphisms in the feline interferon-γ gene. *Vet. Res.* **45,** 1–8 (2014).
77. Zijenah, L. S. *et al.* Association of high HIV-1 RNA levels and homozygosity at HLA class II DRB1 in adults coinfected with Mycobacterium tuberculosis in Harare, Zimbabwe. *Hum. Immunol.* **63,** 1026–1032 (2002).
78. Addie, D. D. *et al.* Feline leucocyte antigen class II polymorphism and susceptibility to feline infectious

peritonitis. *J. Feline Med. Surg.* **6,** 59–62 (2004).
79. Gorbalenya, A. E., Enjuanes, L., Ziebuhr, J. & Snijder, E. J. Nidovirales: Evolving the largest RNA virus genome. *Virus Res.* **117,** 17–37 (2006).
80. in *Virus Taxonomy* (eds. King, A. M. Q., Adams, M. J., Carstens, E. B. & Lefkowitz, E. J.) 806–828 (Elsevier, 2012). doi:https://doi.org/10.1016/B978-0-12-384684-6.00068-9.
81. González, J. M., Gomez-Puertas, P., Cavanagh, D., Gorbalenya, a. E. & Enjuanes, L. A comparative sequence analysis to revise the current taxonomy of the family Coronaviridae. *Arch. Virol.* **148,** 2207–2235 (2003).
82. Li, F. Structure, function, and evolution of coronavirus spike proteins. *Annu. Rev. Virol.* **3,** 237–261 (2016).
83. Motokawa, K., Hohdatsu, T., Hashimoto, H. & Koyama, H. Comparison of the amino acid sequence and phylogenetic analysis of the peplomer, integral membrane and nucleocapsid proteins of feline, canine and porcine coronaviruses. *Microbiol. Immunol.* **40,** 425–433 (1996).
84. Herrewegh, A. A. P. M., Smeenk, I., Horzinek, M. C., Rottier, P. J. M. & de Groot, R. J. Feline Coronavirus Type II Strains 79-1683 and 79-1146 Originate from a Double Recombination between Feline Coronavirus Type I and Canine Coronavirus. *J. Virol.* **72,** 4508–4514 (1998).
85. McArdle, F. *et al.* Induction and enhancement of feline infectious peritonitis by canine coronavirus. *Am. J. Vet. Res.* **53,** 1500–1506 (1992).
86. Vennema, H. Genetic drift and genetic shift during feline coronavirus evolution. *Vet. Microbiol.* **69,** 139–141 (1999).
87. Kummrow, M. *et al.* Feline Coronavirus Serotypes 1 and 2 : Seroprevalence and Association with Disease in Switzerland. *Clin. Vaccine Immunol.* **12,** 1209–1215 (2005).
88. Benetka, V. *et al.* Prevalence of feline coronavirus types I and II in cats with histopathologically verified feline infectious peritonitis. *Vet. Microbiol.* **99,** 31–42 (2004).
89. Tanaka, Y., Sasaki, T., Matsuda, R., Uematsu, Y. & Yamaguchi, T. Molecular epidemiological study of feline coronavirus strains in Japan using RT-PCR targeting nsp14 gene. *BMC Vet. Res.* **11,** 57 (2015).
90. Amer, A. *et al.* Isolation and molecular characterization of type I and type II feline coronavirus in Malaysia. *Virol. J.* **9,** 278 (2012).
91. Barker, E. N. *et al.* Limitations of using feline coronavirus spike protein gene mutations to diagnose feline infectious peritonitis. *Vet. Res.* **48,** 1–14 (2017).
92. Terada, Y. *et al.* Emergence of pathogenic coronaviruses in cats by homologous recombination between feline and canine coronaviruses. *PLoS One* **9,** (2014).
93. Fehr, A. R. & Perlman, S. Coronaviruses: an overview of their replication and pathogenesis. *Methods Mol. Biol.* **1282,** 1–23 (2015).
94. Beniac, D. R., Andonov, A., Grudeski, E. & Booth, T. F. Architecture of the SARS coronavirus prefusion spike. *Nat. Struct. Mol. Biol.* **13,** 751–752 (2006).
95. Delmas, B. & Laude, H. Assembly of coronavirus spike protein into trimers and its role in epitope expression. *J. Virol.* **64,** 5367–5375 (1990).
96. Stohlman, S. A. & Lai, M. M. Phosphoproteins of murine hepatitis viruses. *J. Virol.* **32,** 672–675 (1979).
97. Tresnan, D. B. & Holmes, K. V. Feline aminopeptidase N is a receptor for all group I coronaviruses. *Adv. Exp. Med. Biol.* **440,** 69–75 (1998).
98. Dye, C., Temperton, N. & Siddell, S. G. Type I feline coronavirus spike glycoprotein fails to recognize aminopeptidase N as a functional receptor on feline cell lines. *J. Gen. Virol.* **88,** 1753–1760 (2007).
99. Hohdatsu, T., Izumiya, Y., Yokoyama, Y., Kida, K. & Koyama, H. Differences in virus receptor for type I and type II feline infectious peritonitis virus. *Arch. Virol.* **143,** 839–850 (1998).
100. Weiss, S. R. & Navas-Martin, S. Coronavirus pathogenesis and the emerging pathogen severe acute respiratory syndrome coronavirus. *Microbiol. Mol. Biol. Rev.* **69,** 635–664 (2005).
101. Regan, A. D. & Whittaker, G. R. Utilization of DC-SIGN for entry of feline coronaviruses into host cells. *J. Virol.* **82,** 11992–11996 (2008).
102. Van Hamme, E., Desmarets, L., Dewerchin, H. L. & Nauwynck, H. J. Intriguing interplay between feline infectious peritonitis virus and its receptors during entry in primary feline monocytes. *Virus Res.* **160,** 32–39 (2011).
103. Olsen, C. W. *et al.* Identification of antigenic sites mediating antibody-dependent enhancement of feline infectious peritonitis virus infectivity. *J. Gen. Virol.* **74,** 745–749 (1993).
104. Takano, T., Kawakami, C., Yamada, S., Satoh, R. & Hohdatsu, T. Antibody-dependent enhancement occurs upon re-infection with the identical serotype virus in feline infectious peritonitis virus infection. *J. Vet. Med. Sci.* **70,** 1315–1321 (2008).
105. Bosch, B. J., Zee, R. Van Der, Haan, C. a M. De & Rottier, P. J. M. The coronavirus spike protein is a class I virus fusion protein: structural and functional characterization of the fusion core complex. *J. Virol.* **77,** 8801–8811 (2003).

106. de Groot, R. J. *et al.* Evidence for a coiled-coil structure in the spike proteins of coronaviruses. *J. Mol. Biol.* **196,** 963–966 (1987).
107. Ziebuhr, J., Snijder, E. J. & Gorbalenya, A. E. Virus-encoded proteinases and proteolytic processing in the Nidovirales. *J. Gen. Virol.* **81,** 853–879 (2000).
108. Bos, E. C., Luytjes, W., van der Meulen, H. V, Koerten, H. K. & Spaan, W. J. The production of recombinant infectious DI-particles of a murine coronavirus in the absence of helper virus. *Virology* **218,** 52–60 (1996).
109. Kindler, E. & Thiel, V. To sense or not to sense viral RNA-essentials of coronavirus innate immune evasion. *Curr. Opin. Microbiol.* **20,** 69–75 (2014).
110. Züst, R. *et al.* Ribose 2'-O-methylation provides a molecular signature for the distinction of self and non-self mRNA dependent on the RNA sensor Mda5. *Nat. Immunol.* **12,** 137–143 (2011).
111. Bouvet, M. *et al.* RNA 3'-end mismatch excision by the severe acute respiratory syndrome coronavirus nonstructural protein nsp10/nsp14 exoribonuclease complex. *Proc. Natl. Acad. Sci. U. S. A.* **109,** 9372–9377 (2012).
112. Denison, M. R., Graham, R. L., Donaldson, E. F., Eckerle, L. D. & Baric, R. S. Coronaviruses: An RNA proofreading machine regulates replication fidelity and diversity. *RNA Biol.* **8,** 270–279 (2011).
113. Li, S.-W. *et al.* SARS coronavirus papain-like protease inhibits the TLR7 signalling pathway through removing Lys63-linked polyubiquitination of TRAF3 and TRAF6. *Int. J. Mol. Sci.* **17,** (2016).
114. Chen, X. *et al.* SARS coronavirus papain-like protease inhibits the type I interferon signalling pathway through interaction with the STING-TRAF3-TBK1 complex. *Protein Cell* **5,** 369–381 (2014).
115. Brown, M. A. Genetic determinants of pathogenesis by feline infectious peritonitis virus. *Vet. Immunol. Immunopathol.* **143,** 265–268 (2011).
116. Drake, J. W. & Holland, J. J. Mutation rates among RNA viruses. *Proc. Natl. Acad. Sci. U. S. A.* **96,** 13910–13913 (1999).
117. Salemi, M. *et al.* Severe acute respiratory syndrome coronavirus sequence characteristics and evolutionary rate estimate from maximum likelihood analysis. *J. Virol.* **78,** 1602–1603 (2004).
118. Battilani, M. *et al.* Quasispecies composition and phylogenetic analysis of feline coronaviruses (FCoVs) in naturally infected cats. *FEMS Immunol. Med. Microbiol.* **39,** 141–147 (2003).
119. Gunn-Moore, D. A., Gunn-Moore, F. J., Gruffydd-Jones, T. J. & Harbour, D. A. Detection of FCoV quasispecies using denaturing gradient gel electrophoresis. *Vet. Microbiol.* **69,** 127–130 (1999).
120. Phillips, J. E., Hilt, D. A. & Jackwood, M. W. Comparative sequence analysis of full-length genome of FIPV at different tissue passage levels. *Virus Genes* **47,** 490–497 (2013).
121. Poland, A. M., Vennema, H. & Foley, J. E. Two related strains of feline infectious peritonitis virus isolated from immunocompromised cats infected with a feline enteric coronavirus. *J. Clin. Microbiol.* **34,** 3180–3184 (1996).
122. Bálint, Á. *et al.* Molecular characterization of feline infectious peritonitis virus strain DF-2 and studies of the role of ORF3abc in viral cell tropism. *J. Virol.* **86,** 6258–6267 (2012).
123. Hsieh, L.-E. *et al.* 3C protein of feline coronavirus inhibits viral replication independently of the autophagy pathway. *Res. Vet. Sci.* **95,** 1241–1247 (2013).
124. Chang, H.-W., de Groot, R. J., Egberink, H. F. & Rottier, P. J. M. Feline infectious peritonitis: Insights into feline coronavirus pathobiogenesis and epidemiology based on genetic analysis of the viral 3c gene. *J. Gen. Virol.* **91,** 415–420 (2010).
125. Borschensky, C. M. & Reinacher, M. Mutations in the 3c and 7b genes of feline coronavirus in spontaneously affected FIP cats. *Res. Vet. Sci.* **97,** 333–340 (2014).
126. Pedersen, N. C. *et al.* Feline infectious peritonitis: role of the feline coronavirus 3c gene in intestinal tropism and pathogenicity based upon isolates from resident and adopted shelter cats. *Virus Res.* **165,** 17–28 (2012).
127. Dedeurwaerder, A. *et al.* The role of accessory proteins in the replication of feline infectious peritonitis virus in peripheral blood monocytes. *Vet. Microbiol.* **162,** 447–455 (2013).
128. Lin, C. N. *et al.* Field strain feline coronaviruses with small deletions in ORF7b associated with both enteric infection and feline infectious peritonitis. *J. Feline Med. Surg.* (2009). doi:10.1016/j.jfms.2008.09.004
129. Dedeurwaerder, A. *et al.* ORF7-encoded accessory protein 7a of feline infectious peritonitis virus as a counteragent against IFN-alpha induced antiviral response. *J. Gen. Virol.* **95,** 393–402 (2014).
130. Licitra, B. N. *et al.* Mutation in spike protein cleavage site and pathogenesis of feline coronavirus. *Emerg. Infect. Dis.* **19,** 1066–1073 (2013).
131. Rottier, P. J. M., Nakamura, K., Schellen, P., Volders, H. & Haijema, B. J. Acquisition of macrophage tropism during the pathogenesis of feline infectious peritonitis is determined by mutations in the feline coronavirus spike protein. *J. Virol.* **79,** 14122–14130 (2005).
132. Chang, H.-W., Egberink, H. F., Halpin, R., Spiro, D. J. & Rottier, P. J. M. Spike protein fusion peptide and feline coronavirus virulence. *Emerg. Infect. Dis.* **18,** 1089–1095 (2012).

133. Porter, E. *et al.* Amino acid changes in the spike protein of feline coronavirus correlate with systemic spread of virus from the intestine and not with feline infectious peritonitis. *Vet. Res.* **45,** 49 (2014).
134. Gunn-Moore, D. A., Caney, S. M., Gruffydd-Jones, T. J., Helps, C. R. & Harbour, D. A. Antibody and cytokine responses in kittens during the development of feline infectious peritonitis (FIP). *Vet. Immunol. Immunopathol.* **65,** 221–242 (1998).
135. Glansbeek, H. L. *et al.* Adverse effects of feline IL-12 during DNA vaccination against feline infectious peritonitis virus. *J. Gen. Virol.* **83,** 1–10 (2002).
136. Haijema, B. J., Volders, H. & Rottier, P. J. M. Live, attenuated coronavirus vaccines through the directed deletion of group-specific genes provide protection against feline infectious peritonitis. *J. Virol.* **78,** 3863–3871 (2004).
137. Bálint, Á., Farsang, A., Szeredi, L., Zádori, Z. & Belák, S. Recombinant feline coronaviruses as vaccine candidates confer protection in SPF but not in conventional cats. *Vet. Microbiol.* **169,** 154–162 (2014).
138. Klotz, D., Baumgärtner, W. & Gerhauser, I. Type I interferons in the pathogenesis and treatment of canine diseases. *Vet. Immunol. Immunopathol.* **191,** 80–93 (2017).
139. Lin, F. & Young, H. A. Interferons: Success in anti-viral immunotherapy. *Cytokine Growth Factor Rev.* **25,** 369–376 (2014).
140. Leal, R. & Gil, S. The Use of Recombinant Feline Interferon Omega Therapy as an Immune-Modulator in Cats Naturally Infected with Feline Immunodeficiency Virus: New Perspectives. *Vet. Sci.* **3,** 32 (2016).
141. Ritz, S., Egberink, H. & Hartmann, K. Effect of feline interferon-omega on the survival time and quality of life of cats with feline infectious peritonitis. *J. Vet. Intern. Med.* **21,** 1193–1197 (2007).
142. Ishida, T., Shibanai, A., Tanaka, S., Uchida, K. & Mochizuki, M. Use of recombinant feline interferon and glucocorticoid in the treatment of feline infectious peritonitis. *J. Feline Med. Surg.* **6,** 107–109 (2004).
143. Hartmann, K. & Ritz, S. Treatment of cats with feline infectious peritonitis. *Vet. Immunol. Immunopathol.* **123,** 172–175 (2008).
144. Tanaka, Y. *et al.* Suppression of feline coronavirus replication in vitro by cyclosporin A. *Vet. Res.* **43,** 41 (2012).
145. Tanaka, Y., Sato, Y. & Sasaki, T. Suppression of coronavirus replication by cyclophilin inhibitors. *Viruses* **5,** 1250–1260 (2013).
146. Qureshi, A., Tantray, V. G., Kirmani, A. R. & Ahangar, A. G. A review on current status of antiviral siRNA. *Rev. Med. Virol.* **28,** e1976 (2018).
147. Shah, P. S. & Schaffer, D. V. Antiviral RNAi: Translating science towards therapeutic success. *Pharm. Res.* **28,** 2966–2982 (2011).
148. McDonagh, P., Sheehy, P. A. & Norris, J. M. Combination siRNA therapy against feline coronavirus can delay the emergence of antiviral resistance in vitro. *Vet. Microbiol.* **176,** 10–18 (2015).
149. Doki, T., Takano, T., Kawagoe, K., Kito, A. & Hohdatsu, T. Therapeutic effect of anti-feline TNF-alpha monoclonal antibody for feline infectious peritonitis. *Res. Vet. Sci.* **104,** (2016).
150. Fischer, Y., Ritz, S., Weber, K., Sauter-Louis, C. & Hartmann, K. Randomized, placebo controlled study of the effect of propentofylline on survival time and quality of life of cats with feline infectious peritonitis. *J. Vet. Intern. Med.* **25,** 1270–1276 (2011).
151. Takano, T. *et al.* The cholesterol transport inhibitor U18666A inhibits type I feline coronavirus infection. *Antiviral Res.* **145,** 96–102 (2017).
152. Weiss, R. C., Cox, N. R. & Boudreaux, M. K. Toxicologic effects of ribavirin in cats. *J. Vet. Pharmacol. Ther.* **16,** 301–316 (1993).
153. Madewell, B. R., Crow, S. E. & Nickerson, T. R. Infectious peritonitis in a cat that subsequently developed a myeloproliferative disorder. *J. Am. Vet. Med. Assoc.* **172,** 169–172 (1978).
154. Watari, T., Kaneshima, T., Tsujimoto, H., Ono, K. & Hasegawa, A. Effect of thromboxane synthetase inhibitor on feline infectious peritonitis in cats. *J. Vet. Med. Sci.* **60,** 657–659 (1998).
155. Kim, Y. *et al.* Reversal of the Progression of Fatal Coronavirus Infection in Cats by a Broad-Spectrum Coronavirus Protease Inhibitor. *PLoS Pathog.* **12,** (2016).
156. Kim, Y., Mandadapu, S. R., Groutas, W. C. & Chang, K.-O. Potent inhibition of feline coronaviruses with peptidyl compounds targeting coronavirus 3C-like protease. *Antiviral Res.* **97,** 161–168 (2013).
157. Pedersen, N. C. *et al.* Efficacy of a 3C-like protease inhibitor in treating various forms of acquired feline infectious peritonitis. *J. Feline Med. Surg.* **20,** 378–392 (2018).
158. Travis, J. On the origin of the immune system. *Science (80-.).* **326,** 580–583 (2009).
159. Carpenter, S. & O'Neill, L. A. J. How important are Toll-like receptors for antimicrobial responses? *Cell. Microbiol.* **9,** 1891–1901 (2007).
160. O'Neill, L. A. J. & Bowie, A. G. Sensing and signalling in antiviral innate immunity. *Curr. Biol.* **20,** R328–R333 (2010).
161. Wiens, M. *et al.* Toll-like receptors are part of the innate immune defense system of sponges

(demospongiae: Porifera). *Mol. Biol. Evol.* **24,** 792–804 (2007).
162. Padmanabhan, M., Cournoyer, P. & Dinesh-Kumar, S. P. The leucine-rich repeat domain in plant innate immunity: a wealth of possibilities. *Cell. Microbiol.* **11,** 191–198 (2009).
163. Kawai, T. & Akira, S. Toll-like receptors and their crosstalk with other innate receptors in infection and immunity. *Immunity* **34,** 637–650 (2011).
164. Iwasaki, A. & Medzhitov, R. Toll-like receptor control of the adaptive immune responses. *Nat. Immunol.* **5,** 987–995 (2004).
165. Ignacio, G., Nordone, S., Howard, K. E. & Dean, G. A. Toll-like receptor expression in feline lymphoid tissues. *Vet. Immunol. Immunopathol.* **106,** 229–237 (2005).
166. Franchini, M. *et al.* Feline pancreatic islet-like clusters and insulin producing cells express functional Toll-like receptors (TLRs). *Vet. Immunol. Immunopathol.* **138,** 70–78 (2010).
167. Robert-Tissot, C. *et al.* Stimulation with a class A CpG oligonucleotide enhances resistance to infection with feline viruses from five different families. *Vet. Res.* **43,** 60 (2012).
168. Watanabe, R., Eckstrand, C., Liu, H. & Pedersen, N. C. Characterization of peritoneal cells from cats with experimentally-induced feline infectious peritonitis (FIP) using RNA-seq. *Vet. Res.* **49,** 81 (2018).
169. Arpaia, N. & Barton, G. M. Toll-like receptors: key players in antiviral immunity. *Curr. Opin. Virol.* **1,** 447–454 (2011).
170. Iwasaki, A. & Medzhitov, R. Regulation of Adaptive Immunity by the Innate Immune System. *Science (80-.).* **327,** 291–296 (2010).
171. Jurk, M. *et al.* Human TLR7 or TLR8 independently confer responsiveness to the antiviral compound R-848 [1]. *Nat. Immunol.* **3,** 499 (2002).
172. Kawasaki, T. & Kawai, T. Toll-like receptor signalling pathways. *Front. Immunol.* **5,** (2014).
173. Carty, M. & Bowie, A. G. Recent insights into the role of Toll-like receptors in viral infection. *Clin. Exp. Immunol.* **161,** 397–406 (2010).
174. Dosch, S. F., Mahajan, S. D. & Collins, A. R. SARS coronavirus spike protein-induced innate immune response occurs via activation of the NF-kappaB pathway in human monocyte macrophages in vitro. *Virus Res.* **142,** 19–27 (2009).
175. Mazaleuskaya, L., Veltrop, R., Ikpeze, N., Martin-Garcia, J. & Navas-Martin, S. Protective role of Toll-like Receptor 3-induced type I interferon in murine coronavirus infection of macrophages. *Viruses* **4,** 901–923 (2012).
176. Totura, A. L. *et al.* Toll-like receptor 3 signalling via TRIF contributes to a protective innate immune response to severe acute respiratory syndrome coronavirus infection. *MBio* **6,** e00638-15 (2015).
177. Poltorak, A. *et al.* Defective LPS signalling in C3H/HeJ and C57BL/10ScCr mice: mutations in Tlr4 gene. *Science (80-.).* **282,** 2085–2088 (1998).
178. Blasius, A. L. & Beutler, B. Intracellular Toll-like receptors. *Immunity* **32,** 305–315 (2010).
179. Kawai, T. & Akira, S. The role of pattern-recognition receptors in innate immunity: update on Toll-like receptors. *Nat. Immunol.* **11,** 373–384 (2010).
180. Lester, S. N. & Li, K. Toll-like receptors in antiviral innate immunity. *J. Mol. Biol.* **426,** 1246–1264 (2014).
181. Barbalat, R., Ewald, S. E., Mouchess, M. L. & Barton, G. M. Nucleic acid recognition by the innate immune system. *Annu. Rev. Immunol.* **29,** 185–214 (2011).
182. Weber, F., Wagner, V., Rasmussen, S. B., Hartmann, R. & Paludan, S. R. Double-stranded RNA is produced by positive-strand RNA viruses and DNA viruses but not in detectable amounts by negative-strand RNA viruses. *J. Virol.* **80,** 5059–5064 (2006).
183. Hu, W., Yen, Y.-T., Singh, S., Kao, C.-L. & Wu-Hsieh, B. A. SARS-CoV Regulates Immune Function-Related Gene Expression in Human Monocytic Cells. *Viral Immunol.* **25,** 277–288 (2012).
184. Heil, F. *et al.* Species-specific recognition of single-stranded RNA via Toll-like receptor 7 and 8. *Science (80-.).* **303,** 1526–1529 (2004).
185. McKenna, K., Beignon, A.-S. & Bhardwaj, N. Plasmacytoid dendritic cells: linking innate and adaptive immunity. *J. Virol.* **79,** 17–27 (2005).
186. Honda, K. *et al.* Spatiotemporal regulation of MyD88-IRF-7 signalling for robust type-I interferon induction. *Nature* **434,** 1035–1040 (2005).
187. Shortman, K., Sathe, P., Vremec, D., Naik, S. & O'Keeffe, M. Plasmacytoid dendritic cell development. *Adv. Immunol.* **120,** 105–126 (2013).
188. Summerfield, A., Auray, G. & Ricklin, M. Comparative dendritic cell biology of veterinary mammals. *Annu. Rev. Anim. Biosci.* **3,** 533–557 (2015).
189. Reizis, B., Bunin, A., Ghosh, H. S., Lewis, K. L. & Sisirak, V. Plasmacytoid dendritic cells: recent progress and open questions. *Annu. Rev. Immunol.* **29,** 163–183 (2011).
190. Laver, W. G. *et al.* The mechanism of antigenic drift in influenza virus: sequence changes in the haemagglutinin of variants selected with monoclonal hybridoma antibodies. *Philos. Trans. R. Soc. Lond.*

B. Biol. Sci. **288,** 313–326 (1980).
191. Anderson, C. S. *et al.* Natural and directed antigenic drift of the H1 influenza virus hemagglutinin stalk domain. *Sci. Rep.* **7,** 14614 (2017).
192. Barbalat, R., Lau, L., Locksley, R. M. & Barton, G. M. Toll-like receptor 2 on inflammatory monocytes induces type I interferon in response to viral but not bacterial ligands. *Nat. Immunol.* **10,** 1200–1207 (2009).
193. Hemmi, H. *et al.* A Toll-like receptor recognizes bacterial DNA. *Nature* **408,** 740–745 (2000).
194. Krieg, A. M. Lymphocyte activation by CpG dinucleotide motifs in prokaryotic DNA. *Trends Microbiol.* **4,** 73–77 (1996).
195. Lai, J. *et al.* Infection with the dengue RNA virus activates TLR9 signalling in human dendritic cells. *EMBO Rep.* e46182 (2018). doi:10.15252/embr.201846182
196. Ng, L. F. *et al.* A human in vitro model system for investigating genome-wide host responses to SARS coronavirus infection. *BMC Infect. Dis.* **4,** 34 (2004).
197. Yasuda, K. *et al.* Endosomal translocation of vertebrate DNA activates dendritic cells via TLR9-dependent and -independent Pathways. *J. Immunol.* **174,** 6129–6136 (2005).
198. Yasuda, K. *et al.* CpG motif-independent activation of TLR9 upon endosomal translocation of 'natural' phosphodiester DNA. *Eur. J. Immunol.* **36,** 431–436 (2006).
199. Zhang, Q. *et al.* Circulating mitochondrial DAMPs cause inflammatory responses to injury. *Nature* **464,** 104–107 (2010).
200. Banchereau, J. & Steinman, R. M. Dendritic cells and the control of immunity. *Nature* **392,** 245–252 (1998).
201. Janeway, C. A. & Medzhitov, R. Innate immune recognition. *Annu. Rev. Immunol.* **20,** 197–216 (2002).
202. Hennessy, E. J., Parker, A. E. & O'Neill, L. A. J. Targeting Toll-like receptors: emerging therapeutics? *Nat. Rev. Drug Discov.* **9,** 293–307 (2010).
203. Jensen, S. & Thomsen, A. R. Sensing of RNA viruses: a review of innate immune receptors involved in recognizing RNA virus invasion. *J. Virol.* **86,** 2900–2910 (2012).
204. Dinarello, C. A. Historical Review of Cytokines. *Eur. J. Immunol.* **37,** S34–S45 (2007).
205. Vanha-aho, L. M., Valanne, S. & Rämet, M. Cytokines in Drosophila immunity. *Immunol. Lett.* **170,** 42–51 (2016).
206. Dinarello, C. A. Overview of the IL-1 family in innate inflammation and acquired immunity. *Immunol. Rev.* **281,** 8–27 (2018).
207. Akdis, M. *et al.* Interleukins, from 1 to 37, and interferon-γ: Receptors, functions, and roles in diseases. *J. Allergy Clin. Immunol.* **127,** 701–721 (2011).
208. Kaiko, G. E., Horvat, J. C., Beagley, K. W. & Hansbro, P. M. Immunological decision-making: How does the immune system decide to mount a helper T-cell response? *Immunology* **123,** 326–338 (2008).
209. Korn, T., Bettelli, E., Oukka, M. & Kuchroo, V. K. IL-17 and Th17 Cells. *Annu. Rev. Immunol.* **27,** 485–517 (2009).
210. Grogan, J. L. *et al.* Early transcription and silencing of cytokine genes underlie polarization of T helper cell subsets. *Immunity* **14,** 205–215 (2001).
211. Turner, M. D., Nedjai, B., Hurst, T. & Pennington, D. J. Cytokines and chemokines: At the crossroads of cell signalling and inflammatory disease. *Biochim. Biophys. Acta* **1843,** 2563–2582 (2014).
212. Schroder, K., Zhou, R. & Tschopp, J. The NLRP3 inflammasome: a sensor for metabolic danger? *Science (80-.).* **327,** 296–300 (2010).
213. Dinarello, C. A., Renfer, L. & Wolff, S. M. Human leukocytic pyrogen: purification and development of a radioimmunoassay. *Proc. Natl. Acad. Sci. U. S. A.* **74,** 4624–4627 (1977).
214. Kishimoto, T. & Ishizaka, K. Regulation of antibody response in vitro. VII. Enhancing soluble factors for IgG and IgE antibody response. *J Immunol* **111,** 1194–1205 (1973).
215. Kishimoto, T. IL-6: From its discovery to clinical applications. *Int. Immunol.* **22,** 347–352 (2010).
216. Tanaka, T., Narazaki, M. & Kishimoto, T. IL-6 in inflammation, immunity, and disease. *Cold Spring Harb. Perspect. Biol.* **6,** 1–16 (2014).
217. Heinrich, P. C., Castell, J. V & Andus, T. Interleukin-6 and the acute phase response. *Biochem. J.* **265,** 621–636 (1990).
218. Maruo, N., Morita, I., Shirao, M. & Murota, S. IL-6 increases endothelial permeability in vitro. *Endocrinology* **131,** 710–714 (1992).
219. Okada, M. *et al.* IL-6/BSF-2 functions as a killer helper factor in the in vitro induction of cytotoxic T cells. *J. Immunol.* **141,** 1543–1549 (1988).
220. Akira, S., Taga, T. & Kishimoto, T. Interleukin-6 in biology and medicine. *Adv. Immunol.* **54,** 1–78 (1993).
221. Ray, A. & Prefontaine, K. E. Physical association and functional antagonism between the p65 subunit of transcription factor NF-kappa B and the glucocorticoid receptor. *Proc. Natl. Acad. Sci. U. S. A.* **91,** 752–

756 (1994).
222. Aoki, Y., Narazaki, M., Kishimoto, T. & Tosato, G. Receptor engagement by viral interleukin-6 encoded by Kaposi sarcoma-associated herpesvirus. *Blood* **98,** 3042–3049 (2001).
223. Kishimoto, T., Akira, S. & Taga, T. Interleukin-6 and its receptor: A paradigm for cytokines. *Science (80-.).* **258,** 593–597 (1992).
224. Taga, T. & Kishimoto, T. Gp130 and the interleukin-6 family of cytokines. *Annu. Rev. Immunol.* **15,** 797–819 (1997).
225. Hunter, C. A. & Jones, S. A. IL-6 as a keystone cytokine in health and disease. *Nat. Immunol.* **16,** 448–457 (2015).
226. Rose-John, S., Winthrop, K. & Calabrese, L. The role of IL-6 in host defence against infections: immunobiology and clinical implications. *Nat. Rev. Rheumatol.* **13,** 399–409 (2017).
227. Schmitz, J., Weissenbach, M., Haan, S., Heinrich, P. C. & Schaper, F. SOCS3 exerts its inhibitory function on interleukin-6 signal transduction through the SHP2 recruitment site of gp130. *J. Biol. Chem.* **275,** 12848–12856 (2000).
228. Tsuji, M., Goitsuka, R., Hirota, Y. & Hasegawa, A. Chemotactic responses of neutrophils in cats with spontaneous feline infectious peritonitis. *Japanese J. Vet. Sci.* **51,** 917–923 (1989).
229. Goitsuka, R. *et al.* IL-6 activity in feline infectious peritonitis. *J. Immunol.* **144,** 2599–2603 (1990).
230. de Waal Malefyt, R., Abrams, J., Bennett, B., Figdor, C. G. & de Vries, J. E. Interleukin 10 (IL-10) inhibits cytokine synthesis by human monocytes: an autoregulatory role of IL-10 produced by monocytes. *J. Exp. Med.* **174,** 1209–1220 (1991).
231. Ouyang, P. *et al.* IL-10 encoded by viruses: A remarkable example of independent acquisition of a cellular gene by viruses and its subsequent evolution in the viral genome. *J. Gen. Virol.* **95,** 245–262 (2014).
232. Jabri, B. & Abadie, V. IL-15 functions as a danger signal to regulate tissue-resident T cells and tissue destruction. *Nat. Rev. Immunol.* **15,** 771–783 (2015).
233. Mishra, A., Sullivan, L. & Caligiuri, M. A. Molecular pathways: Interleukin-15 signalling in health and in cancer. *Clin. Cancer Res.* **20,** 2044–2050 (2014).
234. Jin, W. & Dong, C. IL-17 cytokines in immunity and inflammation. *Emerg. Microbes Infect.* **2,** e60 (2013).
235. Park, H. *et al.* A distinct lineage of CD4 T cells regulates tissue inflammation by producing interleukin 17. *Nat. Immunol.* **6,** 1133–1141 (2005).
236. Camporeale, A. & Poli, V. IL-6, IL-17 and STAT3: a holy trinity in auto-immunity? *Front. Biosci.* **17,** 2306–2326 (2012).
237. Dong, C. TH17 cells in development: An updated view of their molecular identity and genetic programming. *Nat. Rev. Immunol.* **8,** 337–348 (2008).
238. Micheau, O. & Tschopp, J. Induction of TNF receptor I-mediated apoptosis via two sequential signalling complexes. *Cell* **114,** 181–190 (2003).
239. Olyslaegers, D. A. J. *et al.* Altered expression of adhesion molecules on peripheral blood leukocytes in feline infectious peritonitis. *Vet. Microbiol.* **166,** 438–449 (2013).
240. Takano, T., Hohdatsu, T., Toda, A., Tanabe, M. & Koyama, H. TNF-alpha, produced by feline infectious peritonitis virus (FIPV)-infected macrophages, upregulates expression of type II FIPV receptor feline aminopeptidase N in feline macrophages. *Virology* **364,** 64–72 (2007).
241. Safi, N. *et al.* Expression profiles of immune mediators in feline Coronavirus-infected cells and clinical samples of feline Coronavirus-positive cats. *BMC Vet. Res.* **13,** 92 (2017).
242. Harun, M. S. R. *et al.* Transcriptional profiling of feline infectious peritonitis virus infection in CRFK cells and in PBMCs from FIP diagnosed cats. *Virol. J.* **10,** 329 (2013).
243. Ge, B. *et al.* Functional expression of CCL8 and its interaction with chemokine receptor CCR3. *BMC Immunol.* **18,** 4–11 (2017).
244. Moser, B., Wolf, M., Walz, A. & Loetscher, P. Chemokines: Multiple levels of leukocyte migration control. *Trends Immunol.* **25,** 75–84 (2004).
245. Travis, M. A. & Sheppard, D. TGF-β activation and function in immunity. *Annu. Rev. Immunol.* **32,** 51–82 (2014).
246. Mu, Y., Gudey, S. K. & Landström, M. Non-Smad signalling pathways. *Cell Tissue Res.* **347,** 11–20 (2012).
247. Shull, M. M. *et al.* Targeted disruption of the mouse transforming growth factor-beta 1 gene results in multifocal inflammatory disease. *Nature* **359,** 693–699 (1992).
248. Sanjabi, S., Mosaheb, M. M. & Flavell, R. A. Opposing effects of TGF-beta and IL-15 cytokines control the number of short-lived effector CD8+ T cells. *Immunity* **31,** 131–144 (2009).
249. Tinoco, R., Alcalde, V., Yang, Y., Sauer, K. & Zuniga, E. I. Cell-intrinsic transforming growth factor-beta signalling mediates virus-specific CD8+ T cell deletion and viral persistence in vivo. *Immunity* **31,** 145–157 (2009).
250. Cerwenka, A., Kovar, H., Majdic, O. & Holter, W. Fas- and activation-induced apoptosis are reduced in

human T cells preactivated in the presence of TGF-beta 1. *J. Immunol.* **156,** 459–464 (1996).
251. Shuid, A. N. *et al.* Apoptosis transcriptional mechanism of feline infectious peritonitis virus infected cells. *Apoptosis* **20,** 1457–1470 (2015).
252. Hansen, G. *et al.* CD4(+) T helper cells engineered to produce latent TGF-beta1 reverse allergen-induced airway hyperreactivity and inflammation. *J. Clin. Invest.* **105,** 61–70 (2000).
253. Pestka, S., Krause, C. D. & Walter, M. R. Interferons, interferon-like cytokines, and their receptors. *Immunol. Rev.* **202,** 8–32 (2004).
254. Stetson, D. B. & Medzhitov, R. Type I interferons in host defense. *Immunity* **25,** 373–381 (2006).
255. Barton, G. M., Kagan, J. C. & Medzhitov, R. Intracellular localization of Toll-like receptor 9 prevents recognition of self DNA but facilitates access to viral DNA. *Nat. Immunol.* **7,** 49–56 (2006).
256. Schneider, W. M., Chevillotte, M. D. & Rice, C. M. Interferon-stimulated genes: a complex web of host defenses. *Annu. Rev. Immunol.* **32,** 513–545 (2014).
257. Berg, A.-L., Ekman, K., Belák, S. & Berg, M. Cellular composition and interferon-gamma expression of the local inflammatory response in feline infectious peritonitis (FIP). *Vet. Microbiol.* **111,** 15–23 (2005).
258. Giordano, A. & Paltrinieri, S. Interferon-gamma in the serum and effusions of cats with feline coronavirus infection. *Vet. J.* **180,** 396–398 (2009).
259. Gelain, M. E., Meli, M. & Paltrinieri, S. Whole blood cytokine profiles in cats infected by feline coronavirus and healthy non-FCoV infected specific pathogen-free cats. *J. Feline Med. Surg.* **8,** 389–399 (2006).
260. Platanias, L. C. Mechanisms of type-I- and type-II-interferon-mediated signalling. *Nat. Rev. Immunol.* **5,** 375–386 (2005).
261. Schoenborn, J. R. & Wilson, C. B. Regulation of interferon-γ during innate and adaptive immune responses. *Adv. Immunol.* **96,** 41–101 (2007).
262. Valente, G. *et al.* Distribution of interferon-γ receptor in human tissues. *Eur. J. Immunol.* **22,** 2403–2412 (1992).
263. Green, D. S., Young, H. A. & Valencia, J. C. Current prospects of type II interferon γ signalling & autoimmunity. *J. Biol. Chem.* **292,** 13925–13933 (2017).
264. Homberger, F. R. Enterotropic mouse hepatitis virus. *Lab. Anim.* **31,** 97–115 (1997).
265. Kyuwa, S. *et al.* Murine coronavirus-induced subacute fatal peritonitis in C57BL/6 mice deficient in gamma interferon. *J. Virol.* **72,** 9286–9290 (1998).
266. France, M. P., Smith, A. L., Stevenson, R. & Barthold, S. W. Granulomatous peritonitis and pleuritis in interferon-γ gene knockout mice naturally infected with mouse hepatitis virus. *Aust. Vet. J.* **77,** 600–604 (1999).
267. Kyuwa, S. *et al.* MHV-induced fatal peritonitis in mice lacking IFN-gamma. *Adv. Exp. Med. Biol.* **440,** 445–450 (1998).
268. Ushach, I. & Zlotnik, A. Biological role of granulocyte macrophage colony-stimulating factor (GM-CSF) and macrophage colony-stimulating factor (M-CSF) on cells of the myeloid lineage. *J. Leukoc. Biol.* **100,** 481–489 (2016).
269. Hamilton, J. A. Colony-stimulating factors in inflammation and autoimmunity. *Nat. Rev. Immunol.* **8,** 533–544 (2008).
270. Conti, L. & Gessani, S. GM-CSF in the generation of dendritic cells from human blood monocyte precursors: Recent advances. *Immunobiology* **213,** 859–870 (2008).
271. Weischenfeldt, J. & Porse, B. Bone marrow-derived macrophages (BMM): Isolation and applications. *Cold Spring Harb. Protoc.* **3,** 1–7 (2008).
272. Gomis-Rüth, F. X. Catalytic Domain Architecture of Metzincin Metalloproteases. *J. Biol. Chem.* **284,** 15353–15357 (2009).
273. Fanjul-Fernández, M., Folgueras, A. R., Cabrera, S. & López-Otín, C. Matrix metalloproteinases: Evolution, gene regulation and functional analysis in mouse models. *Biochim. Biophys. Acta* **1803,** 3–19 (2010).
274. Gearing, A. *et al.* Processing of tumour necrosis factor-alpha precursor by metalloproteinases. *Lett. to Nat.* **370,** 555–557 (1994).
275. Overall, C. M. Molecular determinants of metalloproteinase substrate specificity: matrix metalloproteinase substrate binding domains, modules, and exosites. *Mol. Biotechnol.* **22,** 51–86 (2002).
276. McQuibban, G. A. *et al.* Matrix metalloproteinase processing of monocyte chemoattractant proteins generates CC chemokine receptor antagonists with anti-inflammatory properties in vivo. *Blood* **100,** 1160–1167 (2002).
277. Page-McCaw, A., Ewald, A. J. & Werb, Z. Matrix metalloproteinases and the regulation of tissue remodelling. *Nat. Rev. Mol. Cell Biol.* **8,** 221–233 (2007).
278. Yan, C. & Boyd, D. D. Regulation of matrix metalloproteinase gene expression. *J. Cell. Physiol.* **211,** 19–26 (2007).
279. Yan, C. & Boyd, D. D. Regulation of matrix metalloproteinase gene expression. *J. Cell. Physiol.* **211,** 19–26

(2007).
280. Vincenti, M. P. & Brinckerhoff, C. E. Signal transduction and cell-type specific regulation of matrix metalloproteinase gene expression: Can MMPs be good for you? *J. Cell. Physiol.* **213,** 355–364 (2007).
281. Uría, J. A., Jiménez, M. G., Balbín, M., Freije, J. M. & López-Otín, C. Differential effects of transforming growth factor-beta on the expression of collagenase-1 and collagenase-3 in human fibroblasts. *J. Biol. Chem.* **273,** 9769–9777 (1998).
282. Leivonen, S.-K., Chantry, A., Hakkinen, L., Han, J. & Kahari, V.-M. Smad3 mediates transforming growth factor-beta-induced collagenase-3 (matrix metalloproteinase-13) expression in human gingival fibroblasts. Evidence for cross-talk between Smad3 and p38 signalling pathways. *J. Biol. Chem.* **277,** 46338–46346 (2002).
283. Nagase, H., Visse, R. & Murphy, G. Structure and function of matrix metalloproteinases and TIMPs. *Cardiovasc. Res.* **69,** 562–573 (2006).
284. Paltrinieri, S. The feline acute phase reaction. *Vet. J.* **177,** 26–35 (2008).
285. Darnell, J. E. STATs and gene regulation. *Science (80-.).* **277,** 1630–1635 (1997).
286. Aaronson, D. S. & Horvath, C. M. A road map for those who don't know JAK-STAT. *Science (80-.).* **296,** 1653–1655 (2002).
287. Murray, P. J. The JAK-STAT signalling pathway: input and output integration. *J. Immunol.* **178,** 2623–2629 (2007).
288. Ji, J. D. *et al.* Inhibition of IL-10-induced STAT3 activation by 15-deoxy-Delta12,14-prostaglandin J2. *Rheumatology (Oxford).* **44,** (2005).
289. Frieman, M. B. *et al.* SARS-CoV pathogenesis is regulated by a STAT1 dependent but a type I, II and III interferon receptor independent mechanism. *PLoS Pathog.* **6,** e1000849 (2010).
290. Schoggins, J. W. & Rice, C. M. Interferon-stimulated genes and their antiviral effector functions. *Curr. Opin. Virol.* **1,** 519–525 (2011).
291. Macpherson, A. J. & Smith, K. Mesenteric lymph nodes at the center of immune anatomy. *J. Exp. Med.* **203,** 497–500 (2006).
292. Henao-Mejia, J., Elinav, E., Thaiss, C. A. & Flavell, R. A. The Intestinal Microbiota in Chronic Liver Disease. *Adv. Immunol.* **117,** 73–97 (2013).
293. Kipar, A., Meli, M. L., Baptiste, K. E., Bowker, L. J. & Lutz, H. Sites of feline coronavirus persistence in healthy cats. *J. Gen. Virol.* **91,** 1698–1707 (2010).
294. Leutenegger, C. M. *et al.* Quantitative real-time PCR for the measurement of feline cytokine mRNA. *Vet. Immunol. Immunopathol.* **71,** 291–305 (1999).
295. Gut, M., Leutenegger, C. M., Huder, J. B., Pedersen, N. C. & Lutz, H. One-tube fluorogenic reverse transcription-polymerase chain reaction for the quantitation of feline coronaviruses. *J. Virol. Methods* **77,** 37–46 (1999).
296. Robert-Tissot, C. *et al.* The innate antiviral immune system of the cat: Molecular tools for the measurement of its state of activation. *Vet. Immunol. Immunopathol.* **143,** 269–281 (2011).
297. Kipar, A. *et al.* Cytokine mRNA levels in isolated feline monocytes. *Vet. Immunol. Immunopathol.* **78,** 305–315 (2001).
298. Taglinger, K., Van Nguyen, N., Helps, C. R., Day, M. J. & Foster, a. P. Quantitative real-time RT-PCR measurement of cytokine mRNA expression in the skin of normal cats and cats with allergic skin disease. *Vet. Immunol. Immunopathol.* **122,** 216–230 (2008).
299. Kuang, J., Yan, X., Genders, A. J., Granata, C. & Bishop, D. J. An overview of technical considerations when using quantitative real-time PCR analysis of gene expression in human exercise research. *PLoS One* **13,** e0196438 (2018).
300. Fonfara, S., Hetzel, U., Hahn, S. & Kipar, A. Age- and gender-dependent myocardial transcription patterns of cytokines and extracellular matrix remodelling enzymes in cats with non-cardiac diseases. *Exp. Gerontol.* **72,** 117–123 (2015).
301. Applied Biosystems. User Bulletin # 2 ABI P RISM 7700 Sequence Detection System SUBJECT : Relative Quantitation of Gene Expression. 1–36 (2001). at <http://linkinghub.elsevier.com/retrieve/pii/S0010945208705197>
302. Cummings, M., Sarveswaran, J., Homer-Vanniasinkam, S., Burke, D. & Orsi, N. M. Glyceraldehyde-3-phosphate Dehydrogenase is an Inappropriate Housekeeping Gene for Normalising Gene Expression in Sepsis. *Inflammation* **37,** 1889–1894 (2014).
303. Kessler, Y. *et al.* Quantitative TaqMan real-time PCR assays for gene expression normalisation in feline tissues. *BMC Mol. Biol.* **10,** 106 (2009).
304. Pfaffl, M. W. A new mathematical model for relative quantification in real-time RT-PCR. *Nucleic Acids Res.* **29,** e45 (2001).
305. Ambion. LCM Staining Kit - AM1935. (2014). at

<https://tools.thermofisher.com/content/sfs/manuals/1935M_LCMStaining_UG.pdf>
306. Cummings, M. *et al.* A robust RNA integrity-preserving staining protocol for laser capture microdissection of endometrial cancer tissue. *Anal. Biochem.* **416,** 123–125 (2011).
307. Applied Biosystems. RNAqueous Micro Kit - Micro Scale RNA Isolation Kit. (2010). at <https://tools.thermofisher.com/content/sfs/manuals/cms_057352.pdf>
308. Bolger, A. M., Lohse, M. & Usadel, B. Trimmomatic: A flexible trimmer for Illumina sequence data. *Bioinformatics* **30,** 2114–2120 (2014).
309. Dobin, A. *et al.* STAR: Ultrafast universal RNA-seq aligner. *Bioinformatics* **29,** 15–21 (2013).
310. Lawrence, M. *et al.* Software for Computing and Annotating Genomic Ranges. *PLoS Comput. Biol.* **9,** 1–10 (2013).
311. Robinson, M. D., McCarthy, D. J. & Smyth, G. K. edgeR: A Bioconductor package for differential expression analysis of digital gene expression data. *Bioinformatics* **26,** 139–140 (2009).
312. Li, B. & Dewey, C. N. RSEM: Accurate transcript quantification from RNA-Seq data with or without a reference genome. *BMC Bioinformatics* **12,** (2011).
313. Herrewegh, A. A. *et al.* Detection of feline coronavirus RNA in feces, tissues, and body fluids of naturally infected cats by reverse transcriptase PCR. *J. Clin. M* **33,** 684–689 (1995).
314. Bateman, A. *et al.* UniProt: the universal protein knowledgebase. *Nucleic Acids Res.* **45,** D158–D169 (2017).
315. Supek, F., Bošnjak, M., Škunca, N. & Šmuc, T. REVIGO Summarizes and Visualizes Long Lists of Gene Ontology Terms. *PLoS One* **6,** e21800 (2011).
316. Meli, M. *et al.* High viral loads despite absence of clinical and pathological findings in cats experimentally infected with feline coronavirus (FCoV) type I and in naturally FCoV-infected cats. *J. Feline Med. Surg.* **6,** 69–81 (2004).
317. Hayashi, T., Goto, N., Takahashi, R. & Fujiwara, K. Systemic vascular lesions in feline infectious peritonitis. *Nihon Juigaku Zasshi.* **39,** 365–377 (1977).
318. Beutler, B. A. TLRs and innate immunity. *Blood* **113,** 1399–1407 (2009).
319. Schindler, C., Levy, D. E. & Decker, T. JAK-STAT signalling: from interferons to cytokines. *J. Biol. Chem.* **282,** 20059–20063 (2007).
320. de Groot-Mijnes, J. D. F., van Dun, J. M., van der Most, R. G. & de Groot, R. J. Natural history of a recurrent feline coronavirus infection and the role of cellular immunity in survival and disease. *J. Virol.* **79,** 1036–1044 (2005).
321. Hsiao, H.-B. *et al.* Toll-like receptor 9-mediated protection of enterovirus 71 infection in mice is due to the release of danger-associated molecular patterns. *J. Virol.* **88,** 11658–11670 (2014).
322. Xia, C., Braunstein, Z., Toomey, A. C., Zhong, J. & Rao, X. S100 proteins as an important regulator of macrophage inflammation. *Front. Immunol.* **8,** 1–11 (2018).
323. Bianchi, M. E. DAMPs, PAMPs and alarmins: all we need to know about danger. *J. Leukoc. Biol.* **81,** 1–5 (2006).
324. Foell, D., Wittkowski, H., Vogl, T. & Roth, J. S100 proteins expressed in phagocytes: a novel group of damage-associated molecular pattern molecules. *J. Leukoc. Biol.* **81,** 28–37 (2006).
325. Yang, H., Wang, H., Czura, C. J. & Tracey, K. J. The cytokine activity of HMGB1. *J. Leukoc. Biol.* **78,** 1–8 (2005).
326. Ibrahim, Z., Armour, C. L., Phipps, S. & Sukkar, M. B. RAGE and TLRs: Relatives, friends or neighbours? *Mol. Immunol.* **56,** 739–744 (2013).
327. Vogl, T. *et al.* Mrp8 and Mrp14 are endogenous activators of Toll-like receptor 4, promoting lethal, endotoxin-induced shock. *Nat. Med.* **13,** 1042–1049 (2007).
328. Turovskaya, O. *et al.* RAGE, carboxylated glycans and S100A8/A9 play essential roles in colitis-associated carcinogenesis. *Carcinogenesis* **29,** 2035–2043 (2008).
329. Poston, R. N. & Hussain, I. F. The immunohistochemical heterogeneity of atheroma macrophages: Comparison with lymphoid tissues suggests that recently blood-derived macrophages can be distinguished from longer-resident cells. *J. Histochem. Cytochem.* **41,** 1503–1512 (1993).
330. Basu, S., Dunn, A. & Ward, A. G-CSF: function and modes of action (Review). *Int. J. Mol. Med.* **10,** 3–10 (2002).
331. Takano, T. *et al.* Neutrophil survival factors (TNF-alpha, GM-CSF, and G-CSF) produced by macrophages in cats infected with feline infectious peritonitis virus contribute to the pathogenesis of granulomatous lesions. *Arch. Virol.* **154,** 775–781 (2009).
332. Teng, G. & Papavasiliou, F. N. Immunoglobulin Somatic Hypermutation. *Annu. Rev. Genet.* **41,** 107–120 (2007).
333. Jacobse-Geels, H. E., Daha, M. R. & Horzinek, M. C. Isolation and characterization of feline C3 and evidence for the immune complex pathogenesis of feline infectious peritonitis. *J. Immunol.* **125,** 1606–

1610 (1980).
334. Takano, T. *et al.* Mutation of neutralizing/antibody-dependent enhancing epitope on spike protein and 7b gene of feline infectious peritonitis virus: influences of viral replication in monocytes/macrophages and virulence in cats. *Virus Res.* **156,** 72–80 (2011).
335. Takano, T. *et al.* Analysis of the mechanism of antibody-dependent enhancement of feline infectious peritonitis virus infection: Aminopeptidase N is not important and a process of acidification of the endosome is necessary. *J. Gen. Virol.* **89,** 1025–1029 (2008).
336. Seillet, C. *et al.* The TLR-mediated response of plasmacytoid dendritic cells is positively regulated by estradiol in vivo through cell-intrinsic estrogen receptor α signalling. *Blood* **119,** 454–464 (2012).
337. Liu, J. *et al.* A five-amino-acid motif in the undefined region of the TLR8 ectodomain is required for species-specific ligand recognition. *Mol. Immunol.* **47,** 1083–1090 (2010).
338. Kadowaki, N. *et al.* Subsets of human dendritic cell precursors express different Toll-like receptors and respond to different microbial antigens. *J. Exp. Med.* **194,** 863–870 (2001).
339. Guilliams, M. *et al.* Dendritic cells, monocytes and macrophages: a unified nomenclature based on ontogeny. *Nat. Rev. Immunol.* **14,** 571–578 (2015).
340. Regan, A. D., Ousterout, D. G. & Whittaker, G. R. Feline lectin activity is critical for the cellular entry of feline infectious peritonitis virus. *J. Virol.* **84,** 7917–7921 (2010).
341. van Berne, A. The role of the dendritic cell in the immunobiology of feline infectious peritonitis. (Utrecht University, 2008).
342. Doyle, S. E. *et al.* Toll-Like receptor 3 mediates a more potent antiviral response than Toll-like receptor 4. *J. Immunol.* **170,** 3565–3571 (2003).
343. Le Goffic, R. *et al.* Detrimental Contribution of the Toll-Like Receptor (TLR)3 to Influenza A Virus–Induced Acute Pneumonia. *PLoS Pathog.* **2,** 525–535 (2006).
344. Han, Y., Bo, Z.-J., Xu, M.-Y., Sun, N. & Liu, D.-H. The Protective Role of TLR3 and TLR9 Ligands in Human Pharyngeal Epithelial Cells Infected with Influenza A Virus. *Korean J. Physiol. Pharmacol.* **18,** 225–231 (2014).
345. Roach, J. C. *et al.* The evolution of vertebrate Toll-like receptors. *Proc. Natl. Acad. Sci.* **102,** 9577–9582 (2005).
346. Hajjar, A. M. *et al.* Cutting Edge: Functional Interactions Between Toll-Like Receptor (TLR) 2 and TLR1 or TLR6 in Response to Phenol-Soluble Modulin. *J. Immunol.* **166,** 15–19 (2001).
347. Wang, Y. & Liu, L. The membrane protein of severe acute respiratory syndrome coronavirus functions as a novel cytosolic pathogen-associated molecular pattern to promote beta interferon induction via a toll-like-receptor-related TRAF3-independent mechanism. *MBio* **7,** 1–14 (2016).
348. Oliveira-Nascimento, L., Massari, P. & Wetzler, L. M. The role of TLR2 in infection and immunity. *Front. Immunol.* **3,** 1–17 (2012).
349. Kurt-Jones, E. A. *et al.* Herpes simplex virus 1 interaction with Toll-like receptor 2 contributes to lethal encephalitis. *Proc. Natl. Acad. Sci.* **101,** 1315–1320 (2004).
350. Khanolkar, A. *et al.* Toll-like receptor 4 deficiency increases disease and mortality after mouse hepatitis virus type 1 infection of susceptible C3H mice. *J. Virol.* **83,** 8946–8956 (2009).
351. Haag, B. A., Hartwig, S. M., Khanolkar, A., Harty, J. T. & Varga, S. M. TLR4-Deficient C3H/HeJ Mice Exhibit Enhanced Disease and Mortality Following Intranasal MHV-1 Infection. *J. Immunol.* **182,** 44.23 (2009).
352. Jude, B. A. *et al.* Subversion of the innate immune system by a retrovirus. *Nat. Immunol.* **4,** 573–578 (2003).
353. van Beijnum, J. R., Buurman, W. A. & Griffioen, A. W. Convergence and amplification of Toll-like receptor (TLR) and receptor for advanced glycation end products (RAGE) signalling pathways via high mobility group B1 (HMGB1). *Angiogenesis* **11,** 91–99 (2008).
354. Pedersen, N. C. An update on feline infectious peritonitis: Virology and immunopathogenesis. *Vet. J.* **201,** 123–132 (2014).
355. Kallinich, T., Wittkowski, H., Keitzer, R., Roth, J. & Foell, D. Neutrophil-derived S100A12 as novel biomarker of inflammation in familial Mediterranean fever. *Ann. Rheum. Dis.* **69,** 677–682 (2010).
356. Giordano, A., Spagnolo, V., Colombo, a. & Paltrinieri, S. Changes in some acute phase protein and immunoglobulin concentrations in cats affected by feline infectious peritonitis or exposed to feline coronavirus infection. *Vet. J.* **167,** 38–44 (2004).
357. Hazuchova, K., Held, S. & Neiger, R. Usefulness of acute phase proteins in differentiating between feline infectious peritonitis and other diseases in cats with body cavity effusions. *J. Feline Med. Surg.* **19,** (2017).
358. Salini, V. *et al.* Inflammatory markers: Serum amyloid A, fibrinogen and C-reactive protein - A revisited study. *Eur. J. Inflamm.* **9,** 95–102 (2011).
359. Kajikawa, T., Furuta, A., Onishi, T., Tajima, T. & Sugii, S. Changes in concentrations of serum amyloid A protein, alpha 1-acid glycoprotein, haptoglobin, and C-reactive protein in feline sera due to induced

inflammation and surgery. *Vet. Immunol. Immunopathol.* **68,** 91–98 (1999).
360. Paltrinieri, S., Giordano, A., Ceciliani, F. & Sironi, G. Tissue distribution of a feline AGP related protein (fAGPrP) in cats with feline infectious peritonitis (FIP). *J. Feline Med. Surg.* **6,** 99–105 (2004).
361. Franz, K. M., Neidermyer, W. J., Tan, Y.-J., Whelan, S. P. J. & Kagan, J. C. STING-dependent translation inhibition restricts RNA virus replication. *Proc. Natl. Acad. Sci.* **115,** 201716937 (2018).
362. Reikine, S., Nguyen, J. B. & Modis, Y. Pattern recognition and signalling mechanisms of RIG-I and MDA5. *Front. Immunol.* **5,** 1–7 (2014).
363. Brown, G. D., Willment, J. A. & Whitehead, L. C-type lectins in immunity and homeostasis. *Nat. Rev. Immunol.* **18,** 374–389 (2018).
364. Graham, L. M. *et al.* The C-type lectin receptor CLECSF8 (CLEC4D) is expressed by myeloid cells and triggers cellular activation through syk kinase. *J. Biol. Chem.* **287,** 25964–25974 (2012).
365. Gramberg, T. *et al.* LSECtin interacts with filovirus glycoproteins and the spike protein of SARS coronavirus. *Virology* **340,** 224–236 (2005).
366. Geijtenbeek, T. B. H. & Gringhuis, S. I. Signalling through C-type lectin receptors: shaping immune responses. *Nat. Rev. Immunol.* **9,** 465–479 (2009).
367. Takano, T., Ohyama, T., Kokumoto, A., Satoh, R. & Hohdatsu, T. Vascular endothelial growth factor (VEGF), produced by feline infectious peritonitis (FIP) virus-infected monocytes and macrophages, induces vascular permeability and effusion in cats with FIP. *Virus Res.* **158,** 161–168 (2011).
368. Chaturvedi, A. & Pierce, S. K. How location governs Toll-like receptor signalling. *Traffic* **10,** 621–628 (2009).
369. Takano, T., Katoh, Y., Doki, T. & Hohdatsu, T. Effect of chloroquine on feline infectious peritonitis virus infection in vitro and in vivo. *Antiviral Res.* **99,** 100–107 (2013).
370. Liu, J., Qian, C. & Cao, X. Post-Translational Modification Control of Innate Immunity. *Immunity* **45,** 15–30 (2016).
371. Bhoj, V. G. & Chen, Z. J. Ubiquitylation in innate and adaptive immunity. *Nature* **458,** 430–437 (2009).
372. Dunne, A. & O'Neill, L. New insights into the post-translational modification of Toll-like receptor signalling molecules. *J. Endotoxin Res.* **11,** 325–332 (2005).
373. Carpenter, S. & O'Neill, L. A. J. Recent insights into the structure of Toll-like receptors and post-translational modifications of their associated signalling proteins. *Biochem. J.* **422,** 1–10 (2009).
374. Yang, Y. *et al.* Heat shock protein gp96 is a master chaperone for Toll-like receptors and is important in the innate function of macrophages. *Immunity* **26,** 215–226 (2007).
375. Walsh, C. *et al.* Elucidation of the MD-2/TLR4 interface required for signalling by lipid IVa1. *J. Immunol.* **181,** 1245–1254 (2008).
376. Hershko, A. & Ciechanover, A. The ubiquitin pathway for the degradation of intracellular proteins. *Prog. Nucleic Acid Res. Mol. Biol.* **33,** 19–56, 301 (1986).
377. Martín-Vicente, M., Medrano, L. M., Resino, S., García-Sastre, A. & Martínez, I. TRIM25 in the Regulation of the Antiviral Innate Immunity. *Front. Immunol.* **8,** 1187 (2017).
378. Ozato, K., Shin, D.-M., Chang, T.-H. & Iii, H. C. M. TRIM family proteins and their emerging roles in innate immunity. *Nat. Rev. Immunol.* **8,** 849–860 (2008).
379. Rajsbaum, R., Stoye, J. P. & O'Garra, A. Type I interferon-dependent and -independent expression of tripartite motif proteins in immune cells. *Eur. J. Immunol.* **38,** 619–630 (2008).
380. Gack, M. U. *et al.* TRIM25 RING-finger E3 ubiquitin ligase is essential for RIG-I-mediated antiviral activity. *Nature* **446,** 916–920 (2007).
381. Heikel, G., Choudhury, N. R. & Michlewski, G. The role of Trim25 in development, disease and RNA metabolism. *Biochem. Soc. Trans.* **44,** 1045–1050 (2016).
382. Pauli, E.-K. *et al.* The ubiquitin-specific protease USP15 promotes RIG-I-mediated antiviral signalling by deubiquitylating TRIM25. *Sci. Signal.* **7,** ra3 (2014).
383. Hu, Y. *et al.* The Severe Acute Respiratory Syndrome Coronavirus Nucleocapsid Inhibits Type I Interferon Production by Interfering with TRIM25-Mediated RIG-I Ubiquitination. *J. Virol.* **91,** e02143-16 (2017).
384. van Tol, S., Hage, A., Giraldo, M. I., Bharaj, P. & Rajsbaum, R. The TRIMendous role of TRIMs in virus-host interactions. *Vaccines* **5,** (2017).
385. Bauhofer, O. *et al.* Classical swine fever virus Npro interacts with interferon regulatory factor 3 and induces Its proteasomal degradation. *J. Virol.* **81,** 3087–3096 (2007).
386. Lei, X. *et al.* Cleavage of interferon regulatory factor 7 by enterovirus 71 3C suppresses cellular responses. *J. Virol.* **87,** 1690–1698 (2013).
387. Bhattacharya, P. *et al.* GM-CSF: An immune modulatory cytokine that can suppress autoimmunity. *Cytokine* **75,** 261–271 (2015).
388. Kabelitz, D. Expression and function of Toll-like receptors in T lymphocytes. *Curr. Opin. Immunol.* **19,** 39–45 (2007).

389. Aguzzi, A., Kranich, J. & Krautler, N. J. Follicular dendritic cells: Origin, phenotype, and function in health and disease. *Trends Immunol.* **35,** 105–113 (2014).
390. Buchta, C. M. & Bishop, G. A. Toll-like receptors and B cells: Functions and mechanisms. *Immunol. Res.* **59,** 12–22 (2014).
391. Forsbach, A. *et al.* Identification of RNA Sequence Motifs Stimulating Sequence-Specific TLR8-Dependent Immune Responses. *J. Immunol.* **180,** 3729–3738 (2008).
392. Suthers, A. N. & Sarantopoulos, S. TLR7/TLR9- and B cell receptor-signalling crosstalk: Promotion of potentially dangerous B Cells. *Front. Immunol.* **8,** 1–8 (2017).
393. Das, A. *et al.* Follicular dendritic cell activation by TLR ligands promotes autoreactive B cell responses. *Immunity* **46,** 106–119 (2017).
394. Garin, A. *et al.* Toll-like Receptor 4 Signalling by Follicular Dendritic Cells Is Pivotal for Germinal Center Onset and Affinity Maturation. *Immunity* **33,** 84–95 (2010).
395. Krautler, N. J. *et al.* Follicular dendritic cells emerge from ubiquitous perivascular precursors. *Cell* **150,** 194–206 (2012).
396. Rollins-Raval, M. A., Marafioti, T., Swerdlow, S. H. & Roth, C. G. The number and growth pattern of plasmacytoid dendritic cells vary in different types of reactive lymph nodes: An immunohistochemical study. *Hum. Pathol.* **44,** 1003–1010 (2013).
397. Cervantes-Barragan, L. *et al.* Control of coronavirus infection through plasmacytoid dendritic-cell-derived type I interferon. *Blood* **109,** 1131–1137 (2007).
398. Turner, B. C., Hemmila, E. M., Beauchemin, N. & Holmes, K. V. Receptor-dependent coronavirus infection of dendritic cells. *J. Virol.* **78,** 5486–5490 (2004).
399. Katze, M. G., He, Y. & Gale, M. Viruses and interferon: A fight for supremacy. *Nat. Rev. Immunol.* **2,** 675–687 (2002).
400. Tecchio, C., Micheletti, A. & Cassatella, M. A. Neutrophil-derived cytokines: Facts beyond expression. *Front. Immunol.* **5,** 1–7 (2014).
401. Amini, P. *et al.* An optimised protocol for isolation of RNA from small sections of laser-capture microdissected FFPE tissue amenable for next-generation sequencing. *BMC Mol. Biol.* **18,** (2017).
402. Luger, K., Mäder, A. W., Richmond, R. K., Sargent, D. F. & Richmond, T. J. Crystal structure of the nucleosome core particle at 2.8 Å resolution. *Nature* **389,** 251–260 (1997).
403. Schäfer, A. & Baric, R. Epigenetic landscape during coronavirus infection. *Pathogens* **6,** 8 (2017).
404. Goldberg, A. D., Allis, C. D. & Bernstein, E. Epigenetics: A landscape takes shape. *Cell* **128,** 635–638 (2007).
405. Balakrishnan, L. & Milavetz, B. Epigenetic regulation of viral biological processes. *Viruses* **9,** 346 (2017).
406. Fang, T. C. *et al.* Histone H3 lysine 9 di-methylation as an epigenetic signature of the interferon response. *J. Exp. Med.* **209,** 661–669 (2012).
407. Kaikkonen, M. U., Lam, M. T. Y. & Glass, C. K. Non-coding RNAs as regulators of gene expression and epigenetics. *Cardiovasc. Res.* **90,** 430–440 (2011).
408. Menachery, V. D. *et al.* MERS-CoV and H5N1 influenza virus antagonize antigen presentation by altering the epigenetic landscape. *Proc. Natl. Acad. Sci.* **115,** E1012–E1021 (2018).
409. Sawicki, S. G., Lu, J. H. & Holmes, K. V. Persistent infection of cultured cells with mouse hepatitis virus (MHV) results from the epigenetic expression of the MHV receptor. *J. Virol.* **69,** 5535–5543 (1995).
410. Milne, T. A., Zhao, K. & Hess, J. L. Chromatin immunoprecipitation (ChIP) for analysis of histone modifications and chromatin-associated proteins. *Methods Mol. Biol.* **538,** 409–423 (2009).
411. Mehrbod, P., Harun, M. S. R., Shuid, A. N. & Omar, A. R. Transcriptome analysis of feline infectious peritonitis virus infection. *Coronaviruses Methods Protoc. Methods Mol. Biol.* **1282,** 241–250 (2015).
412. Harun, M. S. R. *et al.* Transcriptional profiling of feline infectious peritonitis virus infection in CRFK cells and in PBMCs from FIP diagnosed cats. *Virol. J.* **10,** 1–9 (2013).
413. Rakyan, V. K., Down, T. A., Balding, D. J. & Beck, S. Epigenome-wide association studies for common human diseases. *Nat. Rev. Genet.* **12,** 529–541 (2011).
414. Felten, S. *et al.* Sensitivity and specificity of a real-time reverse transcriptase polymerase chain reaction detecting feline coronavirus mutations in effusion and serum/plasma of cats to diagnose feline infectious peritonitis. *BMC Vet. Res.* **13,** 228 (2017).
415. Felten, S. *et al.* Detection of feline coronavirus spike gene mutations as a tool to diagnose feline infectious peritonitis. *J. Feline Med. Surg.* **19,** 321–335 (2017).
416. Sangl, L. *et al.* Detection of feline coronavirus mutations in paraffin-embedded tissues in cats with feline infectious peritonitis and controls. *J. Feline Med. Surg.* 1–10 (2018). doi:10.1177/1098612X18762883
417. Horzinek, M. C., Herrewegh, A. A. & de Groot, R. J. Perspectives on feline coronavirus evolution. *Feline Pract.* (1995).
418. Ruch, T. R. & Machamer, C. E. The coronavirus E protein: Assembly and beyond. *Viruses* **4,** 363–382 (2012).

419. DeDiego, M. L. *et al.* Coronavirus virulence genes with main focus on SARS-CoV envelope gene. *Virus Res.* **194,** 124–137 (2014).
420. DeDiego, M. L. *et al.* A severe acute respiratory syndrome coronavirus that lacks the E gene is attenuated in vitro and in vivo. *J. Virol.* **81,** 1701–1713 (2007).
421. Siu, K. L. *et al.* Severe acute respiratory syndrome coronavirus M protein inhibits type I interferon production by impeding theformation of TRAF3·TANK·TBK1/IKKε complex. *J. Biol. Chem.* **284,** 16202–16209 (2009).
422. de Sousa Abreu, R., Penalva, L. O., Marcotte, E. M. & Vogel, C. Global signatures of protein and mRNA expression levels. *Mol. Biosyst.* **5,** 1512–1526 (2009).
423. Vogel, C. & Marcotte, E. M. Insights into the regulation of protein abundance from proteomic and transcriptomic analyses. *Nat. Rev. Genet.* **13,** 227–232 (2012).
424. Koussounadis, A., Langdon, S. P., Um, I. H., Harrison, D. J. & Smith, V. A. Relationship between differentially expressed mRNA and mRNA-protein correlations in a xenograft model system. *Sci. Rep.* **5,** 1–9 (2015).
425. Edfors, F. *et al.* Gene-specific correlation of RNA and protein levels in human cells and tissues. *Mol. Syst. Biol.* **12,** 883 (2016).

Curriculum Vitae

First name Family name	Alexandra Malbon
Date of birth	19/02/83
Place of birth	Preston, UK
Nationality	British

School education

09/1994 – 06/1999	Queen Mary's School, Lytham, UK
09/1999 – 06/2001	Cardinal Newman College, Preston, UK

Studies

09/2002 – 07/2008	Bachelor of Veterinary Science (BVSc), University of Liverpool, UK
09/2005 – 05/2006	Bachelor of Veterinary Pathology, Royal Veterinary College, London, UK
03/2014 – 11/2015	Dr. med. vet, University of Zurich, Switzerland
01/2016 – 11 / 2018	Preparation of the thesis under the direction of Prof. Dr. med. vet. Anja Kipar at the Institute of Veterinary Pathology of the Vetsuisse Faculty University of Zurich Director: Prof. Dr.med.vet.Anja Kipar
09/2008 – 08/2009	Veterinary Surgeon, Border, Brownlow & Castle, Shropshire, UK
10 / 2009 – 02 / 2010	Intern, The Horse Hospital, Wadham Park, Canungra, Queensland, Australia
02/2010 – 06 / 2010	Veterinary Surgeon, Anvet, Upper Coomera, Queensland, Australia
08/2010 – 02 / 2011	Intern in Veterinary Pathology, University of Liverpool, UK
03/2011 – 02 / 2014	Resident in Veterinary Pathology, University of Liverpool, UK

Declaration of Originality

Last name, first name: Malbon, Alexandra

Matriculation number: 13-705-587

I hereby declare that this thesis represents my original work and that I have used no other sources except as noted by citations.

All data, tables, figures and text citations which have been reproduced from any other source, including the internet, have been explicitly acknowledged as such.

I am aware that in case of non-compliance, the Senate is entitled to withdraw the doctorate degree awarded to me on the basis of the present thesis, in accordance with the "Statut der Universität Bern (Universitätsstatut; UniSt)", Art. 69, of 7 June 2011.

Place, date

Zürich, 19.11.2018

Signature